EFFECTS OF PARENTAL DIVERGENCE ON HYBRIDIZATION AND HYBRIDS IN THE HUMAN PATHOGENIC *CRYPTOCOCCUS*

EFFECTS OF PARENTAL DIVERGENCE ON HYBRIDIZATION AND HYBRIDS IN THE HUMAN PATHOGENIC *CRYPTOCOCCUS*

BY

MAN YOU, B.Eng.

A THESIS SUBMITTED TO THE DEPARTMENT OF BIOLOGY AND THE SCHOOL OF GRADUATE STUDIES OF MCMASTER UNIVERSITY IN PARTIAL FULFILMENT OF THE REQUIREMENTS FOR THE DEGREE OF DOCTOR OF PHILOSOPHY

Doctor of Philosophy, 2021 McMaster University
Department of Biology Hamilton, Ontario, Canada

TITLE: Effects of parental divergence on hybridization and hybrids in the human pathogenic *Cryptococcus*

AUTHOR: Man You
B.Eng (Food Science and Engineering)
Sichuan Agricultural University, Ya'an, Sichuan, China

SUPERVISOR: Dr. Jianping Xu

NUMBER OF PAGES: xiv, 200

Lay Abstract

The role of hybridization in evolution can vary widely, giving rise to hybrid vigor and hybrid weakness. Hybridization plays an important role in plants and animals, especially crops, with advantages of increased yield and quality of products. However, the emergence of hybrid vigor in pathogens with increased virulence is an increasing threat to plant, animal, and human healths. My PhD thesis aimed at understanding the effects of parental divergence on hybridization and hybrids in the human pathogenic *Cryptococcus*. Here, I investigated basidiospore germination rate and hybrid progeny genotypes and phenotypes from diverse genetic crosses in this group of pathogens. My findings contribute towards understanding cryptococcal hybrids and establishing treatment plans against infections by these hybrids.

Abstract

Hybridization refers to mating between species or between genetically differentiated populations of the same species. Although hybrid offspring may exhibit sterility and/or inviability, hybridization can generate novel genotypic and phenotypic diversities, leading to the origin of new traits and new species, the expansion into ecological niches outside of the parental range (e.g., host range), and altered virulence properties in pathogens. However, the relationship between parental genetic divergence and hybrid performance remains largely unknown. The human pathogenic *Cryptococcus* (HPC) is an ideal model to study the impacts of parental divergence on the genetic and phenotypic consequences of hybridization. HPC consists of a group of divergent lineages with various degrees of interfertility. These yeasts are the etiologic agents of cryptococcosis, a potentially lethal disease in humans and animals. In this thesis, I examined the effects of parental divergence on cryptococcal hybrids from multiple aspects. I conducted genetic crosses between different lineages to evaluate the mating success and the germination of sexual spores (i.e., basidiospores) under various environmental conditions. Then, I investigated the genotypic and phenotypic diversities among the hybrids under different environmental conditions. Furthermore, I examined the genome stability of diploid inter-lineage hybrids through laboratory experimental evolution and the effect of antifungal drug stress on the loss of heterozygosity (LOH) in these hybrids. We found that parental genetic divergence plays an important role in genotypic and phenotypic diversities among hybrid progeny in HPC. However, our results indicate that parental genetic divergence alone can't explain most of the observed variations. Instead, genetic divergence along with specific parental strains, environmental factors, and their interactions all contributed to hybridization success and to hybrid genotypic and phenotypic variations. My findings will broaden the current understanding of the phenotypic and genotypic consequences of hybridization and explore the connection between genetic architecture and hybrid speciation in the human pathogenic *Cryptococcus*.

Acknowledgements

First and most importantly, I want to thank my supervisor Dr. Jianping Xu. I am indebted to him for his guidance and support throughout the completion of this thesis. I appreciate that Dr. Xu always keeps his door open to answer questions or discuss and has allowed me to pursue my ideas and projects. I would also like to thank my committee members for the active academic support and constructive feedback, Dr. Jim Quinn and Dr. Ze-Chun Yuan. Many thanks to Dr. Rama Singh for chairing my transfer exam, Dr. Jon Stone for chairing my comprehensive exam and for being on my PhD thesis examination committee, Dr. Yan Wang for being my external examiner, and Dr. Jonathan Dushoff for chairing my PhD defence.

Next, I would like to thank the present and past lab members, my thesis would not have been completed without the support of Dr. Eta Ashu, Dr. Adrian Forsythe, Himeshi Samarasinghe, Greg Korfanty, YuYing Fan, Sarah Sandor, Heather Yoell, Lu Yi, Wang Yue, Meagan Archer, Renad Alijohani, Wenjing Hua and Kelly Dong. I also really enjoyed lots of fun time we spent outside of the lab. In addition, I am grateful to my undergraduate students, Yuxin (Monica) Lin and Annamaria Dobrin, who helped with the work presented in chapters 4 and 5 of this thesis. I also want to thank Dr. Yongmei Li and Dr. Xiaodan Yu for their helpful advice. Also, many people on the faculty and staff of the Biology Department have helped, assisted, and encouraged me in many ways over the last five years.

Then, I am very appreciative of all my family for their constant love and support, mom, dad, grandma, grandpa, uncles, aunts, and cousins. Thanks to my best friends in China for always being there for me. Thanks to the Seidlitzs (Eric, Wendy, Adam, Parker, and Maddy) for being my Canadian family in the past two years. Finally, I want to thank all those who have helped and supported in carrying out my research and life in the past five years again. It was a wonderful journey of studying and living abroad.

Table of Contents

List of Figures

List of Tables

Abbreviations

Acronyms

HPC the human pathogenic *Cryptococcus*

CNSC the *Cryptococcus neoformans* species complex

CGSC the *Cryptococcus gattii* species complex

VN variety *neoformans*

VG variety *gattii*

MIC minimum inhibitory concentration

MLST multi-locus sequence typing

PCR-RFLP polymerase chain reaction-restrction fragment length polymorphism

MLST multi-locus sequence typing

AFLP amplified fragment length polymorphism

UV ultra-violet

MLG multi-locus genotype

MHP multi-locus heterozygosity pattern

RPMI rosewell park memorial institute

YEPD yeast extract peptone dextrose

SD sabouraud dextrose

QTL quantitative trait loci

MAT mating type

LOH loss of heterozygosity

Chapter 1: Introduction

1.1 Hybridization

Generally, hybridization is defined as the process that leads to successful mating products between genetically distinct individuals, producing offspring of mixed genetic ancestry (Barton & Hewitt, 1985). However, hybridization also occurs between two species or divergent populations within a species in most sexually reproducing organisms. Natural hybridization has been observed in both plants and animals. That is, about 25% of plant species and 10% of animal species were estimated to be derived from hybridization (Arnold, 1997; Mallet, 2005).

Due to its positive (i.e., hybrid vigor) and negative (i.e., hybrid weakness) effects, the role of hybridization in evolution has long been considered from two extreme viewpoints among biologists. At one extreme, hybridization is regarded as a potent evolutionary force that creates opportunities for speciation and adaptive evolution. In this view, hybridization increases the genetic diversity and brings novel gene combinations, generating novel and/or extreme (i.e., transgressive) phenotypes and leading to significant adaptive potential in heterogeneous environments (Barton, 2001; Rieseberg *et al*., 2003). The contrasting position considers hybridization as evolutionary noise with only transient effects in evolution and little long-term importance. This opposing view is based on the fact that hybrid offspring are often sterile or inviable due to genetic incompatibility. One common model to explain hybrid incompatibility is the Dobzhansky-Muller model, where incompatibility resulted from alterations at two or more genetic loci in different populations, and hybrid sterility or inviability arose from the subsequent interactions of these genetic changes in the hybrid population (Coyne & Orr, 2004).

Although hybrid offspring in some groups of organisms show hybrid weakness (e.g., sterility or inviability), there is evidence of hybrid vigor or heterosis in other species. Hybrid vigor refers to the superior performance of hybrids shown as increasing yield, fertility, growth rate, biomass, and resistance to infectious diseases and insect pests. Hybrid vigor has been discovered in many plants, especially in agricultural and horticultural crops, such as rice (*Oryza sativa*), Arabidopsis (*Arabidopsis thaliana*), maize (*Zea mays*), and sunflowers (*Helianthus annuus* L.) (Z. J. Chen, 2010; Groszmann *et al*., 2014; Hochholdinger & Hoecker, 2007; Huang *et al*., 2016; Owens *et al*., 2019; L. Wang *et al*., 2015; Yang *et al*., 2017). Both hybrid vigor and hybrid

weakness have also been observed in animals, such as fruit fly (*Drosophila)*, domestic dog (*Canis lupus familiaris*), tephritid fly (*Dacus tryoni)*, and stickleback fish (*Gasterosteus aculeatus*) (Brideau *et al*., 2006; Z. J. Chen, 2010; Lewontin & Birch, 1966; Lucek *et al*., 2010).

Unlike plants and animals, all fungi can undergo asexual reproduction. Thus, even sterile hybrids can reproduce through asexual/clonal reproduction and have continuous evolutionary effects. Another unique characteristic of fungi is that they generally have a short reproductive cycle and can achieve large populations in a relatively short time (days or weeks given the right conditions). Both features can contribute to the possibility that hybrid progeny with high fitness could emerge during hybridization in fungi and spread quickly. By mixing divergent genetic materials, hybridization can generate novel genetic diversity and interactions, which may allow them to adapt to new ecological niches such as new host species (Li *et al*., 2012; Mixão & Gabaldón, 2018; Schardl & Craven, 2003). Indeed, natural, clinical, and artificial hybridization events have been frequently reported in fungi, including in the human fungal pathogen *Cryptococcus* (Boekhout *et al*., 2001; Kunitski *et al*., 2019; Leducq *et al*., 2016; Litvintseva *et al*., 2007; Mixão *et al*., 2019; Xu *et al*., 2000). These provide evidence that hybridization could lead to genotypic and phenotypic diversity, resulting in geographic and ecological niche expansions.

1.2 The human pathogenic *Cryptococcus* (HPC)

The human pathogenic *Cryptococcus* consists of two species complexes, *C. neoformans* species complex (CNSC) and *C. gattii* species complex (CGSC). They are the causative agents of the potentially life-threatening disease - cryptococcosis. Cryptococcosis affects the lungs, skin, the central nervous system (the brain and spinal cord), and other body sites in mammals, including humans. Strains of HPC are commonly found in pigeon droppings, soil, tree, and tree hollows (Kwon-Chung *et al*., 2014). Annually, 220,000 cases of cryptococcal infections are reported worldwide with 180,000 resulting in mortality (Rajasingham *et al*., 2017). In 1894, *Cryptococcus neoformans* was first isolated from peach juice by Sanfelice, and Busse isolated the first clinical culture from a sarcoma-like lesion in a patient's tibia (Busse, 1894; Sanfelice, 1894). In 1896, Curtis isolated a yeast-like fungus from a tumor in a patient's lumbar

region which was later determined to be the first clinical isolate of *Cryptococcus gattii* (Curtis, 1896; Kwon-Chung *et al*., 2002).

C. neoformans species complex is an opportunistic pathogen that primarily infects immunocompromised patients and has been found worldwide. *C. gattii* species complex is a primary pathogen that often infects immunocompetent individuals. CGSC was traditionally considered a pathogen only associated with tropical and subtropical regions (Herkert *et al*., 2017; Litvintseva *et al*., 2005). However, the recent outbreaks of CGSC infection on the Vancouver Island in Canada and the United States Pacific Northwestern, as well as the identification of CGSC isolates in other countries (e.g., Greece and Spain), suggest that its ecological niche has expanded to temperate climates (Byrnes *et al*., 2009; Colom *et al*., 2005; MacDougall *et al*., 2007; Velegraki *et al*., 2001).

There are five main serotypes in the human pathogenic *Cryptococcus*: A, B, C, D, and AD (hybrids between serotypes A and D) on the basis of capsular agglutination reactions (Belay *et al*., 1996). Based on multi-locus sequence typing (MLST) and other molecular typing techniques, such as amplified fragment length polymorphism (AFLP) and restriction fragment length polymorphism (RFLP) analyses, CNSC and CGSC are divided into several distinct molecular types/lineages, including VNI, VNII, VNIII, and VNIV (VN = variety *neoformans*) belonging to CNSC, and VGI, VGII, VGIII and VGIV (VG = variety *gattii*) belonging to CGSC (Farrer *et al*., 2019; Hagen *et al*., 2015; Hong *et al*., 2021; Kwon-Chung *et al*., 2017). According to DNA sequencing and molecular clock analysis, it has been estimated that CNSC and CGSC have separated ~100 million years (Casadevall *et al*., 2017; Sharpton *et al*., 2008). Within CNSC, serotypes A and D diverged ~24.5 million years ago (mya), and VNI and VNII split ~4.7 mya (Ngamskulrungroj *et al*., 2009). Within CGSC, VGII diverged from other VG molecular types ~12.5 mya, VGIV separated ~11.7 mya, and VGI and VGIII split ~8.5 mya (Ngamskulrungroj *et al*., 2009). Among these distinct molecular types, strains of VNI are the predominant etiologic agents of cryptococcosis isolated worldwide (63%), followed by VGI (9%), VGII (7%), VNII and VNIII (6% each), VNIV (5%), VGIII (3%), and VGIV (1%) (Kwon-Chung *et al*., 2014). More recently, a new molecular type/lineage of CGSC has been reported, named VGV (Farrer *et al*., 2019).

The human pathogenic *Cryptococcus* has several virulence factors responsible for its survival and proliferation within the host (Alspaugh, 2015; Kwon-Chung *et al*.,

2014). The three essential factors are the synthesis of melanin, the formation of a polysaccharide capsule, and the ability to grow at 37 °C (mammalian body temperature). Melanin has antiphagocytic and antioxidant activities, protecting cryptococcal cells from antifungal agents, such as amphotericin B and azoles, and decreases susceptibility to UV light and temperatures (Cordero & Casadevall, 2017; Ikeda *et al*., 2003; Liu *et al*., 2021; Pacelli *et al*., 2017; Rosas & Casadevall, 1997; Y. Wang & Casadevall, 1994). The polysaccharide capsule protects the cells from being phagocytosed by host phagocytic cells, allowing these cells to evade the host immune system (Almeida *et al*., 2015; Casadevall *et al*., 2019; Leopold Wager *et al*., 2016). These traits, combined with the ability to grow at 37 °C, allow strains of HPC to be a pathogen and thrive within human and animal hosts.

1.3 Life cycle of the human pathogenic *Cryptococcus*

In the environment, haploid strains of HPC are found as yeast cells. They have a bipolar mating system with either of two mating types, mating type **a** (*MAT***a**) or mating type α (*MAT*α). Cryptococcal strains normally reproduce asexually through budding, however, under certain environmental conditions, they can undergo sexual reproduction via mating. Under mating-inducing conditions (e.g., low nitrogen and dehydration), mating occurs between cells of the opposite mating types, resulting in forming a filamentous cell type (dikaryon) containing nuclei of *MAT***a** and *MAT*α. In contrast, the same mating-type mating occurs between *MAT*α cells establishing monokaryon with nuclei of *MAT*α. Either dikaryon or monokaryon generates chains of haploid spores following nuclear fusion (only exists in sexual mating), meiosis, rounds of mitosis, and sporulation, producing four chains of recombinant basidiospores (i.e., sexual spores) (Kwon-Chung, 1976; Zhao *et al*., 2019). However, *MAT*α strains are predominant in natural populations, and consequently, most clinical isolates are *MAT*α strains (J. Chen *et al*., 2008; Kwon-Chung *et al*., 2014; Kwon-Chung & Bennett, 1978; Litvintseva *et al*., 2005).

Despite the divergence between molecular types/lineages in the human pathogenic *Cryptococcus*, intra- and inter-lineage mating occurs with natural hybrid isolates being found, as well as artificial hybrids generated under certain laboratory conditions (Boekhout *et al*., 2001; Bovers *et al*., 2006, 2008; Forsythe *et al*., 2016; Li *et al*., 2012;

Lin *et al*., 2007; Litvintseva *et al*., 2007; Vogan & Xu, 2014). For example, the first reported serotype AD hybrid (strain CBS132) was isolated from peach juice over three decades ago (Ikeda *et al*., 1985). The frequency of AD hybrid strains is ~6% among global clinical isolates, with up to 30% among European clinical isolates and 6% among North American isolates (Cogliati, 2013; Meyer *et al*., 2010). In addition, hybrid weakness and hybrid vigor have been observed among cryptococcal hybrids (Lin *et al*., 2007; Shahid *et al*., 2008; Vogan *et al*., 2016; Vogan & Xu, 2014).

1.4 Objectives

The overall objective of my PhD thesis was to investigate the effects of parental genetic divergence on hybridization and hybrid performance in the human pathogenic *Cryptococcus*. More specifically, my PhD included one review chapter and three main data chapters, focusing on objectives described in detail in Chapters 2 to 5 of this thesis. In Chapter 2, I reviewed the roles of hybridization in fungal evolution and adaptation using two fungal pathogens, the human pathogenic *Cryptococcus* and the amphibian chytrid pathogen *Batrachochytrium dendrobatidis*. In Chapter 3, I conducted diverse genetic crosses to study the mating success and hybrid spore germination under different laboratory conditions. In Chapter 4, I investigated the effects of parental divergence on genotypic diversity and phenotypic variation among hybrid progeny under various environmental conditions. In Chapter 5, by means of mutation accumulation, I investigated genome stability of diploid inter-lineage hybrids and their genetic and phenotypic changes during mitotic divisions.

1.5 References

Almeida, F., Wolf, J. M., & Casadevall, A. (2015). Virulence-Associated Enzymes of *Cryptococcus neoformans*. *Eukaryotic Cell*, *14*(12), 1173–1185.

Alspaugh, J. A. (2015). "Virulence Mechanisms and *Cryptococcus neoformans* pathogenesis." *Fungal Genetics and Biology : FG & B*, *78*, 55–58.

Arnold, M. L. (1997). *Natural Hybridization and Evolution*. Oxford University Press, USA.

Barton, N. H. (2001). The role of hybridization in evolution. *Molecular Ecology*, *10*(3), 551–568.

Barton, N. H., & Hewitt, G. M. (1985). Analysis of Hybrid Zones. *Annual Review of Ecology and Systematics*, *16*(1), 113–148.

Belay, T., Cherniak, R., O'Neill, E. B., & Kozel, T. R. (1996). Serotyping of *Cryptococcus neoformans* by dot enzyme assay. *Journal of Clinical Microbiology*, *34*(2), 466–470.

Boekhout, T., Theelen, B., Diaz, M., Fell, J. W., Hop, W. C. J., Abeln, E. C. A., Dromer, F., & Meyer, W. (2001). Hybrid genotypes in the pathogenic yeast *Cryptococcus neoformans*. *Microbiology (Reading, England)*, *147*(Pt 4), 891–907.

Bovers, M., Hagen, F., Kuramae, E. E., Diaz, M. R., Spanjaard, L., Dromer, F., Hoogveld, H. L., & Boekhout, T. (2006). Unique hybrids between the fungal pathogens *Cryptococcus neoformans* and *Cryptococcus gattii*. *FEMS Yeast Research*, *6*(4), 599–607.

Bovers, M., Hagen, F., Kuramae, E. E., Hoogveld, H. L., Dromer, F., St-Germain, G., & Boekhout, T. (2008). AIDS Patient Death Caused by Novel *Cryptococcus neoformans* × *C. gattii* Hybrid. *Emerging Infectious Diseases*, *14*(7), 1105–1108.

Brideau, N. J., Flores, H. A., Wang, J., Maheshwari, S., Wang, X., & Barbash, D. A. (2006). Two Dobzhansky-Muller genes interact to cause hybrid lethality in Drosophila. *Science (New York, N.Y.)*, *314*(5803), 1292–1295.

Busse, O. (1894). Uber parasitare zelleinschlusse und ihre zuchtung. *Zentralbl Bakteriol*, *16*, 175–180.

Byrnes, E. J., Bildfell, R., Frank, S. A., Mitchell, T. G., Marr, K., & Heitman, J. (2009). Molecular Evidence that the Vancouver Island *Cryptococcus gattii* Outbreak has Expanded into the United States Pacific Northwest. *The Journal of Infectious Diseases*, *199*(7), 1081–1086.

Casadevall, A., Coelho, C., Cordero, R. J. B., Dragotakes, Q., Jung, E., Vij, R., & Wear, M. P. (2019). The capsule of *Cryptococcus neoformans*. *Virulence*, *10*(SI2), 822–831.

Casadevall, A., Freij, J. B., Hann-Soden, C., & Taylor, J. (2017). Continental Drift and Speciation of the *Cryptococcus neoformans* and *Cryptococcus gattii* Species Complexes. *MSphere*, *2*(2), e00103-17.

Chen, J., Varma, A., Diaz, M. R., Litvintseva, A. P., Wollenberg, K. K., & Kwon-Chung, K. J. (2008). *Cryptococcus neoformans* strains and infection in apparently immunocompetent patients, China. *Emerging Infectious Diseases*, *14*(5), 755–762.

Chen, Z. J. (2010). Molecular mechanisms of polyploidy and hybrid vigor. *Trends in Plant Science*, *15*(2), 57–71.

Cogliati, M. (2013). Global Molecular Epidemiology of *Cryptococcus neoformans* and *Cryptococcus gattii*: An Atlas of the Molecular Types. *Scientifica*, *2013*, e675213.

Colom, M. F., Frasés, S., Ferrer, C., Jover, A., Andreu, M., Reus, S., Sánchez, M., & Torres-Rodríguez, J. M. (2005). First case of human cryptococcosis due to *Cryptococcus neoformans* var. *Gattii* in Spain. *Journal of Clinical Microbiology*, *43*(7), 3548–3550.

Cordero, R. J. B., & Casadevall, A. (2017). Functions of fungal melanin beyond virulence. *Fungal Biology Reviews*, *31*(2), 99–112.

Coyne, J. A., & Orr, H. A. (2004). *Speciation*. Sunderland, MA, Sinauer Associate.

Curtis, F. (1896). Contribution a l'etude de la saccharomycose humaine. *Ann Inst Pasteur*, *10*, 449–468.

Farrer, R. A., Chang, M., Davis, M. J., Dorp, L. van, Yang, D.-H., Shea, T., Sewell, T. R., Meyer, W., Balloux, F., Edwards, H. M., Chanda, D., Kwenda, G., Vanhove, M., Chang, Y. C., Cuomo, C. A., Fisher, M. C., & Kwon-Chung, K. J. (2019). A New Lineage of *Cryptococcus gattii* (VGV) Discovered in the Central Zambezian Miombo Woodlands. *MBio*, *10*(6).

Forsythe, A., Vogan, A., & Xu, J. (2016). Genetic and environmental influences on the germination of basidiospores in the *Cryptococcus neoformans* species complex. *Scientific Reports*, *6*(1), 33828.

Groszmann, M., Gonzalez-Bayon, R., Greaves, I. K., Wang, L., Huen, A. K., Peacock, W. J., & Dennis, E. S. (2014). Intraspecific Arabidopsis Hybrids Show Different Patterns of Heterosis Despite the Close Relatedness of the Parental Genomes. *Plant Physiology*, *166*(1), 265–280.

Hagen, F., Khayhan, K., Theelen, B., Kolecka, A., Polacheck, I., Sionov, E., Falk, R., Parnmen, S., Lumbsch, H. T., & Boekhout, T. (2015). Recognition of seven species in the *Cryptococcus gattii*/*Cryptococcus neoformans* species complex. *Fungal Genetics and Biology: FG & B*, *78*, 16–48.

Herkert, P. F., Hagen, F., Pinheiro, R. L., Muro, M. D., Meis, J. F., & Queiroz-Telles, F. (2017). Ecoepidemiology of *Cryptococcus gattii* in Developing Countries. *Journal of Fungi*, *3*(4), 62.

Hochholdinger, F., & Hoecker, N. (2007). Towards the molecular basis of heterosis. *Trends in Plant Science*, *12*(9), 427–432.

Hong, N., Chen, M., & Xu, J. (2021). Molecular Markers Reveal Epidemiological Patterns and Evolutionary Histories of the Human Pathogenic *Cryptococcus*. *Frontiers in Cellular and Infection Microbiology*, *11*.

Huang, X., Yang, S., Gong, J., Zhao, Q., Feng, Q., Zhan, Q., Zhao, Y., Li, W., Cheng, B., Xia, J., Chen, N., Huang, T., Zhang, L., Fan, D., Chen, J., Zhou, C., Lu, Y., Weng, Q., & Han, B. (2016). Genomic architecture of heterosis for yield traits in rice. *Nature*, *537*(7622), 629–633.

Ikeda, R., Nishikawa, A., Shinoda, T., & Fukazawa, Y. (1985). Chemical characterization of capsular polysaccharide from *Cryptococcus neoformans* serotype AD. *Microbiology and Immunology*, *29*(10), 981–991.

Ikeda, R., Sugita, T., Jacobson, E. S., & Shinoda, T. (2003). Effects of melanin upon susceptibility of *Cryptococcus* to antifungals. *Microbiology and Immunology*, *47*(4), 271–277.

Kunitski, M., Eicke, N., Huber, P., Köhler, J., Zeller, S., Voigtsberger, J., Schlott, N., Henrichs, K., Sann, H., Trinter, F., Schmidt, L. P. H., Kalinin, A., Schöffler, M. S., Jahnke, T., Lein, M., & Dörner, R. (2019). Double-slit photoelectron interference in strong-field ionization of the neon dimer. *Nature Communications*, *10*(1), 1.

Kwon-Chung, K. J. (1976). Morphogenesis of Filobasidiella *neoformans*, the sexual state of *Cryptococcus neoformans*. *Mycologia*, *68*(4), 821–833.

Kwon-Chung, K. J., & Bennett, J. E. (1978). Distribution of alpha and alpha mating types of *Cryptococcus neoformans* among natural and clinical isolates. *American Journal of Epidemiology*, *108*(4), 337–340.

Kwon-Chung, K. J., Bennett, J. E., Wickes, B. L., Meyer, W., Cuomo, C. A., Wollenburg, K. R., Bicanic, T. A., Castañeda, E., Chang, Y. C., Chen, J., Cogliati, M., Dromer, F., Ellis, D., Filler, S. G., Fisher, M. C., Harrison, T. S., Holland, S. M., Kohno, S., Kronstad, J. W., … Casadevall, A. (2017). The Case for Adopting the

"Species Complex" Nomenclature for the Etiologic Agents of Cryptococcosis. *MSphere*, *2*(1), e00357-16.

Kwon-Chung, K. J., Boekhout, T., Fell, J. W., & Diaz, M. (2002). (1557) Proposal to conserve the name *Cryptococcus gattii* against C. hondurianus and C. bacillisporus (Basidiomycota, Hymenomycetes, Tremellomycetidae). *TAXON*, *51*(4), 804–806.

Kwon-Chung, K. J., Fraser, J. A., Doering, T. L., Wang, Z. A., Janbon, G., Idnurm, A., & Bahn, Y.-S. (2014). *Cryptococcus neoformans* and *Cryptococcus gattii*, the Etiologic Agents of Cryptococcosis. *Cold Spring Harbor Perspectives in Medicine*, *4*(7), a019760.

Leducq, J.-B., Nielly-Thibault, L., Charron, G., Eberlein, C., Verta, J.-P., Samani, P., Sylvester, K., Hittinger, C. T., Bell, G., & Landry, C. R. (2016). Speciation driven by hybridization and chromosomal plasticity in a wild yeast. *Nature Microbiology*, *1*, 15003.

Leopold Wager, C. M., Hole, C. R., Wozniak, K. L., & Wormley, F. L. (2016). *Cryptococcus* and Phagocytes: Complex Interactions that Influence Disease Outcome. *Frontiers in Microbiology*, *7*, 105.

Lewontin, R. C., & Birch, L. C. (1966). Hybridization as a source of variation for adaptation to new environments. *Evolution; International Journal of Organic Evolution*, *20*(3), 315–336.

Li, W., Averette, A. F., Desnos-Ollivier, M., Ni, M., Dromer, F., & Heitman, J. (2012). Genetic Diversity and Genomic Plasticity of *Cryptococcus neoformans* AD Hybrid Strains. *G3: Genes|Genomes|Genetics*, *2*(1), 83–97.

Lin, X., Litvintseva, A. P., Nielsen, K., Patel, S., Floyd, A., Mitchell, T. G., & Heitman, J. (2007). αADα Hybrids of *Cryptococcus neoformans*: Evidence of Same-Sex Mating in Nature and Hybrid Fitness. *PLOS Genetics*, *3*(10), e186.

Litvintseva, A. P., Lin, X., Templeton, I., Heitman, J., & Mitchell, T. G. (2007). Many globally isolated AD hybrid strains of *Cryptococcus neoformans* originated in Africa. *PLoS Pathogens*, *3*(8), e114.

Litvintseva, A. P., Thakur, R., Reller, L. B., & Mitchell, T. G. (2005). Prevalence of clinical isolates of *Cryptococcus gattii* serotype C among patients with AIDS in Sub-Saharan Africa. *The Journal of Infectious Diseases*, *192*(5), 888–892.

Liu, S., Youngchim, S., Zamith-Miranda, D., & Nosanchuk, J. D. (2021). Fungal Melanin and the Mammalian Immune System. *Journal of Fungi (Basel, Switzerland)*, *7*(4), 264.

Lucek, K., Roy, D., Bezault, E., Sivasundar, A., & Seehausen, O. (2010). Hybridization between distant lineages increases adaptive variation during a biological invasion: Stickleback in Switzerland. *Molecular Ecology*, *19*(18), 3995–4011.

MacDougall, L., Kidd, S. E., Galanis, E., Mak, S., Leslie, M. J., Cieslak, P. R., Kronstad, J. W., Morshed, M. G., & Bartlett, K. H. (2007). Spread of *Cryptococcus gattii* in British Columbia, Canada, and Detection in the Pacific Northwest, USA. *Emerging Infectious Diseases*, *13*(1), 42–50.

Mallet, J. (2005). Hybridization as an invasion of the genome. *Trends in Ecology & Evolution*, *20*(5), 229–237.

Meyer, W., Gilgado, F., Ngamskulrungroj, P., Trilles, L., Hagen, F., Castañeda, E., & Boekhout, T. (2010). Molecular Typing of the *Cryptococcus neoformans*/*Cryptococcus gattii* Species Complex. In *Cryptococcus* (pp. 327–357). John Wiley & Sons, Ltd.

Mixão, V., & Gabaldón, T. (2018). Hybridization and emergence of virulence in opportunistic human yeast pathogens. *Yeast (Chichester, England)*, *35*(1), 5–20.

Mixão, V., Hansen, A. P., Saus, E., Boekhout, T., Lass-Florl, C., & Gabaldón, T. (2019). Whole-Genome Sequencing of the Opportunistic Yeast Pathogen Candida inconspicua Uncovers Its Hybrid Origin. *Frontiers in Genetics*, *10*, 383.

Ngamskulrungroj, P., Gilgado, F., Faganello, J., Litvintseva, A. P., Leal, A. L., Tsui, K. M., Mitchell, T. G., Vainstein, M. H., & Meyer, W. (2009). Genetic Diversity of the *Cryptococcus* Species Complex Suggests that *Cryptococcus gattii* Deserves to Have Varieties. *PLOS ONE*, *4*(6), e5862.

Owens, G. L., Baute, G. J., Hubner, S., & Rieseberg, L. H. (2019). Genomic sequence and copy number evolution during hybrid crop development in sunflowers. *Evolutionary Applications*, *12*(1), 54–65.

Pacelli, C., Bryan, R. A., Onofri, S., Selbmann, L., Shuryak, I., & Dadachova, E. (2017). Melanin is effective in protecting fast and slow growing fungi from various types of ionizing radiation. *Environmental Microbiology*, *19*(4), 1612–1624.

Rajasingham, R., Smith, R. M., Park, B. J., Jarvis, J. N., Govender, N. P., Chiller, T. M., Denning, D. W., Loyse, A., & Boulware, D. R. (2017). Global burden of disease of HIV-associated cryptococcal meningitis: An updated analysis. *The Lancet. Infectious Diseases*, *17*(8), 873–881.

Rieseberg, L. H., Raymond, O., Rosenthal, D. M., Lai, Z., Livingstone, K., Nakazato, T., Durphy, J. L., Schwarzbach, A. E., Donovan, L. A., & Lexer, C. (2003). Major ecological transitions in wild sunflowers facilitated by hybridization. *Science (New York, N.Y.)*, *301*(5637), 1211–1216.

Rosas, A. L., & Casadevall, A. (1997). Melanization affects susceptibility of *Cryptococcus neoformans* to heat and cold. *FEMS Microbiology Letters*, *153*(2), 265–272.

Sanfelice, F. (1894). Contributo alla morfologia e biologia dei blastomiceti che si sviluppano nei succhi di alcuni frutti. *Ann Igien*, *4*.

Schardl, C. L., & Craven, K. D. (2003). Interspecific hybridization in plant-associated fungi and oomycetes: A review. *Molecular Ecology*, *12*(11), 2861–2873.

Shahid, M., Han, S., Yoell, H., & Xu, J. (2008). Fitness distribution and transgressive segregation across 40 environments in a hybrid progeny population of the human-pathogenic yeast *Cryptococcus neoformans*. *Genome*, *51*(4), 272–281.

Sharpton, T. J., Neafsey, D. E., Galagan, J. E., & Taylor, J. W. (2008). Mechanisms of intron gain and loss in *Cryptococcus*. *Genome Biology*, *9*(1), R24.

Velegraki, A., Kiosses, V. G., Pitsouni, H., Toukas, D., Daniilidis, V. D., & Legakis, N. J. (2001). First report of *Cryptococcus neoformans* var. *Gattii* serotype B from Greece. *Medical Mycology*, *39*(5), 419–422.

Vogan, A. A., Khankhet, J., Samarasinghe, H., & Xu, J. (2016). Identification of QTLs Associated with Virulence Related Traits and Drug Resistance in *Cryptococcus neoformans*. *G3 Genes|Genomes|Genetics*, *6*(9), 2745–2759.

Vogan, A. A., & Xu, J. (2014). Evidence for genetic incompatibilities associated with post-zygotic reproductive isolation in the human fungal pathogen *Cryptococcus neoformans*. *Genome*, *57*(6), 335–344.

Wang, L., Greaves, I. K., Groszmann, M., Wu, L. M., Dennis, E. S., & Peacock, W. J. (2015). Hybrid mimics and hybrid vigor in Arabidopsis. *Proceedings of the National Academy of Sciences*, *112*(35), E4959–E4967.

Wang, Y., & Casadevall, A. (1994). Decreased susceptibility of melanized *Cryptococcus neoformans* to UV light. *Applied and Environmental Microbiology*, *60*(10), 3864–3866.

Xu, J., Vilgalys, R., & Mitchell, T. G. (2000). Multiple gene genealogies reveal recent dispersion and hybridization in the human pathogenic fungus *Cryptococcus neoformans*. *Molecular Ecology*, *9*(10), 1471–1481.

Yang, J., Mezmouk, S., Baumgarten, A., Buckler, E. S., Guill, K. E., McMullen, M. D., Mumm, R. H., & Ross-Ibarra, J. (2017). Incomplete dominance of deleterious alleles contributes substantially to trait variation and heterosis in maize. *PLoS Genetics*, *13*(9), e1007019.

Zhao, Y., Lin, J., Fan, Y., & Lin, X. (2019). Life Cycle of *Cryptococcus neoformans*. *Annual Review of Microbiology*, *73*, 17–42.

Chapter 2: Hybridization facilitates adaptive evolution in two major fungal pathogens

2.1 Preface

The role of hybridization in evolution has long been debated. This review paper discusses how recent hybridizations have played an important role in the evolution and adaptation of two fungal pathogens, the human pathogenic *Cryptococcus* and the amphibian chytrid fungus *Batrachochytrium dendrobatidis*. This review paper is now published in Genes 2020, 11(1), 101. I am a co-first author of this work. The *Cryptococcus* related section was contributed equally by Himeshi Samarasinghe and myself. References in this chapter appear as they are in the originally published manuscript.

2.2 Abstract

Hybridization is increasingly recognized as an important force impacting adaptation and evolution in many lineages of fungi. During hybridization, divergent genomes and alleles are brought together into the same cell, potentiating adaptation by increasing genomic plasticity. Here, we review hybridization in fungi by focusing on two fungal pathogens of animals. Hybridization is common between the basidiomycete yeast species *Cryptococcus neoformans* × *Cryptococcus deneoformans*, and hybrid genotypes are frequently found in both environmental and clinical settings. The two species show 10 − 15% nucleotide divergence at the genome level, and their hybrids are highly heterozygous. Though largely sterile and unable to mate, these hybrids can propagate asexually and generate diverse genotypes by nondisjunction, aberrant meiosis, mitotic recombination, and gene conversion. Under stress conditions, the rate of such genetic changes can increase, leading to rapid adaptation. Conversely, in hybrids formed between lineages of the chytridiomycete frog pathogen *Batrachochytrium dendrobatidis* (*Bd*), the parental genotypes are considerably less diverged (0.2% divergent). *Bd* hybrids are formed from crosses between lineages that rarely undergo sex. A common theme in both species is that hybrids show genome plasticity via aneuploidy or loss of heterozygosity and leverage these mechanisms as a rapid way to generate genotypic/phenotypic diversity. Some hybrids show greater fitness and survival in both virulence and virulence-associated phenotypes than parental lineages under certain conditions. These studies showcase how experimentation in model species such as

Cryptococcus can be a powerful tool in elucidating the genotypic and phenotypic consequences of hybridization.

2.3 Introduction

Hybridization refers to the interbreeding of individuals from genetically distinct populations or species. Through hybridization, genes and alleles that have diverged significantly from each other are brought together into the same cells and individuals, potentially creating the scenario of novel interactions among genes and genomes. There are two contrasting views on the roles of hybridization in organic evolution. On the one hand, hybridization is considered an evolutionary noise with limited long-term effects. Indeed, under a model in which species diverge by adaptation to different niches, the majority of hybrids are expected to show lower fitness than either parental genotype in parental niches [1,2]. On the other hand, certain hybrid progenies may display transgressive segregation/extreme phenotypes or fitness, both positive and negative, that exceed parental values, especially in novel ecological niches. Because of this, the contrasting view believes that hybridization plays critical roles in generating evolutionary novelty and can impact long-term evolution [3,4].

Hybrids may be either homoploid or polyploid. Homoploid hybrids have the same ploidy as the parents, but they may face obstacles to further sexual reproduction due to potential chromosomal incompatibilities. If homoploid hybrids can self-fertilize or backcross, the resulting offspring often reveals high genetic and phenotypic variance, including the generation of transgressive phenotypes [5]. Polyploid hybrids, specifically allopolyploids, have a higher ploidy generated typically by chromosome duplication, either in gametogenesis or after zygote formation following the mating of different species [6]. The presence of pairs of homologous chromosomes from each parental species alleviates the problems in meiosis due to low sequence similarity or structural rearrangements that lead to hybrid sterility in homoploids. Outcomes of hybridization are diverse. For example, in plants, hybridization may lead to the formation of novel hybrid species that are genetically isolated and phenotypically distinct from progenitors [3,5]. In other contexts, the extent of hybridization may be limited to a geographic region (or hybrid zone) maintained by either environment-genotype interactions or through a balance between migration and selection. In any case, hybridization also makes possible

the introgression of alleles from one parental species into another, which is becoming easier to identify through genome sequencing [7,8].

In all major groups of eukaryotes, such as plants, animals, and fungi, natural hybridization has been reported, with some groups showing over 20% of extant species as hybrids. Previously, however, hybridization in fungi was either ignored or discounted, and only since the molecular revolution has hybridization in fungi been increasingly accepted as playing important roles [9,10]. Fungi are unique from the better-studied plants and animals in that they often produce copious (literally millions or billions) amounts of recombinants from a single mating event, which could lead to the generation of immense diversity. They are also unique because their dispersal is not considered particularly limited, such that traditional hybrid zones of a limited geographic extent seem unlikely. On the other hand, many fungi display a mixed mode of reproduction, with extensive generations of asexual reproduction interspersed with rare sexual reproduction [11]. Such versatility in reproduction could allow hybrids to propagate asexually for extended periods of time without suffering from a potential segregation load [12]. In fungi, F1 hybrids often display aneuploidy, diploidy, or higher ploidy, and because of the extra chromosome copies they can continue to diversify and adapt through mechanisms such as mitotic recombination and the gain/loss of individual chromosomes.

In this review, we explore these issues with a fungal view of hybridization described using two major fungal pathogens, the human-pathogenic *Cryptococcus* species and the amphibian chytrid fungus *Batrachochytrium dendrobatidis*. We argue that hybridization in these two groups of fungi reveals much about how speciation and hybridization in fungi is unique, and how hybridization will become an increasingly important concern for both the environment and human health in this era of rapid fungal evolution. The choice of these two species is based off of the authors' experiences. However, the pair complement each other nicely. On the one hand, *Cryptococcus* (Basidiomycota) is a model system and easily manipulated in the lab, while *B. dendrobatidis* (Chytridiomycota), a species of great ecological significance, is far from a model system and lacks genetic tools. Insights into hybridization in these species require different approaches, but much has been revealed and facilitated by genomics.

2.4 Hybridization in *Cryptococcus* species complex

2.4.1 *Cryptococcus* species complex

The human pathogenic *Cryptococcus* species complex comprises a group of closely related, basidiomycetous yeast species, responsible for over 220,000 annual, global infections with a mortality rate of ~80% [13]. Cryptococcal infections, known to occur in multiple forms including respiratory infections, skin lesions, and meningoencephalitis, are collectively called cryptococcosis and are a leading cause of death among HIV/AIDS patients worldwide. Commonly found in association with soil, bird droppings and tree barks, *Cryptococcus* species has a global distribution with strains having been discovered from all continents except Antarctica [14]. Currently, seven evolutionarily divergent lineages are recognized as pathogenic *Cryptococcus* species, which can be distinguished based on their genetic and molecular characterization, with each species having been assigned specific molecular types (Figure 2.1) [15,16]. Historically, *Cryptococcus* strains were categorized into serotypes based on the structure of polysaccharides at the cell surface. An alternative classification system aims to maintain two major species that are subdivided into varieties and/or molecular types [17,18]. In this review, we will use the seven-species classification system with (i) *C. neoformans* (serotype A, molecular types VNI, VNII and VNB; VN = variety *neoformans*), (ii) *C. deneoformans* (serotype D, molecular type VNIV), (iii) *C. gattii* (molecular type VGI; VG = variety *gattii*), (iv) *C. bacillisporus* (molecular type VGIII), (v) *C. deuterogattii* (molecular type VGII), (vi) *C. tetragattii* (molecular type VGIV) and (vii) *C. decagattii* (molecular type VGIV/VGIIIc) (the last five species share serotypes B and C). To maintain consistency with the previous literature, we will categorize cryptococcal hybrids based on the serotypes of the parental species. For example, hybrids of *C. neoformans* and *C. deneoformans* will be referred to as AD hybrids.

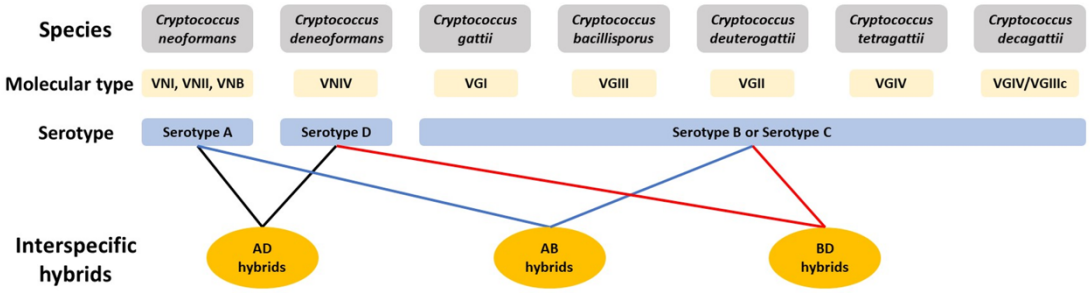

Figure 2.1. The currently recognized species in the pathogenic *Cryptococcus* species complex. The seven species of this complex can be distinguished based on genetic and molecular differences, and each is assigned a distinct molecular type. Historically, cryptococcal strains were broadly categorized into serotypes based on the antigens found at the cell surface. Hybrids arising from mating between species are named based on the serotypes of the parental strains.

The seven species are believed to be descended from a common ancestor that existed on the supercontinent Pangea [19]. It is hypothesized that the ancestral population was split into two distinct groups following the breakup of Pangea and subsequent continental drift further spatially isolated the subgroups, leading to the emergence of two major, independently evolving populations in South America and Africa. This theory is supported by the fact that the estimated split of VN molecular types from VG molecular types occurred ~100 million years ago (mya) which coincides with the breakup of Pangea [19]. Furthermore, genomic analyses have revealed the origin of VN molecular types to be Africa, while VG molecular types originated in South America. The ancestral populations of VN and VG molecular types continued to diverge and evolve, likely due to local niche differences, eventually splitting into the seven species observed today. *C. neoformans* and *C. deneoformans* are believed to have diverged ~24.5 mya [19,20,21,22]. More recently, within *C. neoformans*, VNI and VNII split from each other ~4.7 mya. Among VG lineages, VGII diverged from other VG lineages ~12.5 mya, followed by VGIV splitting ~11.7 mya. VGI and VGIII were the last to diverge from each other, approximately 8.5 mya [21].

In the last century, historical spatial barriers between the seven cryptococcal species have been challenged with the significant increase in international commercial and

human travel. The different lineages are now thrust back into contact due to anthropogenic transfer of cryptococcal cells/strains across countries and continents. Despite significant genomic nucleotide divergence, these species are still sufficiently compatible to initiate mating with each other, making interspecific hybridization a significant force that shapes their ongoing evolution. In fact, cryptococcal hybrids with superior fitness to parental strains have been recovered from both natural and laboratory settings while the proportion of infections caused by *C. neoformans* × *C. deneoformans* (AD) hybrids is on the rise, especially in Europe, where these hybrids are responsible for nearly 40% of all cryptococcal infections. The implications of interspecific hybridization on the adaptive evolution of the pathogenic *Cryptococcus* species complex are discussed below.

2.4.2 Sexual cycle of *Cryptococcus*

Cryptococcus species are haploid basidiomycete yeasts that can reproduce asexually via budding or sexually via mating (Figure 2.2). The sexual cycle of *Cryptococcus* was first observed by Kwon-Chung four decades ago [23,24]. Under nutrient-limiting conditions (e.g., low nitrogen) and dehydration, cells of opposite mating types (*MAT***a** and *MAT*α) could be triggered to fuse and form a zygote. A germ tube originating from the *MAT***a** end of the zygote extends out and subsequently develops into dikaryotic hyphae with the two parental nuclei maintained as separate entities. During hyphal growth, a specialized hypha called a clamp connection forms across septa and fuses with the subapical neighboring cell. One of the two daughter nuclei in the apical cell is transferred to the subapical cell via the clamp connection to reform the dikaryon. Haploid blastospores can form along the hyphae: blastospores are vegetative, yeast-like cells that bud from the hyphae. Some hyphal cells can also enlarge and form chlamydospores, which are thick-walled vegetative cells with a condensed cytoplasm. Chlamydospores can facilitate the long-term survival of cells in harsh environments [25]. At the onset of meiosis, the tip of an aerial hypha enlarges to form a basidium within which the two parental nuclei fuse and meiosis occurs to produce four recombinant, haploid nuclei. The daughter nuclei undergo repeated mitotic divisions with individual nuclei packaged into individual basidiospores that bud off from the basidium, consequently forming four chains of basidiospores [26,27,28].

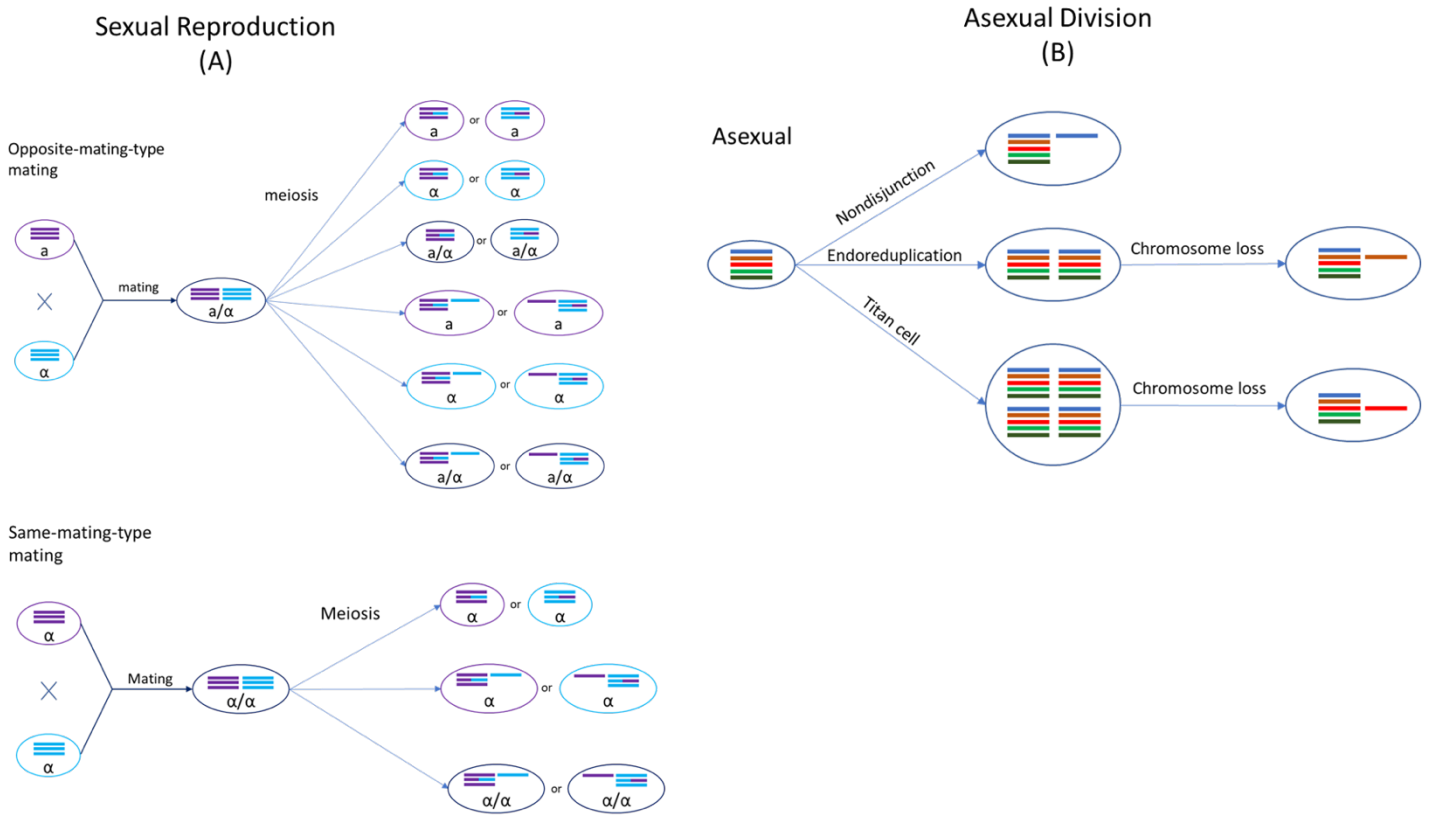

Figure 2.2. Genomic changes of *Cryptococcus* occur in sexual and asexual processes. (A) In sexual mating and subsequent meiosis, resulting in the formation of recombinant cells, both euploidy and aneuploidy can be observed; (B) Asexual replication can undergo nondisjunction, endoreduplication or the formation of titan cells to cause genomic changes.

Sexual mating in *Cryptococcus* is normally restricted to cells of opposite mating types. However, cryptococcal cells of the same mating type could be induced to mate with each other under nutrient-limiting conditions, referred to as same-mating-type reproduction [29,30,31]. Mating between genetically different strains of the same mating type can produce a high frequency of recombinants, similar to opposite-mating-type mating [27]. Even though both *MAT***a** and *MAT*α cells can undergo same-mating-type reproduction, the presence of cells with opposite mating types significantly enhances this process [32]. *MAT*α is the predominant mating type in natural populations, with >99% of *C. neoformans* strains and ~95% of other cryptococcal strains belonging to this mating type [14,33,34]. During same-mating-type mating, haploid *MAT*α cells become α/α diploids, either by endoduplication or by nuclear fusion following cell – cell fusion between two α cells [27,35]. The newly formed diploid nucleus then undergoes one round of meiosis to produce four, recombinant haploid nuclei, which are then packaged into basidiospores [36]. Evidence for same-mating-type mating in *Cryptococcus* has also been found in nature: particularly, same-mating-type reproduction could be beneficial due to natural populations in both clinical and environmental settings being predominantly of the same mating type, *MAT*α [37,38].

Both mating processes confer two major benefits to *Cryptococcus*: (i) they result in the production of basidiospores which act as the unit of long-distance dispersal, and (ii) they are known to be mutagenic, generating both genetic and phenotypic variation, as described in the sections below [39]. Strains of different cryptococcal species have been successfully mated with each other in the laboratory, albeit generally with low spore germination rates [40]. Unlike haploid parental strains, the resulting interspecific hybrids are often diploid or aneuploid, indicating that genomic divergence between parental lineages could hinder chromosomal disjunction and proper meiosis during gamete formation.

2.4.3 Hybrids in the *Cryptococcus* species complex

Cryptococcal hybrids, discussed below, are categorized according to the serotypes of the parental lineages.

AB and BD hybrids: To the best of our knowledge, hybrids arising from the mating of *C. neoformans* (serotype A) or *C. deneoformans* (serotype D) with one of *C. gattii*,

C. bacillisporus, *C. deuterogattii*, *C. tetragattii* or *C. decagattii* (serotypes B or C) have not been recovered from the environment. However, there have been several reports of infections caused by AB (serotype A × serotype B) and BD (serotype B × serotype D) hybrid strains. The first such hybrid was reported in 2006, when three strains isolated from the cerebrospinal fluid of two patients in the Netherlands were determined to be diploid strains of serotype BD [41]. Based on these findings, it was estimated that BD hybrids made up about 1% of the clinical isolates found in the Netherlands between 1977 and 2005. A cryptococcal hybrid of serotype A × serotype B was first reported in 2008, when a strain isolated from an AIDS patient in Canada was determined to be an AB hybrid [42]. In 2012, four AB hybrid strains were identified among clinical samples obtained from the cerebrospinal fluid of patients in Brazil (n = 2), Columbia (n = 1) and India (n = 1) [43]. AB and BD hybrids have since been reported in Germany [44], Denmark [45], and the United States [46], all from clinical sources. Even though mating between the parental lineages can be induced in the laboratory, the mating cells often fail to complete the sexual cycle, indicating a strong post-zygotic reproductive barrier [24]. These observations suggest that, while these species are still genetically and phenotypically compatible enough to initiate mating, they produce relatively few viable hybrid progenies, leading to their rare occurrence in environmental and clinical samples. Furthermore, to date, cryptococcal hybrids of serotypes AC and CD have never been reported in the literature.

AD hybrids: Hybridization between A and D serotypes is a significantly more common occurrence than the hybridization of A or D serotypes with B or C serotypes. Indeed, *C. neoformans* × *C. deneoformans* hybrids, commonly referred to as AD hybrids, are the most common of all cryptococcal hybrids. AD hybrids are assigned their own molecular type of VNIII. Since their initial discovery in 1977, their prevalence has been steadily increasing, with AD hybrids currently causing up to 40% of all cryptococcal infections in Europe [47,48,49,50]. They have been recovered from clinical and environmental sources in many countries, across most continents [51]. AD hybrids are typically diploid or aneuploid and experience frequent loss of heterozygosity during vegetative growth [52,53,54].

BC hybrids: Under mating-inducing conditions, strains of different VG molecular types (serotypes B and C) are capable of mating with each other in the laboratory

[40,55,56,57]. However, to the best of our knowledge, diploid/aneuploid VG hybrid strains (BC hybrids) have not been recovered from environmental or clinical sources. One likely explanation might be that VG lineages are still sufficiently compatible with each other to produce haploid, recombinant progeny: nucleotide divergence between VG lineages is less extensive in comparison to that between VNI and VNIV (see Section 2.4.1). In fact, when strains of serotypes B and C are mated with each other, they produced proper dikaryotic hyphae with clamp connections that were morphologically similar to those produced when VG strains of the same serotype are mated with each other [24,55]. However, spore viability was found to be very low (< 1%) in lab-derived reciprocal crosses of VGII (*MAT*α) × VGIII (*MAT***a**) and VGII (*MAT***a**) × VGIII (*MAT*α): among the spores that successfully germinated, 18/18 and 9/16 were diploid/aneuploid in the two crosses, respectively [58]. Furthermore, almost all collected F1 hybrid progeny were determined to be diploid/aneuploid when VG lineages were mated with each other, or VGIII was mated with VN lineages in the laboratory (You *et al*., unpublished data). Together, these observations suggest that VG hybrids can be produced, and the apparent absence of diploid/aneuploid VG hybrids in nature is likely due to these hybrids' failure to successfully compete with parental lineages in their natural habitats.

2.5 Outcomes of hybridization between cryptococcal lineages

2.5.1 Hybrid inviability

Spore germination rates in hybrid cryptococcal crosses are typically low, indicating significant post-zygotic reproductive isolation between these species. Studies have reported ~5 – 20% of hybrid spores to be viable in lab-derived hybrid crosses between *C. neoformans* and *C. deneoformans* [52,59,60]. However, the true germination rate might be slightly higher, since we have observed some AD hybrid spores to display an abortive phenotype where, following germination, growth is aborted after several mitotic divisions, indicating genetic incompatibilities within the nucleus [61]. Recent studies detected significant variability in spore germination rates in crosses between strains of *C. gattii*, *C. bacillisporus*, *C. deuterogattii*, *C. tetragattii* and *C. decagattii*, with a range of ~1 – 98% [29,40,60]: however, since the ploidy of germinated spores was not deter-

mined in the study by You *et al*., the proportion of viable progeny that were diploid/aneuploid is not known. You *et al*. also found spore viability to vary between ~1 – 43% in a series of crosses where a *C. bacillisporus* strain was crossed with different *C. neoformans* and *C. deneoformans* strains [29]. The significant variation in spore viability observed across multiple studies highlights the complex interplay of determinants, including parental genetic backgrounds as well as environmental and genotype-environment interaction effects, on the germination of hybrid cryptococcal spores [29,58,59].

2.5.2 Hybrid sterility

While most cryptococcal hybrids are heterozygous at multiple loci across the genome and contain alleles for both mating types (i.e., heterozygous at the *MAT* locus), few are self-fertile or can mate with other strains [52,61]. Basidiospores produced by three self-fertile AD hybrids containing both mating types germinated at a very low rate of ~5% in laboratory conditions: these three AD hybrids did not produce any sexual spores when co-incubated with haploid *MAT***a** and *MAT*α strains of *C. neoformans* and *C. deneoformans* [52]. However, sterility does not pose a barrier to cryptococcal hybrid success, as they can propagate asexually via mitosis.

2.5.3 Phenotypic diversity and Hybrid vigor

Studies investigating the phenotypes and virulence of cryptococcal hybrids have found variable results with some reporting hybrid vigor (heterosis) while others have found hybrids to be inferior to parental strains. In general, AD hybrids are less virulent than either *C. neoformans* or *C. deneoformans* haploid strains, though this result is not always observed [62]. However, increasing evidence of hybrid vigor in both natural and laboratory-constructed AD hybrids has been found. For example, AD hybrids might be better able to adapt to new environmental niches than *C. neoformans* and *C. deneoformans* isolates. Natural AD hybrid strains are more resistant to UV irradiation than native *C. neoformans* strains from Botswana [63]. Laboratory-constructed AD hybrids also showed hybrid vigor with higher resistance to both UV irradiation and high temperatures than *C. neoformans* and *C. deneoformans* parents [63,64]. Another study found the majority of 31 investigated global AD isolates to be resistant to the antifungal drug FK506 [54,65]. A small proportion of hybrid strains in an AD hybrid population derived

from a cross between CDC15 (*C. neoformans*, *MAT*α) and JEC20 (*C. deneoformans*, *MAT***a**) was found to surpass both parents in the expression of essential virulence factors, including melanin production, capsule production, growth at 37 °C, resistance to the antifungal fluconazole, and cell size [66]. The remaining hybrid offspring displayed intermediate phenotypes or inferior phenotypes to both parents. At present, similar phenotypic data on other cryptococcal hybrids are not available due to their rarity compared to AD hybrids. However, the presence of these hybrids in clinical settings suggests that at least some are capable of causing fatal infections in humans.

The phenotypic diversity found among cryptococcal hybrids indicates the presence of extensive genetic diversity in hybrid populations. Due to significant genomic differences between the parental species, frequent chromosome nondisjunction is observed during meiosis, with hybrids often inheriting novel and/or unique combinations of chromosomes. For example, evidence of homozygosity (or hemizygosity) interspersed with heterozygosity is observed across AD hybrid genomes [59,66,67]. Homozygosity could be derived through either chromosome loss or mitotic gene conversion, leading to loss of heterozygosity [54,65,68]. The generation of novel allelic and chromosomal combinations can offer cryptococcal hybrids a significant advantage in adapting to a diversity of environmental niches and competing with parental lineages for resources.

2.6 Genetics of cryptococcal hybrids

2.6.1 Aneuploidy in cryptococcal hybrids

AD hybrids are either diploid or aneuploid, as determined by fluorescence-activated cell sorting (FACS) analysis [49,52]. Previous studies revealed that aneuploidy in AD hybrids is most likely caused by the non-disjunction of homologous chromosomes during meiosis due to nucleotide sequence divergence (10 − 15%), as well as genetic incompatibilities, between *C. neoformans* and *C. deneoformans* genomes [52,69,70]. Sun and Xu found that at least one out of 114 screened co-dominant loci was heterozygous in the majority of lab-derived AD hybrid offspring strains, with an average heterozygosity of ~75% per strain [53]. Recombination between markers located on the same chromosome was observed, confirming the involvement of a meiotic process in the generation of these progeny, although the rate of crossovers was significantly lower

during hybridization than that observed in intraspecific crosses of *C. neoformans* and *C. deneoformans*. Another analysis of a hybrid cross between H99 (*C. neoformans*, *MAT*α) and JEC20 (*C. deneoformans*, *MAT***a**) suggested that the resulting hybrid progeny were likely generated via random nuclear fusion of two of the four recombinant nuclei generated from meiosis, which could result in heterozygous hybrids with doubled ploidy levels [71].

Clinical BD hybrid strains have also been found to be diploid or aneuploid by Bovers *et al*. [42]. These hybrids have a unique Amplified Fragment Length Polymorphism (AFLP) genotype (AFLP genotype group 8), revealing that they likely originated from hybridization between a *MAT*α, serotype B strain (AFLP genotype 4) and a *MAT***a**, serotype D strain (AFLP genotype 2). Interestingly, these hybrids were heterozygous at two of the genotyped loci, namely RNA polymerase II (RPB2) and laccase (LAC): however, they were homozygous for the serotype B parent's genotype at the Internal Transcribed Spacer (ITS) regions of the nuclear ribosomal RNA gene cluster. In addition, most BD hybrids were homozygous for the serotype B allele at the Intergenic Spacer (IGS) sequence of the nuclear ribosomal RNA gene cluster, while the remaining hybrids were homozygous for the serotype D allele.

While diploid/aneuploid hybrid strains of *C. gattii*, *C. bacillisporus*, *C. deuterogattii*, *C. tetragattii* and *C. decagattii* have not been recovered from nature, lab-derived hybrids of such crosses often display diploidy or aneuploidy. In two laboratory crosses between *C. bacillisporus* and *C. deuterogattii*, 18/18 and 9/16 of the spores that successfully germinated were determined to be diploid/aneuploid, respectively [58]. Furthermore, almost all collected F1 hybrid progeny were determined to be diploid/aneuploid when these five species were mated with each other, or when *C. bacillisporus* was mated with *C. neoformans* and *C. deneoformans* in the laboratory (You *et al*., unpublished data).

2.6.2 Loss of heterozygosity

The definition of loss of heterozygosity (LOH) is the loss of one parental allele in a certain genomic region in a heterozygous individual. LOH can be caused by multiple mechanisms, such as unbalanced chromosome rearrangements, gene conversion, mitotic recombination, and loss of a chromosome or a chromosomal segment. Double-strand

break repair can give rise to short-range LOH events by gene conversion without crossover. In contrast, long-range LOH events are mostly caused by single crossovers or break-induced replication [72]. In addition, whole-chromosome LOH can arise from chromosome loss through nondisjunction, followed by duplication of the remaining homolog [73]. The duplication of a chromosome is a common occurrence in whole-chromosome LOH. With complete duplication of the remaining genetic material, the appearance of a normal karyotype is maintained, even though there may have been a wholesale loss of genetic diversity. Generally, LOH is not reversible, however, cells can regain the lost heterozygous alleles via outcrossing or mutation.

The emergence of LOH is considered a major mechanism of generating genetic diversity in populations of diploid heterozygous organisms. Unlike the parental haploid lineages, cryptococcal AD hybrids are often highly heterozygous, and may be prone to LOH, both during hybridization events and during asexual growth following germination [39,49,52,54,64]. During sexual mating, the two parental nuclei have been observed to fuse at earlier stages of sexual development (e.g., in the zygote or hyphae), providing opportunities for mitotic recombination to facilitate LOH at certain chromosomal regions before meiosis. A recent analysis of 297 lab-derived AD hybrid progeny strains generated from a single cross revealed the hybrids to experience extensive loss of chromosomes [74]. Both partial and complete chromosome loss and duplication have been observed in some AD hybrids. Partial chromosome loss may result in genome rearrangement or the formation of novel chromosomes through truncation or translocation [54]. Li *et al*. found that the progeny strain P5 (progeny of a self-fertile AD strain CDC228) partially lost some chromosomes (Chromosomes 8 and 10 from the *C. neoformans* parent) and completely lost some others (Chromosomes 5 and 13 from *C. neoformans*, and Chromosomes 3 and 12 from *C. deneoformans*), giving rise to a highly unique genome organization [54].

Interestingly, natural AD hybrids show a preferential retention of specific alleles and chromosomes from one of the two parents, suggesting that those alleles may offer survival and growth benefits under specific conditions [68]. Allele distributions in the genomes of AD hybrids often show significant departures from Mendelian ratios with alleles of one parent preferred over that of the other at certain loci [74]. In fact, Sama-

rasinghe *et al*. found genome-wide allele distribution in 297 AD hybrids to be significantly skewed in favor of the *C. deneoformans* parent from which the hybrids inherited mitochondria [75]. It is hypothesized that given the uniparental mitochondrial inheritance seen in cryptococcal species, hybrids prefer to retain chromosomes of the mitochondria-donor parent to minimize incongruence between their mitochondrial and nuclear genomes.

A very recent study conducted by Dong *et al*. estimated the rate of LOH during mutation accumulation in a laboratory-constructed diploid AD hybrid (CDC15 × JEC20) during mitotic divisions. They used 33 genetic markers located on 14 chromosomes to determine genome-wide allele distributions in the AD hybrid [76]. The parental haploid strain CDC15 (serotype A, *MAT*α) is more resistant to fluconazole (minimum inhibitory concentration [MIC] = 64 μg/mL) than the other parent JEC20 (serotype D, *MAT***a**, MIC = 4 μg/mL). Their findings showed that only a few LOH events occurred over 800 generations of propagation on nutrient-rich medium, with an estimated rate of 6.44×10^{-5} LOH events per mitotic division. However, fluconazole exposure resulted in a dramatic 50-fold increase in LOH rate at two markers on Chromosome 1. Interestingly, Chromosome 1 contains two genes, *ERG11* (the fluconazole target gene) and *AFR1* (a major transporter for triazoles), both of which play major roles in the development of antifungal resistance in *C. neoformans* [66,75]. Here, the AD hybrid lost the fluconazole-susceptible allele of both genes inherited from JEC20 while maintaining the alleles from CDC15. In these evolved strains, the copy number of Chromosome 1 inherited from CDC15 also increased. Results from this study suggested that hybridization can facilitate the rapid adaptation of *Cryptococcus* to stressful environmental conditions.

2.6.3 Dynamic ploidy changes in *Cryptococcus*

Ploidy change is often associated with sexual reproduction. Fungal cells generally mate with cells of identical ploidy levels, resulting in intermediate sexual structures with double the genomic content. Subsequent meiosis reduces the DNA content by half, reinstating the original ploidy of the parental strains. Some fungi, like *Saccharomyces*

cerevisiae, favor propagation in the diploid state while other fungi, like *Schizosaccharomyces pombe*, prefer to propagate in the haploid state with a transient diploid state, as is the case observed in *Cryptococcus* [77,78,79].

Cryptococcal cells isolated from clinical and environmental settings are normally haploid with 14 chromosomes. FACS analyses have revealed an appreciable proportion of AD hybrids to be diploid [46,52,80]. However, it is possible that the diploid AD hybrids are not heterozygous at all loci across the genome: the remaining copy of a chromosome is often duplicated following LOH events, maintaining diploidy. Environmental stress has been observed to induce chromosome mis-segregation causing chromosomal instability. For example, exposure to a high-dose fluconazole treatment can result in the amplification of Chromosome 1 in both haploid *C. neoformans* and AD hybrids [77,78]. A comparison of haploid and diploid *C. neoformans* cells found that haploid cells were generally more virulent than diploid cells in a murine inhalation model of cryptococcosis [64]. However, in a rabbit infection model, diploids displayed similar virulence levels to haploid forms [79]. Higher ploidy was found to be associated with larger cell size in *C. neoformans*. For example, titan cells that can grow up to an impressive 100 μm in diameter contain 16, 32, 64 or more copies of the genome [81]. The large size facilitates the survival of titan cells during infection by hindering ingestion by host macrophages and by imparting resistance to oxidative and nitrosative stresses [73]. However, in certain cases, increased ploidy has been shown to have modest detrimental effects on virulence in a murine inhalation model, growth at high temperature, and melanization [64]. In addition, melanin production was found to be correlated with monosomy at Chromosome 13, while disomic variants produced less melanin and were less virulent in mice in *C. neoformans* cells isolated from AIDS patients [82]. The plasticity of their genomes provides cryptococcal hybrids with the flexibility to alter their ploidy, via chromosome loss/gain or duplication, which in turn promotes adaptation to a wide range of environmental conditions.

2.6.4 *Cryptococcus* as a model system for fungal hybridization

Hybrids face significant challenges to survival and functionality due to two divergent genomes residing in the same cell. In a process referred to as genome stabilization, hybrids eliminate unfavorable combinations of the two parental genomes via a variety

of mechanisms including recombination, gene conversion and chromosome loss [76]. The rate at which genome stabilization is achieved in a hybrid may be related to the extent of divergence between the two parental genomes, since incompatibilities between more differentiated genomes will be resolved faster within the hybrids. For example, aneuploidy is commonly found in hybrids derived from two divergent parents, while frequent LOH events can be viewed as a mechanism of achieving genome stabilization.

Chromosomal nondisjunction during meiosis coupled with LOH during vegetative growth leads to the creation of cryptococcal hybrids with novel and unique allelic combinations not found in parental species. The novelty and plasticity of their genomes have put cryptococcal hybrids at a unique position to dynamically adapt to novel environmental niches and compete with parental lineages in current habitats. In fact, hybrid vigor, displayed by some hybrids in laboratory settings, and the increasing presence of AD hybrids in clinical samples suggest an advantage of cryptococcal hybrids to successfully adapt to the changing environment. In summary, genomic plasticity likely facilitates the rapid adaptation of hybrids to new environmental niches (e.g., harsh environments) or genetic perturbations.

In a world where frequent international commerce and human travel is blurring geographical and spatial boundaries, hybridization between closely related taxa is an increasingly likely outcome across all kingdoms of life. The seven species of the *Cryptococcus* species complex provide an excellent model system for studying hybridization in fungi. Many tools have been developed and optimized for the study of these yeasts, including transformation [83], ploidy estimation by flow cytometry [84], and a strain-typing system integrating numerous well-characterized strains [85]. Importantly, there are multiple host models of cryptococcal infections that make in vivo experiments feasible [86]. Furthermore, whole genome sequences of hundreds of isolates from various geographical origins are available on online databases (e.g., NCBI, FungiDB) while gene editing in these species can now be carried out with high efficiency using specially adapted CRISPR-Cas9 [87]. Finally, experimenting on haploid yeasts such as *Cryptococcus* is more convenient, and the findings can be more generalizable to understanding pathogenicity as compared to the well-established model *Saccharomyces cerevisiae*, which is primarily diploid in nature and the lab. Insights gained from

cryptococcal hybrid research can be used to guide research strategies on hybridization in lesser known pathogenic fungi such as *B. dendrobatidis*, discussed in the remaining sections of this review. The major obstacles in understanding the process of hybridization in non-model species are typically the lack of genetic tools, such as ability to conduct gene disruption, the inability to perform genetic crosses, or both. Fortunately, much can be understood about the process of hybridization using genomic characterization of wild collected strains. The genomic tools developed in model systems can be adapted to study the non-model fungal hybrids.

2.7 Hybridization in an aquatic chytrid fungus associated with amphibian declines

2.7.1 The amphibian chytrid *Batrachochytrium Dendrobatidis*

The chytrid fungus *Batrachochytrium dendrobatidis* (*Bd*) is a broad host-range pathogen that is known to infect close to 700 species of frogs, salamanders, and caecilians worldwide [88]. *Bd* is now recognized as the major contributor to near-simultaneous amphibian population declines in the 1980s and 1990s that are correlated with arrival of the pathogen [89,90]. To date, Bd has been detected on every continent except Antarctica [91] and is most likely introduced from source populations in east Asia [92].

Bd is composed of at least four deeply divergent evolutionary lineages with varying geographical histories and virulence against hosts. The most widespread and well documented of these lineages is a globally-distributed, hypervirulent diploid genotype, BdGPL (Global Panzootic Lineage) [93]. The other, putatively less virulent lineages of Bd include: a Brazilian lineage endemic to the Atlantic Forest region of southern Brazil, BdBrazil (also known as BdBrazil/Asia2) [92,94]; an African lineage endemic to the Cape region of South Africa, BdCape [93]; and an endemic Asian lineage BdAsia1, believed to be closest to the source of origin for *Bd* diversity [92]. Recently, the existence of an additional endemic lineage, BdAsia3, widespread throughout southeast Asia was reported from amphibian swabs [95].

2.7.2 Hybrids in *Batrachochytrium Dendrobatidis*

Intraspecific hybrid strains resulting from outcrossing between parental genotypes of divergent lineages are rare, but known to occur. Within the divergent lineages of *Bd*,

reproduction appears to be strictly asexual [96], with the exception of BdAsia1, which has a population signature of a highly recombining population [93]. Both the paucity of outcrossing in natural *Bd* populations and the inability to cross isolates is a major point of contrast between *Bd* (and other non-model species) and the model fungal species with hybrids, such as *Cryptococcus*. Outcrossing among the divergent *Bd* lineages (referred to here as hybridization) is only known to occur in secondary contact zones where divergent lineages have been brought into proximity by human activity. There are currently five hybrid *Bd* isolates reported in the literature from two hybrid zones. Three of these hybrid isolates were documented from the Atlantic Forest of Brazil within a narrowly restricted zone in the southern Brazilian state of Paraná [94,97,98]. This locality is one of the areas where the BdGPL and BdBrazil lineages overlap. The other two known *Bd* hybrids are described from the Eastern Cape Province of South Africa where BdGPL and BdCape overlap. Putative hybrid isolates were also identified from genotyping DNA from amphibian skin swabs, but these could also be explained by co-infection [95]. Unlike the narrow geographic range of the Brazilian hybrid zone, the two South African hybrid isolates were collected approximately 200 km apart from one another [92]. Additional regions where secondary contact could occur along with hybridization are Europe, western Africa, and Central America [92,95,98]. These regions are of interest with respect to hybridization because they harbor BdGPL and BdCape lineages which are already known to hybridize. Evidence of hybridization derives from combination of otherwise lineage-specific alleles into the same genome, increased heterozygosity, and Bayesian admixture analyses [92,97,98]. Most of the hybrids appear to be F1, and an earlier F2 reported [94] was later determined to be an F1 which had undergone some LOH [97]. In most *Cryptococcus* hybrids, divergence in the chromosomal structure greatly hinders the ability to undergo meiosis. As a result, in *Cryptococcus*, most natural hybrids appear to be close to F1, and these data also agree with expectations of chromosomal pairing problems reflected in the 100 million year divergence between *C. neoformans* and *C. deneoformans* [19,20,21,22] and the studies which show meiotic segregation in F1 hybrids to be highly abnormal [53]. On the other hand, for *Bd*, there is no evidence that F1 hybrids have higher ploidy than the parental genotypes and, though the timeframe of divergence between the lineages of *Bd* is deba-

ted [92,97], the extreme end of an estimate of 100,000 years of divergence before hybridization is three orders of magnitude younger than cryptococcal hybrids. These data would predict that hybrids should be fertile.

While clear genetic evidence of hybridization in *Bd* exists, mating and hybridization have not yet been observed in situ or in the laboratory. Likewise, specialized meiotic structures have never been reported for this species. The cellular process of hybridization in *Bd* is of special interest to understanding the dispersal ecology of this pathogen, because sexual reproduction in related members of the Chytridiomycota results in the production of harsh environment-resistant resting spores which may facilitate environmental or long-range transmission. Alternative cellular mechanisms of outcrossing that do not involve meiosis have also been proposed. One alternative mechanism by which *Bd* may be outcrossing is through a parasexual cycle [98]. Parasexual reproduction is well documented in other groups of pathogenic fungi, such as *Candida albicans* [99,100]. This mode of reproduction involves the fusion of diploid cells without meiosis. The resulting cell is a tetraploid intermediate which, in most cases, loses chromosomal copies back to a diploid state (Figure 2.3). Such a reproductive mechanism may explain the varying levels of aneuploidy prevalent throughout individual *Bd* isolates, as well as the lack of obvious meiotic structures or resting spores in this species. On the other hand, given the diversity of mechanisms possible to create aneuploidy, as discussed above for *Cryptococcus*, it is plausible that the sexual cycle of *Bd* is typical for other fungi, cryptic as it may be.

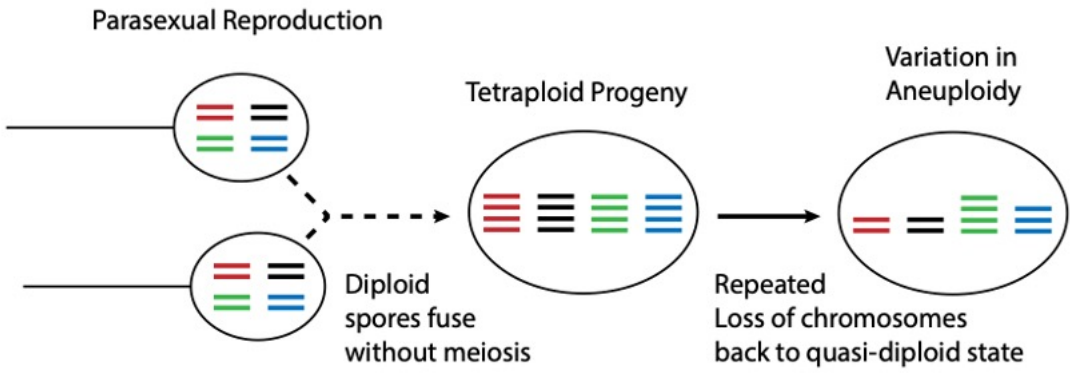

Figure 2.3. Parasexuality is a process of reproducing without a reductive cell division (meiosis). With parasexuality, a tetraploid offspring is produced which is a transient stage followed by random loss of chromosomes during vegetative growth.

2.7.3 Outcomes of hybridization in *Batrachochytrium Dendrobatidis*

The phenotypic outcomes of hybridization in *Bd* remain largely unknown. It is unclear whether hybrids are favored by natural selection in the habitats in which they were created. In order to test this, it would be useful to return to regions where hybridization has occurred in order to attempt reisolation of the same hybrid genotypes and to estimate the frequencies of hybrids related to parental species. Both measures can test whether hybrid genotypes are on the increase, which is predicted if they are favored by selection. In the only currently available study on hybrid phenotypes, Greenspan *et al*. [101] showed that hybrid virulence and pathogenicity was highly dependent on the infected host species. In a virulence challenge assay, the authors infected two endemic Brazilian, direct-developing frog species with BdGPL, BdBrazil, or hybrid isolates produced by the two lineages. In one host species, the high-altitude endemic pumpkin toadlet (*Brachycephalus ephippium*), hybrid isolates were more virulent (causing greater mortality in host animals) than either BdGPL or BdBrazil isolates. The endemic BdBrazil was the least virulent in this host species. In the other host species tested, the robber frog (*Ischnocnema parva*), hybrid isolates displayed an intermediate degree of virulence, with BdGPL being the most and BdBrazil being the least virulent.

Hybrid pathogenicity also varied according to host context. In the Greenspan *et al*. study, the authors examined pathogenicity among isolates in three host species by assessing pathogen load upon host mortality [101]. Again, the pathogenicity phenotypes of hybrids depended on the host species. In the host species, *B. ephippium*, where hybrid isolates were most virulent, the hybrids were also more pathogenic, with hybrid strains producing the highest spore loads on hosts at the time of mortality. In *I. parva*, the host species in which hybrid virulence was intermediate between BdGPL and BdBrazil, spore loads produced by hybrid isolates were comparable to those of BdGPL. The third species examined in the Greenspan *et al*. [101] study, the habitat-generalist, swamp treefrog (*Dendropsophus minutus*), is known to be more tolerant to *Bd* infection in laboratory challenge assays [102]. Because of this, infection experiments did not produce sufficient mortality in this species to analyze differences in virulence. However, the authors showed that *Bd* pathogenicity varied by genotype in this host species. Hybrid isolates produced spore loads intermediate between BdGPL (highest loads) and BdBrazil (lowest) when the host animals were assessed 60 days post-inoculation.

In summary, much work remains to be completed in understanding the cellular processes and phenotypic outcomes of hybridization in *Bd*. However, the Greenspan *et al*. study documents two interesting results. First, hybrid genotypes do show some degree of heterosis (hybrid vigor) in both virulence and pathogenicity characteristics. Second, and very importantly, this increase in the virulence and pathogenicity of the hybrid strains are context-dependent on the host species being infected. These results highlight that predicting the phenotypic characteristics of hybrid *Bd* genotypes is very complex, and further experimental work should focus on assessing hybrid characteristics in a broad range of host species.

2.7.4 Aneuploidy in *Batrachochytrium Dendrobatidis*

Although most fungi are considered to have zygotic meiosis where the diploid stage is highly limited, this is a gross generalization. In fact, there are no extensive studies of the genetics of Chytridiomycota that would allow ploidy changes during the life cycle to be fully elucidated. In *Bd*, an outcome of hybridization is the creation of genomes that are approximately 0.233% heterozygous [97]. This level of divergence is considerably lower than other hybrids, like the cryptococcal hybrids. and presumably

should not provoke chromosome incompatibilities. Nonetheless, the presence of chromosomal rearrangements across *Bd* lineages has not been explored. Like *Cryptococcus*, *Bd* is also capable of generating genetic diversity via dynamic genome mutations including aneuploidy and LOH. While the *Bd* genome is generally considered to be diploid, chromosomal copy number can vary greatly. Whole genome sequencing studies of *Bd* finds a high variation in aneuploidy within individuals and among closely related isolates. Chromosomal copy number in *Bd* can vary between 1 (monosomic) to 5 (pentasomic). In 51 *Bd* genomes that have been sequenced and analyzed for copy number variation, two studies together show that approximately 58.7% of Bd chromosomes are disomic, 29.0% are trisomic, 11.3% are tetrasomic, and less than 1% monosomic or pentasomic [97,103].

The widespread nature of aneuploidy across major lineages of *Bd* suggests that it may be an important mechanism in the generation of genetic variation, especially given the rarity of sexual reproduction observed in this species. Links between variation in chromosomal copy number and phenotypic effect, however, have been difficult to establish in this species. This is largely due to the paucity of phenotyped Bd isolates with accompanying whole genome sequences. Comparatively, no obvious patterns have emerged to link highly aneuploid genomes to the hypervirulent BdGPL clade. The BdGPL lineage contains representative isolates displaying disomic, trisomic, and tetrasomic genomes throughout its phylogeny [97,103]. While the sample sizes of analyzed genomes outside the better-studied BdGPL clade are very small, some phylogenetic trends are beginning to emerge around *Bd* aneuploidy with respect to lineage. In the novel, enzootic *Bd* lineages, the BdCape isolates analyzed so far (n = 5) show a mix of trisomic (60%) and tetrasomic (40%) genomes [103]. Three representative isolates assigned to BdCH were mostly trisomic. BdBrazil isolates (n = 2) were mostly disomic [97]. Finally, the single BdGPL/BdBrazil hybrid analyzed is also mostly disomic, with 13/17 of its major chromosomes disomic and 4/17 trisomic [97].

In addition to observations of widespread aneuploidy in *Bd*, chromosomal copy number has also been shown to be mutable over short timescales. Farrer *et al*. [103] examined replicate laboratory lines of an ancestrally trisomic *Bd* isolate serially passaged over 40 passages under differing growth conditions. One line was passaged in a standard media while the other was passaged in a selective media containing defensive

antimicrobial peptides collected from the European water frog (*Pelophylax esculentus*) [104]. After approximately 40 weekly passages, the culture sequenced from standard media lost a copy of one chromosome (supercontig IV) and gained a copy of another (supercontig V), while the culture passaged in antimicrobial peptide media gained a chromosomal copy at supercontig V. Another study investigated the genomic changes in an isolate, JEL427, before and after 30 transfers in the lab [105]. The isolate showed lower virulence and spore production after the passages [106]. The major change in the isolate over the 30 passages was a reduction in ploidy, going from an average of 3.6 copies per chromosome (in practice genomic scaffold as the genomic map is not available) to 3.1. The difference between the two laboratory evolution studies may relate to their divergent starting points, but both results show that aneuploidy changes can occur rapidly in *Bd*, perhaps serving as a mechanism for rapid genomic adaptation to changing selective pressures. While the functional underpinnings of these pattern are difficult to tease out, they may suggest that specific *Bd* chromosomes more readily gain or lose copies. This pattern is also reported in another major study investigating aneuploidy in *Bd*, where the authors find that supercontig V is one of the *Bd* chromosomes more likely to present higher than average copy numbers [97].

Characterization of the ploidy of additional hybrid isolates will be essential for understanding whether meiosis and sex result from the fusion of haploid gametes or through a parasexual cycle. The general reduction in chromosome number over time from an ancestor of higher than disomic average chromosome numbers would tend to support parasexuality, however, the absence of more than two alleles per locus suggests that it is more likely that an endoduplication of all or part of the genome occurs sometime after hybridization via a heretofore undetected standard sexual cycle. Either way, hybrid genotypes present a greater deal of allelic diversity, which could facilitate adaptation by LOH. Understanding whether LOH occurs primarily at the chromosome level, i.e., aneuploidy, or at the gene level, e.g., gene conversion, in hybrid isolates is critical for understanding the nature and magnitude of the selective forces they experience.

2.7.5 LOH in *Batrachochytrium Dendrobatidis*

Loss of heterozygosity is a well-known feature contributing to genome diversity in *Bd*. LOH is hypothesized to occur during asexual reproduction of Bd through mitotic

recombination, chromosome loss, or gene conversion [96]. In addition to changes in chromosome copy number, LOH has a great capacity to generate genotypic diversity without the input of new alleles [107]. This may be particularly important in clonally dominant pathogen lineages such as in *Bd*, such as the BdGPL lineage which typically shows a maximum of two alleles per locus, despite being frequently trisomic. The genotypic diversity generated by LOH should alter combinations of alleles within and across loci, displaying overdominance, underdominance, or epistasis, which can then be subject to selection pressure with presumably advantageous tracts of LOH sweeping to fixation in a population.

The most prominent example of this in *Bd* may be a large, shared LOH region on supercontig II that is present in all members of BdGPL [92,97,103]. The conserved nature of this LOH feature throughout the globally invasive clade may reveal clues to the successful proliferation of this lineage. Gene functions, enriched in shared LOH regions of BdGPL, included processes related to reactive oxygen metabolism, L-serine metabolism, and superoxide dismutase/oxidoreductase [97]. These gene classes, in addition to various peptidases identified through comparative genomics with the closely related non-pathogenic chytrid *Homolaphlyctis polyrhiza* [108], and transcriptomic studies of *Bd* infections [109,110], are possibly involved in the genomic evolution underpinning the adaptive success of BdGPL in varied habitats worldwide.

In clonally reproducing diploid organisms such as *Bd*, the lack of outcrossing results in regions of LOH in the genome persisting in lineages through time. Because of this, shared homologous regions of LOH can be a powerful tool to inform populations of closely related clonal strains. For example, homologies in patterns of LOH have been used to distinguish evolutionary subclades within the global BdGPL [96,107]. Further geographic sampling and improved computational methods to detect homologies in LOH patterns hold the promise of resolving their finer-scale, intra-lineage population structure, and providing a more refined picture of the geographic history of this ecologically important pathogen.

2.8 Conclusions and Perspectives

Hybridization and genomic plasticity appear to be shared hallmarks contributing to rapid adaptation in fungal pathogens. The shared mechanisms of hybridization, aneuploidy, and LOH between the two major fungal pathogens *Cryptococcus* and *B. dendrobatidis* span the fungal tree of life (phylum Basidiomycota to Chytridiomycota) and appear to reflect a global pathway for rapid adaptation in pathogens across the fungal kingdom. Themes emerging from multiple studies of fungal hybrids are that they demonstrate increased ploidy, heterosis, and novel ecological niches. Prime examples of successful hybrids with these traits across the fungal tree of life are readily found. For example, hybridization in the plant endophytic species Epichlöe leads to asexual diploids/polyploids with major benefits to the host, and hence the fungus [111]. Likewise for the pathogen, *Verticillium longisporum*, hybridization is associated with an expanded host range and diploidization [112,113]. Ancient hybridization is involved in the diversification of *Saccharomycete* yeasts [114], while more recent hybridization and polyploidization is involved in the formation of yeasts (*Saccharomyces* spp.) involved in beer brewing [115,116]. Finally, two examples of human pathogenic species appear to be largely of hybrid origin: the halophilic black yeast *Hortaea warnecki* is the cause of superficial skin infection, tinea nigra [117] and the recently described, but rare, *Candida metapsilosis* [118].

The above-mentioned fungal hybrids generally are discovered as F1 and have higher ploidy than their parental species or lineages. This appears to be the case for *Cryptococcus* hybrids but not for Bd, for which hybrids are the same ploidy as the parental genotypes. *Bd* hybrids are therefore similar to homoploid hybrids, good examples of which, in fungi, are *Zymoseptoria pseudotritici* and *Microbotryum* spp. [119,120]. Following the formation of F1 hybrids, persistence and adaptation is facilitated by the mechanisms of genomic plasticity during asexual growth, such as ploidy cycling and LOH. The high number of successful asexual F1 hybrids with heterosis across species suggests that any reproductive isolation caused by genetic incompatibilities are likely to be recessive as predicted by theory [1]. Overall, however, it is plausible that the importance of hybridization in fungal adaptation may be overinterpreted, as the likelihood of identifying or observing failed hybrids is low. The community would benefit from additional work synthesizing hybrids in the lab to understand and predict the outcome

of hybridization on evolution, such as has been conducted for investigating reproductive isolation in *Neurospora* and *Microbotryum* [121,122]. More needs to be known about fungal adaptation to ecological gradients in order to understand whether hybrid zones are likely to exist at the boundaries in which allopatric species meet.

Understanding the evolutionary dynamics of better studied pathogens such as *Cryptococcus* can inform the biology of less characterized, or newly discovered, fungal pathogens such as *Bd*. As we have discussed, the *Cryptococcus* system has served as a model for establishing the relationship between divergence, chromosomal pairing, and sterility. As *Bd* hybrids are not as diverged as *Cryptococcus*, and may not even represent the fusion of distinct species, we predict that F2 and further generation of hybrids of *Bd* are likely to exist, and it would be appropriate to account for this possibility when conducting additional sampling in regions of admixture, perhaps even as more subtle forms of introgression. Model species, like *Cryptococcus*, not only allow specific gene hypotheses to be tested through gene manipulation [123], they also generally have easy to trigger sexual cycles and selectable markers that allow for crossing designs to understand the genetics of complex traits [66]. As another example, crosses have established that the mitochondrial genotype in *Cryptococcus* is not known to have an impact on hybrid fitness, yet this has been demonstrated in other species of fungal hybrids, using crossing designs that create identical nuclear genomes in alternative mitochondrial association [79,124]. More work should be done to develop a crossing system in *Bd* that could allow for mitochondrial-nuclear genetic interactions to be tested. Finally, in *Cryptococcus*, same-mating-type mating was first demonstrated to occur in nature, because the mating type locus had been well described and easily genotyped [37]. This is a large hurdle for a species like *Bd*, but the fact that *Bd* hybrids exist should provide impetus to determine the genetic basis of mating types which may reveal similar same-mating-type mating dynamics.

Regardless of the underlying genetic differences between *Cryptococcus* and *Bd*, this review has highlighted several commonalities regarding their hybridization. Hybrids in both genera show increased genomic plasticity, with the potential to generate transgressive phenotypes, unleashed following both meiotic and mitotic recombination. Hybrids in both genera reveal that it is a subset of environments, rather than all, in which they have higher fitness. Finally, the spread of both pathogen genera likely involves

human-assisted migration that led to subsequent admixture. Given the potential adaptive benefits of hybridization in both *Cryptococcus* and *Bd*, improved measures for pathogen containment to prevent increased opportunities for hybridization should be put in place, both in clinical and environmental settings.

2.9 References

1. Barton, N.H. The role of hybridization in evolution. Mol. Ecol. 2001, 10, 551–568.
2. Barton, N.H.; Hewitt, G.M. Analysis of hybrid zones. Annu. Rev. Ecol. Syst. 1985, 16, 113–148.
3. Rieseberg, L.H. Hybrid origins of plant species. Annu. Rev. Ecol. Syst. 1997, 28, 359–389.
4. Arnold, M.L.; Hodges, S.A. Are natural hybrids fit or unfit relative to their parents? Trends Ecol. Evol. (Amsterdam) 1995, 10, 67–71.
5. Mallet, J. Hybrid speciation. Nature 2007, 446, 279–283.
6. Ramsey, J.; Schemske, D.W. Neopolyploidy in Flowering Plants. Annu. Rev. Ecol. Syst. 2002, 33, 589–639.
7. Harrison, R.G.; Larson, E.L. Hybridization, introgression, and the nature of species boundaries. J. Hered. 2014, 105 (Suppl. 1), 795–809.
8. Dunn, B.; Richter, C.; Kvitek, D.J.; Pugh, T.; Sherlock, G. Analysis of the *Saccharomyces cerevisiae* pan-genome reveals a pool of copy number variants distributed in diverse yeast strains from differing industrial environments. Genome Res. 2012, 22, 908–924.
9. Schardl, C.L.; Craven, K.D. Interspecific hybridization in plant-associated fungi and oomycetes: A review. Mol. Ecol. 2003, 12, 2861–2873.
10. Stukenbrock, E.H. The role of hybridization in the evolution and emergence of new fungal plant pathogens. Phytopathology 2016, 106, 104–112.
11. Nieuwenhuis, B.P.S.; James, T.Y. The frequency of sex in fungi. Philos. Trans. R. Soc. Lond. B Biol. Sci. 2016, 371, 20150540.
12. Haag, C.R.; Roze, D. Genetic load in sexual and asexual diploids: Segregation, dominance and genetic drift. Genetics 2007, 176, 1663–1678.
13. Rajasingham, R.; Smith, R.M.; Park, B.J.; Jarvis, J.N.; Govender, N.P.; Chiller, T.M.; Denning, D.W.; Loyse, A.; Boulware, D.R. Global burden of disease of HIV-

associated cryptococcal meningitis: An updated analysis. Lancet Infect. Dis. 2017, 17, 873–881.

14. Cogliati, M. Global Molecular Epidemiology of *Cryptococcus neoformans* and *Cryptococcus gattii*: An Atlas of the Molecular Types. Scientifica 2013, 2013, 1–23.

15. Hagen, F.; Khayhan, K.; Theelen, B.; Kolecka, A.; Polacheck, I.; Sionov, E.; Falk, R.; Parnmen, S.; Lumbsch, H.T.; Boekhout, T. Recognition of seven species in the *Cryptococcus gattii*/*Cryptococcus neoformans* species complex. Fungal Genet. Biol. 2015, 78, 16–48.

16. Hagen, F.; Lumbsch, H.T.; Arsic Arsenijevic, V.; Badali, H.; Bertout, S.; Billmyre, R.B.; Bragulat, M.R.; Cabañes, F.J.; Carbia, M.; Chakrabarti, A.; *et al*. Importance of resolving fungal nomenclature: The case of multiple pathogenic species in the *Cryptococcus* genus. mSphere 2017, 2, e00238-17.

17. Kwon-Chung, K.J.; Bennett, J.E.; Wickes, B.L.; Meyer, W.; Cuomo, C.A.; Wollenburg, K.R.; Bicanic, T.A.; Castañeda, E.; Chang, Y.C.; Chen, J.; *et al*. The case for adopting the "species complex" nomenclature for the etiologic agents of cryptococcosis. mSphere 2017, 2, e00357-16.

18. Dromer, F.; Gueho, E.; Ronin, O.; Dupont, B. Serotyping of *Cryptococcus neoformans* by using a monoclonal antibody specific for capsular polysaccharide. J. Clin. Microbiol. 1993, 31, 359–363.

19. Casadevall, A.; Freij, J.B.; Hann-Soden, C.; Taylor, J. Continental drift and speciation of the *Cryptococcus neoformans* and *Cryptococcus gattii* species complexes. mSphere 2017, 2, e00103-17.

20. Xu, J.; Vilgalys, R.; Mitchell, T.G. Multiple gene genealogies reveal recent dispersion and hybridization in the human pathogenic fungus *Cryptococcus neoformans*. Mol. Ecol. 2000, 9, 1471–1481.

21. Ngamskulrungroj, P.; Gilgado, F.; Faganello, J.; Litvintseva, A.P.; Leal, A.L.; Tsui, K.M.; Mitchell, T.G.; Vainstein, M.H.; Meyer, W. Genetic diversity of the *Cryptococcus* species complex suggests that *Cryptococcus gattii* deserves to have varieties. PLoS ONE 2009, 4, e5862.

22. Sharpton, T.J.; Neafsey, D.E.; Galagan, J.E.; Taylor, J.W. Mechanisms of intron gain and loss in *Cryptococcus*. Genome Biol. 2008, 9, R24.

23. Kwon-Chung, K.J. A New Genus, Filobasidiella, the Perfect State of *Cryptococcus neoformans*. Mycologia 1975, 67, 1197–1200.
24. Kwon-Chung, K.J. A new species of Filobasidiella, the sexual state of *Cryptococcus neoformans* B and C serotypes. Mycologia 1976, 68, 943–946.
25. Lin, X.; Heitman, J. Chlamydospore formation during hyphal growth in *Cryptococcus neoformans*. Eukaryot. Cell 2005, 4, 1746–1754.
26. Lin, X. *Cryptococcus neoformans*: Morphogenesis, infection, and evolution. Infect. Genet. Evol. 2009, 9, 401–416.
27. Lin, X.; Hull, C.M.; Heitman, J. Sexual reproduction between partners of the same mating type in *Cryptococcus neoformans*. Nature 2005, 434, 1017–1021.
28. Zhao, Y.; Lin, J.; Fan, Y.; Lin, X. Life Cycle of *Cryptococcus neoformans*. Annu. Rev. Microbiol. 2019, 73, 17–42.
29. Hull, C.M.; Heitman, J. Genetics of *Cryptococcus neoformans*. Annu. Rev. Genet. 2002, 36, 557–615.
30. Wang, P.; Perfect, J.R.; Heitman, J. The G-protein beta subunit GPB1 is required for mating and haploid fruiting in *Cryptococcus neoformans*. Mol. Cell. Biol. 2000, 20, 352–362.
31. Wickes, B.L.; Mayorga, M.E.; Edman, U.; Edman, J.C. Dimorphism and haploid fruiting in *Cryptococcus neoformans*: Association with the alpha-mating type. Proc. Natl. Acad. Sci. USA 1996, 93, 7327–7331.
32. Lin, X.; Huang, J.C.; Mitchell, T.G.; Heitman, J. Virulence attributes and hyphal growth of *C. neoformans* are quantitative traits and the *MAT*α allele enhances filamentation. PLoS Genet. 2006, 2, e187.
33. Kwon-Chung, K.J.; Bennett, J.E. Distribution of alpha and alpha mating types of *Cryptococcus neoformans* among natural and clinical isolates. Am. J. Epidemiol. 1978, 108, 337–340.
34. Yan, Z.; Li, X.; Xu, J. Geographic distribution of mating type alleles of *Cryptococcus neoformans* in four areas of the United States. J. Clin. Microbiol. 2002, 40, 965–972.
35. Fu, C.; Heitman, J. PRM1 and KAR5 function in cell-cell fusion and karyogamy to drive distinct bisexual and unisexual cycles in the *Cryptococcus* pathogenic species complex. PLoS Genet. 2017, 13, e1007113.

36. Lin, X.; Heitman, J. The biology of the *Cryptococcus neoformans* species complex. Annu. Rev. Microbiol. 2006, 60, 69–105.

37. Lin, X.; Litvintseva, A.P.; Nielsen, K.; Patel, S.; Floyd, A.; Mitchell, T.G.; Heitman, J. αADα hybrids of *Cryptococcus neoformans*: Evidence of same-sex mating in nature and hybrid fitness. PLoS Genet. 2007, 3, e186.

38. Rhodes, J.; Desjardins, C.A.; Sykes, S.M.; Beale, M.A.; Vanhove, M.; Sakthikumar, S.; Chen, Y.; Gujja, S.; Saif, S.; Chowdhary, A.; *et al*. Tracing genetic exchange and biogeography of *Cryptococcus neoformans* var. *grubii* at the global population level. Genetics 2017, 207, 327–346.

39. Ni, M.; Feretzaki, M.; Li, W.; Floyd-Averette, A.; Mieczkowski, P.; Dietrich, F.S.; Heitman, J. Unisexual and heterosexual meiotic reproduction generate aneuploidy and phenotypic diversity de novo in the yeast *Cryptococcus neoformans*. PLoS Biol. 2013, 11, e1001653.

40. You, M.; Xu, J. The effects of environmental and genetic factors on the germination of basidiospores in the *Cryptococcus gattii* species complex. Sci. Rep. 2018, 8, 1–15.

41. Bovers, M.; Hagen, F.; Kuramae, E.E.; Diaz, M.R.; Spanjaard, L.; Dromer, F.; Hoogveld, H.L.; Boekhout, T. Unique hybrids between the fungal pathogens *Cryptococcus neoformans* and *Cryptococcus gattii*. FEMS Yeast Res. 2006, 6, 599–607.

42. Bovers, M.; Hagen, F.; Kuramae, E.E.; Hoogveld, H.L.; Dromer, F.; St-Germain, G.; Boekhout, T. AIDS patient death caused by novel *Cryptococcus neoformans* × *C. gattii* hybrid. Emerg. Infect. Dis. 2008, 14, 1105–1108.

43. Aminnejad, M.; Diaz, M.; Arabatzis, M.; Castañeda, E.; Lazera, M.; Velegraki, A.; Marriott, D.; Sorrell, T.C.; Meyer, W. Identification of novel hybrids between *Cryptococcus neoformans* var. *grubii* VNI and *Cryptococcus gattii* VGII. Mycopathologia 2012, 173, 337–346.

44. Smith, I.M.; Stephan, C.; Hogardt, M.; Klawe, C.; Tintelnot, K.; Rickerts, V. Cryptococcosis due to *Cryptococcus gattii* in Germany from 2004 to 2013. Int. J. Med. Microbiol. 2015, 305, 719–723.

45. Hagen, F.; Hare Jensen, R.; Meis, J.F.; Arendrup, M.C. Molecular epidemiology and in vitro antifungal susceptibility testing of 108 clinical *Cryptococcus neoformans*

sensu lato and *Cryptococcus gattii sensu lato* isolates from Denmark. Mycoses 2016, 59, 576–584.

46. Rhodes, J.; Desjardins, C.A.; Sykes, S.M.; Beale, M.A.; Vanhove, M.; Sakthikumar, S.; Chen, Y.; Gujja, S.; Saif, S.; Chowdhary, A.; *et al*. Population genomics of *Cryptococcus neoformans* var. *grubii* reveals new biogeographic relationships and finely maps hybridization. BioRxiv 2017, 132894.

47. Bennett, J.E.; Kwon-Chung, K.J.; Howard, D.H. Epidemiologic differences among serotypes of *Cryptococcus neoformans*. Am. J. Epidemiol. 1977, 105, 582–586.

48. Maduro, A.P.; Mansinho, K.; Teles, F.; Silva, I.; Meyer, W.; Martins, M.L.; Inácio, J. Insights on the genotype distribution among *Cryptococcus neoformans* and *C. gattii* Portuguese clinical isolates. Curr. Microbiol. 2014, 68, 199–203.

49. Cogliati, M.; Esposto, M.C.; Clarke, D.L.; Wickes, B.L.; Viviani, M.A. Origin of *Cryptococcus neoformans* var. *neoformans* diploid strains. J. Clin. Microbiol. 2001, 39, 3889–3894.

50. Viviani, M.A.; Antinori, S.; Cogliati, M.; Esposto, M.C.; Pinsi, G.; Casari, S.; Bergamasco, A.F.; Santis, M.D.; Ghirga, P.; Bonaccorso, C.; *et al*. European Confederation of Medical Mycology (ECMM) prospective survey of cryptococcosis: Report from Italy. Med. Mycol. 2002, 40, 507–517.

51. Samarasinghe, H.; Xu, J. Hybrids and hybridization in the *Cryptococcus neoformans* and *Cryptococcus gattii* species complexes. Infect. Genet. Evol. 2018, 66, 245–255.

52. Lengeler, K.B.; Cox, G.M.; Heitman, J. Serotype AD strains of *Cryptococcus neoformans* are diploid or aneuploid and are heterozygous at the mating-type locus. Infect. Immun. 2001, 69, 115–122.

53. Sun, S.; Xu, J. Genetic analyses of a hybrid cross between serotypes A and D strains of the human pathogenic fungus *Cryptococcus neoformans*. Genetics 2007, 177, 1475–1486.

54. Li, W.; Averette, A.F.; Desnos-Ollivier, M.; Ni, M.; Dromer, F.; Heitman, J. Genetic diversity and genomic plasticity of *Cryptococcus neoformans* AD hybrid strains. G3 (Bethesda) 2012, 2, 83–97.

55. Campbell, L.T.; Fraser, J.A.; Nichols, C.B.; Dietrich, F.S.; Carter, D.; Heitman, J. Clinical and environmental isolates of *Cryptococcus gattii* from Australia that retain sexual fecundity. Eukaryot. Cell 2005, 4, 1410–1419.

56. Kidd, S.E.; Hagen, F.; Tscharke, R.L.; Huynh, M.; Bartlett, K.H.; Fyfe, M.; Macdougall, L.; Boekhout, T.; Kwon-Chung, K.J.; Meyer, W. A rare genotype of *Cryptococcus gattii* caused the cryptococcosis outbreak on Vancouver Island (British Columbia, Canada). Proc. Natl. Acad. Sci. USA 2004, 101, 17258–17263.

57. Fraser, J.A.; Subaran, R.L.; Nichols, C.B.; Heitman, J. Recapitulation of the sexual cycle of the primary fungal pathogen *Cryptococcus neoformans* var. *gattii*: Implications for an outbreak on Vancouver Island, Canada. Eukaryot. Cell 2003, 2, 1036–1045.

58. Voelz, K.; Ma, H.; Phadke, S.; Byrnes, E.J.; Zhu, P.; Mueller, O.; Farrer, R.A.; Henk, D.A.; Lewit, Y.; Hsueh, Y.-P.; *et al*. Transmission of hypervirulence traits via sexual reproduction within and between lineages of the human fungal pathogen *Cryptococcus gattii*. PLoS Genet. 2013, 9, e1003771.

59. Vogan, A.A.; Khankhet, J.; Xu, J. Evidence for mitotic recombination within the basidia of a hybrid cross of *Cryptococcus neoformans*. PLoS ONE 2013, 8, e62790.

60. Forsythe, A.; Vogan, A.; Xu, J. Genetic and environmental influences on the germination of basidiospores in the *Cryptococcus neoformans* species complex. Sci. Rep. 2016, 6, 1–12.

61. Tanaka, R.; Nishimura, K.; Miyaji, M. Ploidy of serotype AD strains of *Cryptococcus neoformans*. Nihon Ishinkin Gakkai Zasshi 1999, 40, 31–34.

62. Desnos-Ollivier, M.; Patel, S.; Raoux-Barbot, D.; Heitman, J.; Dromer, F.; French Cryptococcosis Study Group. Cryptococcosis serotypes impact outcome and provide evidence of *Cryptococcus neoformans* speciation. MBio 2015, 6, e00311.

63. Litvintseva, A.P.; Lin, X.; Templeton, I.; Heitman, J.; Mitchell, T.G. Many globally isolated AD hybrid strains of *Cryptococcus neoformans* originated in Africa. PLoS Pathog. 2007, 3, e114.

64. Lin, X.; Nielsen, K.; Patel, S.; Heitman, J. Impact of mating type, serotype, and ploidy on the virulence of *Cryptococcus neoformans*. Infect. Immun. 2008, 76, 2923–2938.

65. Li, M.; Liao, Y.; Chen, M.; Pan, W.; Weng, L. Antifungal susceptibilities of *Cryptococcus* species complex isolates from AIDS and non-AIDS patients in Southeast China. Braz. J. Infect. Dis. 2012, 16, 175–179.

66. Vogan, A.A.; Khankhet, J.; Samarasinghe, H.; Xu, J. Identification of QTLs associated with virulence related traits and drug resistance in *Cryptococcus neoformans*. G3 (Bethesda) 2016, 6, 2745–2759.

67. Sun, S.; Xu, J. Chromosomal rearrangements between serotype A and D strains in *Cryptococcus neoformans*. PLoS ONE 2009, 4, e5524.

68. Hu, G.; Liu, I.; Sham, A.; Stajich, J.E.; Dietrich, F.S.; Kronstad, J.W. Comparative hybridization reveals extensive genome variation in the AIDS-associated pathogen *Cryptococcus neoformans*. Genome Biol. 2008, 9, R41.

69. Kavanaugh, L.A.; Fraser, J.A.; Dietrich, F.S. Recent evolution of the human pathogen *Cryptococcus neoformans* by intervarietal transfer of a 14-gene fragment. Mol. Biol. Evol. 2006, 23, 1879–1890.

70. Vogan, A.A.; Xu, J. Evidence for genetic incompatibilities associated with postzygotic reproductive isolation in the human fungal pathogen *Cryptococcus neoformans*. Genome 2014, 57, 335–344.

71. Cogliati, M.; Esposto, M.C.; Tortorano, A.M.; Viviani, M.A. *Cryptococcus neoformans* population includes hybrid strains homozygous at mating-type locus. FEMS Yeast Res. 2006, 6, 608–613.

72. Llorente, B.; Smith, C.E.; Symington, L.S. Break-induced replication: What is it and what is it for? Cell Cycle 2008, 7, 859–864.

73. Bennett, R.J.; Forche, A.; Berman, J. Rapid mechanisms for generating genome diversity: Whole ploidy shifts, aneuploidy, and loss of heterozygosity. Cold Spring Harb. Perspect. Med. 2014, 4, a019604.

74. Samarasinghe, H.; Vogan, A.; Pum, N.; Xu, J. Patterns of allele distribution in a hybrid population of the *Cryptococcus neoformans* species complex. Mycoses 2019.

75. Sionov, E.; Lee, H.; Chang, Y.C.; Kwon-Chung, K.J. *Cryptococcus neoformans* overcomes stress of azole drugs by formation of disomy in specific multiple chromosomes. PLoS Pathog. 2010, 6, e1000848.

76. Dong, K.; You, M.; Xu, J. Genetic changes in experimental populations of a hybrid in the *Cryptococcus neoformans* species complex. Pathogens 2020, 9, 3.

77. Lin, X.; Patel, S.; Litvintseva, A.P.; Floyd, A.; Mitchell, T.G.; Heitman, J. Diploids in the *Cryptococcus neoformans* serotype A population homozygous for the alpha mating type originate via unisexual mating. PLoS Pathog. 2009, 5, e1000283.

78. Hata, K.; Ohkusu, M.; Aoki, S.; Ito-Kuwa, S.; Pienthaweechai, K.; Takeo, K. Cells of different ploidy are often present together in *Cryptococcus neoformans* strains. Nihon Ishinkin Gakkai Zasshi 2000, 41, 161–167.

79. Toffaletti, D.L.; Nielsen, K.; Dietrich, F.; Heitman, J.; Perfect, J.R. *Cryptococcus neoformans* mitochondrial genomes from serotype A and D strains do not influence virulence. Curr. Genet. 2004, 46, 193–204.

80. Skosireva, I.; James, T.Y.; Sun, S.; Xu, J. Mitochondrial inheritance in haploid x non-haploid crosses in *Cryptococcus neoformans*. Curr. Genet. 2010, 56, 163–176.

81. Zaragoza, O.; Nielsen, K. Titan cells in *Cryptococcus neoformans*: Cells with a giant impact. Curr. Opin. Microbiol. 2013, 16, 409–413.

82. Hu, G.; Wang, J.; Choi, J.; Jung, W.H.; Liu, I.; Litvintseva, A.P.; Bicanic, T.; Aurora, R.; Mitchell, T.G.; Perfect, J.R.; *et al*. Variation in chromosome copy number influences the virulence of *Cryptococcus neoformans* and occurs in isolates from AIDS patients. BMC Genom. 2011, 12, 526.

83. Toffaletti, D.L.; Rude, T.H.; Johnston, S.A.; Durack, D.T.; Perfect, J.R. Gene transfer in *Cryptococcus neoformans* by use of biolistic delivery of DNA. J. Bacteriol. 1993, 175, 1405–1411.

84. Tanaka, R.; Taguchi, H.; Takeo, K.; Miyaji, M.; Nishimura, K. Determination of ploidy in *Cryptococcus neoformans* by flow cytometry. J. Med. Vet. Mycol. 1996, 34, 299–301.

85. Meyer, W.; Aanensen, D.M.; Boekhout, T.; Cogliati, M.; Diaz, M.R.; Esposto, M.C.; Fisher, M.; Gilgado, F.; Hagen, F.; Kaocharoen, S.; *et al*. Consensus multi-locus sequence typing scheme for *Cryptococcus neoformans* and *Cryptococcus gattii*. Med. Mycol. 2009, 47, 561–570.

86. Sabiiti, W.; May, R.C.; Pursall, E.R. Experimental models of cryptococcosis. Int. J. Microbiol. 2012, 2012, 626745.

87. Fan, Y.; Lin, X. Multiple Applications of a transient CRISPR-Cas9 coupled with electroporation (TRACE) system in the *Cryptococcus neoformans* species complex. Genetics 2018, 208, 1357–1372.

88. Xie, G.Y.; Olson, D.H.; Blaustein, A.R. Projecting the global distribution of the emerging amphibian fungal pathogen, *Batrachochytrium dendrobatidis*, based on IPCC climate futures. PLoS ONE 2016, 11, e0160746.

89. Berger, L.; Speare, R.; Daszak, P.; Green, D.E.; Cunningham, A.A.; Goggin, C.L.; Slocombe, R.; Ragan, M.A.; Hyatt, A.D.; McDonald, K.R.; *et al*. Chytridiomycosis causes amphibian mortality associated with population declines in the rain forests of Australia and Central America. PNAS 1998, 95, 9031–9036.

90. Rachowicz, L.J.; Knapp, R.A.; Morgan, J.A.T.; Stice, M.J.; Vredenburg, V.T.; Parker, J.M.; Briggs, C.J. Emerging infectious disease as a proximate cause of amphibian mass mortality. Ecology 2006, 87, 1671–1683.

91. Olson, D.H.; Aanensen, D.M.; Ronnenberg, K.L.; Powell, C.I.; Walker, S.F.; Bielby, J.; Garner, T.W.J.; Weaver, G.; Bd Mapping Group; Fisher, M.C. Mapping the global emergence of *Batrachochytrium dendrobatidis*, the amphibian chytrid fungus. PLoS ONE 2013, 8, e56802.

92. O'Hanlon, S.J.; Rieux, A.; Farrer, R.A.; Rosa, G.M.; Waldman, B.; Bataille, A.; Kosch, T.A.; Murray, K.A.; Brankovics, B.; Fumagalli, M.; *et al*. Recent Asian origin of chytrid fungi causing global amphibian declines. Science 2018, 360, 621–627.

93. Farrer, R.A.; Weinert, L.A.; Bielby, J.; Garner, T.W.J.; Balloux, F.; Clare, F.; Bosch, J.; Cunningham, A.A.; Weldon, C.; du Preez, L.H.; *et al*. Multiple emergences of genetically diverse amphibian-infecting chytrids include a globalized hypervirulent recombinant lineage. PNAS 2011, 108, 18732–18736.

94. Schloegel, L.M.; Toledo, L.F.; Longcore, J.E.; Greenspan, S.E.; Vieira, C.A.; Lee, M.; Zhao, S.; Wangen, C.; Ferreira, C.M.; Hipolito, M.; *et al*. Novel, panzootic and hybrid genotypes of amphibian chytridiomycosis associated with the bullfrog trade. Mol. Ecol. 2012, 21, 5162–5177.

95. Byrne, A.Q.; Vredenburg, V.T.; Martel, A.; Pasmans, F.; Bell, R.C.; Blackburn, D.C.; Bletz, M.C.; Bosch, J.; Briggs, C.J.; Brown, R.M.; *et al*. Cryptic diversity of a widespread global pathogen reveals expanded threats to amphibian conservation. Proc. Natl. Acad. Sci. USA 2019, 116, 20382–20387.

96. James, T.Y.; Litvintseva, A.P.; Vilgalys, R.; Morgan, J.A.T.; Taylor, J.W.; Fisher, M.C.; Berger, L.; Weldon, C.; du Preez, L.; Longcore, J.E. Rapid global expansion of

the fungal disease chytridiomycosis into declining and healthy amphibian populations. PLoS Pathog. 2009, 5, e1000458.

97. Rosenblum, E.B.; James, T.Y.; Zamudio, K.R.; Poorten, T.J.; Ilut, D.; Rodriguez, D.; Eastman, J.M.; Richards-Hrdlicka, K.; Joneson, S.; Jenkinson, T.S.; *et al*. Complex history of the amphibian-killing chytrid fungus revealed with genome resequencing data. Proc. Natl. Acad. Sci. USA 2013, 110, 9385–9390.

98. Jenkinson, T.S.; Betancourt Román, C.M.; Lambertini, C.; Valencia-Aguilar, A.; Rodriguez, D.; Nunes-de-Almeida, C.H.L.; Ruggeri, J.; Belasen, A.M.; da Silva Leite, D.; Zamudio, K.R.; *et al*. Amphibian-killing chytrid in Brazil comprises both locally endemic and globally expanding populations. Mol. Ecol. 2016, 25, 2978–2996.

99. Giraud, T.; Enjalbert, J.; Fournier, E.; Delmote, F.; Dutech, C. Population genetics of fungal diseases of plants. Parasite 2008, 15, 449–454.

100. Bennett, R.J. The parasexual lifestyle of *Candida albicans*. Curr. Opin. Microbiol. 2015, 28, 10–17.

101. Greenspan, S.E.; Lambertini, C.; Carvalho, T.; James, T.Y.; Toledo, L.F.; Haddad, C.F.B.; Becker, C.G. Hybrids of amphibian chytrid show high virulence in native hosts. Sci. Rep. 2018, 8, 1–10.

102. Becker, C.G.; Rodriguez, D.; Toledo, L.F.; Longo, A.V.; Lambertini, C.; Corrêa, D.T.; Leite, D.S.; Haddad, C.F.B.; Zamudio, K.R. Partitioning the net effect of host diversity on an emerging amphibian pathogen. Proc. Biol. Sci. 2014, 281, 20141796.

103. Farrer, R.A.; Henk, D.A.; Garner, T.W.J.; Balloux, F.; Woodhams, D.C.; Fisher, M.C. Chromosomal copy number variation, selection and uneven rates of recombination reveal cryptic genome diversity linked to pathogenicity. PLoS Genet. 2013, 9, e1003703.

104. Daum, J.M.; Davis, L.R.; Bigler, L.; Woodhams, D.C. Hybrid advantage in skin peptide immune defenses of water frogs (*Pelophylax esculentus*) at risk from emerging pathogens. Infect. Genet. Evol. 2012, 12, 1854–1864.

105. Refsnider, J.M.; Poorten, T.J.; Langhammer, P.F.; Burrowes, P.A.; Rosenblum, E.B. Genomic correlates of virulence attenuation in the deadly amphibian chytrid fungus, *Batrachochytrium dendrobatidis*. G3 (Bethesda) 2015, 5, 2291–2298.

106. Langhammer, P.F.; Lips, K.R.; Burrowes, P.A.; Tunstall, T.; Palmer, C.M.; Collins, J.P. A fungal pathogen of amphibians, *Batrachochytrium dendrobatidis*, attenuates in pathogenicity with in vitro passages. PLoS ONE 2013, 8, e77630.
107. James, T.Y.; Toledo, L.F.; Rödder, D.; da Silva Leite, D.; Belasen, A.M.; Betancourt-Román, C.M.; Jenkinson, T.S.; Soto-Azat, C.; Lambertini, C.; Longo, A.V.; *et al*. Disentangling host, pathogen, and environmental determinants of a recently emerged wildlife disease: Lessons from the first 15 years of amphibian chytridiomycosis research. Ecol. Evol. 2015, 5, 4079–4097.
108. Joneson, S.; Stajich, J.E.; Shiu, S.-H.; Rosenblum, E.B. Genomic transition to pathogenicity in chytrid fungi. PLoS Pathog. 2011, 7, e1002338.
109. Rosenblum, E.B.; Stajich, J.E.; Maddox, N.; Eisen, M.B. Global gene expression profiles for life stages of the deadly amphibian pathogen *Batrachochytrium dendrobatidis*. Proc. Natl. Acad. Sci. USA 2008, 105, 17034–17039.
110. Rosenblum, E.B.; Poorten, T.J.; Joneson, S.; Settles, M. Substrate-specific gene expression in *Batrachochytrium dendrobatidis*, the chytrid pathogen of amphibians. PLoS ONE 2012, 7, e49924.
111. Saikkonen, K.; Young, C.A.; Helander, M.; Schardl, C.L. Endophytic Epichloë species and their grass hosts: From evolution to applications. Plant Mol. Biol. 2016, 90, 665–675.
112. Inderbitzin, P.; Davis, R.M.; Bostock, R.M.; Subbarao, K.V. The ascomycete *Verticillium longisporum* is a hybrid and a plant pathogen with an expanded host range. PLoS ONE 2011, 6, e18260.
113. Fogelqvist, J.; Tzelepis, G.; Bejai, S.; Ilbäck, J.; Schwelm, A.; Dixelius, C. Analysis of the hybrid genomes of two field isolates of the soil-borne fungal species *Verticillium longisporum*. BMC Genom. 2018, 19, 14.
114. Marcet-Houben, M.; Gabaldón, T. Beyond the whole-genome duplication: Phylogenetic evidence for an ancient interspecies hybridization in the baker's yeast lineage. PLoS Biol. 2015, 13, e1002220.
115. Fay, J.C.; Liu, P.; Ong, G.T.; Dunham, M.J.; Cromie, G.A.; Jeffery, E.W.; Ludlow, C.L.; Dudley, A.M. A polyploid admixed origin of beer yeasts derived from European and Asian wine populations. PLoS Biol. 2019, 17, e3000147.

116. Langdon, Q.K.; Peris, D.; Baker, E.P.; Opulente, D.A.; Nguyen, H.-V.; Bond, U.; Gonçalves, P.; Sampaio, J.P.; Libkind, D.; Hittinger, C.T. Fermentation innovation through complex hybridization of wild and domesticated yeasts. Nat. Ecol. Evol. 2019, 3, 1576–1586.

117. Gostinčar, C.; Stajich, J.E.; Zupančič, J.; Zalar, P.; Gunde-Cimerman, N. Genomic evidence for intraspecific hybridization in a clonal and extremely halotolerant yeast. BMC Genom. 2018, 19, 364.

118. Pryszcz, L.P.; Németh, T.; Saus, E.; Ksiezopolska, E.; Hegedűsová, E.; Nosek, J.; Wolfe, K.H.; Gacser, A.; Gabaldón, T. The genomic aftermath of hybridization in the opportunistic pathogen *Candida metapsilosis*. PLoS Genet. 2015, 11, e1005626.

119. Stukenbrock, E.H.; Christiansen, F.B.; Hansen, T.T.; Dutheil, J.Y.; Schierup, M.H. Fusion of two divergent fungal individuals led to the recent emergence of a unique widespread pathogen species. PNAS 2012, 109, 10954–10959.

120. Le Gac, M.; Hood, M.E.; Fournier, E.; Giraud, T. Phylogenetic evidence of host-specific cryptic species in the anther smut fungus. Evolution 2007, 61, 15–26.

121. Turner, E.; Jacobson, D.J.; Taylor, J.W. Genetic architecture of a reinforced, post-mating, reproductive isolation barrier between *Neurospora* species indicates evolution via natural selection. PLoS Genet. 2011, 7, e1002204.

122. Büker, B.; Petit, E.; Begerow, D.; Hood, M.E. Experimental hybridization and backcrossing reveal forces of reproductive isolation in *Microbotryum*. BMC Evol. Biol. 2013, 13, 224.

123. Lin, X.; Chacko, N.; Wang, L.; Pavuluri, Y. Generation of stable mutants and targeted gene deletion strains in *Cryptococcus neoformans* through electroporation. Med. Mycol. 2015, 53, 225–234.

124. Olson, A.; Stenlid, J. Plant pathogens. Mitochondrial control of fungal hybrid virulence. Nature 2001, 411, 438.

Chapter 3: The effects of environmental and genetic factors on the germination of basidiospores in the *Cryptococcus gattii* species complex

3.1 Preface

Spores generated from sexual reproduction in basidiomycete fungi (i.e., basidiospores) are abundant and resistant to various environmental stresses, such as high temperature, desiccation, and oxidative stress. In the human pathogenic *Cryptococcus*, these basidiospores are considered the main infectious propagules that cause cryptococcosis. Previous studies have found that the viability of basidiospores of serotype AD hybrids was highly variable. However, very little is known about hybridization and hybrids from crosses between lineages within CGSC and between CNSC and CGSC. In this study, I found that the germination rates of basidiospores significantly decreased at 37 °C than at 30 °C, while the two media (a rich medium and a poor medium) did not show significant differences in supporting spore germination. In addition, although basidiospores from intra-species crosses germinated better than those from inter-species crosses, the genetic distance between parents did not show any significant negative correlations with spore germination. This work is now published in Scientific Reports, 8(1), 15260. The referencing style in this chapter is as in the originally published manuscript. I am the primary contributor of this work.

3.2 Abstract

Natural and artificial hybridization has been frequently reported among divergent lineages within and between the two closely related human pathogenic fungi *Cryptococcus gattii* species complex and *Cryptococcus neoformans* species complex. However, the biological effects of such hybridization are not well known. Here we used five strains of the *C. neoformans* species complex and twelve strains of the *C. gattii* species complex to investigate the potential effects of selected environmental and genetic factors on the germination of their basidiospores from 29 crosses. We found that the germination rates varied widely among crosses and environmental conditions, ranging from 0% to 98%. Overall, the two examined media showed relatively little difference on spore germination while temperature effects were notable, with the high temperature (37 °C) having an overall deleterious effect on spore germination. Within the *C. gattii* species complex, one intra-lineage VGIII × VGIII cross had the highest germination rates among all crosses at all six tested environmental conditions. Our analyses indicate

significant genetic, environmental, and genotype-environment interaction effects on the germination of basidiospores within the *C. gattii* species complex.

3.3 Introduction

The genus *Cryptococcus* was created by Kützing in 1833[1]. This genus currently includes 37 species, two of which are well-known human fungal pathogens, the *Cryptococcus neoformans* species complex and the *Cryptococcus gattii* species complex[2,3]. Cryptococcosis caused by the *C. neoformans* species complex and *C. gattii* species complex is among the most serious fungal diseases and claims hundreds of thousands of lives each year, with an estimated global infection burden of 223,100 cases annually[4]. Current epidemiological studies suggest that the *C. neoformans* species complex infects primarily immunocompromised patients, whereas the *C. gattii* species complex is commonly found infecting immunocompetent individuals.

The *C. gattii* species complex was traditionally considered a pathogen associated with tropical and subtropical regions. However, over the last decade, strains of the *C. gattii* species complex has been commonly found in temperate regions of North America and Europe[5-11]. Recent molecular phylogenetic studies identified significant diversity and genetic divergence within both the *C. neoformans* species complex and the *C. gattii* species complex. In one study, the divergent lineages within each of the two species complexes were proposed as different species: the *C. neoformans* species complex was divided into two species (*C. neoformans* and *C. deneoformans*) and the *C. gattii* species complex into five species (*C. gattii, C. deuterogattii, C. bacillisporus, C. tetragattii* and *C. decagattii*) (Table 3.1). However, there is an ongoing debate about whether the observed differences warrant naming the different lineages as different species and on how species should be named in this and other groups of fungal taxa. Here we used the conservative naming system to call strains of lineages VNI to VNIV as belonging to the *C. neoformans* species complex while those of lineages VGI to VGIV as belonging to the *C. gattii* species complex. Regardless of the naming disagreements, these lineages/species are readily identified using a variety of molecular markers, including multi-locus sequence typing (MLST) and amplified fragment length polymorphism (AFLP) analysis (Table 3.1)[12,13]. Within the *C. gattii* species complex, Bovers *et al*. reported that VGI and VGIII are the most closely related, VGIV clusters basal to

them, whereas VGII is the most distantly related to others. Within the *C. neoformans* species complex, VNI and VNII are sister groups, VNIV being the most distantly related, and VNIII representing the hybrids between VNI or VNII with VNIV[14].

Hybridization is defined as the process that leads to successful mating between individuals of genetically distinct populations or species, producing offspring of mixed genetic ancestry[15]. Hybridization and hybrids have been observed in animals and plants since antiquity, but the scientific study of hybrids did not begin until the mid-18th century when Kölreuter showed that hybrid progeny often had intermediate phenotypes of the parents and that most of them were sterile[16]. Since then, hybridization has been continuously reported. However, the role of hybridization in long-term evolution has been debated and there are two opposite viewpoints among biologists. At one extreme, hybridization is regarded as a potent evolutionary force that creates opportunities for speciation and adaptive evolution. Biologists holding this view believe hybridization increases the genetic diversity and brings novel gene combinations, which could lead to significantly increased adaptive potential in heterogeneous environments. The contrary considers hybridization as evolutionary noise, with only transient effects on populations and relatively little long-term evolutionary importance[17,18]. Recent genetic and genomic evidence suggest that hybridization is very common and has likely played a significant role in speciation and other biological processes of many organisms[19-21].

Table 3.1. Correspondence among the names that have been used to describe the various lineages within the human pathogenic *Cryptococcus* species complexes.

Name in this manuscript	**Common / variety name**	**Lineage / Molecular type**	**Proposed name**[12]
Cryptococcus neoformans **species complex**	*C. neoformans var. grubii*	VNI/VNII/VN (AFLP1,AFLP1A, AFLP1B, VNB)	*C. neoformans*
	C. neoformans var. neoformans	VNIV (AFLP2)	*C. neoformans*
	AD hybrid	VNIII (AFLP3)	*C. neoformans* × *C. neoformans hybrid*
Cryptococcus gattii **species complex**	*C. gattii*	VGI (AFLP4)	*C. gattii*
		VGII (AFLP6)	*C. deuterogattii*
		VGIII (AFLP5)	*C. bacillisporus*
		VGIV (AFLP7)	*C. tetragattii*
		VGIV/VGIIIc (AFLP10)	*C. decagattii*
Cryptococcal interspecific hybrids	DB hybrid	AFLP8	*C. neoformans* × *C. gattii hybrid*
	AB hybrid	AFLP9	*C. neoformans* × *C. gattii hybrid*
	AB hybrid	AFLP11	*C. neoformans* × *C. deuterogattii hybrid*

The impact of hybridization on fungal evolution differs from those in the majority of plants and animals in several aspects. For example, unlike in plants and animals, most fungal species can reproduce both sexually and asexually. As a result, sexually sterile hybrid progeny can continue to reproduce through asexual/clonal reproduction and thus can have continuous evolutionary effects. Another unique characteristic of fungi is that they generally have short reproductive cycles and can achieve large population sizes in a relatively short period of time. Both features can contribute to the possibility that hybrid progeny with high fitness could emerge during hybridization in fungi.

Although most studies of hybridization have focused on animals and plants, natural and artificial hybridization has been frequently reported in many microbial groups, including the human pathogenic *Cryptococcus*. Both the *C. neoformans* species complex and the *C. gattii* species complex have a bipolar mating system with two different mating types, *MAT***a** and *MAT*α. Under appropriate conditions, strains of different mating types from the same or different lineages and species complexes can mate with each other to generate meiotic progeny. The hybridization process includes cell fusion, formation of dikaryotic hyphae, and the generation of basidiospores through meiosis[22]. In addition, natural hybrid strains have been frequently reported in the human pathogenic *Cryptococcus* species. For example, strains of *C. neoformans* var. *grubii* × *C. neoformans* var. *neoformans* (or VNI × VNIV and VNII × VNIV hybrids) have been observed in both the natural environments and in patients[23]. Indeed, the frequency of *C. neoformans* var. *grubii* × *C. neoformans* var. *neoformans* hybrids is reported to be ~6% among global clinical isolates and 30% among European clinical isolates[24,25]. In addition to the *C. neoformans* var. *grubii* × *C. neoformans* var. *neoformans* hybrids, both inter-lineage and inter-species hybrids have been described in the *C. neoformans* / *C. gattii* species complex. Specifically, three *C. neoformans* var. *neoformans* VNIV × *C. gattii* VGI hybrids from two HIV-negative patients in the Netherlands, one *C. neoformans* var. *grubii* VNI × *C. gattii* VGI hybrid from an HIV-positive person in Canada, and one novel *C. neoformans* var. *grubii* VNI × *C. gattii* VGII hybrid from South America, have been reported[14,26-29]. In addition, Kavanaugh *et al*. reported an ancient introgression event that a fragment of the *C. neoformans* var. *grubii* gene region (~40kb) non-reciprocally transferred to a strain of the *C. neoformans* var. *neoformans*[30]. These results suggest that hybridization is common in the human pathogenic *Cryptococcus* species complexes

and that they represent great model organisms for understanding the effects of hybridization on fungal evolution.

One of the key indicators of evolution and speciation is the viability of sexual offspring. In the human pathogenic *Cryptococcus*, the sexual basidiospores are also considered the infectious propagules. These spores can be abundant, stress resistant, and readily aerially dispersed. As a result, animals may encounter spores more often than other infectious forms[31]. A previous study described that spores from the *C. neoformans* species complex were much more infectious than yeast cells in mice[32]. Both the *C. neoformans* species complex and the *C. gattii* species complex have defined sexual cycles that can produce abundant basidiospores capable of infecting patients[31]. However, based on the low spore germination rate at 37 °C, several studies also suggested that basidiospores might not be the only nor most important infectious propagule in *Cryptococcus*[33-35].

A recent study reported that basidiospores from intra-lineage crosses within the *C. neoformans* species complex had an overall greater germination potential than those from inter-lineage crosses over a range of environmental conditions[33]. Their results showed that temperature had a greater influence than medium on spore germination, with lower germination at 37 °C than at 23 °C and 30 °C in most crosses. Whether a similar result will be found in the *C. gattii* species complex remains unknown. As described previously, the *C. neoformans* species complex and *C. gattii* species complex differ in several aspects, including geographic distributions, epidemiology, and mitochondrial inheritance[36,37].

Here, we examined the germination of basidiospores from VGI × VGIII, VGII × VGIII, VGIII × VGIII crosses within the *C. gattii* species complex under selected environmental conditions. In addition, we performed several crosses between strains belonging to the two different species complexes *C. gattii* species complex and *C. neoformans* species complex. These results were compared with those reported previously for the *C. neoformans* species complex. We hypothesize that similar to what was observed in the *C. neoformans* species complex, basidiospores from the VGIII × VGIII crosses in the *C. gattii* species complex should show higher basidiospore germination rates than those of inter-lineage crosses. Furthermore, because *C. gattii* is mainly found in tropical and subtropical regions, we hypothesize that basidiospores from crosses within the *C.*

gattii species complex should germinate well at a high temperature due to their historical adaptation.

3.4 Results

In this study, we used a total of twelve strains of the *C. gattii* species complex and five strains of the *C. neoformans* species complex, including three VGI strains, three VGII strains, six VGIII strains, three VNI strains and two VNIV strains (Table 3.2). Among these 17 strains, eight were *MAT***a** and nine were *MAT*α. Fifteen of these strains were wildtype while two strains JF101 (*MAT*α) and JF109 (*MAT***a**) had mutations at the *crg1* gene[38]. The *crg1* gene is a suppressor of the mating pathway in *C. gattii* species complex and its knockout enabled these two strains to mate much more efficiently than wildtype strains. However, the knockout is not known to have other notable effects, including meiosis and sporulation[38]. These strains were used to create 46 mating pairs. For each successful cross, we examined the basidiospore germination rates on two media and at three temperatures. Below we describe the effects of the examined environmental and genetic factors on basidiospore germination among our mating crosses.

Table 3.2. Strains used in this study.

Strain	Lineage / Molecular Type (GenBank accession numbers for *GPD1*, *LAC1*, and *PLB1*)	Mating Type	Strain source
B4545	VGI (DQ096396; DQ096404; DQ096353)	*MAT* **a**	Clinical, USA
B4492	VGI (MG891763; MG891768; MG891773)	*MAT* α	Clinical, USA
B4495	VGI (MG891764; MG891769; MG891774)	*MAT* **a**	Clinical, Australia
LA55n	VGII (HM990744; AY973087; HM990885)	*MAT* **a**	Clinical, Brazil
LA61n	VGII (HM990746; AY973089; HM990887)	*MAT* α	Clinical, Brazil
R265	VGII (DQ096377; DQ096400; DQ096343)	*MAT* α	Clinical, Canada
B4544	VGIII (MG891765; MG891771; MG891776)	MATα	Clinical, USA
B4546	VGIII (DQ096383; DQ096405; AY327616)	*MAT* **a**	Clinical, USA
B4499	VGIII (MG891766; MG891770; MG891775)	*MAT* α	Clinical, Australia
ATCC32608	VGIII (DQ096388; DQ096406; FJ705950)	*MAT* **a**	Clinical, USA
JF101	VGIII (DQ096378; FJ706051; AY327615)	*MAT* α	Lab, derivative of NIH312
JF109	VGIII (DQ096383; FJ706051; AY327616)	*MAT* **a**	Lab, derivative of B4546
CDC15	VNI (MG891767; MG891772; MG891777)	*MAT* α	Clinical, USA
KN99a	VNI (GU079851; EF211594; GU079701)	*MAT* **a**	Lab, derivative of H99
KN99α	VNI (GU079851; EF211594; GU079701)	*MAT* α	Lab, derivative of H99
JEC20a	VNIV (HQ851613; EF211637; EU408650)	*MAT* **a**	Lab
JEC21α	VNIV (HQ851614; EF211638; HQ851729)	*MAT* α	Lab

3.4.1 Mating success

Among the forty-six attempted crosses, twenty-nine were successful (Table 3.3). Our results indicated that mating success differed among the different types of crosses among the tested strains. Among strains between VGI and VGIII lineages, six of the nine hybrid crosses mated successfully (~66.7%). Seven out of the nine hybrid crosses between strains of the VGII and VGIII lineages were successful (~77.8%). All nine VGIII × VGIII crosses mated successfully (100%) and all seven VGIII × VN (*Cryptococcus neoformans*) were successful (100%). Despite multiple tries, we were unable to successfully cross strains from within and between other lineages of the *C. gattii* species complex and *C. neoformans* species complex. These included two VGI × VGI, two VGII × VGII, five VGI × VGII, two VGI × VNI, and one VGII × VNI (Table 3.3).

Of the 29 successful crosses, all involved strains from VGIII and 15 of which involved either JF101 or JF109. However, a comparison of the crosses involving VGIII strains with or without the *crg1Δ* mutation showed that the high mating success rate for VGIII strains observed here was not due to the *crg1Δ* mutation in strains JF101 and JF109. Specifically, even though crosses involving JF101 and JF109 mated more readily and produced more hyphae (a signature of mating product for the *C. gattii* species complex and the *C. neoformans* species complex) than other crosses (data not shown), for strains within VGIII, there was no noticeable difference in mating success rate between wildtype strains and the two *crg1Δ* mutants JF101 and JF109. Indeed, excluding the 15 crosses involving JF101 and JF109 from our comparisons of mating success still showed that VGIII strains were more fertile than strains in other lineages examined in this study (Table 3.3).

Table 3.3. Mating success among the 46 attempted crosses in this study.

***MAT*a Strain**			***MATα* Strain**		**Successful on V8**
VGI × VGI					
B4545	VGI	×	B4492	VGI	--
B4495	VGI	×	B4492	VGI	--
VGI × VGII					
B4545	VGI	×	LA61	VGII	--
B4545	VGI	×	R265	VGII	--
B4495	VGI	×	LA61	VGII	--
B4495	VGI	×	R265	VGII	--
VGI × VGIII					
B4545	VGI	×	B4544	VGIII	+
B4545	VGI	×	B4499	VGIII	+
B4545	VGI	×	JF101	VGIII	+
B4495	VGI	×	B4544	VGIII	+
B4495	VGI	×	B4499	VGIII	+
B4495	VGI	×	JF101	VGIII	+
VGII × VGI					
LA55n	VGII	×	B4492	VGI	--
VGII × VGII					
LA55n	VGII	×	LA61	VGII	--
LA55n	VGII	×	R265	VGII	--
VGII × VGIII					
LA55n	VGII	×	B4544	VGIII	--
LA55n	VGII	×	B4499	VGIII	--
LA55n	VGII	×	JF101	VGIII	+
VGIII × VGI					
B4546	VGIII	×	B4492	VGI	--
ATCC32608	VGIII	×	B4492	VGI	--
JF109	VGIII	×	B4492	VGI	--
VGIII × VGII					

B4546	VGIII	×	LA61	VGII	+
B4546	VGIII	×	R265	VGII	+
ATCC32608	VGIII	×	LA61	VGII	+
ATCC32608	VGIII	×	R265	VGII	+
JF109	VGIII	×	LA61	VGII	+
JF109	VGIII	×	R265	VGII	+
VGIII × VGIII					
B4546	VGIII	×	B4544	VGIII	+
B4546	VGIII	×	B4499	VGIII	+
B4546	VGIII	×	JF101	VGIII	+
ATCC32608	VGIII	×	B4544	VGIII	+
ATCC32608	VGIII	×	B4499	VGIII	+
ATCC32608	VGIII	×	JF101	VGIII	+
JF109	VGIII	×	B4544	VGIII	+
JF109	VGIII	×	B4499	VGIII	+
JF109	VGIII	×	JF101	VGIII	+
C. gattii* × *C. neoformans					
B4545	VGI	×	CDC15	VNI	--
B4495	VGI	×	CDC15	VNI	--
LA55n	VGII	×	CDC15	VNI	--
B4546	VGIII	×	CDC15	VNI	+
ATCC32608	VGIII	×	CDC15	VNI	+
JF109	VGIII	×	CDC15	VNI	+
JF109	VGIII	×	JEC21α	VNIV	+
JF109	VGIII	×	KN99α	VNI	+
JEC20**a**	VNIV	×	JF101	VGIII	+
KN99**a**	VNI	×	JF101	VGIII	+

'+' indicates succeeded attempts; '--' indicates failed attempts.

3.4.2 Basidiospore germination

The rates of basidiospore germination were examined from the twenty-nine successful crosses. The basidiospores were spread-plated on two different media (a nutrient-rich YEPD medium and a nutrient-limited SD medium) and incubated at three different temperatures (23 °C, 30 °C and 37 °C). These crosses were divided into four groups based on the lineage associations of the parental strains: VGI × VGIII, VGII × VGIII, VGIII × VGIII and VN × VGIII. The summary of basidiospore germination rates is shown in Table 3.4.

Table 3.4. Rates of basidiospore germination after 7 days of incubation for the 29 successful crosses under six environmental conditions. Values represent means ± sd of three independent tests.

Mating Cross	Medium	Temperature	Mean rates of basidiospores germinated (N=300)
B4545 (VGI) × B4544 (VGIII)	SD	23 °C	9.67 ± 0.94
		30 °C	13.33 ± 0.47
		37 °C	1.67 ± 0.47
	YEPD	23 °C	11.00 ± 0.82
		30 °C	7.67 ± 1.25
		37 °C	3.33 ± 0.47
B4545 (VGI) × JF101(VGIII)	SD	23 °C	20.00 ± 3.56
		30 °C	28.67 ± 0.29
		37 °C	4.67 ± 0.94
	YEPD	23 °C	19.67 ± 4.50
		30 °C	26.67 ± 1.70
		37 °C	8.67 ± 1.25
B4495 (VGI) × B4544 (VGIII)	SD	23 °C	29.00 ± 4.32
		30 °C	27.33 ± 3.09
		37 °C	8.67 ± 2.05
	YEPD	23 °C	27.00 ± 5.72
		30 °C	25.67 ± 3.68
		37 °C	28.33 ± 2.49
B4495 (VGI) × JF101 (VGIII)	SD	23 °C	14.33 ± 3.68
		30 °C	12.00 ± 0.82
		37 °C	1.17 ± 0.47
	YEPD	23 °C	15.50 ± 4.32
		30 °C	13.00 ± 3.27
		37 °C	1.33 ± 1.25
B4545 (VGI) × B4499 (VGIII)	SD	23 °C	6.00 ± 3.74
		30 °C	7.67 ± 6.60
		37 °C	0.67 ± 1.25
	YEPD	23 °C	12.00 ± 0.82
		30 °C	5.83 ± 5.31
		37 °C	2.17 ± 1.25
B4495 (VGI) × B4499 (VGIII)	SD	23 °C	1.67 ± 0.47
		30 °C	1.17 ± 0.94
		37 °C	1.67 ± 0.47
	YEPD	23 °C	2.00 ± 0.00
		30 °C	3.17 ± 0.94
		37 °C	3.00 ± 3.56

LA55n (VGII) × JF101 (VGIII)	SD	23 °C	7.67 ± 2.36
		30 °C	6.33 ± 0.47
		37 °C	2.67 ± 0.94
	YEPD	23 °C	6.00 ± 2.16
		30 °C	3.67 ± 1.25
		37 °C	5.33 ± 0.47
B4546 (VGIII) × R265 (VGII)	SD	23 °C	13.33 ± 1.70
		30 °C	14.67 ± 1.70
		37 °C	12.67 ± 0.94
	YEPD	23 °C	17.33 ± 3.40
		30 °C	21.67 ± 2.87
		37 °C	13.67 ± 3.40
ATCC32608 (VGIII) × LA61n (VGII)	SD	23 °C	11.33 ± 2.05
		30 °C	3.67 ± 1.25
		37 °C	10.33 ± 1.70
	YEPD	23 °C	9.67 ± 0.94
		30 °C	19.00 ± 2.16
		37 °C	10.00 ± 1.41
ATCC32608 (VGIII) × R265 (VGII)	SD	23 °C	47.67 ± 6.80
		30 °C	53.67 ± 0.94
		37 °C	36.33 ± 3.68
	YEPD	23 °C	44.33 ± 1.25
		30 °C	55.00 ± 1.41
		37 °C	53.67 ± 1.25
JF109 (VGIII) × LA61n (VGII)	SD	23 °C	15.67 ± 4.71
		30 °C	9.33 ± 0.47
		37 °C	13.67 ± 3.09
	YEPD	23 °C	14.00 ± 2.83
		30 °C	13.00 ± 0.82
		37 °C	14.67 ± 2.49
JF109 (VGIII) × R265 (VGII)	SD	23 °C	38.67 ± 4.78
		30 °C	40.00 ± 5.72
		37 °C	30.33 ± 1.25
	YEPD	23 °C	31.67 ± 4.50
		30 °C	34.33 ± 5.31
		37 °C	30.00 ± 2.83
B4546 (VGIII) × LA61n (VGII)	SD	23 °C	11.00 ± 0.82
		30 °C	12.33 ± 1.25
		37 °C	11.67 ± 1.25
	YEPD	23 °C	16.33 ± 4.11
		30 °C	15.67 ± 4.78
		37 °C	15.33 ± 1.25
B4546 (VGIII) × B4544 (VGIII)	SD	23 °C	80.00 ± 4.55
		30 °C	86.67 ± 0.94

		37 °C	58.33 ± 2.36
	YEPD	23 °C	98.33 ± 0.47
		30 °C	89.67 ± 0.94
		37 °C	89.00 ± 4.32
B4546 (VGIII) × B4499 (VGIII)	SD	23 °C	42.33 ± 10.87
		30 °C	30.00 ± 0.00
		37 °C	25.33 ± 4.19
	YEPD	23 °C	30.33 ± 2.05
		30 °C	32.33 ± 8.18
		37 °C	27.00 ± 1.63
B4546 (VGIII) × JF101 (VGIII)	SD	23 °C	11.67 ± 2.87
		30 °C	11.33 ± 1.25
		37 °C	12.67 ± 2.62
	YEPD	23 °C	12.00 ± 0.00
		30 °C	5.33 ± 0.47
		37 °C	10.33 ± 1.25
ATCC32608 (VGIII) × B4544 (VGIII)	SD	23 °C	23.67 ± 4.19
		30 °C	27.00 ± 1.41
		37 °C	1.00 ± 0.82
	YEPD	23 °C	18.67 ± 1.70
		30 °C	23.67 ± 2.05
		37 °C	21.67 ± 0.47
ATCC32608 (VGIII) × B4499 (VGIII)	SD	23 °C	28.67 ± 1.70
		30 °C	31.67 ± 2.05
		37 °C	29.33 ± 4.11
	YEPD	23 °C	27.33 ± 6.13
		30 °C	35.00 ± 5.10
		37 °C	23.67 ± 0.47
ATCC32608 (VGIII) × JF101 (VGIII)	SD	23 °C	0.67 ± 0.94
		30 °C	0.67 ± 0.47
		37 °C	1.33 ± 1.25
	YEPD	23 °C	0.00 ± 0.00
		30 °C	0.33 ± 0.47
		37 °C	0.00 ± 0.00
JF109 (VGIII) × B4544 (VGIII)	SD	23 °C	15.33 ± 0.47
		30 °C	16.00 ± 2.83
		37 °C	13.00 ± 3.56
	YEPD	23 °C	17.67 ± 2.05
		30 °C	19.33 ± 2.05
		37 °C	22.33 ± 0.47
JF109 (VGIII) × B4499 (VGIII)	SD	23 °C	22.00 ± 2.45
		30 °C	29.67 ± 3.09
		37 °C	23.00 ± 2.16
	YEPD	23 °C	27.00 ± 4.55

		30 °C	26.00 ± 7.26
		37 °C	22.67 ± 3.77
JF109 (VGIII) × JF101 (VGIII)	SD	23 °C	1.00 ± 0.82
		30 °C	0.50 ± 0.00
		37 °C	1.50 ± 1.41
	YEPD	23 °C	1.33 ± 0.47
		30 °C	2.17 ± 0.47
		37 °C	2.00 ± 0.00
B4546 (VGIII) × CDC15 (VNI)	SD	23 °C	36.00 ± 2.94
		30 °C	42.00 ± 0.82
		37 °C	41.67 ± 0.94
	YEPD	23 °C	43.33 ± 4.19
		30 °C	39.33 ± 1.25
		37 °C	34.67 ± 1.70
ATCC32608 (VGIII) × CDC15 (VNI)	SD	23 °C	33.00 ± 5.66
		30 °C	29.33 ± 3.40
		37 °C	24.00 ± 2.94
	YEPD	23 °C	35.00 ± 8.60
		30 °C	29.00 ± 1.41
		37 °C	14.33 ± 4.50
JF109 (VGIII) × CDC15 (VNI)	SD	23 °C	3.67 ± 2.36
		30 °C	4.83 ± 2.87
		37 °C	3.17 ± 1.70
	YEPD	23 °C	4.00 ± 0.00
		30 °C	1.83 ± 1.25
		37 °C	1.00 ± 1.41
JF109 (VGIII) × KN99α (VNI)	SD	23 °C	1.33 ± 0.47
		30 °C	7.00 ± 0.82
		37 °C	1.17 ± 1.70
	YEPD	23 °C	1.83 ± 1.25
		30 °C	2.00 ± 0.00
		37 °C	1.83 ± 1.89
KN99**a** (VNI) × JF101 (VGIII)	SD	23 °C	1.33 ± 0.47
		30 °C	1.33 ± 0.47
		37 °C	3.67 ± 0.94
	YEPD	23 °C	2.67 ± 0.47
		30 °C	1.00 ± 0.82
		37 °C	0.67 ± 0.47
JF109 (VGIII) × JEC21α (VNIV)	SD	23 °C	3.00 ± 1.41
		30 °C	1.33 ± 0.47
		37 °C	1.00 ± 0.00
	YEPD	23 °C	1.67 ± 0.47
		30 °C	0.67 ± 0.47
		37 °C	0.00 ± 0.00

JEC20**a** (VNIV) × JF101 (VGIII)	SD	23 °C	15.67 ± 3.09
		30 °C	22.00 ± 4.55
		37 °C	15.00 ± 7.12
	YEPD	23 °C	20.67 ± 4.64
		30 °C	16.00 ± 0.82
		37 °C	14.00 ± 2.45

Our comparisons of the basidiospore germination rate differences between the mating groups indicated significant differences between several groups: VGI × VGIII vs. VGII × VGIII ($p = 0.05$), VGI × VGIII vs. VGIII × VGIII ($p = 0.001$), and VGIII × VGIII vs. VN × VGIII ($p < 0.0001$). In all these cases, crosses involving genetically closely related strains on average produced basidiospores with higher germination rates than those from crosses involving more distantly related parental strains (Table 3.4). However, separating the comparisons into six different environmental conditions and compared each pair separately, significant differences were only found between two groups VN × VGIII vs. VGIII × VGIII on SD medium at 30 °C and YEPD medium at 37 °C, where *p* values were 0.0491 and 0.0342 respectively.

As shown previously, the deletion of *crg1* gene enhanced the fertility of strains JF101 and JF109 as compared to their ancestral strains NIH312 and B4546 respectively[37]. Here we compared crosses involving strains B4546 and its *crg1Δ* derivative JF109 to examine the influence of *crg1* gene on basidiospore germination. A total of four pairwise comparisons were made: between B4546 × R265 and JF109 × R265; between B4546 × LA61n and JF109 × LA61n; between B4546 × B4544 and JF109 × B4544; between B4546 × JF101 and JF109 × JF101; and between B4546 × CDC15 and JF109 × CDC15. The results showed that in three of the four pairwise comparisons, the crosses containing B4546 had significantly higher germination rates than those containing JF109, consistent with *crg1* gene playing a role in spore germination. However, in one of the four pairwise comparisons, B4546 × R265 and JF109 × R265, the germination rate involving JF109 was significantly higher than that of involving B4546 ($p < 0.0001$).

3.4.3 Effects of temperature on spore germination

Our results showed that temperature had a significant influence on basidiospore germination and that the effects were different for different crosses (Table 3.4; Figure 3.1). The highest basidiospore germination rate was found from the intra-lineage cross between strains within VGIII lineage (B4546 × B4544) at all three temperatures, followed by an inter-lineage cross between VGII and VGIII strains (ATCC32608 × R265). In contrast, in two crosses, a VGIII intra-lineage cross (ATCC32608 × JF101, at 23 °C and 37 °C on YEPD) and an inter-species cross JF109 (VGIII) × JEC21α (VNIV) (at 37ºC on YEPD), there was no germination. Of the 29 successful crosses, three (two inter-lineage crosses ATCC32608 × LA61n and B4546 × LA61n, and one intra-lineage cross JF109 × B4544) showed minor differences in their spore germination rates among the three temperature treatments.

In general, among the three temperature environments, the 37 °C had the lowest germination rate for most crosses while the 23 °C and 30 °C temperature environments supported similar germination rates. However, there were some exceptions. For example, though statistically insignificant, seven crosses (KN99a × JF101; JF109 × JF101; JF109 × B4544; ATCC32607 × JF101; B4546 × JF101; JF109 × LA61n; and B4595 × B4499; Figure 3.1) showed a comparable or higher germination rate at the 37 °C temperature than at the two lower temperatures. In addition, the spores in two inter-lineage crosses, ATCC32608 × R265 and B4545 × JF101, showed significantly higher germination rates at 30 °C than at 23 °C ($p < 0.0001$ in both cases). The detailed data and statistical comparisons among temperatures for each cross are shown in Table 3.4 and Figure 3.1.

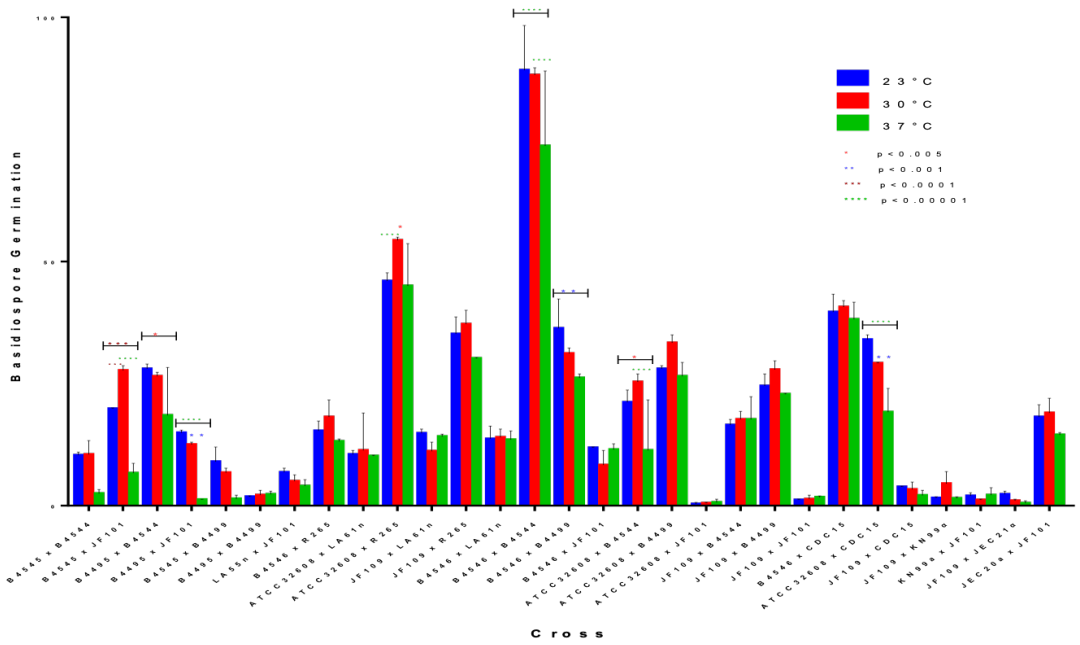

Figure 3.1. The mean rates of basidiospores germination at three different temperatures (23 °C, 30 °C and 37 °C). Values represent means ± sd.

The above comparisons were based on basidiospore germination at seven days after incubation. We also attempted to obtain colony counts on day 2 and day 3 after incubation. At day 2, few basidiospores germinated to form visible colonies. By day 3, there were visible colonies for most crosses. The comparisons in colony counts between day 3 and 7 revealed that while most crosses showed similar spore germination between the two time-points in each of the six environmental conditions, several crosses did show significant differences (Data not shown). Specifically, the intra-lineage cross B4546 × B4544 ($p < 0.001$) at 23 °C, and the intra-lineage cross ATCC32608 × B4499 ($p < 0.0001$), the inter-lineage ATCC32608 × R265 ($p < 0.0001$) and the inter-species cross B4546 × CDC15 ($p < 0.0001$) at 37 °C on SD medium, all showed significant increases in basidiospore germination from day 3 to day 7. Overall, for most crosses, the fastest germination was observed at the 30 °C environment, followed by that at 37 °C and then at 23 °C (Data not shown).

3.4.4 Effects of medium on spore germination

Compared to the large effects of temperature observed for many crosses, the effects of medium are overall relatively minor. However, there are several notable observations. First, two crosses, the intra-lineage cross ATCC32608 × JF101 (at 23 °C and 37 °C) and the inter-species cross JF109 × JEC21α (at 37 °C), showed no germinated basidiospores on the rich YEPD medium while germinations were observed on the minimal SD medium (Table 3.4). Second, significant differences between the two medium treatments were found for three crosses (inter-lineage cross B4546 × LA61n, intra-lineage crosses B4546 × B4499 and B4546 × B4544) at 23 °C, two crosses (inter-lineage cross ATCC32608 × LA61n and intra-lineage cross JF109 × B4499) at 30 °C, and six crosses (two inter-lineage crosses B4495 × B4544 and ATCC32608 × LA61n; three intra-lineage crosses B4546 × B4544, ATCC32608 × B4544 and JF109 × B4544; one inter-species cross B4546 × CDC15) at 37 °C with $p < 0.001$. In most of the above cases, the rich YEPD medium supported greater spore germination than the minimal SD medium. The exceptions were two crosses B4546 × CDC15 (at 37 °C) and JF109 × KN99α (at 30 °C) where the SD medium supported higher spore germination rates than the YEPD medium.

As indicated above, the media contributions to differences in germination rates from those crosses were temperature-specific. We thus further explored whether there was a broad temperature-medium interaction effect on basidiospore germination including all crosses and all environmental conditions. Using a generalized linear mixed model approach, we found no significant temperature-medium interaction effect on basidiospore germination in our crosses (Data not shown).

3.4.5 Effect of genetic divergence between parental strains on their progeny basidiospore germination

To examine the potential effects of nucleotide sequence divergence between parental strains on their progeny basidiospore germination, we obtained the DNA sequences at three gene fragments (*GPD*1, *LAC*1 and *PLB*1) for all parental strains. Of the 17 strains that resulted in successful crosses, 12 already had their sequences at these three loci deposited in GenBank and these were retrieved for our analyses. We obtained the sequences for the remaining five strains (B4492, B4495, B4544, B4499 and CDC15)

using the method described previously. The sequence accession numbers of all the 51 sequences are presented in Table 3.2. A Neighbor-Joining tree based on the concatenated sequences was constructed using MEGA7 (Figure 3.2). The phylogenetic tree showed the expected relationships among parental strains used in this study, with the strains from the same lineage grouped together. The Kimura-2-parameter genetic distances between each pair of mating parents were used to analyze its relationship with basidiospore germination rate.

The computed pairwise nucleotide sequence distances between parental strains are summarized in Table 3.S1. Based on the basidiospore germination data in Table 3.4 and the nucleotide sequence divergence data in Table 3.S1, we conducted a series of correlation tests. These included each of the six environmental conditions and for different types of cross populations. The summary results are presented in Table 3.S2. Our correlation analyses showed that when all 29 crosses were included, there was a negative correlation between genetic distance of parental strains and the rate of basidiospore germination in all tested environments. This result is consistent with the hypothesis that sequence divergence contributes to lower progeny basidiospore viability. However, the correlations were statistically insignificant in any of the six individual environmental conditions (Table 3.S2).

To further explore the relationship between genetic distance and basidiospore germination rate, we divided the 29 crosses into four groups based on strain lineage relationships and examined the relationships between genetic distance and basidiospore germination rate within each type of crosses. These four groups were VGI × VGIII, VGII × VGIII, VGIII × VGIII, and VN × VGIII. Our analyses revealed that of the four groups, only the VGIII × VGIII group showed a slight negative relationship between genetic distance and spore germination rate (Table 3.S2). In contrast, the other three groups all showed slight positive correlations. However, none of the four correlations were statistically significant ($p > 0.1$).

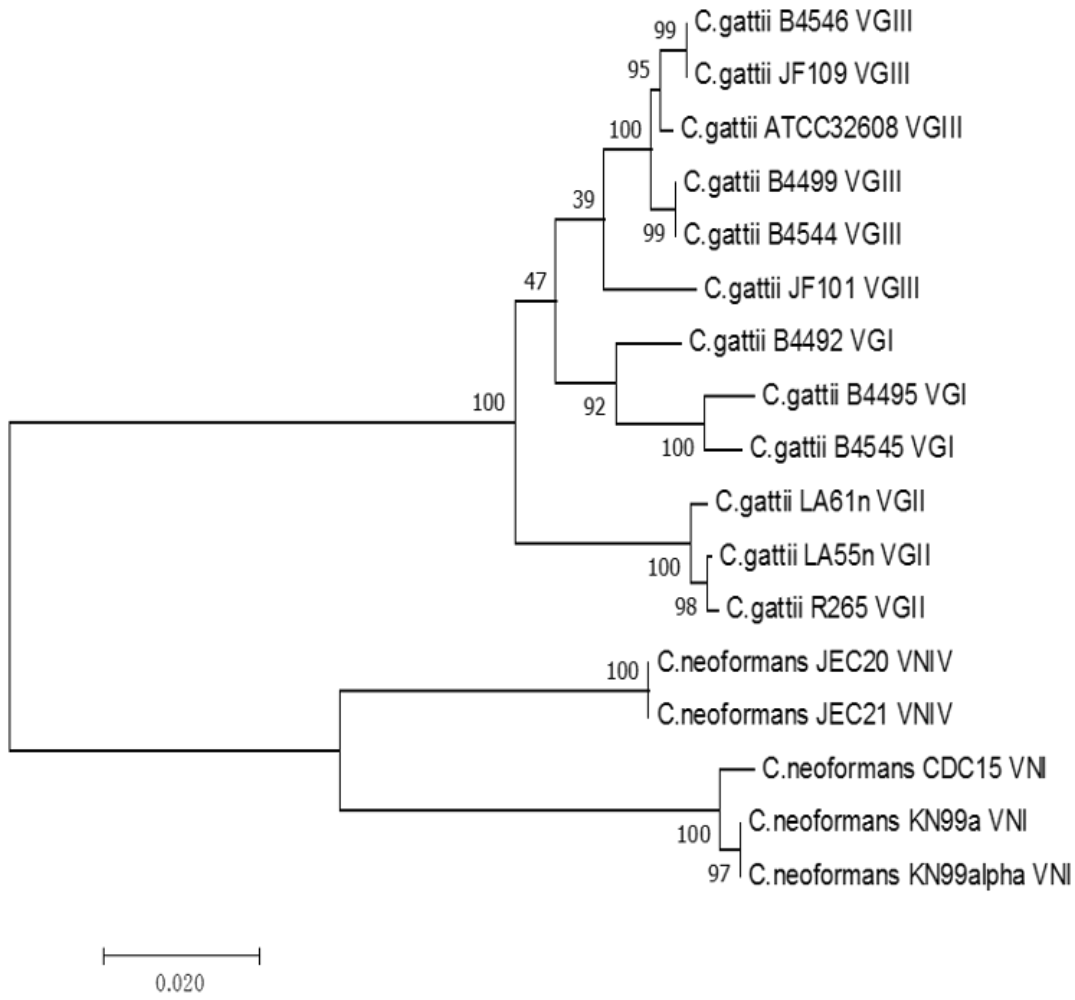

Figure 3.2. The genetic relationships among strains of the *Cryptococcus gattii* species complex and the *Cryptococcus neoformans* species complex analyzed in this study. The relationships were inferred based on DNA sequences at three gene fragments.

3.5 Discussion

In this study, we examined the germination rates of basidiospores from crosses involving strains from within and between diverged lineages in the *C. gattii* species complex and the *C. neoformans* species complex under six different environmental conditions. Interestingly, all our successful crosses involved at least one VGIII strain. This result is consistent with several previous studies that showed VGIII strains as being more fertile than strains of other VG groups[37-41]. Among the successful crosses, we found large variations in germination ability among crosses and among the tested environmental conditions. The basidiospore germination rates of an intra-VGIII lineage cross B4546 × B4544 were higher (average of ~84% and range from 58.33% to 98.33% among the six conditions) than other crosses. While media showed an overall relatively minor effects, temperature showed a significant influence on basidiospore germination, with the high temperature (37 °C) having an inhibitory effect for spores from many of the crosses. Below we discuss the spore germination rates observed here and compare with those in the *C. neoformans* species complex.

3.5.1 Comparison of spore germination rates with those in the *C. neoformans* species complex

Previous studies have estimated the germination rates of basidiospores from crosses in the *C. neoformans* species complex, with a range of 5.5%[42] to 95%[33]. The highest rate of basidiospore germination in the *C. neoformans* species complex was found from an intra-lineage cross between two isogenic strains JEC20**a** × JEC21α belonging to the VNIV lineage on the minimal SD medium at 30 °C (~95%) and 23 °C (~90%), followed by two other intra-specific crosses KN99**a** × KN99α (~70%) and KN99**a** × CDC15 (~60%) belonging to the VNI lineage at 23 °C on SD medium. The lowest rate in that study was found in certain hybrid crosses between strains of VNI and VNIV. Our results showed that basidiospores from different crosses in the *C. gattii* species complex could also have highly variable germination rates, from 0% to 98%. The 0% germination was observed in two crosses: an inter-specific cross between VGIII and VNIV (JF109 × JEC21α) and an intra-lineage cross within VGIII (ATCC32608 × JF101) when their spores were placed under certain conditions. The highest germination rate was found in one of the intra-lineage crosses (VGIII, B4546 × B4544) at 23 °C (~98%), 30 °C (~90%)

and 37 °C (89%) on YEPD medium. However, the second highest was an inter-lineage cross (VGIII × VGII, ATCC32608 × R265) at 30 °C (~55%) and 37 °C (~54%) on the YEPD medium. Similar to that observed in *C. neoformans*[33], the germination rates of basidiospores from most crosses were less than 50%. Overall, lower rates of spore germination were found in the VGII × VGIII mating crosses. This observation is similar to that by Voelz *et al*. showing that both the VGII**a** × VGIIIα and VGIIα × VGIII**a** mating pairs had a low spore germination rate[43]. At present, the reason(s) for the overall lower germination rate of spores from VGII × VGIII crosses remains unknown.

3.5.2 Effects of environmental factors on spore germination and their implications

This study examined whether environmental factors (3 temperatures × 2 media) influenced the germination potential of basidiospores from hybrid crosses in *C. gattii* species complex. For human fungal pathogens, one of the most important characteristics is the ability to survive and grow at high temperatures (≥ 37 °C). However, for most crosses, our results demonstrated that high temperature had an inhibitory effect on basidiospore germination. This result is similar to what was found for basidiospores in all six crosses among strains within the *C. neoformans* species complex reported by Forsythe *et al*.[33]. Interestingly, different from what was found in *C. neoformans* species complex where the same two media did not show any noticeable effect on spore germination[33], for several of the crosses examined here, media showed a significant effect on basidiospore germination, especially at 37 °C. For example, the rich YEPD medium supported a greater germination rate for 17/29 crosses than the minimum SD medium at both 23 °C and 37 °C (Table 3.4). The greater germination rate on YEPD medium than on SD medium for the *C. gattii* species complex spores may suggest that higher nutrient levels are more conducive for *C. gattii* species complex spore germination at low (23 °C) and high (37 °C) temperature rather than at intermediate (30 °C) temperature.

At present, the reasons for the diverse basidiospore germination rates among the different environmental conditions and among crosses are not known. One potential explanation might be related to mitochondrial inheritance. Previous studies have shown that different crosses in the *C. gattii* species complex showed very different mitochondrial inheritance patterns and that environmental factors such as temperature

and UV irradiation can have significant effects on mitochondrial inheritance in both the *C. neoformans* species complex and the *C. gattii* species complex but to different degrees[37,44]. In general, Wang *et al*. noted that crosses among strains within the *C. gattii* species complex have more variable mtDNA inheritance patterns than those within the *C. neoformans* species complex and that parental strains, strain combinations, and diverse environmental factors can all contribute to the different mtDNA inheritance patterns in the *C. gattii* species complex[37]. The heterogeneous mitochondrial genotypes, including recombination genotypes, among basidiospore progeny may influence their energy generation and spore viability.

3.5.3 Genetic contributions

Since all our successful matings involved at least one strain from the VGIII lineage, the specific characteristics of VGIII isolates might also have played a key role in the variable spore germinations observed here. Previous studies have shown that the VGIII lineage is genotypically highly diverse[45] and that strains of both *MAT***a** and *MAT*α have been reported from clinical, veterinary and environmental VGIII isolates, consistent with sexual reproduction and recombination in natural populations of this lineage[46,47]. Frequent mating and recombination of these strains in nature could help explain the high mating success and high spore germination rates of the VGIII × VGIII crosses.

Our results indicate that c*rg1* gene plays a role on basidiospore germination with the effects differ among crosses. However, since not all crosses were similarly affected, the effects of the *crg1* mutation on basidiospore germination likely involve interacting with other gene(s) in the mating partner genome that likely differ among the parental strains. Several studies have reported that the deletion of *crg1* gene can enhance mating efficiency in both the *C. neoformans* species complex and the *C. gattii* species complex but may reduce the viability of basidiospores[38,43,48,49], though no directional effect of the *crg1* gene on mitochondrial inheritance in *C. gattii* was found[50]. Voelz *et al*. used VGIII strains carrying the *crg1::NEO* mutation mated with a VGII strain and found none of the dissected 63 basidiospores were viable[43]. Among our crosses, two (ATCC32608 × JF101 and JF109 × JEC20**a**) showed 0% of basidiospore germination rate under certain conditions. Of the four crosses where direct comparisons could be made about the role of *crg1* gene in basidiospore germination, three crosses showed

significantly reduced spore viability when *crg1* was deleted while one cross showed the opposite. The results suggest that the effect of *crg1* gene on basidiospore germination is mating partner and incubation condition-dependent. Interestingly, strain R265 that showed a higher germination rate when mated with JF109 than when mated with B4546 represents the dominant genotype responsible for the cryptococcosis outbreak in western North America including British Columbia in Canada and Washington and Oregon States in the US. The potential ecological significance of this observation remains to be investigated.

Overall, our results suggested that nucleotide sequence divergence between two parental strains may be related to their progeny basidiospore germination. However, this result should be interpreted with caution. A previous study used the Cross-Match analysis revealed that the nucleotide sequence divergence between the VGI (WM276) and VGII (R265) genomes was ~7.6%, while that between VNI and VNIV was ~10%[51]. The similarity of concatenated sequences based on the consensus loci for multi-locus sequence typing (MLST) is 95% to 96% among the lineages of the *C. gattii* species complex and 84% to 86% between the *C. neoformans* species complex and the *C. gattii* species complex[14]. The average sequence divergence between mating pairs based on the three concatenated loci (*GPD*1, *LAC*1 and *PLB*1) used in this study was 1.1% for VGIII × VGIII crosses, 4.05% for VGI × VGIII crosses, 4.74% for VGII × VGIII crosses and 17.7% for VN × VGIII crosses. Thus, though there were some minor differences, overall, the amounts of sequence divergences among lineages within and between the *C. neoformans* species complex and the *C. gattii* species complex estimated using the different methods were similar to each other. As expected, there was an overall negative correlation between genetic divergence and germination rate when all crosses were included, consistent with a previous study reported for the *C. neoformans* species complex[33]. However, the observed correlation was not statistically significant in the present study. This was not surprising as there were large variations among crosses within each of the four mating categories analyzed here (Table 3.4 and Figure 3.1). To eliminate some of the confounding factors associated with both parental strains being different in the comparison, we further assessed the relationship between genetic distance and basidiospore germination rate for crosses all involving a shared mating

partner. Here, we focused on JF101, the only strain that successfully mated with representative strains from all lineages (VNI, VNIV, VGI, VGII, and VGIII) in this study. A total of eight crosses involving strain JF101 were included in this analysis (Tables 3.3 and 3.4). Correlational analyses between the pairwise parental strain genetic distances (Table 3.S1) and basidiospore germination rates (Table 3.4) in each of the six conditions did not yield any statistically significant correlation (*p* values all greater than 0.5). Overall, the results suggest that in the crosses examined here, the level of genetic divergence between parental strains is a relatively minor contributor to differences in basidiospore germination rate. In contrast, other factors such as genome structure differences (e.g. translocations and inversions) and mutations in genes involved in basidiospore germination likely play important roles. At present, almost nothing is known about the potential genome structural differences and mutations among the majority of investigated parental strains in this study.

Overall, our study identified that multiple factors can influence basidiospore germination rate differences, including parental strains/strain combination, temperature, medium, and some combinations of these factors. At present, the genetic bases for the observed differences are largely unknown. A previous study identified evidence for Bateson-Dobzjansky-Muller (BDM) incompatibility factors affecting the viability of basidiospores in a hybrid cross in the *C. neoformans* species complex[52]. In addition, several studies have also shown evidence that hybrids are unable to go through normal meiosis to generate haploid basidiospore progeny[13,41,42,52-55]. Both of which could contribute to genetic abnormality and low spore viability. However, this and earlier analyses have also shown that certain hybrid crosses between genetically divergent strains can generate highly viable spores with some showing superior phenotypic traits such as much faster growth rates and higher resistance to environmental stresses and antifungal drugs than parental strains[33,55,56]. In this study, we showed that novel hybrids could be readily generated in the laboratory among the divergent lineages within the *C. gattii* species complex and between strains of the *C. gattii* species complex and the *C. neoformans* species complex.

3.6 Conclusions

This study described the potential environmental and genetic factors influencing the germination of basidiospores from among twenty-nine crosses within the *C. gattii* species complex and between the *C. gattii* species complex and the *C. neoformans* species complex. We examined the effects of two media, three temperatures, and genetic divergence between pairs of parental strains on the germination rates of basidiospores. Our analyses indicated that all examined factors (temperature, medium, parental strain and strain pair) could influence basidiospore germination. Unlike in *C. neoformans* species complex where nucleotide sequence divergence between parental strains was negatively correlated with basidiospore germination rate, the results from the *C. gattii* species complex were more variable and complex. The highest spore germination rate was found in an intra-lineage VGIII × VGIII cross. In addition, while environmental factors can significantly influence the pattern of basidiospore germination, most of the environmental influences are not universal but are cross-specific. Our results also suggest that novel hybrids among certain lineages within the *C. gattii* species complex and between the *C. gattii* species complex and the *C. neoformans* species complex could be readily generated under laboratory conditions. The genotypic and phenotypic consequences of these hybridizations and their hybrids await further investigations.

3.7 Materials and Methods

3.7.1 Strains

Twelve strains of the *Cryptococcus gattii* species complex and five strains of the *Cryptococcus neoformans* species complex were used in this study. The twelve *C. gattii* species complex strains belonged to three lineages: VGI, VGII and VGIII. Strains B4545, B4492 and B4495 belong to the VGI lineage; strains LA55n, LA61n and R265 belong to the VGII lineage; and strains B4544, B4546, B4499, ATCC32608, JF101 and JF109 belong to the VGIII lineage. Strain JF109 is a derivative of a clinical strain B4546 with the *crg1* gene deleted while strain JF101 is derived from a clinical strain NIH312 with the deletion of *crg1* gene. Four of the five *C. neoformans* species complex strains correspond to two pairs of isogenic isolates, one pair is JEC20**a** and JEC21α, the other one is KN99**a** and KN99α. The isogenic strain pairs differ at the mating type locus but

are otherwise identical. CDC15 is a clinical isolate of the VNI lineage of the *C. neoformans* species complex. Strains B4544, B4492, B4499, LA61n, JF101, R265, JEC20**a** and KN99**a** are of mating type **a** while the remaining nine strains have the α mating type. The information of the parental strains used for mating crosses in this study is shown in Table 3.2.

3.7.2 Mating and Germination of basidiospores

The main objective of this study was to examine the rate of basidiospore germination for crosses involving strains within and among lineages of the *C. gattii* species complex. Not all 72 pairwise strain combinations between the *MAT***a** and *MAT*α types were crossed with each other. Instead, 46 pairwise combinations, including all 36 possible pairs within the *C. gattii* species complex were attempted (Table 3.3). To prepare for mating, all parental strains were first cultured on Yeast Extract-Peptone-Dextrose (YEPD) agar medium for 2−3 days at 30 °C. Actively growing cells were then re-suspended in sterile distilled water and 10 μl of the adjusted cell suspension (~10^5 cells/ml) from each parental strain was completely mixed together and then spotted on the V8-juice mating agar medium. Each plate contained six spots (10 μl/spot): four for the mixed cells and two for pure parental cells as negative controls. Mating plates were incubated in the dark at room temperature (around 23 °C) for 7−30 days to allow for mating and sexual spore formation. Successful mating was indicated by the formation of hyphae at the periphery of the mating spots containing yeast cells from the two parents.

For those pairs that failed to mate at the first try, additional attempts were made, including by changing the pH of V8-juice agar medium, from pH 7 to pH 5. For all successful crosses, sections of agar with hyphae and basidiospores (i.e., no parental yeast cells) were cut and transferred to a new blank plate. The hyphae and basidiospores were gently washed by applying sterile 0.5% Tween 20 solution to the mycelial surface of each agar block and four layers of sterile cheesecloth (Loblaws Inc. Toronto, Canada) were used as filter to obtain pure spore solutions. Basidiospore suspensions were diluted with additional sterile 0.5% Tween 20 solution to a final density (approx. 3×10^3 spores/ml). 100 μl of the diluted basidiospore suspensions was spread on either the common rich medium (YEPD agar medium) or the minimal Synthetic Dextrose (SD) agar

medium and incubated at each of the tested temperatures (23 °C, 30 °C and 37 °C) for seven days. The number of all visible colonies formed by germinated basidiospores was counted on each plate at three and seven days respectively after incubation. For each cross × temperature × medium combination, we performed at least three repeats. The germination of basidiospores was determined as a ratio of the number of observed colonies to the estimated total number of basidiospores plated.

3.7.3 Sequencing

To estimate the genetic divergence among parental strains, sequences in fragments of three protein-coding genes (*GPD*1, *LAC*1 and *PLB*1) were obtained from either the GenBank or through PCR followed by sequencing. For sequences of the strains that have already been deposited in the GenBank, their sequences were directly retrieved from the GenBank database. Those that were not found in the GenBank were obtained by PCR and sequencing of PCR products. Briefly, DNA was extracted from the parental strains following protocol outlined in Xu *et al*.[57]. The diluted DNA extraction was used as template to amplify the three gene fragments, following the PCR conditions listed in Table 3.S3. The amplificated PCR products were checked on a 1.2% agarose gel in 1x Tris-Acetic-Acid-EDTA buffer. The PCR products were then sequenced by MOBIX Lab at McMaster University (Hamilton, Ontario). The obtained sequences were edited using FinchTV 1.4.0 (Geospiza, Inc.; Seattle, WA, USA; http://www.geospiza.com) and aligned using MEGA 7.0 before being combined for phylogenetic analyses using the Neighbor-joining program. Bootstrap values were computed using 1000 replicates. In addition, the pairwise strain genetic distances were computed using MEGA 7.0. The relationship between genetic distances between mating partners and the basidiospore germination rates of the crosses was analyzed using a Pearson correlation test through the GraphPad Prism program (version 7.0; GraphPad Software, San Diego CA, USA).

3.7.4 Statistical analyses

To compare the differences of basidiospore germination rate among crosses on tested conditions and the effects of environmental and genetic factors which contribute to the differences, we used the paired T-tests, the generalized linear mixed model using R[58], and Pearson's correlation and visualization using GraphPad Prism (version 7.0;

GraphPad Software, San Diego CA, USA). $P < 0.05$ was considered statistically significant. Sequence alignment, genetic distance calculations and phylogenetic tree construction were performed using MEGA 7.0[59,60].

3.8 Appendix

Table 3.S1. The genetic distances between two parental strains. Genetic distances were calculated using the Maximum Composite Likelihood model.

Species 1	Species 2	Genetic Distance	Standard Error
C. gattii B4545 VGI	*C. gattii* B4544 VGIII	0.036	0.007
C. gattii B4545 VGI	*C. gattii* JF101 VGIII	0.046	0.008
C. gattii B4495 VGI	*C. gattii* B4544 VGIII	0.038	0.007
C. gattii B4495 VGI	*C. gattii* JF101 VGIII	0.049	0.008
C. gattii B4545 VGI	*C. gattii* B4499 VGIII	0.036	0.007
C. gattii B4495 VGI	*C. gattii* B4499 VGIII	0.038	0.007
C. gattii LA55n VGII	*C. gattii* JF101 VGIII	0.031	0.005
C. gattii R265 VGII	*C. gattii* B4546 VGIII	0.052	0.008
C. gattii LA61n VGII	*C. gattii* ATCC32608 VGIII	0.048	0.007
C. gattii R265 VGII	*C. gattii* ATCC32608 VGIII	0.049	0.008
C. gattii LA61n VGII	*C. gattii* JF109 VGIII	0.05	0.008
C. gattii R265 VGII	*C. gattii* JF109 VGIII	0.052	0.008
C. gattii LA61n VGII	*C. gattii* B4546 VGIII	0.05	0.008
C. gattii B4544 VGIII	*C. gattii* B4546 VGIII	0.008	0.002
C. gattii B4499 VGIII	*C. gattii* B4546 VGIII	0.008	0.002
C. gattii B4546 VGIII	*C. gattii* JF101 VGIII	0.014	0.004
C. gattii ATCC32608 VGIII	*C. gattii* B4544 VGIII	0.006	0.002
C. gattii ATCC32608 VGIII	*C. gattii* B4499 VGIII	0.006	0.002
C. gattii ATCC32608 VGIII	*C. gattii* JF101 VGIII	0.02	0.004
C. gattii B4544 VGIII	*C. gattii* JF109 VGIII	0.008	0.002
C. gattii B4499 VGIII	*C. gattii* JF109 VGIII	0.008	0.002
C. gattii JF101 VGIII	*C. gattii* JF109 VGIII	0.021	0.004
C. gattii B4546 VGIII	*C. neoformans* CDC15 VNI	0.182	0.022
C. gattii ATCC32608 VGIII	*C. neoformans* CDC15 VNI	0.18	0.022
C. gattii JF109 VGIII	*C. neoformans* CDC15 VNI	0.182	0.022
C. gattii JF109 VGIII	*C. neoformans* KN99α VNI	0.178	0.022
C. gattii JF101 VGIII	*C. neoformans* KN99a VNI	0.178	0.022
C. neoformans JF109 VGIII	*C. gattii* JEC21 VNIV	0.17	0.021
C. neoformans JF101 VGIII	*C. gattii* JEC20 VNIV	0.169	0.021

Table 3.S2. The Pearson correlation coefficient between environmental factors and the genetic distance.

Group		Genetic distance vs. YEPD (23°C)	Genetic distance vs. YEPD (30°C)	Genetic distance vs. YEPD (37°C)	Genetic distance vs. SD (23°C)	Genetic distance vs. SD (30°C)	Genetic distance vs. SD (37°C)
Mean Rates (N=29)	Pearson r	-0.16	-0.2263	-0.2721	-0.2136	-0.1661	-0.09351
	P-value (two-tailed)	0.4071	0.2377	0.1533	0.2659	0.3891	0.6295
VGI x VGIII (N=6)	Pearson r	0.3257	0.6088	-0.08069	0.3546	0.5353	0.1261
	P-value (two-tailed)	0.5287	0.1996	0.8792	0.4903	0.2738	0.8118
VGII x VGIII (N=7)	Pearson r	0.4839	0.5244	0.4154	0.3928	0.3504	0.5457
	P-value (two-tailed)	0.2712	0.2269	0.354	0.3834	0.441	0.2051
VGIII x VGIII (N=9)	Pearson r	-0.4775	-0.5511	-0.5042	-0.5516	-0.551	-0.4782
	P-value (two-tailed)	0.1936	0.1241	0.1663	0.1237	0.1241	0.1929
VN x VGIII (N=7)	Pearson r	0.3654	0.3831	0.3165	0.3831	0.3509	0.3997
	P-value (two-tailed)	0.4202	0.3963	0.4892	0.3963	0.4403	0.3744

Table 3.S3. Primers and PCR protocols for obtaining sequences of three genes. For all sets of primers the following PCR protocols were used.

Gene locus	Gene product	Primer Sequences (5'-3')	Amplification conditions	Fragment size (bp)	Ref.
GPD1	Glyceraldehyde-3-phosphate dehydroenase	**GPD1F:** CCACCGAACCCTTCTAGGATA **GPD1R:** CTTCTTGGCACCTCCCTTGAG	94°C 3min; 35 cycles: 94°C 45s, 63°C 1min, 72°C 2min	543	61
		Alternative: **GPD1F:** TAGCGTTAGTACTAAACGAG **GPD1R:** GTATTCGGCACCAGCCTCA	12 cycles 62-56°C, step down 2°C every 2 cycles	222	62
LAC1	Laccase	**LAC1F:** AACATGTTCCCTGGGCCTGTG **LAC1R:** ATGAGAATTGAA TCGCCTTGT	94°C 3min; 35 cycles: 94°C 30s, 53°C 30s, 72°C 1min	469	61
		Alternative: **LAC1F:** GGCGATACTATTATCGTA **LAC1R:** TTCTGGAGTGGCTAGAGC	94°C 3min; 35 cycles: 94°C 1min, 50°C 1min, 72°C 1min	565	14
PLB1	Phospholipase	**PLB1F:** CTTCAGGCGGAGAGAGGTTT **PLB1R:** GATTTGGCGTTGGTTTCAGT	94°C 3min; 35 cycles: 94°C 45s, 58°C 45s, 72°C 1min	532	61

3.9 References

1. Benham, R. W. The genus *Cryptococcus*. *Bacteriol. Rev*. **20**, 189-201 (1956).

2. Casadevall, A. & Perfect, J. *Cryptococcus neoformans*. ASM Press, Washington, DC 407-456 (1998).

3. Heitman, J., Kozel, T. R., Kwon-Chung, K. J., Perfect, J. R. & Casadevall, A. *Cryptococcus*: From Human Pathogen to Model Yeast. ASM Press, Washington, DC (2011).

4. Rajasingham, R. *et al*. Global burden of disease of HIV-associated cryptococcal meningitis: an updated analysis. *Lancet. Infect. Dis.* **17**, 873-881 (2017).

5. Speed, B. & Dunt, D. Clinical and host differences between infections with the two varieties of *Cryptococcus neoformans*. *Clin Infect Dis*. **21**, 28-34 (1995).

6. Sorrell, T. C. *Cryptococcus neoformans* variety *gattii*. *Med Mycol*. **39**, 155-68 (2001).

7. Kwon-Chung, K. J. & Bennett, J. E. Epidemiological differences between the two varieties of *Cryptococcus neoformans*. *Am J Epidemiol*. **120**, 123-30 (1984).

8. Dixit, A., Carroll, S. F. & Qureshi, S. T. *Cryptococcus gattii*: an emerging cause of fungal disease in North America. *Interdiscip Perspect Infect Dis*. **2009**, 840452 (2009).

9. Kidd, S. E. *et al*. A rare genotype of *Cryptococcus gattii* caused the cryptococcosis outbreak on Vancouver Island (British Columbia, Canada). *Proc Natl Acad Sci.* USA **101**, 17258-17263 (2004).

10. MacDougall, L. *et al*. Spread of *Cryptococcus gattii* in British Columbia, Canada, and detection in the Pacific Northwest, USA. *Emerg Infect Dis*. **13**, 42-50 (2007).

11. Viviani, M. A. *et al*. European Confederation of Medical Mycology (ECMM) Cryptococcosis Working Group. Molecular analysis of 311 *Cryptococcus neoformans* isolates from a 30-month ECMM survey of cryptococcosis in Europe. *FEMS Yeast Res*. **6**, 614-619 (2006).

12. Kwon-Chung, K. J. *et al*. The case for adopting the "species complex" nomenclature for the etiologic agents of cryptococcosis. *mSphere* **2**, e00357-e16 (2017).

13. Hagen, F. *et al*. Recognition of seven species in the *Cryptococcus gattii*/ *Cryptococcus neoformans* species complex. *Fungal Genet. Biol*. **78**, 16-48 (2015).

14. Bovers, M., Hagen, F., Kuramae, E. E. & Boekhout, T. Six monophyletic lineages

identified within *Cryptococcus neoformans* and *Cryptococcus gattii* by multi-locus sequence typing. *Fungal Genet.Biol*. **45,** 400-421 (2008a).

15. Stebbins, G. L. The role of hybridization in evolution. *Proc. Am. Phil. Soc*. **103**, 231-251 (1959).

16. Barton, N. H. & Hewitt, G. M. Analysis of hybrid zones. *Ann. Rev. Ecol. Syst*. **16**, 113-148 (1985).

17. Riesberg, L. H. *et al*. Major Ecological Transitions in Wild Sunflowers Facilitated by Hybridization. *Science* **301**, 1211-1216 (2003).

18. Barton, N. H. The Role of Hybridization in Evolution. *Molecular Ecology* **10**, 551-568 (2001).

19. Wolf, D. E., Takebayashi, N. & Rieseberg, L. H. Predicting the risk of extinction through hybridization. *Conserv. Biol*. **15**, 1039-1053 (2001).

20. Rieseberg, L. H. Hybrid origins of plant species. *A. Rev. Ecol. Syst*. **28**, 359-389 (1997).

21. Otto, S. P. & Whitton, J. Polyploid incidence and evolution. *A. Rev. Genet*. **34**, 401-437 (2000).

22. Kwon-Chung, K. J. Morphogenesis of *Filobasidiella neoformans*, the sexual state of *Cryptococcus neoformans*. *Mycologia* **68**(4), 821-833 (1976).

23. Brandt, M. E. *et al*. Molecular subtype distribution of *Cryptococcus neoformans* in four areas of the United States. Cryptococcal Disease Active Surveillance Group. *J. clin. Microbial* **34**, 912-917 (1996).

24. Meyer, W. *et al*. Molecular typing of the *Cryptococcus neoformans*/*Cryptococcus gattii* species complex. 327-357 (2011). In Heitman J, Kogure T, Kwon-Chung KJ, Perfect JR, Casadevall A (ed), *Cryptococcus*: from human pathogen to model yeast. ASM Press, Washington, DC.

25. Cogliati, M. Global molecular epidemiology of *Cryptococcus neoformans* and *Cryptococcus gattii*: an atlas of the molecular types. *Scientifica* **2013**, 675213 (2013).

26. Bovers, M. *et al*. Unique hybrids between fungal pathogens *Cryptococcus neoformans* and *Cryptococcus gattii*. *FEMS Yeast Res*. **6**, 599-607 (2006).

27. Bovers, M. *et al*. AIDS patient death caused by novel *Cryptococcus neoformans* x *C. gattii* hybrid. *Emerg Infect Dis*. **14**, 1105-1108 (2008b).

28. Lin, X. *et al*. Diploids in the *Cryptococcus neoformans* serotype A population homozygous for the a mating type originate via unisexual mating. *PLoS Pathogens*. **5**, 1-18 ((2009).

29. Aminnejad, M. *et al*. Identification of novel hybrids between *Cryptococcus neoformans* var. *grubii* VNI and *Cryptococcus gattii* VGII. *Mycopathologia* **173**, 337-346 (2012).

30. Kavanaugh, L. A., Fraser, J. A., Dietrich, F. S. Recent evolution of the human pathogen *Cryptococcus neoformans* by intervarietal transfer of a 14-gene fragment. *Mol. Biol. Evol*. **23**, 1879-1890 (2006).

31. Velagapudi, R., Hsueh, Y. P., Geunes-Boyer, S., Wright, J. R. & Heitman, J. Spores as infectious propagules of *Cryptococcus neoformans*. *Infect. Immun*. **77**, 4345-4355 (2009).

32. Sukroongreung, S., Kitiniyom, K., Nilakul, C. & Tantimavanich, S. Pathogenicity of basidiospores of *Filobasidiella neoformans* var. *neoformans*. *Med. Mycol*. **36**, 419-424 (1998).

33. Forsythe, A., Vogan, A. & Xu, J. Genetic and environmental influences on the germination of basidiospores in the *Cryptococcus neoformans* species complex. *Scientific Reports* **6,** 33828; doi: 10.1038/srep33828 (2016).

34. Shahid, M., Han, S., Yoell, H. & Xu, J. Fitness distribution and transgressive segregation across 40 environments in a hybrid progeny population of the human-pathogenic yeast *Cryptococcus neoformans*. *Genome* **51**, 272-281 (2008).

35. Steen, B. R. *et al*. Temperature-Regulated Transcription in the Pathogenic Fungus *Cryptococcus neoformans*. *Genome Res*. **12**, 1386-1400 (2002).

36. Cogliati, M. Global molecular epidemiology of *Cryptococcus neoformans* and *Cryptococcus gattii*: an atlas of the molecular types. *Scientifica* **2013**, 23 (2013).

37. Wang, Z., Wilson, A. & Xu, J. Mitochondrial DNA inheritance in the human fungal pathogen *Cryptococcus gattii*. *Fungal Genet. Biol*. **75**, 1-10 (2015).

38. Fraser, J. A., R. L. Subaran, C. B. Nichols & J. Heitman. Recapitulation of the sexual cycle of the primary fungal pathogen *Cryptococcus neoformans* var. *gattii*: implications for an outbreak on Vancouver Island, Canada. *Eukaryot. Cell* **2**, 1036-1045 (2003).

39. Fraser, J. A. *et al*. Same-sex mating and the origin of the Vancouver Island *Cryptococcus gattii* outbreak. *Nature* **437**, 1360-1364 (2005).

40. Campbell, L. T. *et al*. Clinical and environmental isolates of *Cryptococcus gattii* from Australia that retain sexual fecundity. *Eukaryot Cell* **4**, 1410-1419 (2005).

41. Lin, X. *et al*. aADa hybrids of *Cryptococcus neoformans*: evidence of same-sex mating in nature and hybrid fitness. *PLoS Genetics* **3**, e186 (2007).

42. Lengeler, K. B., Cox, G. M. & Heitman, J. Serotype AD strains of *Cryptococcus neoformans* are diploid or aneuploid and are heterozygous at the mating-type locus. *Infect Immun*. **69**, 115-122 (2001).

43. Voelz, K. *et al*. Transmission of Hypervirulence Traits via Sexual Reproduction within and between Lineages of the Human Fungal Pathogen *Cryptococcus gattii*. *PLoS Genet*. **9**(9), e1003771 (2013).

44. Yan, Z., Sun, S., Shahid, M. & Xu, J. Environment factors can influence mitochondrial inheritance in the fungus *Cryptococcus neoformans*. *Fungal Genet*. *Biol*. **44**, 315-322 (2007a).

45. Firacative, C. *et al*. MLST and wholegenome-based population analysis of *Cryptococcus gattii* VGIII links clinical, veterinary and environmental strains, and reveals divergent serotype specific sub-populations and distant ancestors. *PLoS Negl Trop Dis*. **10**, e0004861 (2016).

46. Lockhart, S. R. *et al*. *Cryptococcus gattii* in the United States: genotypic diversity of human and veterinary isolates. *PLoS One* **8**, e74737 (2013).

47. Byrnes, E. J. III, Bartlett, K. H., Perfect, J. R. & Heitman J. *Cryptococcus gattii*: an emerging fungal pathogen infecting humans and animals. *Microbes Infect*. **13**, 895-907 (2011).

48. Nielsen, K. *et al*. Sexual cycle of *Cryptococcus neoformans* var. *grubii* and virulence of congenic a and α isolates. *Infect. Immun*. **71**, 4831–4841(2003).

49. Wang, P., Cutler, J., King, J. & Palmer, D. Mutation of the regulator of G protein signalling Crg1 increases virulence in *Cryptococcus neoformans*. *Eukaryot. Cell* **3**, 1028–1035(2004).

50. Wilson, A. Highly Variable Mitochondrial Inheritance in Intra- and Inter-lineage Crosses of *Cryptococcus gattii*. MSc Thesis. Department of Biology, McMaster University, Hamilton, Canada (2011).

51. D'Souza, C. A. *et al*. Genome variation in *Cryptococcus gattii*, an emerging pathogen of immunocompetent hosts. *mBio* **2**(1), e00342-10 (2011).

52. Vogan, A. A. & Xu, J. Evidence for genetic incompatibilities associated with post-zygotic reproductive isolation in the human fungal pathogen *Cryptococcus neoformans*. *Genome* **344**, 335-344 (2014).
53. Kwon-Chung, K. J. & Varma, A. Do major species concepts support one, two or more species within *Cryptococcus neoformans*? *FEMS Yeast Res*. **6**, 574-587 (2006).
54. Vogan, A. A., Khankhet, J. & Xu, J. Evidence for mitotic recombination within the basidia of a hybrid cross of *Cryptococcus neoformans*. *PLoS One* **8**, e62790 (2013).
55. Vogan, A. A., Khankhet, J., Samarasinghe, H. & Xu, J. Identification of QTLs associated with virulence related traits and drug resistance in *Cryptococcus neoformans*. *G3 (Bethesda)* **6**, 2745–2759 (2016).
56. Shahid, M., Han, S., Yoell, H., and Xu, J. Fitness distribution and transgressive segregation across 40 environmental conditions in a hybrid progeny population of the human pathogenic yeast *Cryptococcus neoformans*. *Genome* **51**, 272-281 (2008)
57. Xu, J. *et al*. Uniparental mitochondrial transmission in sexual crosses in *Cryptococcus neoformans*. *Current Microbiology* **40**(4), 269-273 (2000).
58. R Core Team. R: A Language and Environment for Statistical Computing. Vienna, Austria: R Foundation for Statistical Computing (2015).
59. Tamura, K. & Nei, M. Estimation of the number of nucleotide substitutions in the control region of mitochondrial DNA in humans and chimpanzees. *Molecular Biology and Evolution* **10**, 512-526 (1993).
60. Kumar, S., Stecher, G. & Tamura, K. MEGA7: Molecular Evolutionary Genetics Analysis version 7.0 for bigger datasets. *Molecular Biology and Evolution* **33**, 1870-1874 (2016).
61. Meyer, W. *et al*. Consensus multi-locus sequence typing scheme for *Cryptococcus neoformans* and *Cryptococcus gattii*. *Med Mycol.* **47**, 561–570 (2009).
62. Litvintseva, A. P., Lin, X., Templeton, I., Heitman, J. & Mitchell, T. G. Many globally isolated AD hybrid strains of *Cryptococcus neoformans* originated in Africa. *PLoS Pathog*. **3**(8), e114 (2007).

Chapter 4: What are the best parents for hybrid progeny? An investigation into the human pathogenic fungus *Cryptococcus*

4.1 Preface

Hybridization between more divergent organisms is likely to generate more novel genetic interactions and genetic variations. However, the relationship between parental genetic divergence and progeny phenotypic variation remains largely unknown. In this paper, I investigated the patterns of such relationship using the human pathogenic *Cryptococcus*. The results indicate that, as genetic distance increases between parental strains, hybrid progeny showed increased fluconazole resistance and growth at 37 °C but decreased melanin production under various stresses. However, under each tested condition, there was a diversity of phenotypic variations among progeny, including: (i) similar to one of the parents; (ii) intermediate between the parents; (iii) outside the parental phenotypic range. This work is now published in Journal of Fungi, 7(4), 299. References in this chapter appear as they are in the originally published manuscript. I am the primary contributor of this work.

4.2 Abstract

Hybridization between more divergent organisms is likely to generate progeny with more novel genetic interactions and genetic variations. However, the relationship between parental genetic divergence and progeny phenotypic variation remains largely unknown. Here, using strains of the human pathogenic *Cryptococcus*, we investigated the patterns of such a relationship. Twenty-two strains with up to 15% sequence divergence were mated. Progeny were genotyped at 16 loci. Parental strains and their progeny were phenotyped for growth ability at two temperatures, melanin production at seven conditions, and susceptibility to the antifungal drug fluconazole. We observed three patterns of relationships between parents and progeny for each phenotypic trait, including (i) similar to one of the parents, (ii) intermediate between the parents, and (iii) outside the parental phenotypic range. We found that as genetic distance increases between parental strains, progeny showed increased fluconazole resistance and growth at 37 °C but decreased melanin production under various oxidative and nitrosative stresses. Our findings demonstrate that, depending on the traits, both evolutionarily more similar strains and more divergent strains may be better parents to generate progeny

with hybrid vigor. Together, the results indicate the enormous potential of *Cryptococcus* hybrids in their evolution and adaptation to diverse conditions.

4.3 Introduction

Hybridization refers to crosses between two closely related species or divergent populations within a species. Natural hybridization has been reported in most groups of eukaryotes. A diversity of phenotypes has been observed for hybrids, including heterosis (hybrid vigor), outbreeding depression, and intermediate between parents [1−4]. At present, despite our long history of studying hybrids and hybridization, the mechanisms for hybrid offspring phenotype variation remain largely unknown. A longstanding and unsolved issue is the relationship between parental population divergence and hybrid progeny phenotype. In 1936, East proposed that as the genetic distance between parental populations increases, heterosis should become more prevalent [5]. However, there has been limited critical testing of this intriguing hypothesis.

The human pathogenic *Cryptococcus* (HPC) represents an ideal group of organisms to study this hypothesis and investigate the relationships between the genetic divergence of parental strains and offspring phenotypes. HPC consists of multiple evolutionary divergent lineages that have been classified into different species complexes, species, varieties, serotypes, and molecular types [6,7]. For example, there are two species complexes within HPC, the *Cryptococcus neoformans* species complex (CNSC) and the *Cryptococcus gattii* species complex (CGSC), corresponding to an estimated divergence time of ~80 – 100 million years. Each of the two species complexes contains multiple divergent lineages. Importantly, these lineages show a range of nucleotide sequence divergence at the whole genome level, ranging from 2% to ~15% [6,8−11].

HPC has several virulence factors that play crucial roles in the survival and proliferation within the hosts [12]. The three essential virulence factors are the synthesis of melanin, the formation of a polysaccharide capsule, and the ability to grow at mammalian body temperature (37 °C). Melanin has antiphagocytic and antioxidant activities, protecting cryptococcal cells against environmental stressors (e.g., ultraviolet (UV) irradiation and high temperature) and antifungal agents (e.g., amphotericin B) [13,14]. The polysaccharide capsule protects the cells from being phagocytized by host phagocytic cells and allows them to evade the host immune system attack [15,16]. Combined

with the ability to grow at 37 °C, these virulence-related traits allow *Cryptococcus* strains to be a pathogen and thrive in human and animal hosts.

Apart from hybrids, strains of the human pathogenic *Cryptococcus* are generally haploid. They exist in one of the two mating types, *MAT*α and *MAT***a**, with most environmental and clinical strains belonging to *MAT*α [17−19]. Haploid cells typically propagate asexually by budding until strains of the opposite mating types (**a**-α) or even the same mating type (α-α) encounter each other to initiate mating and sexual reproduction [20]. Sexual reproduction can give rise to the generation of diverse genotypes via recombination. This diversity and the resulting phenotypic variation could be key factors in promoting adaptation to changing environments. Evidence of mating and recombination has been reported in the human pathogenic *Cryptococcus* [18,21−24]. Although sexual reproduction is typically rare except in a few regions (e.g., Botswana and Brazil) where it is relatively frequent, evidence of both α-α and **a**-α matings generating diploid/aneuploid hybrids has been found [23,25−32]. Serotype AD hybrids, derived from mating between the VNI (serotype A) and VNIV lineages (serotype D) within CNSC, have been reported in environmental and clinical samples [23,28,33]. However, hybrids between CGSC and CNSC lineages have only been reported from clinical settings and the laboratory [34−37]. Of all reported hybrid populations, serotype AD hybrids are the most common, with a prevalence of 18% in Europe and 6% in the United States [38]. Among the hybrids, there are increasing reports showing evidence of hybrid vigor and transgressive segregation [1,23,39,40]. For example, serotype AD hybrids are often more resistant to UV irradiation and antifungal drugs than their parental strains, as well as more thermotolerant.

In this study, the aim was to address the following question: What are the best parents for hybrid progeny in the human pathogenic *Cryptococcus*? To broadly address this question, we selected 22 parental strains representing six evolutionarily distinct lineages of this fungus to construct crosses. We investigated the effects of parental phenotypic variations on progeny phenotypic variations and the relationship between parental strain sequence divergence and progeny phenotypes. A number of phenotypes were assayed, including growth at 30 °C and 37 °C, melanin production under various oxidative and nitrosative stresses, and susceptibility to the antifungal drug fluconazole. We observed various degrees of phenotypic variation and phenotypic plasticity among

the progeny. We also identified different relationships between parental genetic divergence and progeny phenotypes among the measured traits.

4.4 Materials and Methods

4.4.1 Parental strains and Progeny

Twenty-two *Cryptococcus* strains were used as parental strains in this study (Table 4.1). There were six VGI strains (two *MAT***a** and four *MAT*α), four VGII strains (one *MAT***a** and three *MAT*α), six VGIII strains (three *MAT***a** and three *MAT*α), one VGIV strain (*MAT*α), three VNI strains (one *MAT***a** and two *MAT*α), and two VNIV strains (one *MAT***a** and one *MAT*α). These *MAT***a** strains and *MAT*α strains were mated on V8 agar, following the protocol described in You and Xu [37]. After two to six weeks of incubation at room temperature (~23 °C), hyphae started to form. To collect progeny, once formed, hyphae without parental cells were streaking out on new yeast extract–peptone–dextrose (YEPD) agar plates and incubated at 37 °C for three days. The 37 °C temperature was used to select diploid yeast cells from dikaryotic hyphae. Then, all single yeast colonies on each plate were picked and purified. The mating types of these colonies were determined by using the primers of *STE20***a** and *STE12*α genes. Only those containing both mating types were selected for further analyses in this study.

Genetic distance between mating partners was calculated to estimate the parental genetic divergence, based on five gene loci (*GPD1*, *LAC1*, *PLB1*, *URA5*, and *IGS1*). All gene fragments were amplified using the polymerase chain reaction (PCR) conditions described by Meyer *et al*. [41]. Sequences were obtained from GenBank or sequencing. The phylogenetic analysis, using the neighbor-joining method with 1000 bootstrap replicates, was performed to compute the genetic distances between mating partners in MEGA 7.0 [42]. Details about the primers and PCR conditions are listed in Table 4.2.

Table 4.1. Strains of the *C. neoformans* species complex (CNSC) and *C. gattii* species complex (CGSC) were used as parents in this study.

Species complex	Lineage	Isolate ID	Mating type	Source
CGSC	VGI	B4495	*MAT***a**	Clinical
		B4545	*MAT***a**	Clinical
		WM179	*MAT*α	Human, CSF
		WM276	*MAT*α	*E. tereticornis*
		R794	*MAT*α	Human, CSF
		R299	*MAT*α	Human, CSF
	VGII	LA55	*MAT***a**	Human, CSF
		R265	*MAT*α	Human, BAL
		LA61	*MAT*α	Human, CSF
		KB5746	*MAT*α	Horse
	VGIII	B4546	*MAT***a**	Clinical
		JF109	*MAT***a**	Lab strain
		ATCC32608	*MAT***a**	Human, CSF
		B4544	*MAT*α	Clinical
		JF101	*MAT*α	Lab strain
		B4499	*MAT*α	Clinical
	VGIV	WM779	*MAT*α	Cheetah
CNSC	VNI	KN99**a**	*MAT***a**	Lab strain
		KN99α	*MAT*α	Lab strain
		CDC15	*MAT*α	Clinical
	VNIV	JEC20	*MAT***a**	Lab strain
		JEC21	*MAT*α	Lab strain

Table 4.2. Details of primers, PCR protocols, and restriction enzymes that were used in this study.

Genes	**Primer Sequences (5'-3')**	**Amplification conditions**	**Restriction enzymes**
STE12α	F: CTGAGGAATCTCAAACCAGGGA	94°C 4min; 35 cycles: 94°C 45s, 55°C 45s, 72°C 1min	NA
	R: CCAGGGCATCTAGAAACAATCG		
*STE20***a**	F: GATCTCTCTCAGCAGGCCAC		NA
	R: AAATATCAGCTGCCCAGGTGA		
ND2	F: TATGATGGCCGTAGCGCTATC	94°C 4min; 35 cycles: 94°C 1min, 50°C 30s, 72°C 1min	PvuII
	R: TGGTGGTACTCCTGCCATTG		
ND4	F: GGGAGAATTTGATTCAAGTGCAAC		SacI
	R: ATGATGTTGCATCTGGCATCATAC		
GPD1	F: CCACCGAACCCTTCTAGGATA	94°C 3min; 35 cycles: 94°C 45s, 63°C 1min, 72°C 2min	NA
	R: CTTCTTGGCACCTCCCTTGAG		
LAC1	F: AACATGTTCCCTGGGCCTGTG	94°C 3min; 30 cycles: 94°C 30s, 58°C 30s, 72°C 1min	NA
	R: ATGAGAATTGAATCGCCTTGT		
PLB1	F: CTTCAGGCGGAGAGAGGTTT	94°C 3min; 30 cycles: 94°C 45s, 61°C 45s, 72°C 1min	NA
	R: GATTTGGCGTTGGTTTCAGT		
IGS1	F: ATCCTTTGCAGACGACTTGA		NA

	R: GTGATCAGTGCATTGCATGA	94℃ 3min; 35 cycles: 94℃ 30s, 60℃ 30s, 72℃ 1min	
URA5	F: ATGTCCTCCCA AGCCCTCGAC	94℃ 3min; 35 cycles: 94℃ 45s, 61℃ 1min, 72℃ 2min	HhaI
	R: TTAAGACCTCT GAACACCGTACTC		
CAP59	F: CTCTACGTCGAGCAAGTCAAG	94℃ 3min; 35 cycles: 94℃ 30s, 57℃ 30s, 72℃ 1min	HinfI
	R: TCCGCTGCACAAGTGATACCC		
CNL06810	F: TTAATGGACTGGGCAGATGCTCGTC	94℃ 4min; 36 cycles: 94℃ 45s, 55℃ 45s, 72 1min	HhaI
	R: ATGTCTTCTCCCGCCCTTTTTGCC		
CNI01350	F: GAGCGACATCGTCCCTATGTGA		HinfI
	R: ACTGGTAGCAATGGCGACATG		
CNK01700	F: ACGCACTCTCACAGCTCCTTCG		HpyCH4IV
	R: GCAAAGCTCAGGCTCAAATCCAG		
CNM00180	F: GCTCAAGAACCATACCTGCTCAT		Sau96I/HpyAV
	R: GGCGGCAGGTGACTTCAGTG		
CGND	F: TGCGAGTCGAAGGCRGACTATGATCGTCTGATTGC	94℃ 4min; 36 cycles: 94℃ 45s, 60℃ 45s, 72 1min	HinfI
	R: GCTGGATCCGTTCCTTGATAGCRGCCCACTTTGCG		
CGNM	F: AGCATCGTCGATGGACATCKTGGACCTTCTTCGCC		HpyCH4IV
	R: CAGAGAGCCCAGACRAAGGAGGCGAGGAACATGGC		
ERG11	F: CTTTGGGTGGAAAGATTTCTCAAGTCTCTGCCGAG		AluI/Sau3A

	R: GCGGCGGCAAATCCCTTTTCRTCGTGCCATCGGGC		
CGNA	F: AGGCCCCGAGGTTGTTGCCGARGCTGTCCGAG		AccI
	R: TCGGGGGCACCGGCGAGAGACGCAGARGGGAGGAG		
CNB00360	F: AGTGCTCAGAGTCTGGGGCTGG		HincII
	R: GCCATTCGCAGGGGTGGAGG		
CNE00250	F: TGGCGTCTCTTTGAACGCGATC		HaeII
	F: ATGGCGGAATGTCCGGCTTT		
CNH02750	F: TTGGATCGCTTGCTCGCGAA		XhoI
	R: AGGCCCGAGCAAAGGAATGA		

4.4.2 Ploidy analyses

The ploidy levels of both parents and progeny were determined by fluorescence-activated cell sorting (FACS), similar to the protocol used by Skosireva *et al*. [43]. Briefly, cells grown overnight were harvested from YEPD agar medium (~10^7 cells/mL), washed once in phosphate-buffered saline (PBS), and then fixed in 1mL of 70% ethanol at 4 °C for at least 6 h. Fixed cells were washed once in NS buffer, then stained with 5 µL of propidium iodide (10 mg/mL) in 180 µL NS buffer adding 20 µL of RNaseA (10 mg/mL) and incubated with agitation for 3 h at room temperature or overnight at 4 °C 50 µL of stained cells were diluted into 2 mL of 50 mM Tris-HCl (pH 8.0) and sonicated for 10s. Flow cytometry was performed on a Becton–Dickinson LSR II model with ~10^4 cells. Data were analyzed and visualized by ModFit LT 5.0 (Verity Software House). Parental strain JEC21 was used as a haploid control, and D15 (RAS strain) was used as a diploid control [44].

4.4.3 Polymerase chain reaction-restriction length polymorphism (PCR-RFLP) genotyping

Fourteen nuclear markers and two mitochondrial markers (*ND2* and *ND4*) were used for genotyping. The 14 nuclear markers are located on 10 of 14 chromosomes, including *CAP59*, *CGNA*, *ERG11*, *CNB00360*, *CNK01700*, *CNL06810*, *CGND*, *MAT* locus (*STE12*α and *STE20***a**), *CNE00250*, *URA5*, *CNI01350*, *CNM00180*, *CGNM2*, and *CNH02750*. Except for the *MAT* locus, the remaining 15 markers were used for polymerase chain reaction-restriction length polymorphism (PCR-RFLP) genotyping, distinguishing the parental strains for each successful cross. The choice of markers to represent the chromosomes was based on the genome annotation of the model strain JEC21 (of the VNIV lineage). These PCR-RFLP markers were either obtained from the previous studies [45,46,47] or designed using Prifi [48] based on the whole genome sequences of KN99 (VNI lineage), JEC21 (VNIV lineage), R265 (VGII lineage), and WM276 (VGI lineage). PCR products were analyzed on 1.0% agarose gels. All restriction digestions were performed following the manufacturer's instructions (NEB, UK) and separated on 2.0% agarose gels at 80 V for 2 h. Figure 4.1 shows the locations of the twelve nuclear markers across chromosomes. The information on the markers and restriction enzymes used for PCR-RFLP genotyping is listed in Table 4.2.

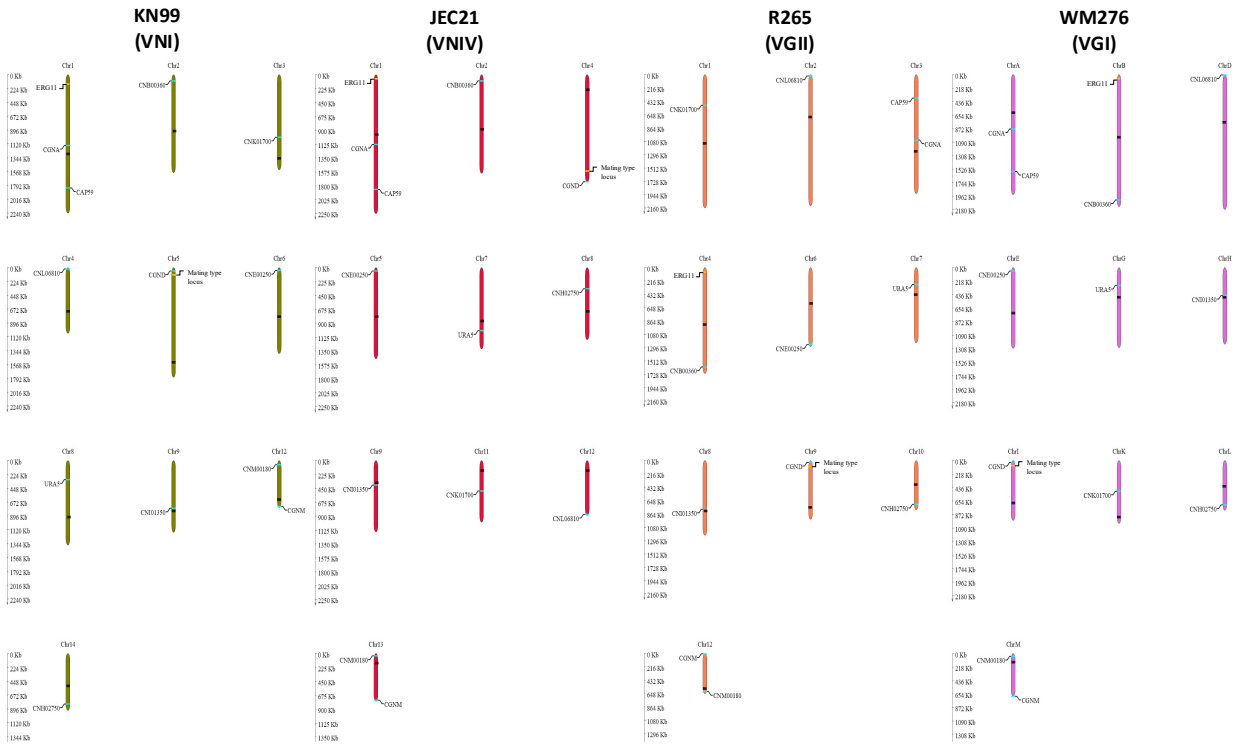

Figure 4.1. Chromosomal locations of the fourteen polymerase chain reaction-restriction length polymorphism (PCR-RFLP) markers that were used for progeny genotyping in this study. These markers were located across 10 chromosomes (out of 14) on the four reference genomes of strains, KN99 (VNI lineage), JEC21 (VNIV lineage), R265 (VGII lineage), and WM276 (VGI lineage). Dark text indicates the location of centromeres.

4.4.4 Phenotype assays

Parental strains and progeny were grown on YEPD agar for two days at 30 °C. Fresh cells were suspended in sterile water for the following phenotyping experiments.

For growth assay, the cell density was adjusted to ~10^6 cells/mL in medium Roswell Park Memorial Institute (RPMI) 1640. 200 µL of each strain, with three replicates, was then inoculated in 96-well microplates and incubated at 30 °C or 37 °C for three days. The growth potential was determined by spectrophotometer using optical density (OD) of 600 nm.

For melanin assay, cell density was adjusted to ~10^6 cells/mL in sterile water. Oxidative stresses caused by reactive oxygen species (ROS) and nitrosative stresses caused by reactive nitrogen species (RNS) were generated by adding hydrogen peroxide (H_2O_2) and sodium nitrite ($NaNO_2$) to the caffeic acid agar, respectively, with three concentrations (0.25 mM, 0.5 mM, and 1 mM) of each. The regular caffeic-acid agar [49] without any added stress was used as the control. 5 µL of each cell suspension for each strain, with four replicates, was spotted onto the agar plates and incubated at 30 °C for seven days. Melanin production was approximated by light reflection using ImageJ [50]. Parental strains and their progeny were plated on the same plates to mitigate the potential batch effects. Additionally, JEC21 (VNIV lineage) was used as a reference on each plate for data standardization.

For antifungal susceptibility assay, concentrations of 0 µg/mL, 0.5 µg/mL, 1 µg/mL, 2 µg/mL, 4 µg/mL, 8 µg/mL, 16 µg/mL, 32 µg/mL, 64 µg/mL, and 128 µg/mL of fluconazole were evaluated, following the M27-A3 guidelines (the Clinical and Laboratory Standards Institute, CLSI) [51]. The adjusted cells were inoculated in 96-well plates and incubated for 72h at 35 °C (the CLSI recommended temperature) and 37 °C (the mammalian body temperature), respectively. The minimum inhibitory concentration (MIC) was determined in the treated samples.

4.4.5 Statistical analysis

The coefficient of variation (CV) was used as an index to determine (i) phenotypic variation between parental strain pairs and among progeny from each cross; and (ii) phenotypic plasticity of each strain across environments for each trait. We analyzed the

amounts of phenotypic variations among progeny from each cross and compared them with their parents under the same experimental condition, using CV_s values. A higher CV_s value indicates a greater phenotypic variation. We calculated two CV_i values for individual progeny and each parental strain, one for growth under two temperature conditions and the other for melanin production under seven conditions, and compared them with their parental strains. A high CV_i value indicates high phenotypic plasticity in the specific trait for the strain, while a low CV_i value suggests that the trait is relatively stably expressed under diverse conditions for the strain. The details of CV_s and CV_i are shown in Table 4.S1. The Pearson correlation tests were used to determine the potential relationships between parental genetic distance and the phenotypic values of progeny under each environmental condition.

The better-parent heterosis (BPH) was calculated to determine progeny performance as compared to their parents. BPH is the percentage of progeny that had a higher phenotypic value than the high-phenotype value parent. In addition, the Pearson correlation tests were performed to determine its potential relationship with parental genetic distance. Furthermore, evidence for transgressive segregation was evaluated for progeny by comparing their phenotypic values with the phenotype range of their respective parents for each of the traits. Trait values that are two standard deviations higher than the high-value parent or two standard deviations lower than the low-value parent are referred to as positive and negative transgressive segregants, respectively.

All statistical analyses and visualization of data were performed using R (version 4.0.3) [52]. The progeny multi-locus genotypes were determined using the R package "poppr" [53]. The relationships between parental genetic distances and progeny phenotypes were estimated by performing a generalized linear model using the R package "lme4" and displayed and predicted by effect plots using the R package "effects" [54,55]. The Pearson correlation tests were used to determine the correlation between parental genetic distance and progeny phenotype, phenotypic plasticity, and BPH rates. All figures were visualized using the R package "ggplot2" [56].

4.5 Results

We constructed genetic crosses and collected progeny. The ploidy levels of all progeny were determined by FACS. For all parental strains and their progeny, we obtained

the quantitative phenotype values of their growth ability, melanin production, and fluconazole susceptibility. Based on the quantitative data, several analyses were performed. Below we describe the results of our genotypic and phenotypic assays of the progeny.

4.5.1 Progeny collection and Ploidy analyses

In our previous analyses, we found that strains of VGIII lineage were generally more fertile than those of other lineages. Thus, we constructed crosses using at least one VGIII strain in each cross. By using 22 parental strains, 58 genetic crosses were attempted and 22 of them were successful. These 22 successful crosses consisted of six (out of nine attempted) intra-VGIII crosses, three (of 18 attempted) inter-lineage VGI × VGIII crosses, two (of 13 attempted) inter-lineage VGII × VGIII crosses, one (of three attempted) inter-lineage VGIV × VGIII cross, five (of nine attempted) inter-lineage VNI × VGIII crosses, and five (of six attempted) inter-lineage VNIV × VGIII crosses. Details of successful crosses and their progeny are listed in Table 4.3.

Table 4.3. Information on crosses, the genetic distance between parental strains, ploidy levels of progeny, multi-locus genotypes (MLG), and minimum inhibitory concentration (MIC) values to fluconazole.

Mating Groups	Genetic Crosses	*MAT*a parent	*MAT*α parent	Genetic distances between parents	Progeny ID	Ploidy	Multilocus genotypes	MIC
Intra-lineage group	VGIIIxVGIII	B4546 (VGIII) MIC=1	B4544 (VGIII) MIC=4	0.005	YMA79	A	NA	4
				0.005	YMA80	A	NA	4
				0.005	YMD81	D	NA	4
		JF109 (VGIII) MIC=2	B4544 (VGIII) MIC=4	0.005	YMA62	A	NA	8
				0.005	YMA63	A	NA	8
				0.005	YMA64	A	NA	8
		ATCC32608 (VGIII) MIC=4	B4544 (VGIII) MIC=4	0.005	YMA65	A	NA	8
				0.005	YMA66	A	NA	8
				0.005	YMA68	A	NA	8
		B4546 (VGIII) MIC=1	JF101 (VGIII) MIC=4	0.009	YMA73	A	NA	4
				0.009	YMA74	A	NA	4
				0.009	YMA138	A	NA	2
		JF109 (VGIII) MIC=2	JF101 (VGIII) MIC=4	0.009	YMA102	A	NA	4
				0.009	YMA125	A	NA	4
				0.009	YMA136	A	NA	1
		ATCC32608 (VGIII) MIC=4	JF101 (VGIII) MIC=4	0.009	YMA77	A	NA	4
				0.009	YMA78	A	NA	4
				0.009	YMA105	A	NA	4
Inter-lineage group	VGIxVGIII	B4495 (VGI) MIC=2	B4544 (VGIII) MIC=4	0.033	YMD53	D	MLG.21	4
				0.033	YMD90	D	MLG.19	2
				0.033	YMD96	D	MLG.12	4
		B4495 (VGI) MIC=2	JF101 (VGIII) MIC=4	0.038	YMD69	D	MLG.20	4
				0.038	YMA71	A	MLG.20	4
				0.038	YMD72	D	MLG.20	4
		B4545 (VGI) MIC=2	JF101 (VGIII) MIC=4	0.04	YMD85	D	MLG.18	4
				0.04	YMD86	D	MLG.17	4
	VGIVxVGIII	JF109 (VGIII) MIC=2	WM779 (VGIV) MIC=2	0.045	YMD36	D	MLG.11	2
	VGIIxVGIII	LA55 (VGII) MIC=32	JF101 (VGIII) MIC=4	0.128	YMD111	D	MLG.13	8
		B4546 (VGIII) MIC=1	R265 (VGII) MIC=4	0.135	YMD132	D	MLG.8	8
				0.135	YMD135	D	MLG.8	8
				0.135	YMD150	D	MLG.7	8
	VNIxVGIII	JF109 (VGIII) MIC=2	KN99α (VNI) MIC=1	0.17	YMD112	D	MLG.5	4
				0.17	YMD113	D	MLG.5	8
				0.17	YMD114	D	MLG.5	8
		B4546 (VGIII) MIC=1	KN99α (VNI) MIC=1	0.17	YMD29	D	MLG.5	4
				0.17	YMT33	T	MLG.5	4
		KN99a (VNI) MIC=1	JF101 (VGIII) MIC=4	0.171	YMD1	D	MLG.1	1
				0.171	YMD5	D	MLG.1	2
				0.171	YMD10	D	MLG.1	2
		JF109 (VGIII) MIC=2	CDC15 (VNI) MIC=32	0.172	YMA162	A	MLG.4	16
				0.172	YMD164	D	MLG.6	32
				0.172	YMD165	D	MLG.4	16
		B4546 (VGIII) MIC=1	CDC15 (VNI) MIC=32	0.172	YMD34	D	MLG.4	16
				0.172	YMD83	D	MLG.2	16
				0.172	YMT98	T	MLG.3	4
	VNIVxVGIII	JF109 (VGIII) MIC=2	JEC21 (VNIV) MIC=1	0.172	YMD87	D	MLG.9	4
		B4546 (VGIII) MIC=1	JEC21 (VNIV) MIC=1	0.172	YMD88	D	MLG.10	4
				0.172	YMD89	D	MLG.9	4
		JEC20 (VNIV) MIC=1	JF101 (VGIII) MIC=4	0.173	YMD16	D	MLG.15	4
				0.173	YMD17	D	MLG.16	4
		JEC20 (VNIV) MIC=1	B4544 (VGIII) MIC=4	0.171	YMD11	D	MLG.14	8
				0.171	YMD12	D	MLG.22	8
		ATCC32608 (VGIII) MIC=4	JEC21 (VNIV) MIC=1	0.171	YMD25	D	MLG.10	4
				0.171	YMD26	D	MLG.10	4
				0.171	YMD27	D	MLG.1	4

A: aneuploidy; D: diploidy; T: triploidy.
NA: genotype was not able to be determined.

Previous studies have shown that the human pathogenic *Cryptococcus* hybrids are often diploid/aneuploid and are heterozygous at the mating-type locus. Thus, to standardize our comparison, we selected only progeny that contained mating-type genes from both parents for downstream analyses. From the 22 crosses, 55 progeny were collected for further study by confirming the heterozygosity at the *MAT* locus. FACS analyses revealed that 34 out of 55 progeny (~62%) were likely diploid, with twice the amount of DNA of the haploid parental strains and similar to the diploid control. Nineteen progeny (~35%) had FACS profiles intermediate between haploidy and diploidy, consistent with aneuploidy. The remaining two progeny had ploidy levels higher than the diploid reference strain, with profiles consistent with triploidy. Figure 4.2 shows the representative FACS profiles of the obtained progeny. The ploidy estimates of all 55 progeny are presented in Table 4.3.

4.5.2 Genotypic diversity and Variable mtDNA inheritance

Aside from the *MAT* locus, we analyzed 13 nuclear and two mitochondrial markers using PCR-RFLP for progeny genotyping. However, due to the high sequence similarities among the VGIII parental strains, the 18 progeny from the six intra-VGIII lineage crosses could not be distinguished from each other using these PCR-RFLP markers. For the remaining 37 hybrid progeny from the 16 inter-lineage crosses, their multi-locus genotypes were determined.

All 37 hybrids were heterozygous at *ERG11* and *MAT* locus, while they were homozygous at one locus *CAP59* (Table 4.S1). Most hybrids were heterozygous at the remaining 11 nuclear loci. Across the 14 nuclear loci, the rates of heterozygosity among the hybrids ranged from ~57% to ~93% (Table 4.S1). We found that the parental genetic distance was significantly negatively correlated with the frequency of progeny that were homozygous for alleles from the *MAT***a** parents ($r = -0.4$, $p = 0.014$). That is, with an increasing genetic distance between parental strains, there was a significant decrease in the proportion of progeny that were homozygous for alleles from the *MAT***a** parents. The 37 hybrids were assigned to 22 unique multi-locus genotypes (Table 4.3). Among these hybrids, 11 hybrids from four crosses had identical genotypes at the assayed loci with their siblings, whereas 26 hybrids from another nine crosses had different genotypes.

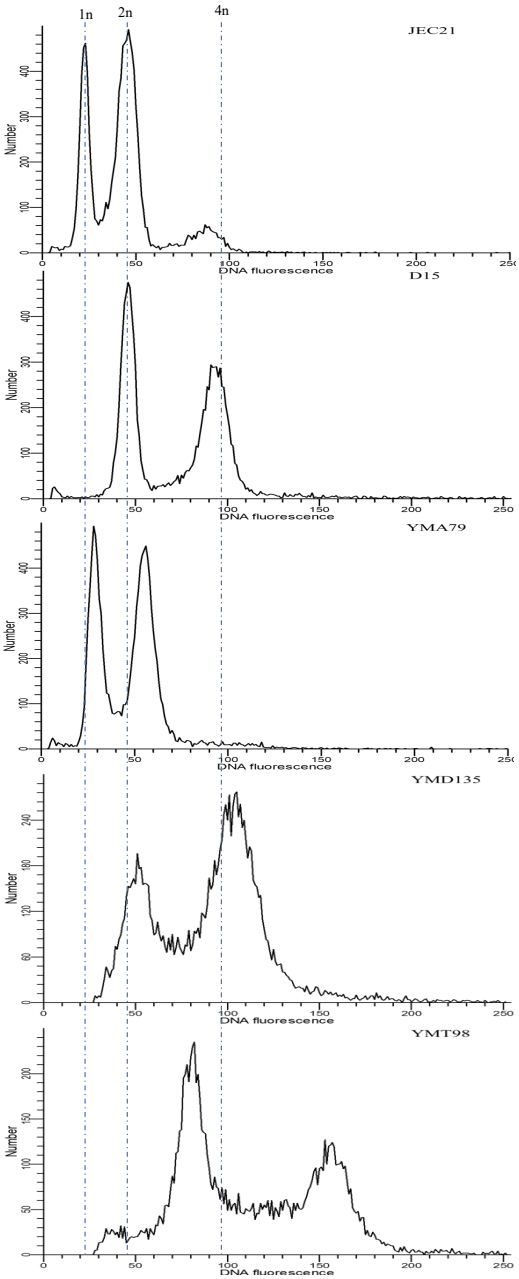

Figure 4.2. Three different ploidy levels were observed among progeny. Fluorescence-activated cell sorting (FACS) profiles of haploid control JEC21 (1n), diploid control D15 (2n), likely aneuploid progeny YMA79 (between 1n and 2n), likely diploid progeny YMD135 (2n), and likely triploid progeny YMT98 (between 2n and 4n) are shown here. 1n, 2n, and 4n indicate nuclear DNA content. The x-axis shows the relative fluorescence intensity of DNA content, and the y-axis represents the number of the counted cells of each fluorescence intensity category.

Analyses of the two mitochondrial markers identified three mitochondrial inheritance patterns among the 37 hybrids (Table 4.S1). They included that 20 hybrids inherited mtDNA from the *MAT***a** parents (~54%), seven inherited from the *MAT***α** parents (~19%), and ten hybrids had recombinant mitochondrial genotypes (~27%, with each having a combination of alleles from the *MAT***α** and *MAT***a** parents for the two different mitochondrial marker genes). Interestingly, all recombinant mitochondrial genotypes were found in progeny derived from the inter-lineage crosses between strains of the two species complexes, CNSC and CGSC. Of the 10 hybrids with recombinant mitochondria, all had the *ND2* allele from the *MAT***α** parents and the *ND4* allele from the *MAT***a** parents.

4.5.3 Growth at 30 °C and 37 °C

4.5.3.1 Phenotypic Variation

As shown in Table 4.S2, parental strains showed a range of growth ability at both 30 °C and 37 °C. CV_s values of parental strains ranged from 0.011 to 0.664 at 30 °C and from 0.004 to 0.356 at 37 °C. The big ranges were found for both evolutionarily similar and divergent strain pairs. For example, at 30 °C, divergent parental pair JEC21 (VNIV lineage) and JF109 (VGIII lineage) grew similarly (CV_s = 0.011) while another divergent pair KN99**α** (VNI lineage) and B4546 (VGIII lineage) showing a CV_s value of 0.664. An intra-VGIII parental strain pair B4546 and B4544 showed a notable difference at 30 °C (CV_s = 0.650) while little difference at 37 °C (CV_s = 0.017). The wide range of parental phenotype variations enabled us to examine the effects of parental strain divergence on progeny phenotype relative to such variations.

We also found a range of CV_s values among progeny, ranging from 0.022 to 0.246 at 30 °C and from 0.013 to 0.348 at 37 °C (Table 4.S2). The progeny from the intra-VGIII cross JF109 × JF101 showed the greatest CV_s at 30 °C (CV_s = 0.246). At 37 °C, the progeny from KN99**a** × JF101 (VNI × VGIII) showed the most variation (CV_s = 0.348). The progeny from JEC20 × JF101 (VNIV × VGIII) had relatively low CV_s values at both temperatures (CV_s values 0.053 and 0.013, respectively). Of the 19 crosses with each having two or more progeny, the progeny of five crosses (~26%, 5/19) showed a greater CV_s at 30 °C while the progeny from nine crosses (~47%, 9/19) showed

higher CV_s at 37 °C than those of their respective parental pairs (highlighted in Table 4.S2). Progeny of two inter-lineage crosses, CDC15 × JF109 (VNI × VGIII) and JEC21 × ATCC32608 (VNIV × VGIII), displayed greater differences in growth at both temperatures than those between parental strains.

Between the two temperatures, the progeny showed overall greater growth differences than parental strains, mainly due to an overall higher growth reduction of most progeny at 37 °C ($p < 0.001$). In contrast, the parental strains remained relatively stable at the two temperatures ($p = 0.301$).

Interestingly, the observed phenotypic variation between parents was significantly negatively associated with that between progeny at 37 °C ($r = -0.46$, $p = 0.049$), while not at 30 °C ($r = -0.19$, $p = 0.435$). In addition, there was a significant negative correlation between ploidy levels and growth ability at both 30 °C ($r = -0.32$, $p = 0.008$) and 37 °C ($r = -0.47$, $p < 0.001$) when both parental strains and progeny were included in the analyses. Similarly, parental genetic distance was significantly negatively correlated with the relative growth rates of progeny at both 30 °C ($r = -0.57$, $p < 0.001$) and 37 °C ($r = -0.46$, $p < 0.001$). However, when progeny from the intra-VGIII crosses were excluded, parental genetic distance was found significantly positively correlated with progeny growth at 37 °C ($r = 0.34$, $p = 0.037$) while not significantly correlated at 30 °C ($r = -0.21$, $p = 0.220$).

4.5.3.2 Better-parent heterosis and Transgressive segregation

Of the 55 progeny, 14 (~26%) at 30 °C and 21 (~38%) at 37 °C displayed BPH (Table 4.S3). Ten progeny showed BPH at both temperatures, including three progeny (YMA62, YMA63, and YMA64) from JF109 × B4544 (intra-VGIII). Significantly, the genetic distance between parents was negatively associated with BPH rates of progeny at both 30 °C ($r = -0.54$, $p < 0.001$) and 37 °C ($r = -0.32$, $p = 0.017$) (Figure 4.3). Also, transgressive segregation in both positive and negative directions was observed at both temperatures (Table 4.S3). At 30 °C, five progeny (~9%) showed positive transgressive phenotypes, whereas three progeny (~6%) had negative transgressive phenotypes. At 37 °C, 14 progeny (~26%) displayed positive transgressive segregation, while nine (~16%) exhibited negative transgressive segregation.

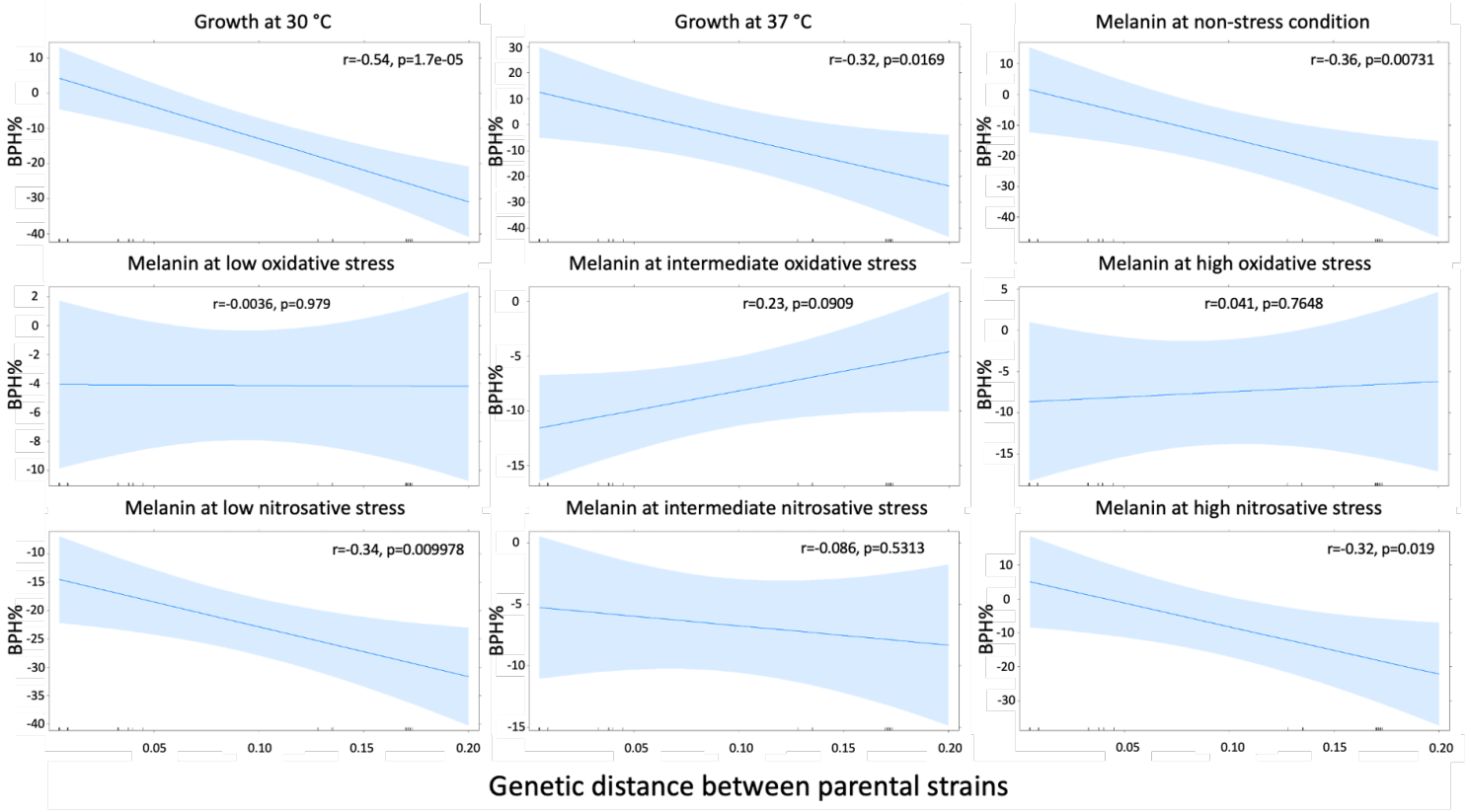

Figure 4.3. Effects of parental genetic divergence on %BPH (better-parent heterosis) in growth (30 °C and 37 °C) and melanin synthesis (non-stress, low oxidative stress, intermediate oxidative stress, high oxidative stress, low nitrosative stress, intermediate nitrosative stress, and high nitrosative stress). The x-axis shows the genetic distance between parental pairs. The y-axis represents the percentage of BPH.

4.5.3.3 Phenotypic plasticity

We found a range of CV_i values in growth for both parental strains and their progeny (Table 4.S2). CV_i values ranged from 0.065 to 0.488 among parental strains and from 0.055 to 0.553 among progeny. The range of variation was not related to specific lineages among parental strains. For example, JF101 (VGIII lineage) had a very low CV_i value of 0.064, whereas B4544 (VGIII lineage) had the highest CV_i value of 0.488. Among progeny, the overall highest CV_i values were found from B4495 × B4544 (VGI × VGIII) where all three progeny had CV_i values ranged from 0.534 to 0.553. In contrast, two progeny YMA162 and YMD165 from CDC15 × JF109 (VNI × VGIII) had the lowest CV_i values (0.055 and 0.082, respectively).

When comparing each progeny with its respective parents, we found several patterns. Some progeny showed more variation in growth than their parents. However, others showed variations either in-between the parents or less than both parents. Overall, 20 of the 55 progeny (~36%) had higher CV_i values than both parents (highlighted in Table 4.S2), indicating that they displayed greater plasticity than their parents in growth. For the remaining 35 progeny, 14 progeny had lower CV_i values than both parents, while 21 had intermediate CV_i values between their parents. Among the 22 crosses, we found: all progeny of four crosses had greater CV_i values than their parental strains; all progeny of four other crosses had lower CV_i values than both parents; the remaining 14 crosses had progeny as intermediates of the parental strains or a mixture of patterns. However, there was no correlation between parental genetic distance and progeny phenotypic plasticity in growth ($r = -0.02$, $p = 0.8712$). Our data showed a variety of growth patterns for the progeny when compared to their parents when exposed to different temperatures.

4.5.4 Melanin production at various environmental conditions

4.5.4.1. Melanin at the non-stress condition

4.5.4.1.1 Phenotypic variation

The CV_s values between parents varied from 0.010 to 0.567 (Table 4.S2). Both genetically divergent and closely related parental pairs had a wide range of CV_s values.

For example, among intra-VGIII crosses, the parental pair ATCC32608 and JF101 showed little difference (CV_s = 0.010), while the parental pair ATCC32608 and B4544 displayed big differences (CV_s = 0.477). Similarly, among inter-lineage crosses, parental pair KN99a (VNI lineage) and JF101 (VGIII lineage) produced comparable melanin (CV_s = 0.047), whereas parental pair JEC20 (VNIV lineage) and B4544 (VGIII lineage) produced notably different amount of melanin (CV_s = 0.567).

Similarly, progeny also had a range of CV_s values, from 0.019 to 0.554 (Table 4.S2). For example, the progeny from the inter-lineage VGI × VGIII cross B4545 × JF101 showed the most difference in melanin (CV_s = 0.554), while progeny of the inter-lineage VNIV × VGIII cross JEC20 × B4544 produced the most similar amount of melanin (CV_s = 0.019). In total, progeny of six crosses showed greater variation in melanin than that between their parents (highlighted in Table 4.S2). However, the observed variation between parents was not associated with that among progeny (r = 0.32, p = 0.182).

4.5.4.1.2 Better-parent heterosis and Transgressive segregation

Of the 55 progeny, 10 progeny (~18%) showed evidence of BPH (Table 4.S3). Eight out of these ten were from five intra-VGIII crosses and two were from two inter-lineage VGI × VGIII crosses. Significantly, parental genetic distance was negatively correlated with the BPH rates of progeny (r = −0.36, p = 0.007) (Figure 4.3). Also, transgressive segregation in both directions was observed (Table 4.S3). Among the 55 progeny, three (~5%) displayed transgressive phenotypes in the positive direction, while four (~7%) had negative transgressive phenotypes. Surprisingly, all three progeny of KN99**a** × JF101 (VNI × VGIII) displayed negative transgressive phenotypes. Three out of the 10 progeny with BPH showed positive transgressive segregation. Overall, our results suggest that genetically more divergent parents generated fewer progeny with BPH in melanin production at the non-stress condition.

4.5.4.2 Melanin at oxidative stress conditions

4.5.4.2.1 Phenotypic variation

Parental strains showed a range of melanin production at the three oxidative stress levels (Table 4.S2). CV_s values varied from 0.001 to 0.436 at low, from 0.001 to 0.212

at intermediate, and from 0.001 to 0.535 at high oxidative stresses. Of the 22 parental pairs, 20 (~91%) at low, 19 (~86%) at intermediate, and 16 (~73%) at high oxidative stresses showed relatively small differences with CV_s values less than 0.1. Low and high CV_s values were observed for both evolutionarily similar and divergent strain pairs, although most pairs had small CV_s values under three oxidative stresses. The results indicate that most parental pairs, either evolutionarily similar or divergent, produced similar amounts of melanin at oxidative stresses.

Variations among progeny were also observed under three oxidative stresses (Table 4.S2). CV_s values ranged from 0.008 to 0.324 at low, from 0.003 to 0.245 at intermediate, and from 0.004 to 0.420 at high oxidative stresses. Under low oxidative stress, progeny from 17 (~89%, 17/19) crosses had CV_s values less than 0.1, with progeny of ATCC32608 × B4544 (intra-VGIII) showing the most variation (CV_s = 0.324), while progeny of JF109 × B4544 (intra-VGIII) showing the least difference (CV_s = 0.008). Interestingly, both parental strains and progeny from ATCC32608 × B4544 (intra-VGIII) showed the most variation as compared to other crosses at low oxidative stress. Under intermediate stress, progeny from 17 out of 19 (~89%) crosses had CV_s values less than 0.1. Progeny from B4545 × JF101 (VGI × VGIII) showed the highest CV_s of 0.245, while progeny of ATCC32608 × B4544 (intra-VGIII) produced the most comparable melanin (CV_s = 0.003). Under high oxidative stress, progeny from 14 crosses (~74%, 14/19) had CV_s values less than 0.1. Progeny of CDC15 × JF109 (VNI × VGIII) had the smallest CV_s value of 0.004, whereas progeny from B4546 × B4544 (intra-VGIII) had the greatest CV_s value of 0.420.

Similar to parental strains, most progeny produced comparable melanin under all oxidative stresses. Of the 19 crosses with progeny having CV_s values, progeny of ten (~53%) crosses at low, nine (~47%) crosses at intermediate, and seven (~37%) crosses at high oxidative stresses had greater CV_s values than their parents (highlighted in Table 4.S2). Interestingly, there were significant positive correlations between the observed parental variation and progeny variation at low ($r = 0.79$, $p < 0.001$) and high ($r = 0.694$, $p = 0.001$) oxidative stresses. However, no correlation was found at intermediate oxidative stress ($r = 0.05$, $p = 0.835$).

4.5.4.2.2 Better-parent heterosis and Transgressive segregation

Of the 55 progeny, 18 (~33%) at low, five (~9%) at intermediate, and 18 (~33%) at high oxidative stresses showed BPH (Table 4.S3). Four progeny (YMA73, YMA74, YMD85, and YMD1) displayed BPH at all three stresses. Eight progeny (~15%, 8/55) showed BPH at both low and high oxidative stresses. However, parental genetic distance was not correlated with the progeny BPH rates at any of the three tested oxidative stresses ($r = 0.003$, $p = 0.979$, at low stress; $r = 0.23$, $p = 0.091$, at intermediate stress; $r = 0.04$, $p = 0.765$, at high stress; Figure 4.3).

Transgressive segregation was also observed (highlighted in Table 4.S3). Specifically, 11 progeny (20%, 11/55) at low, one progeny (~2%, 1/55) at intermediate, and 10 progeny (~18%, 10/55) at high oxidative stresses showed positive transgressive segregation. Two progeny, YMA73 and YMD85, exhibited positive transgressive phenotypes at all three stresses. In contrast, seven progeny (~13%, 7/55) at low, nine progeny (~16%, 9/55) at intermediate, and six progeny (~11%, 6/55) at high stresses showed negative transgressive segregation. Among these, four progeny (YMD25, YMD26, YMD27, and YMD87) from inter-lineage crosses showed negative transgressive phenotypes at all three stresses. Interestingly, YMD16 showed negative transgressive phenotypes at low and intermediate stresses but positive transgressive phenotypes at high oxidative stress. Overall, more progeny showed BPH and transgressive segregation at low and high oxidative stresses than the intermediate stress.

4.5.4.3 Melanin at nitrosative stress conditions

4.5.4.3.1 Phenotypic Variation

Parental pairs in both intra-VGIII and inter-lineage crosses varied in melanin production under nitrosative stresses (Table 4.S2). CV_s values of parental pairs ranged from 0.012 to 0.368 at low and from 0.016 to 0.267 at intermediate stresses. Among the 22 crosses, 15 crosses (~68%) at low stress and 12 crosses (~55%) at intermediate stress had CV_s values greater than 0.1. Similarly, variations were also observed among progeny. CV_s values of progeny varied from 0.011 to 0.258 at low stress and from 0.003 to 0.159 at intermediate stress. Under low nitrosative stress, progeny of KN99α × B4546

(VNI × VGIII) produced the most similar amount of melanin (CV_s = 0.011), while progeny of B4545 × JF101 (VGI × VGIII) showed the greatest variation (CV_s = 0.258). Under intermediate stress, progeny from B4545 × JF101 (VGI × VGIII) showed the least differences (CV_s = 0.003), while progeny from JF109 × JF101 (intra-VGIII) displayed the most variation (CV_s = 0.159). In contrast, parental pair B4495 and JF101 (VGI × VGIII) showed little variation at low stress (CV_s = 0.012) but notable differences at intermediate stress (CV_s = 0.115). Of the 19 crosses with ≥ two progeny, progeny of three crosses (~16%) had greater CV_s values than those of their parents at low and intermediate stresses, respectively (highlighted in Table 4.S2). Different from parental strains, progeny from most crosses had CV_s values less than 0.1 at low (~79%, 15/19) and intermediate (~74%, 14/19) stresses. Additionally, no correlations were found between parental variation and progeny variation under these two conditions.

However, by contrast with low and intermediate stress conditions, eight parental strains failed to grow under high nitrosative stress. They were: VGIII strains B4546, B4544, JF109, ATCC32608, and JF101; VGI strain B4545; VGIV strain WM779; VGII strain LA55. In total, there were nine crosses involving these parental strains that neither was able to grow at high nitrosative stress. Among these nine crosses, progeny from eight crosses also all failed to grow at high nitrosative stress. Surprisingly, although neither parental strain grew at high nitrosative stress, progeny YMD85 survived. Another two progeny, YMD150 and YMD16, failed to grow, although their siblings grew. We found 14 crosses having at least one progeny that grew, in spite of one parental strain (VGIII lineage) being unable to grow. Because of the low viability and small sample size, we were able to calculate CV_s values of progeny for only 11 crosses that had at least two progeny growing (excluding all non-viable progeny; Table 4.S2). Among these 11 crosses, CV_s values of progeny ranged from 0.011 to 0.1967. Progeny of JEC21xATCC32608 (VNIV × VGIII) showed the most variation in melanin (CV_s = 0.197), whereas progeny of KN99α × B4546 (VNI × VGIII) had little difference in melanin (CV_s = 0.011). Of these 11 crosses, only two crosses (~18%) had progeny with CV_s values greater than 0.1. Together, under all nitrosative stresses, most parental strains showed notable variations while most of their progeny produced comparable melanin.

4.5.4.3.2 Better-parent heterosis and Transgressive segregation

Of the 55 progeny, five (~9%) at low, 16 (~29%) at intermediate, and seven (~13%) at high nitrosative stresses displayed BPH (Table 4.S3). Although no progeny showed BPH at all nitrosative stresses, six progeny (~11%, 6/55) showed BPH at two stresses. For example, YMD36 and YMD111 showed BPH at both intermediate and high nitrosative stresses. There were significant negative associations between parental genetic distance and progeny BPH rates at low and high nitrosative stresses ($r = -0.34$, $p = 0.010$ at low; $r = -0.32$, $p = 0.019$ at high; Figure 4.3). However, there was no such correlation at intermediate nitrosative stress ($r = -0.086$, $p = 0.531$; Figure 4.3).

Additionally, transgressive segregation in both directions was observed at all nitrosative stresses (highlighted in Table 4.S3). Among the 55 progeny, three progeny (~5%) at low stress, seven progeny (~13%) at intermediate stress, and three progeny (~5%) at high stress had positive transgressive phenotypes. Although no progeny showed positive transgressive segregation at all three nitrosative stress levels, three progeny were positive transgressive segregants: progeny YMD86 at low and high nitrosative stresses; while progeny YMD36 and YMD111 at both intermediate and high nitrosative stresses (Table 4.S3). In contrast, five progeny (~9%, 5/55) at low and one progeny (~2%, 1/55) at intermediate stress levels displayed negative transgressive phenotypes, but none of the progeny showed negative transgressive segregation at high nitrosative stress. Overall, though the rate of progeny showing transgressive segregation was low, positive transgressive phenotypes were observed at all three tested nitrosative stresses.

4.5.4.4 Phenotypic plasticity

A range of CV_i values was observed for both parental strains and their progeny in melanin production across the tested six or seven conditions (Table 4.S2). CV_i values ranged from 0.071 to 0.556 among parental strains and from 0.094 to 0.651 among progeny. Of the 22 parental strains, B4545 (VGI lineage) had the greatest CV_i value, while JEC21 (VNIV lineage) had the smallest CV_i value. Interestingly, except for JEC21, all other parental strains had CV_i values of >0.1, with most strains in most lineages showing a range of CV_i values. Among the 55 progeny, YMD85 had the highest CV_i value, while YMD16 had the smallest CV_i value. Except for YMD16, all progeny had CV_i values

greater than 0.1. Of the 55 progeny, ten progeny (~18%) had greater CV_i values than that of both parents (highlighted in Table 4.S2). Fourteen progeny (~25%, 14/55) had lower CV_i values than both parents, whereas another 31 progeny (~56%, 31/55) had intermediate CV_i values between parents. Among the 22 crosses, all three progeny of one cross had higher CV_i values than their parents, all progeny of two crosses had lower CV_i values than their parents, and progeny of the remaining 19 crosses had a mixture of lower, intermediate, and/or higher CV_i values (Table 4.S2). However, parental plasticity in melanin production was not correlated with progeny plasticity ($r = 0.30$, $p = 0.093$). Significantly, there was a negative correlation between parental genetic distance and progeny plasticity in melanin ($r = -0.54$, $p < 0.001$). Overall, we found that progeny showed three types (less, intermediate, and greater) of plasticity in melanin as compared to their respective parental strains.

4.5.4.5 Relationships between Oxidative and Nitrosative Stresses

First, we compared melanin production between oxidative stresses separately for the parental strains and the progeny population. For parental strains, melanin production at intermediate oxidative stress was significantly positively correlated with that at high oxidative stress ($r = 0.75$, $p < 0.001$). However, such a significant correlation was not observed between low and intermediate oxidative stresses ($r = 0.23$, $p = 0.140$) or between low and high oxidative stresses ($r = 0.27$, $p = 0.075$). For progeny, we found significantly positive correlations between low and high oxidative stresses ($r = 0.34$, $p = 0.012$) and between intermediate and high oxidative stresses ($r = 0.36$, $p = 0.006$), while not found between low and intermediate stresses ($r = 0.25$, $p = 0.069$).

Second, we compared melanin production between nitrosative stresses. For parental strains, there were significant positive correlations in melanin productions between low and intermediate nitrosative stresses ($r = 0.43$, $p = 0.004$), and between low and high nitrosative stresses ($r = 0.67$, $p = 0.012$). However, no correlation was found between intermediate and high nitrosative stresses ($r = -0.42$, $p = 0.16$). For progeny, a significant positive correlation was observed between low and intermediate nitrosative stresses ($r = 0.60$, $p < 0.001$), while no correlation was observed between intermediate and high stresses ($r = -0.06$, $p = 0.75$) or between low and high stresses ($r = 0.08$, $p = 0.65$).

Third, we investigated the relationships between oxidative and nitrosative stresses (Table 4.S4). For parental strains, there were significant positive correlations between melanin production at low oxidative stress and low nitrosative stress (r = 0.32, p = 0.033), between high oxidative and low nitrosative stresses (r = 0.55, p < 0.001), and between high oxidative and intermediate nitrosative stresses (r = 0.53, p < 0.001). However, no correlations were found between other stresses. The results indicate that those parental strains that produced more melanin under low and/or high oxidative stresses are likely to produce more melanin at low and/or intermediate nitrosative stresses.

Similarly, we also found several correlations for progeny between oxidative and nitrosative stresses. There were significant positive correlations in melanin production between low oxidative stress and low nitrosative stress (r = 0.66, p < 0.001), between intermediate oxidative and low nitrosative stresses (r = 0.37, p = 0.006), between high oxidative and low nitrosative stresses (r = 0.47, p < 0.001), and between high oxidative and intermediate nitrosative stresses (r = 0.34, p = 0.010). However, no correlations were observed between other stresses. Our data demonstrate that those progeny that produced more melanin under any of the three oxidative stresses are likely to produce more melanin at low and/or intermediate nitrosative stress. Overall, our findings suggest, for parental strains and progeny, there were both shared and distinct mechanisms for melanin biosynthesis between oxidative and nitrosative stresses at different levels.

4.5.4.6 Effects of potential factors on melanin production

Compared to the non-stress condition, both the parental strains and the progeny overall produced significantly less melanin at all oxidative and two lower nitrosative stresses (p values < 0.001; Figures 4.S1 and 4.S2). Among oxidative stresses, both parental strains and progeny had more melanin production on average at the intermediate oxidative stress than the other two levels. Significantly, we found that parental strains at intermediate oxidative stress produced more melanin than at high oxidative stress (p < 0.001), while such a significant difference was not observed in progeny. Among nitrosative stresses, for both parental strains and progeny, significant differences in melanin production were found between low and intermediate (p values = 0.003 and < 0.001 respectively) and between low and high nitrosative stresses (p values = 0.01 and < 0.001 respectively).

We found significant negative correlations between parental genetic distance and progeny melanin production at non-stress condition ($r = -0.64$, $p < 0.001$), all three oxidative stress levels ($r = -0.42$, $p = 0.002$ at low; $r = -0.35$, $p = 0.01$ at intermediate; $r = -0.44$, $p < 0.001$ at high), and low nitrative stress ($r = -0.44$, $p < 0.001$). When progeny from all intra-VGIII crosses were excluded from analyses, significant negative correlations were still found at non-stress condition ($r = -0.43$, $p = 0.009$) and all oxidative stresses ($r = -0.55$, $p = 0.001$ at low; $r = -0.43$, $p = 0.009$ at intermediate; $r = -0.55$, $p < 0.001$ at high), while no correlations were found at any nitrosative stresses. In addition, we found significant negative correlations between ploidy levels and melanin production at non-stress ($r = -0.37$, $p = 0.003$) and low nitrosative stress ($r = -0.32$, $p = 0.009$) conditions, while no correlations were found at other stresses.

Taken together, our results here illustrate that, for both parental strains and progeny, melanin production could be affected by both environmental stresses and ploidy changes. Under non-stress and oxidative stress conditions, progeny of evolutionarily more similar parental pairs produced overall more melanin than those from evolutionarily more divergent parents.

4.5.4.5 Susceptibility to antifungal drug fluconazole

Susceptibility to fluconazole was evaluated for all parental strains and their progeny, obtaining their minimal inhibitory concentration (MIC) values (Table 4.3). Consistently, we obtained the same MIC values for each tested strain at 35 °C and 37 °C. The MIC values of parental strains ranged from 1 μg/mL to 32 μg/mL. Among them, two parental strains had MIC values of 32 μg/mL, four had MIC of 4 μg/mL, four had MIC of 2 μg/mL, and five had MIC of 1 μg/mL. Among strains used in this study, parental strains of CGSC had overall higher MIC values than those of CNSC.

Similarly, progeny also had MIC values ranging from 1 μg/mL to 32 μg/mL. Of the 55 progeny, 19 (~35%) had greater MIC values than both of their parents; 24 (~44%) had the same MIC values as their more resistant parents; nine (~16%) had intermediate MIC values; two (~4%) had the same MIC values as their less resistant parents; one (~2%) had a lower MIC value than both of its parents. We found a significantly positive correlation between parental genetic distance and MIC values of progeny ($r = 0.28$, $p = 0.039$). However, when the five progeny of CDC15 (VNI lineage) with MIC values of

≥ 16 μg/mL were excluded, there was no correlation between parental genetic distance and progeny MIC values ($r = 0.02$, $p = 0.873$).

Additionally, we standardized progeny MIC values by calculating the percentage of progeny MIC values to the mean MIC values of two parental strains. A significant positive correlation was observed between parental genetic distance and the standardized MIC values ($r = 0.32$, $p = 0.019$). The results indicate that a greater proportion of progeny from more evolutionarily divergent crosses overall had higher MIC values than intermediate parental MIC values or both parental MIC values. Altogether, our findings suggest that both the individual parental strains and the hybridization process contribute to the susceptibility of progeny to fluconazole.

4.6 Discussion

In this study, we found that both parental strains and progeny can be significantly influenced by different stressors, including temperatures on their growth and oxidative and nitrosative stresses on melanin production. A range of phenotypic variations was observed between parental strains and among progeny under the tested conditions. Our results demonstrate that parental genetic divergence can impact progeny relative phenotype values, progeny phenotypic variation and plasticity, and BPH rates of progeny under some tested environmental conditions. Below we discuss our observations in more detail.

4.6.1 Aneuploidy

We determined the ploidy levels of progeny from intra-VGIII and inter-lineage crosses by FACS. Unlike their haploid parents, cryptococcal hybrids are often diploid/aneuploid [28,31,32,34−36,46,57]. Consistently, most progeny collected in this study were also diploid/aneuploid. Surprisingly, despite using the same selection criteria (i.e., heterozygosity at the *MAT* locus) for all progeny, only one out of 18 progeny from the intra-VGIII crosses was diploid, while over 90% of progeny from inter-lineage crosses were diploid (Table 4.3). These diploids were likely derived from two processes. First, they might be from the artificially terminated sexual process when we collected the dikaryotic hyphae before meiosis happened. Alternatively, they might be derived from chromosomal non-disjunction after meiosis. Due to the high similarity and

compatibility between VGIII parental strains, the potentially faster mating between parental strains and more frequent chromosomal disjunction during meiosis would lower ploidy levels among progeny from the intra-VGIII crosses. In CNSC, diploidy and aneuploidy in AD hybrids are primarily caused by meiotic non-disjunction, likely due to genome divergence and genetic incompatibilities between parental strains [31,58,59]. Chromosome structural differences have been observed among the divergent lineages in the human pathogenic *Cryptococcus* [60−63]. Thus, it is tempting to speculate that the observed genome sequence and genome structure divergence between lineages facilitate the generation and maintenance of diploidy among progeny from inter-lineage crosses.

4.6.2 Mitochondrial inheritance

In general, uniparental mitochondrial inheritance is the dominant pattern in animals, plants, and fungi [64,65]. In *C. neoformans* species complex, mitochondria inheritance of both clinical and natural AD hybrids was uniparental from the *MAT***a** parent [47,66]. Additionally, Yan and Xu demonstrated that the *MAT*α mitochondria were selectively eliminated at an early stage during **a**-α mating [66]. One possibility for the uniparental inheritance of *MAT***a** parental mitochondria is that during mating, there is unidirectional migration of the *MAT*α nucleus into the *MAT***a** cell via a conjugation tube [67]. However, mitochondria might not migrate. The newly formed dikaryotic cell would germinate to produce hyphae on the side of the mated *MAT***a** cell away from the *MAT*α parent. Consequently, progeny developed from these hyphae would only contain the *MAT***a** mitochondria.

However, in *C. gattii* species complex, highly variable mitochondrial inheritance patterns, including from *MAT***a** parent only, *MAT*α parent only, and recombinant mitochondrial genotypes, have been observed in previous studies and this study [68,69]. Similarly, biparental mitochondrial inheritance has been found in some other fungi, such as *Saccharomyces cerevisiae* and *Schizosaccharomyces prome* [64,70]. One potential of mitochondrial recombination in our crosses is the breakdown of genetic interactions between the parental cells governing the uniparental mitochondrial inheritance. The observation of recombinant mitochondrial genotypes only for progeny from inter-lineage VNI × VGIII and VNIV × VGIII crosses is consistent with the hypothesis of

the hybrid breakdown of the mechanisms governing uniparental inheritance between divergent parents. Previously, Gyawali and Lin demonstrated that a pre-zygotic factor, Mat2, plays a crucial role in determining the mitochondrial inheritance in *C. neoformans* species complex [71]. They found that if Mat2 preactivates the pheromone pathway in the *MAT*α parent, it can preserve the *MAT*α mtDNA in the progeny, and vice versa. Additionally, two specific genes, *Sxi1*α and *Sxi2***a**, were identified as essential to ensure uniparental mitochondrial inheritance. The deletion of either *Sxi1*α and *Sxi2***a** gave rise to biparental mitochondrial inheritance, with a high proportion of progeny with recombinant mitochondrial genomes [71,72].

We examined the potential effects of mitochondria on hybrid phenotypes in this study. At most tested conditions, different mitochondrial inheritance patterns did not result in any significant phenotypic differences among progeny. However, we found that progeny with *MAT*α mitochondria produced significantly more melanin on average than those with *MAT***a** mitochondria or recombinant mitochondrial genotypes at the non-stress condition ($p < 0.02$). This result suggests a potential adaptive significance of *MAT*α mitochondrial inheritance. As demonstrated previously, the *MAT*α mitochondrial inheritance and mitochondrial recombination were frequently observed under environmental stress conditions, such as ultraviolet (UV) irradiation and high temperatures, in both *C. neoformans* species complex and *C. gattii* species complex [69,73].

4.6.3 Susceptibility to the antifungal drug fluconazole

Fluconazole, a triazole antifungal drug, is widely used as the first-line treatment for cryptococcal meningitis [74]. However, the frequency of drug-resistant fungal pathogens is increasing, causing severe threats to human health. Mutations in genes responsible for fluconazole resistance, such as the azole target gene *ERG11*, have been identified in fungi, including in *Candida* species and *Cryptococcus* species [75−80]. Previous studies have reported that the accumulation of aneuploidies, especially Chromosome 1 disomy, is one of the main reasons for clinical treatment failure and drug resistance in *C. neoformans* [74,81]. In this study, we found that 19 out of 55 progeny had fluconazole MIC values higher than both of their parental strains. Because all progeny were either diploid or aneuploid while parental strains were haploid, the increased fluconazole MIC values in these 19 progeny were consistent with the ploidy effects

observed previously. Indeed, the only progeny (YMA136) with a lower MIC value than both parents was found to have a DNA content only slightly higher than the haploid parental strains (Figure 4.S3). However, ploidy alone cannot explain all the observed MIC values as the remaining 36 aneuploid/diploid progeny showed no obvious advantage over haploid parental strains.

Because of the short time frame during mating and zygote analyses, the observed higher MIC values than parental strains for the 19 progeny were more likely due to gene dosage and gene expression differences rather than to de novo mutations in the progeny. For example, the gene(s) responsible for drug resistance obtained from the more resistant parent might be overexpressed in these progeny. Alternatively, epigenetic mechanisms, such as chromatin modification, could also be involved [82]. Specifically, histone acetylation has been found associated with the regulations of azole resistance in *Candida albicans* [83,84]. Also, inhibitors of histone deacetylases can impact the antifungal drug susceptibility in both *Cryptococcus neoformans* and *Aspergillus fumigatus* [85,86]. Further studies should investigate if these inhibitors impact haploid and diploid strains differently.

4.6.4 Effects of parental genetic divergence on progeny performance

In this study, all crosses contained at least one VGIII strain due to the high fertility of VGIII strains [87,88]. Indeed, strains of VGIII lineage are genotypically highly diverse, likely due to frequent sexual recombination in nature [87,89−92]. Also, two genetically modified VGIII strains, JF101 and JF109, that have enhanced fertility were used in this study [93]. On the other hand, the fertility of strains in other lineages is relatively low. The use of one lineage (VGIII) in all crosses allows us to critically evaluate the impact of parental strain genetic divergence on progeny phenotypes.

Our analyses identified an overall negative correlation between parental genetic divergence and the growth ability of progeny at 30 °C and 37 °C. The negative correlation was likely related to genetic compatibility between the parental genomes regulating cell cycles and cell divisions. Progeny derived from inter-lineage parental strains (either evolutionarily closely related or divergent to VGIII) are likely to experience genetic incompatibility to negatively impact growth as compared to progeny of the intra-

VGIII crosses. However, when progeny from intra-VGIII lineage crosses were excluded, there was a positive correlation between parental genetic distance and the growth of hybrid progeny from the inter-lineage crosses at 37 °C. At present, the exact mechanisms for the observed positive correlation are not known.

We also noticed that the presence of H_2O_2 led to a significant decrease in melanin production of both parents and progeny as compared to the non-stress condition. However, there was no significant difference in melanin production among the three oxidative stress levels. Previous studies have shown that actively growing *C. neoformans* cells can degrade the additional H_2O_2 (1 mM) within 30 min, and *C. gattii* strains are all highly tolerant to high oxidative stress (1 mM H_2O_2) [94,95]. Thus, the significant impact of oxidative stress on melanin production was unexpected. Surprisingly, all VGIII parental strains and progeny from the intra-VGIII crosses were not able to grow at 1 mM $NaNO_2$ condition. A previous study found that strains R265 of VGII lineage and H99 of VNI lineage did not grow at 1.2 mM $NaNO_2$ [96], suggesting that a higher concentration of $NaNO_2$ may arrest the growth of all strains in this study. Furthermore, while many parental strains and their progeny grew at the 1 mM $NaNO_2$ condition, they produced very limited amounts of melanin.

Our results revealed that progeny from evolutionarily more similar parents produced significantly more melanin under non-stress and all oxidative stresses than those from divergent parents. Progeny from intra-VGIII crosses produced significantly more melanin on average than progeny from inter-lineage crosses at low nitrosative stresses. However, most progeny from either intra-VGIII crosses or inter-lineage crosses under low and intermediate nitrosative stress, and progeny from inter-lineage crosses under high nitrosative stress produced similar amounts of melanin. Overall, our results suggest that dominant alleles are likely associated with the significant differences in responses to oxidative and nitrosative stresses in our strains, as well as the growth and melanin production under high nitrosative stress. For human pathogens, tolerance to nitrosative stress is important for their pathogenicity. Fungal pathogens (including HPC) can respond to nitrosative stress via either enzymatic defenses or non-enzymatic defenses [97]. The most common non-enzymatic defenses against nitrosative stress include melanin, mannitol, and trehalose. For example, 1,8-dihydroxynaphthalene (DHN)-melanin can protect the pathogenic fungus *Sporothrix schenckii* from nitrogen-derived radicals

and macrophage-mediated killing [98]. Some proteins, such as protein kinase C (Pkc1) and isocitrate dehydrogenase (Idp1), are known to protect cell wall integrity or repair DNA damage, enabling *C. neoformans* cells to be resistant to nitrosative stress [99,100]. Similarly, transcription factor Cta4 is involved in nitrosative stress response by regulating the reactive nitrogen species (RNS) induced genes in *Candida albicans* [101]. The differential responses among lineages and their progeny to high nitrosative stress could be related to the expressions of these and/or other genes.

4.6.5 Transgressive segregation

It has been reported that transgressive segregation occurs more frequently in plants than in animals [102]. In *Cryptococcus neoformans* species complex, Shahid *et al*. previously examined the vegetative fitness of serotype AD hybrids under 40 environmental conditions, including variations in temperatures, media, and fluconazole concentrations [40]. They found evidence of transgressive segregation in 39 of the 40 tested conditions. In this study, we found transgressive segregation in intra-VGIII and inter-lineage crosses under various environmental conditions in both directions. Several mechanisms have been proposed for such transgressive phenotypes in segregating populations [103,104]. Due to mitotic and meiotic recombination between parental genomes in hybrids, novel gene and allelic combinations are created, both of which could contribute to generating transgressive phenotypes in hybrid populations. Indeed, different gene and allelic combinations could generate transgressive segregations for different traits. Our observed transgressive segregations suggest the enormous capacity and potential of cryptococcal hybrids in adapting to diverse ecological niches.

4.6.6 Potential effect of temperature for selecting hybrids

In this study, we used the 37 °C temperature to select for diploid hybrids from the diverse crosses. While this process ensured that we were able to recover a large number of diploid hybrids, this temperature could potentially bias the progeny population in favor of those capable of growing at 37 °C. Indeed, the observed positive correlation between parental genetic divergence and hybrid progeny growth at 37 °C could be partly due to this selection protocol. However, for several reasons, we believe that the potential

effect of the 37 °C selection temperature on the overall observed patterns is likely minor. First, as described in Results Section 4.5.3.1, the hybrid progeny population showed similar or even greater declines in overall growth at 37 °C (vs. at 30 °C) than the parental strains. Second, there were wide ranges of both CV_s and CV_i values among progeny in their growth at the 37 °C, with an overall pattern similar to those of their respective parental strains. Third, although there were slightly higher rates of both BPH and positive transgressive segregation in growth rate at 37 °C than at 30 °C, the differences were not statistically significant. Furthermore, there was also a slightly higher frequency of negative transgressive segregation at 37 °C than at 30 °C. Despite these observations, we would like to note that if the hybrid progeny selection temperature were lower (e.g., at 25 °C, which likely would require screening far more colonies to identify diploid hybrids), some of the progeny might not be able to grow at the 37 °C temperature and thus might impact our results on the measured hybrid growth abilities at this temperature [105]. In this study, all progeny selected at 37 °C grew well at both 30 °C and 37 °C. Additional experiments are needed in order to determine the potential impacts of different selection protocols on hybrid performance.

4.7 Conclusions

This study investigated the relationships between parental differences (both genetic and phenotypic) and their progeny phenotypes for three medically important traits in the human pathogenic *Cryptococcus*: growth at 37 °C, melanin production, and fluconazole susceptibility. We found several types of relationships, with progeny from each type of cross showing superior performance potential than both parents in some traits under certain conditions. There are other medically important traits in the human pathogenic *Cryptococcus*, including resistance/tolerance to other antifungal drugs, the secretion of a number of extracellular enzymes, and capsule production. At present, the relationships between parental divergence (both genetic and phenotypic) and progeny phenotype at other traits are not known and worth investigating. For capsule production, our previous research [39] and pilot experiment for this study (unpublished) revealed that, for most parental strains and progeny, their capsule size was highly variable among cells of the same sample that were grown under the same condition and measured under the same microscopic field. Often, the standard deviations were larger than the means,

making most comparisons among parental strains and progeny meaningless. In this study, we analyzed highly reproducible traits, including melanin production under seven conditions, growth ability at two temperatures, and fluconazole susceptibility, all of which showed very low standard deviation when compared to the mean among repeats of the same strain. Our analyses of the three medically important traits suggest the enormous capacity and potential of cryptococcal hybrids in adapting to diverse ecological niches.

4.8 Appendix

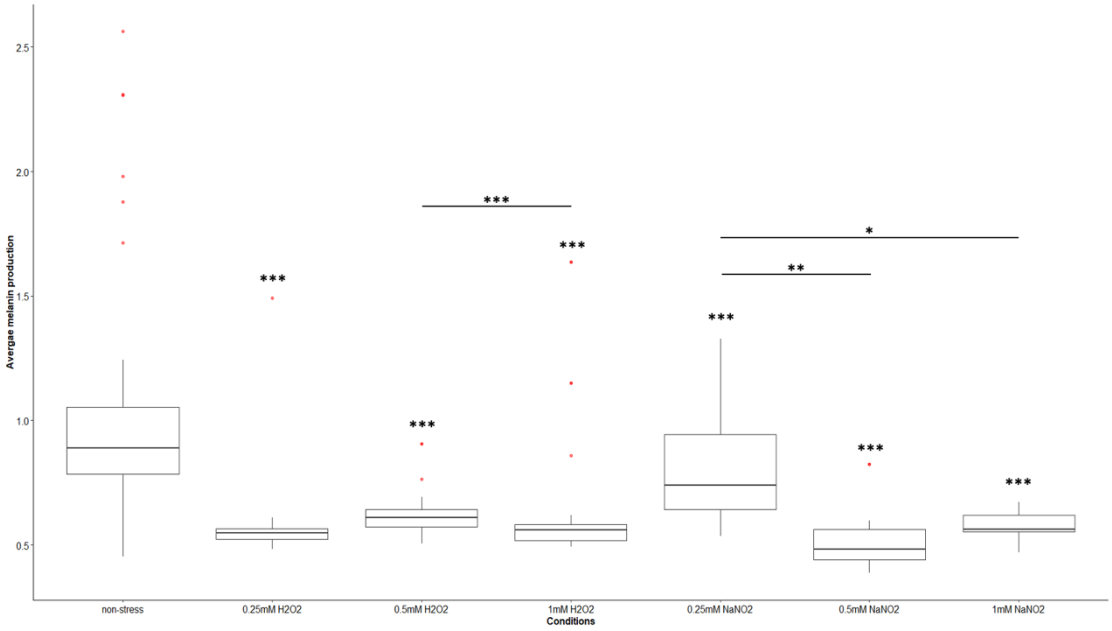

Figure 4.S1. Effects of oxidative and nitrosative stress on average melanin production of parental strains. At high nitrosative stress, we excluded those parental strains that did not grow. Pairwise comparisons were performed between stresses. Red dots represent outliers. * indicates p values < 0.05; ** indicates p values < 0.005; *** indicates p values < 0.001.

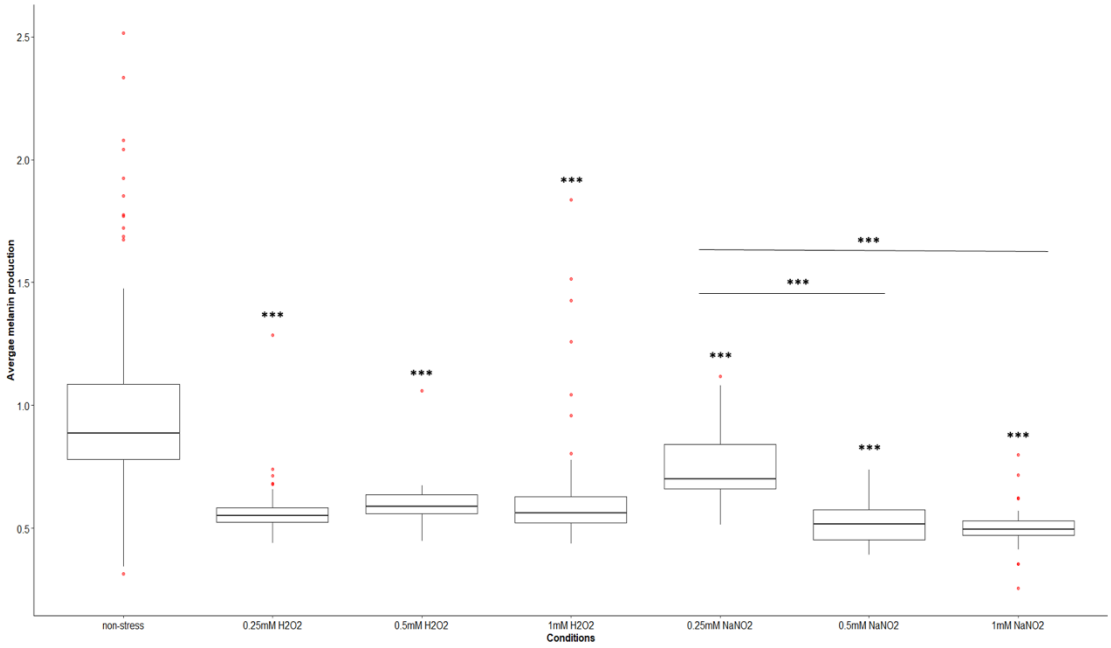

Figure 4.S2. Effects of oxidative and nitrosative stress on average melanin production of progeny. Seven environmental conditions, including non-stress, oxidative stress (low, intermediate, and high), and nitrosative stress conditions (low, intermediate, and high) were tested in this study. At high nitrosative stress, we excluded progeny that did not grow. Red dots represent outliers. *** indicates that the *p* value is less than 0.001.

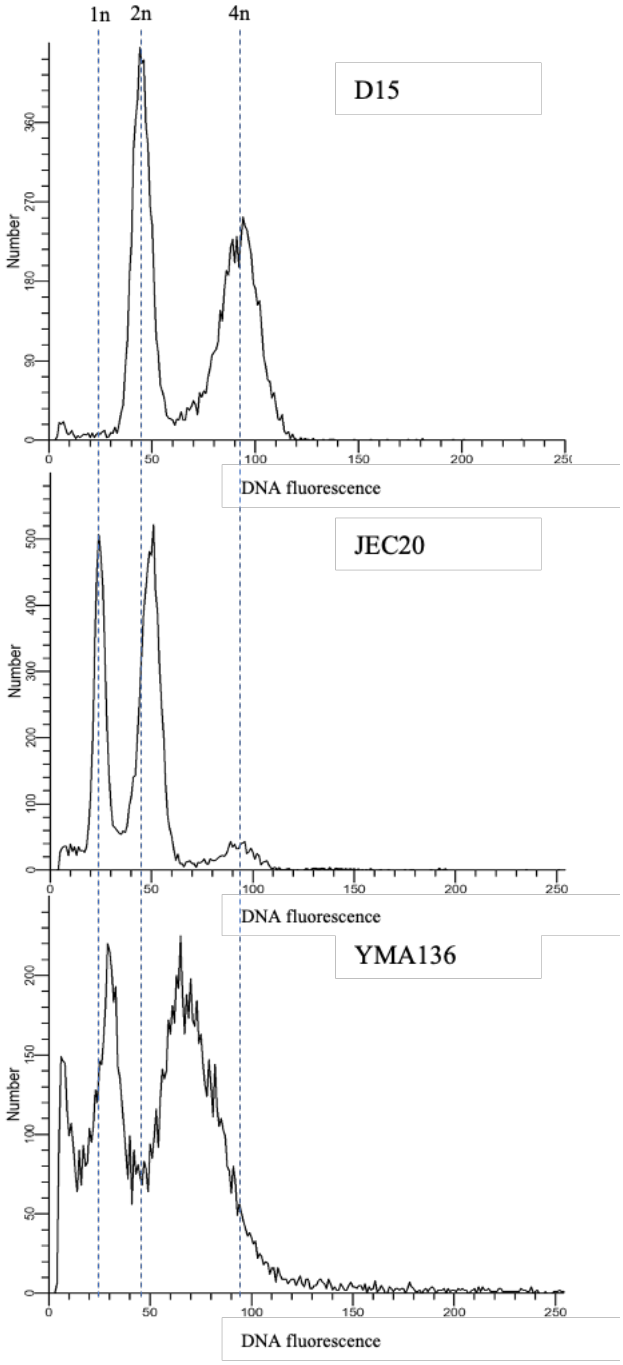

Figure 4.S3. FACS profile of YMA136 comparing to the haploid control and diploid control.

Table 4.S1. Information on genotyping and mitochondrial inheritance.

Progeny ID	Nuclear genotype			Mitochondrial inheritance	Nucler loci														Mitochondrial loci	
	Heterozygous loci (%)	Homologous *MAT* **a** (%)	Homologous *MAT* **α**(%)		*CAP59*	*CGNA*	*ERG11*	*CNB00360*	*CNK01700*	*CNL06810*	*CGND*	*MAT locus*	*CNE00250*	*URA5*	*CNI01350*	*CNM00180*	*CGNM2*	*CNH02750*	*ND2*	*ND4*
YMA79	NA	NA	NA	NA	NA	NA	NA	NA	NA	NA	NA	3	NA	NA	NA	NA	NA	NA	NA	NA
YMA80	NA	NA	NA	NA	NA	NA	NA	NA	NA	NA	NA	3	NA	NA	NA	NA	NA	NA	NA	NA
YMD81	NA	NA	NA	NA	NA	NA	NA	NA	NA	NA	NA	3	NA	NA	NA	NA	NA	NA	NA	NA
YMA62	NA	NA	NA	NA	NA	NA	NA	NA	NA	NA	NA	3	NA	NA	NA	NA	NA	NA	NA	NA
YMA63	NA	NA	NA	NA	NA	NA	NA	NA	NA	NA	NA	3	NA	NA	NA	NA	NA	NA	NA	NA
YMA64	NA	NA	NA	NA	NA	NA	NA	NA	NA	NA	NA	3	NA	NA	NA	NA	NA	NA	NA	NA
YMA65	NA	NA	NA	NA	NA	NA	NA	NA	NA	NA	NA	3	NA	NA	NA	NA	NA	NA	NA	NA
YMA66	NA	NA	NA	NA	NA	NA	NA	NA	NA	NA	NA	3	NA	NA	NA	NA	NA	NA	NA	NA
YMA68	NA	NA	NA	NA	NA	NA	NA	NA	NA	NA	NA	3	NA	NA	NA	NA	NA	NA	NA	NA
YMA73	NA	NA	NA	NA	NA	NA	NA	NA	NA	NA	NA	3	NA	NA	NA	NA	NA	NA	NA	NA
YMA74	NA	NA	NA	NA	NA	NA	NA	NA	NA	NA	NA	3	NA	NA	NA	NA	NA	NA	NA	NA
YMA138	NA	NA	NA	NA	NA	NA	NA	NA	NA	NA	NA	3	NA	NA	NA	NA	NA	NA	NA	NA
YMA102	NA	NA	NA	NA	NA	NA	NA	NA	NA	NA	NA	3	NA	NA	NA	NA	NA	NA	NA	NA
YMA125	NA	NA	NA	NA	NA	NA	NA	NA	NA	NA	NA	3	NA	NA	NA	NA	NA	NA	NA	NA
YMA136	NA	NA	NA	NA	NA	NA	NA	NA	NA	NA	NA	3	NA	NA	NA	NA	NA	NA	NA	NA
YMA77	NA	NA	NA	NA	NA	NA	NA	NA	NA	NA	NA	3	NA	NA	NA	NA	NA	NA	NA	NA
YMA78	NA	NA	NA	NA	NA	NA	NA	NA	NA	NA	NA	3	NA	NA	NA	NA	NA	NA	NA	NA
YMA105	NA	NA	NA	NA	NA	NA	NA	NA	NA	NA	NA	3	NA	NA	NA	NA	NA	NA	NA	NA
YMD53	71.43	21.43	7.14	*MAT* **a**	1	1	3	2	3	3	3	3	3	1	3	3	3	3	1	1
YMD90	78.57	7.14	14.29	*MAT* **a**	1	3	3	2	3	3	2	3	3	3	3	3	3	3	1	1
YMD96	78.57	7.14	14.29	*MAT* **a**	1	3	3	2	3	3	3	3	3	3	2	3	3	3	1	1
YMD69	92.86	7.14	0.00	*MAT* α	1	3	3	3	3	3	3	3	3	3	3	3	3	3	2	2
YMA71	92.86	7.14	0.00	*MAT* α	1	3	3	3	3	3	3	3	3	3	3	3	3	3	2	2
YMD72	92.86	7.14	0.00	*MAT* α	1	3	3	3	3	3	3	3	3	3	3	3	3	3	2	2
YMD85	78.57	7.14	14.29	*MAT* α	1	3	3	2	3	2	3	3	3	3	3	3	3	3	2	2
YMD86	71.43	21.43	7.14	*MAT* α	1	2	3	1	3	3	3	3	3	3	3	3	3	1	2	2
YMD36	64.29	35.71	0.00	*MAT* **a**	1	1	3	3	3	3	3	3	3	1	1	3	1	3	1	1
YMD111	57.14	28.57	14.29	*MAT* α	1	3	3	3	1	3	3	3	2	1	3	1	3	2	2	2
YMD132	78.57	0.00	21.43	*MAT* **a**	2	3	3	3	3	3	3	3	2	2	3	3	3	3	1	1
YMD135	78.57	0.00	21.43	*MAT* **a**	2	3	3	3	3	3	3	3	2	2	3	3	3	3	1	1
YMD150	71.43	14.29	14.29	*MAT* **a**	2	3	3	3	3	3	1	3	1	2	3	3	3	3	1	1
YMD112	85.71	7.14	7.14	*MAT* **a**	2	3	3	3	3	3	3	3	3	3	3	1	3	3	1	1
YMD113	85.71	7.14	7.14	*MAT* **a**	2	3	3	3	3	3	3	3	3	3	3	1	3	3	1	1
YMD114	85.71	7.14	7.14	*MAT* **a**	2	3	3	3	3	3	3	3	3	3	3	1	3	3	1	1
YMD29	85.71	7.14	7.14	*MAT* **a**	2	3	3	3	3	3	3	3	3	3	3	1	3	3	1	1
YMT33	85.71	7.14	7.14	*MAT* **a**	2	3	3	3	3	3	3	3	3	3	3	1	3	3	1	1
YMD1	85.71	0.00	14.29	*MAT* **a**	2	3	3	3	3	3	3	3	3	3	3	2	3	3	1	1
YMD5	85.71	0.00	14.29	*MAT* **a**	2	3	3	3	3	3	3	3	3	3	3	2	3	3	1	1
YMD10	85.71	0.00	14.29	*MAT* **a**	2	3	3	3	3	3	3	3	3	3	3	2	3	3	1	1

YMA162	85.71	7.14	7.14	Recombinant	2	3	3	3	3	3	3	3	3	3	3	1	3	3	2	1
YMD164	78.57	7.14	7.14	Recombinant	2	3	3	0	3	3	3	3	3	3	3	1	3	3	2	1
YMD165	85.71	7.14	7.14	Recombinant	2	3	3	3	3	3	3	3	3	3	3	1	3	3	2	1
YMD34	85.71	7.14	7.14	Recombinant	2	3	3	3	3	3	3	3	3	3	3	1	3	3	2	1
YMD83	78.57	14.29	7.14	Recombinant	2	3	3	3	1	3	3	3	3	3	3	1	3	3	2	1
YMT98	85.71	7.14	7.14	*MAT* α	2	3	3	3	3	3	3	3	3	3	3	1	3	3	2	2
YMD87	92.86	0.00	7.14	Recombinant	2	3	3	3	3	3	3	3	3	3	3	3	3	3	2	1
YMD88	92.86	0.00	7.14	*MAT* **a**	2	3	3	3	3	3	3	3	3	3	3	3	3	3	1	1
YMD89	92.86	0.00	7.14	Recombinant	2	3	3	3	3	3	3	3	3	3	3	3	3	3	2	1
YMD16	85.71	14.29	0.00	Recombinant	1	3	3	3	3	3	3	3	3	1	3	3	3	3	2	1
YMD17	85.71	14.29	0.00	*MAT* **a**	1	3	3	3	3	3	3	3	3	1	3	3	3	3	1	1
YMD11	92.86	7.14	0.00	Recombinant	1	3	3	3	3	3	3	3	3	3	3	3	3	3	2	1
YMD12	71.43	14.29	7.14	Recombinant	1	3	3	0	2	3	3	3	3	1	3	3	3	3	2	1
YMD25	92.86	0.00	7.14	*MAT* **a**	2	3	3	3	3	3	3	3	3	3	3	3	3	3	1	1
YMD26	92.86	0.00	7.14	*MAT* **a**	2	3	3	3	3	3	3	3	3	3	3	3	3	3	1	1
YMD27	85.71	0.00	14.29	*MAT* **a**	2	3	3	3	3	3	3	3	3	3	3	2	3	3	1	1

Table 4.S2. Coefficient of variation (CV) in growth and melanin under various environmental conditions.

Cross	Sample	CVs									CVi	
		Growth		Melanin							Growth	Melanin
		At 30°C	At 37°C	Non-stress	Low oxidative stress	Intermediate oxidative stress	High oxidative stress	Low nitrosative stress	Intermediate nitrosative stress	High nitrosative stress		
B4546xB4544	B4546	0.649988578	0.016859099	0.400448694	0.041898548	0.195883469	0.474851785	0.220160908	0.196424938	NA	0.22184127	0.477468284
	B4544										0.48753862	0.619107453
	YMA79	0.078103385	0.072655222	0.306180017	0.066817088	0.065302226	0.420101299	0.146000694	0.15680331	NA	0.275594239	0.672252899
	YMA80										0.273246024	0.640872218
	YMD81										0.290637191	0.470640527
JF109xB4544	JF109	0.095072024	0.013854933	0.425275292	0.111906779	0.211585953	0.535144051	0.237307351	0.181417281	NA	0.422985217	0.488872997
	B4544										0.48753862	0.632250537
	YMA62	0.049208999	0.107088609	0.091564576	0.007966127	0.013488237	0.41464036	0.013312614	0.022013804	NA	0.16943918	0.638900513
	YMA63										0.238778438	0.690160579
	YMA64										0.267313383	0.768660855
ATCC32608xB4544	ATCC32608	0.151008049	0.077835434	0.476912395	0.435752864	0.153677044	0.249076084	0.282511923	0.130213366	NA	0.293746205	0.467539263
	B4544										0.48753862	0.665108275
	YMA65	0.038598507	0.076043374	0.228392541	0.323517403	0.003404941	0.054366761	0.042961646	0.070002384	NA	0.235673895	0.803403431
	YMA66										0.288209607	0.560652719
	YMA68										0.28194828	0.62305039
B4546xJF101	B4546	0.489035271	0.239066823	0.050695451	0.015123092	0.005266357	0.031364414	0.071179677	0.10046436	NA	0.22184127	0.447882173
	JF101										0.065322436	0.44991713
	YMA73	0.138425368	0.05133405	0.047205523	0.041972219	0.012215661	0.050614668	0.030202701	0.004445293	NA	0.368518619	0.443891505
	YMA74										0.317141668	0.440750476
	YMA138										0.201352758	0.436577967
JF109xJF101	JF109	0.144116943	0.236231656	0.068456719	0.000857628	0.044378974	0.010560037	0.083686953	0.204131374	NA	0.422985217	0.460951052
	JF101										0.065322436	0.44837275
	YMA102	0.24581314	0.127919124	0.350415601	0.073549001	0.023402485	0.242249288	0.190741449	0.159387299	NA	0.31056394	0.691892404
	YMA125										0.289298382	0.635257951
	YMA136										0.161773399	0.457810416
ATCC32608xJF101	ATCC32608	0.088086606	0.147838826	0.010433502	0.037962099	0.058776411	0.0686946	0.126740711	0.045126298	NA	0.293746205	0.501108972
	JF101										0.065322436	0.505281746
	YMA77	0.107909646	0.071334131	0.048845359	0.011786902	0.013526583	0.021112955	0.021303214	0.027023026	NA	0.355345554	0.510600327
	YMA78										0.168620953	0.479068208
	YMA105										0.209602081	0.506802917
B4495xB4544	B4495	0.298453794	0.144434224	0.19843038	0.043237372	0.032544088	0.345224522	0.289146956	0.266811436	1	0.354390837	0.541855532
	B4544										0.48753862	0.741983273
	YMD53	0.098124918	0.078131461	0.157415754	0.092878737	0.050138679	0.192136108	0.075445478	0.046957254	0.068009317	0.553065747	0.450170195
	YMD90										0.547487238	0.300925626
	YMD96										0.533961253	0.432611657
B4495xJF101	B4495	0.067232415	0.356067162	0.015094956	0.006831091	0.043432445	0.012894845	0.070883126	0.102698925	1	0.354390837	0.203649814
	JF101										0.065322436	0.459002563
	YMD69	0.054126218	0.067650847	0.031591616	0.021850679	0.02455654	0.048252618	0.032390511	0.122515313	0.01375476	0.396598749	0.214901141
	YMA71										0.404617254	0.206777244
	YMD72										0.4102967	0.219549125
B4545xJF101	B4545	0.280325623	0.09819864	0.165179218	0.040226392	0.093763775	0.018297086	0.01230549	0.114618035	NA	0.423514652	0.556401918
	JF101										0.065322436	0.452586358
	YMD85	0.171824786	0.089047005	0.553780873	0.155088972	0.24486448	0.251260287	0.257472817	0.003272522	1	0.51807916	0.651282623
	YMD86										0.301238155	0.441354712
WM779xJF109	WM779	0.169565431	0.003628821	0.187696327	0.080094543	0.027023517	0.111859176	0.117018412	0.016367078	NA	0.276355422	0.529198218
	JF109										0.422985217	0.473909659
	YMD36	NA	NA	NA	NA	NA	NA	NA	NA	NA	0.31576498	0.224064774

LA55xJF101	LA55	0.066340239	0.260194643	0.018142282	0.014372971	0.00076268	0.004461718	0.01797289	0.058818161	NA	0.259241363	0.476034084
	JF101										0.065322436	0.471894818
	YMD111	NA	NA	NA	NA	NA	NA	NA	NA	NA	0.374802319	0.17844922
R265xB4546	R265	0.475027844	0.059225013	0.147897365	0.049299798	0.026619148	0.001735813	0.291513931	0.060812341	1	0.336593697	0.398646411
	B4546										0.22184127	0.464430092
	YMD132	0.022131027	0.138841736	0.055345659	0.008140738	0.008029295	0.01063898	0.094926182	0.048283467	0.709148745	0.372776311	0.249867517
	YMD135										0.365980522	0.284233536
	YMD150										0.224391521	0.477643372
KN99alphaxJF109	KN99alpha	0.118594003	0.155543926	0.06450466	0.062568281	0.014176219	0.081835618	0.139104419	0.096222897	1	0.39157595	0.284166096
	JF109										0.422985217	0.497262578
	YMD112	0.141463314	0.091633737	0.081026509	0.023470183	0.024509992	0.02335581	0.077704045	0.073143823	0.156572828	0.205408886	0.2231738
	YMD113										0.454147143	0.233839873
	YMD114										0.360660137	0.189229925
KN99alphaxB4546	KN99alpha	0.66351856	0.158474724	0.106832144	0.007804092	0.030550556	0.001009198	0.121318076	0.11161797	1	0.39157595	0.338298152
	B4546										0.22184127	0.501632106
	YMD29	0.04631184	0.041599999	0.033392564	0.020537121	0.006800705	0.009484416	0.011249644	0.026411423	0.011038993	0.398534944	0.242531066
	YMT33										0.39455635	0.207121383
KN99axJF101	KN99a	0.295653546	0.030625503	0.047148544	0.037827014	0.034351004	0.07691249	0.15048371	0.067450648	1	0.327058253	0.35849655
	JF101										0.065322436	0.485135023
	YMD1	0.163892773	0.34819816	0.050444844	0.043913435	0.038574591	0.066695479	0.060119928	0.034054852	0.016217191	0.238464984	0.199759349
	YMD5										0.407373553	0.252409442
	YMD10										0.386607	0.218697304
CDC15xJF109	CDC15	0.026752689	0.050328657	0.226955769	0.004249498	0.008496773	0.008589441	0.268753301	0.128585139	1	0.357652847	0.429380409
	JF109										0.422985217	0.476822445
	YMA162	0.111720328	0.134760641	0.055377817	0.013631606	0.008583087	0.004194103	0.058951384	0.050970574	0.036597325	0.055153773	0.268095308
	YMD164										0.139019578	0.232942244
	YMD165										0.081641014	0.214080392
CDC15xB4546	CDC15	0.573793296	0.05332546	0.071306814	0.066108289	0.024874742	0.072293849	0.251886365	0.143859481	1	0.357652847	0.409312402
	B4546										0.22184127	0.489968479
	YMD34	0.145750403	0.204186364	0.06970199	0.028001401	0.031564885	0.047701519	0.084251572	0.026657232	0.047012142	0.202365058	0.246783363
	YMD83										0.123096942	0.20160465
	YMT98										0.288101119	0.242173266
JEC21xJF109	JEC21	0.010711716	0.012345681	0.10469093	0.008001146	0.013034575	0.006941618	0.052765472	0.075640613	1	0.403869262	0.042908897
	JF109										0.422985217	0.429204333
	YMD87	NA	NA	NA	NA	NA	NA	NA	NA	NA	0.347770497	0.143746223
JEC21xB4546	JEC21	0.584457857	0.01534998	0.071307373	0.00097817	0.011199471	0.037023773	0.105229924	0.075507825	1	0.403869262	0.118084117
	B4546										0.22184127	0.462174134
	YMD88	0.0382957	0.084190487	0.01876406	0.080731461	0.078602889	0.049490857	0.075950207	0.136088111	0.710599029	0.311609656	0.12650957
	YMD89										0.282471836	0.102931668
JEC20xJF101	JEC20	0.126406419	0.205601722	0.197938675	0.019672299	0.025274127	0.020768994	0.158339382	0.054819441	1	0.380869565	0.113984959
	JF101										0.065322436	0.465665575
	YMD16	0.053227632	0.012731005	0.035673564	0.028384554	0.127235724	0.011380713	0.017898439	0.137728509	1	0.180594783	0.420699824
	YMD17										0.243608904	0.132255159
JEC20xB4544	JEC20	0.112917517	0.018346814	0.567243325	0.069657388	0.01437432	0.352143275	0.36817982	0.221506591	1	0.380869565	0.113984959
	B4544										0.48753862	0.690541543
	YMD11	0.047223585	0.202513836	0.178558066	0.069584077	0.07190848	0.040978684	0.050595178	0.006201459	0.034493571	0.530846485	0.177326078
	YMD12										0.326326852	0.101302588
JEC21xATCC32608	JEC21	0.046067064	0.079335622	0.06016485	0.063740549	0.059394673	0.012620987	0.093309518	0.093750461	1	0.403869262	0.051251946
	ATCC32608										0.293746205	0.446532138
	YMD25	0.182463591	0.080694682	0.048826915	0.008551926	0.016754613	0.020786889	0.140267276	0.093744507	0.19671822	0.378555109	0.13525235
	YMD26										0.487673291	0.286457215
	YMD27										0.362466857	0.129466769

'NA' indicates that it was not able to calculate the CV either due to one progeny in the cross or none of the samples grew at high nitrosative stress.

Table 4.S3. Better-parent heterosis (BPH) and transgressive segregation found under various environmental conditions.

Crosses	Sample ID	Better parent heterosis (labeld with Y) /transgressive segregation (highlighted, positive in orange, negative in green)								
		Growth at 30°C	Growth at 37°C	Melanin						
				Non-stress	Low oxidative stress	Intermediate oxidative stress	High oxidative stress	Low nitrosative stress	Intermediate nitrosative stress	High nitrosative stress
B4546xB4544	YMA79	Y	Y	Y	Y	/	Y	/	Y	/
	YMA80	/	Y	/	Y	/	/	/	Y	/
	YMD81	Y	Y	/	/	/	/	/	/	/
JF109xB4544	YMA62	Y	Y	/	/	/	/	/	/	/
	YMA63	Y	Y	/	/	/	/	/	/	/
	YMA64	Y	Y	Y	/	/	/	/	/	/
ATCC32608xB4544	YMA65	/	Y	Y	/	/	/	/	Y	/
	YMA66	/	Y	/	/	/	/	/	/	/
	YMA68	/	Y	/	/	/	/	/	Y	/
B4546xJF101	YMA73	Y	/	Y	Y	Y	Y	/	/	/
	YMA74	Y	/	/	Y	Y	Y	/	/	/
	YMA138	Y	/	/	/	Y	/	/	/	/
JF109xJF101	YMA102	Y	Y	Y	Y	/	Y	Y	Y	/
	YMA125	Y	Y	Y	Y	/	Y	Y	Y	/
	YMA136	/	/	/	/	/	N	/	/	/
ATCC32608xJF101	YMA77	Y	/	Y	/	/	/	/	/	/
	YMA105	/	/	Y	/	/	/	/	/	/
B4495xB4544	YMD53	/	/	/	Y	/	Y	/	/	/
	YMD90	/	/	N	Y	/	/	/	/	/
	YMD96	/	/	/	/	N	/	/	/	/
B4495xJF101	YMD69	/	/	/	Y	/	Y	/	/	/
	YMD72	/	/	Y	/	/	/	/	Y	/
B4545xJF101	YMD85	/	N	Y	Y	Y	Y	Y	/	Y
	YMD86	/	/	/	N	/	N	N	/	/

WM779xJF109	YMD36	/	Y	/	/	/	/	/	Y	Y
LA55xJF101	YMD111	/	/	/	/	/	Y	/	Y	Y
R265xB4546	YMD132	Y	Y	/	/	/	Y	/	/	Y
	YMD135	Y	Y	/	/	/	Y	/	Y	/
	YMD150	Y	Y	/	/	/	Y	/	Y	/
KN99alphaxJF109	YMD112	/	/	/	/	/	/	N	/	/
	YMD114	/	/	/	/	N	/	N	/	/
KN99alphaxB4546	YMD29	/	/	/	/	/	/	N	/	/
	YMT33	/	/	/	Y	/	/	N	/	/
KN99axJF101	YMD1	/	/	N	Y	Y	Y	/	Y	/
	YMD5	/	N	N	Y	/	Y	Y	Y	/
	YMD10	/	N	N	/	/	/	/	Y	/
CDC15xJF109	YMA162	N	Y	/	Y	/	/	/	/	Y
	YMD164	N	Y	/	Y	/	/	/	/	Y
	YMD165	/	Y	/	Y	/	/	/	/	/
CDC15xB4546	YMD34	/	N	/	/	/	/	/	Y	/
	YMD83	/	/	/	/	N	/	/	/	/
	YMT98	/	Y	/	Y	/	Y	/	/	/
JEC21xJF109	YMD87	/	Y	/	N	N	N	/	/	/
JEC21xB4546	YMD88	/	N	/	Y	/	Y	/	/	/
JEC20xJF101	YMD16	N	Y	/	N	N	Y	/	/	/
	YMD17	/	/	/	/	/	Y	/	N	/
JEC20xB4544	YMD11	/	N	/	N	N	/	Y	/	/
JEC21xATCC32608	YMD25	/	N	/	N	N	N	/	Y	/
	YMD26	/	N	/	N	N	N	/	/	/
	YMD27	/	N	/	N	N	N	/	/	Y
%BPH (out of 55 progeny)		25.4545455	38.1818182	18.181818	32.72727273	9.090909091	32.72727273	9.090909091	29.09090909	12.72727273

'Y': the progeny showed BPH; 'N': the progeny did not show BPH;
The progeny showed positively transgressive phenotypes labeled in orange;
The progeny displayed negatively transgressive phenotypes labeled in green.

Table 4.S4. Relationships between oxidative stresses and nitrosative stresses.

Stresses	Low Oxidative stress		Intermediate Oxidative Stress		High Oxidative stress	
	Parental strains	Progeny	Parental strains	Progeny	Parental strains	Progeny
Low Nitrosative stress	r=0.32, p=0.033*	r=0.66, p=4e-08*	r=0.26, p=0.089	r=0.37, p=0.0059*	r=0.55, p=1e-04*	r=0.47, p=0.00033*
Intermediate Nitrosative stress	r=0.22, p=0.16	r=0.23, p=0.084	r=0.28, p=0.065	r=0.23, p=0.097	r=0.53, p=2e-04*	r=0.34, p=0.01*
High Nitrosative stress	r=-0.021, p=0.95	r=0.14, p=0.42	r=-0.52, p=0.071	r=0.16, p=0.37	r=-0.17, p=0.57	r=-0.016, p=0.93

* indicates that *p* value is less than 0.05.

4.9 Reference

1. Li, W.; Averette, A.F.; Desnos-Ollivier, M.; Ni, M.; Dromer, F.; Heitman, J. Genetic Diversity and Genomic Plasticity of *Cryptococcus neoformans* AD Hybrid Strains. *G3 (Bethesda)* 2012, *2*, 83–97, doi:10.1534/g3.111.001255.

2. Schardl, C.L.; Craven, K.D. Interspecific Hybridization in Plant-Associated Fungi and Oomycetes: A Review. *Mol. Ecol.* 2003, *12*, 2861–2873, doi:10.1046/j.1365-294x.2003.01965.x.

3. Mixão, V.; Gabaldón, T. Hybridization and Emergence of Virulence in Opportunistic Human Yeast Pathogens. *Yeast* 2018, *35*, 5–20, doi:10.1002/yea.3242.

4. Yuan, L. Progress in Super-Hybrid Rice Breeding. *The Crop Journal* 2017, *5*, 100–102, doi:10.1016/j.cj.2017.02.001.

5. East, E.M. Heterosis. *Genetics* 1936, *21*, 375–397.

6. Hagen, F.; Khayhan, K.; Theelen, B.; Kolecka, A.; Polacheck, I.; Sionov, E.; Falk, R.; Parnmen, S.; Lumbsch, H.T.; Boekhout, T. Recognition of Seven Species in the *Cryptococcus gattii/Cryptococcus neoformans* Species Complex. *Fungal genetics and biology: FG & B* 2015, *78*, 16–48, doi:10.1016/j.fgb.2015.02.009.

7. Kwon-Chung, K.J.; Bennett, J.E.; Wickes, B.L.; Meyer, W.; Cuomo, C.A.; Wollenburg, K.R.; Bicanic, T.A.; Castañeda, E.; Chang, Y.C.; Chen, J.; *et al*. The Case for Adopting the "Species Complex" Nomenclature for the Etiologic Agents of Cryptococcosis. *mSphere* 2017, *2*, e00357-16, doi:10.1128/mSphere.00357-16.

8. Farrer, R.A.; Chang, M.; Davis, M.J.; Dorp, L. van; Yang, D.-H.; Shea, T.; Sewell, T.R.; Meyer, W.; Balloux, F.; Edwards, H.M.; *et al*. A New Lineage of *Cryptococcus gattii* (VGV) Discovered in the Central Zambezian Miombo Woodlands. *mBio* 2019, *10*, doi:10.1128/mBio.02306-19.

9. Xu, J.; Vilgalys, R.; Mitchell, T.G. Multiple Gene Genealogies Reveal Recent Dispersion and Hybridization in the Human Pathogenic Fungus *Cryptococcus neoformans*. *Mol. Ecol.* 2000, *9*, 1471–1481, doi:10.1046/j.1365-294x.2000.01021.x.

10. Ngamskulrungroj, P.; Gilgado, F.; Faganello, J.; Litvintseva, A.P.; Leal, A.L.; Tsui, K.M.; Mitchell, T.G.; Vainstein, M.H.; Meyer, W. Genetic Diversity of the *Cryptococcus* Species Complex Suggests That *Cryptococcus gattii* Deserves to Have Varieties. *PLoS ONE* 2009, *4*, e5862, doi:10.1371/journal.pone.0005862.

11. Kidd, S.E.; Guo, H.; Bartlett, K.H.; Xu, J.; Kronstad, J.W. Comparative Gene Genealogies Indicate That Two Clonal Lineages of *Cryptococcus gattii* in British Columbia Resemble Strains from Other Geographical Areas. *Eukaryot Cell* 2005, *4*, 1629–1638, doi:10.1128/EC.4.10.1629-1638.2005.

12. Alspaugh, J.A. Virulence Mechanisms and *Cryptococcus neoformans* Pathogenesis. *Fungal Genetics and Biology* 2015, *78*, 55–58, doi:10.1016/j.fgb.2014.09.004.

13. Ikeda, R.; Sugita, T.; Jacobson, E.S.; Shinoda, T. Effects of Melanin upon Susceptibility of *Cryptococcus* to Antifungals. *Microbiology and Immunology* 2003, *47*, 271–277, doi:10.1111/j.1348-0421.2003.tb03395.x.

14. Rosas, A.L.; Casadevall, A. Melanization Affects Susceptibility of *Cryptococcus neoformans* to Heat and Cold. *FEMS Microbiol Lett* 1997, *153*, 265–272, doi:10.1111/j.1574-6968.1997.tb12584.x.

15. Leopold Wager, C.M.; Hole, C.R.; Wozniak, K.L.; Wormley, F.L. *Cryptococcus* and Phagocytes: Complex Interactions That Influence Disease Outcome. *Frontiers in Microbiology* 2016, *7*, 1–16, doi:10.3389/fmicb.2016.00105.

16. Almeida, F.; Wolf, J.M. Virulence-Associated Enzymes of *Cryptococcus neoformans*. 2015, *14*, 1173–1185, doi:10.1128/EC.00103-15.Address.

17. Kwon-Chung, K.J.; Bennett, J.E. Distribution of Alpha and Alpha Mating Types of *Cryptococcus neoformans* among Natural and Clinical Isolates. *American Journal of Epidemiology* 1978, *108*, 337–340, doi:10.1093/oxfordjournals.aje.a112628.

18. Litvintseva, A.P.; Kestenbaum, L.; Vilgalys, R.; Mitchell, T.G. Comparative Analysis of Environmental and Clinical Populations of *Cryptococcus neoformans*. *J. Clin. Microbiol.* 2005, *43*, 556–564, doi:10.1128/JCM.43.2.556-564.2005.

19. Chen, J.; Varma, A.; Diaz, M.R.; Litvintseva, A.P.; Wollenberg, K.K.; Kwon-Chung, K.J. *Cryptococcus neoformans* Strains and Infection in Apparently Immunocompetent Patients, China. *Emerging Infect. Dis.* 2008, *14*, 755–762, doi:10.3201/eid1405.071312.

20. Lin, X.; Heitman, J. The Biology of the *Cryptococcus neoformans* Species Complex. *Annu. Rev. Microbiol.* 2006, *60*, 69–105, doi:10.1146/annurev.micro.60.080805.142102.

21. Xu, J.; Mitchell, T.G. Comparative Gene Genealogical Analyses of Strains of Serotype AD Identify Recombination in Populations of Serotypes A and D in the Human

Pathogenic Yeast *Cryptococcus neoformans*. *Microbiology (Reading)* 2003, *149*, 2147–2154, doi:10.1099/mic.0.26180-0.

22. Hiremath, S.S.; Chowdhary, A.; Kowshik, T.; Randhawa, H.S.; Sun, S.; Xu, J. Long-Distance Dispersal and Recombination in Environmental Populations of *Cryptococcus neoformans* Var. g*rubii* from India. *Microbiology (Reading)* 2008, *154*, 1513–1524, doi:10.1099/mic.0.2007/015594-0.

23. Lin, X.; Litvintseva, A.P.; Nielsen, K.; Patel, S.; Floyd, A.; Mitchell, T.G.; Heitman, J. AADα Hybrids of *Cryptococcus neoformans*: Evidence of Same-Sex Mating in Nature and Hybrid Fitness. *PLOS Genetics* 2007, *3*, e186, doi:10.1371/journal.pgen.0030186.

24. Lin, X.; Hull, C.M.; Heitman, J. Sexual Reproduction between Partners of the Same Mating Type in *Cryptococcus neoformans*. *Nature* 2005, *434*, 1017–1021, doi:10.1038/nature03448.

25. Chen, Y.-H.; Yu, F.; Bian, Z.-Y.; Hong, J.-M.; Zhang, N.; Zhong, Q.-S.; Hang, Y.-P.; Xu, J.; Hu, L.-H. Multi-locus Sequence Typing Reveals Both Shared and Unique Genotypes of *Cryptococcus neoformans* in Jiangxi Province, China. *Scientific Reports* 2018, *8*, 1495, doi:10.1038/s41598-018-20054-4.

26. Samarasinghe, H.; Aljohani, R.; Jimenez, C.; Xu, J. Fantastic Yeasts and Where to Find Them: The Discovery of a Predominantly Clonal *Cryptococcus deneoformans* Population in Saudi Arabian Soils. *FEMS Microbiol Ecol* 2019, *95*, doi:10.1093/femsec/fiz122.

27. Rocha, D.F.S.; Cruz, K.S.; Santos, C.S. da S.; Menescal, L.S.F.; Neto, J.R. da S.; Pinheiro, S.B.; Silva, L.M.; Trilles, L.; Souza, J.V.B. de MLST Reveals a Clonal Population Structure for *Cryptococcus neoformans* Molecular Type VNI Isolates from Clinical Sources in Amazonas, Northern-Brazil. *PLOS ONE* 2018, *13*, e0197841, doi:10.1371/journal.pone.0197841.

28. Litvintseva, A.P.; Lin, X.; Templeton, I.; Heitman, J.; Mitchell, T.G. Many Globally Isolated AD Hybrid Strains of *Cryptococcus neoformans* Originated in Africa. *PLOS Pathogens* 2007, *3*, e114, doi:10.1371/journal.ppat.0030114.

29. Chen, Y.; Litvintseva, A.P.; Frazzitta, A.E.; Haverkamp, M.R.; Wang, L.; Fang, C.; Muthoga, C.; Mitchell, T.G.; Perfect, J.R. Comparative Analyses of Clinical and

Environmental Populations of *Cryptococcus neoformans* in Botswana. *Molecular Ecology* 2015, *24*, 3559–3571, doi:https://doi.org/10.1111/mec.13260.

30. Hagen, F.; Ceresini, P.C.; Polacheck, I.; Ma, H.; Nieuwerburgh, F. van; Gabaldón, T.; Kagan, S.; Pursall, E.R.; Hoogveld, H.L.; Iersel, L.J.J. van; *et al*. Ancient Dispersal of the Human Fungal Pathogen *Cryptococcus gattii* from the Amazon Rainforest. *PLOS ONE* 2013, *8*, e71148, doi:10.1371/journal.pone.0071148.

31. Lengeler, K.B.; Cox, G.M.; Heitman, J. Serotype AD Strains of *Cryptococcus neoformans* Are Diploid or Aneuploid and Are Heterozygous at the Mating-Type Locus. *Infect. Immun.* 2001, *69*, 115–122, doi:10.1128/IAI.69.1.115-122.2001.

32. Ni, M.; Feretzaki, M.; Li, W.; Floyd-Averette, A.; Mieczkowski, P.; Dietrich, F.S.; Heitman, J. Unisexual and Heterosexual Meiotic Reproduction Generate Aneuploidy and Phenotypic Diversity De Novo in the Yeast *Cryptococcus neoformans*. *PLOS Biology* 2013, *11*, e1001653, doi:10.1371/journal.pbio.1001653.

33. Samarasinghe, H.; Xu, J. Hybrids and Hybridization in the *Cryptococcus neoformans* and *Cryptococcus gattii* Species Complexes. *Infect. Genet. Evol.* 2018, *66*, 245–255, doi:10.1016/j.meegid.2018.10.011.

34. Aminnejad, M.; Diaz, M.; Arabatzis, M.; Castañeda, E.; Lazera, M.; Velegraki, A.; Marriott, D.; Sorrell, T.C.; Meyer, W. Identification of Novel Hybrids between *Cryptococcus neoformans* Var. *grubii* VNI and *Cryptococcus gattii* VGII. *Mycopathologia* 2012, *173*, 337–346, doi:10.1007/s11046-011-9491-x.

35. Bovers, M.; Hagen, F.; Kuramae, E.E.; Hoogveld, H.L.; Dromer, F.; St-Germain, G.; Boekhout, T. AIDS Patient Death Caused by Novel *Cryptococcus neoformans* × *C. gattii* Hybrid. *Emerg Infect Dis* 2008, *14*, 1105–1108, doi:10.3201/eid1407.080122.

36. Bovers, M.; Hagen, F.; Kuramae, E.E.; Diaz, M.R.; Spanjaard, L.; Dromer, F.; Hoogveld, H.L.; Boekhout, T. Unique Hybrids between the Fungal Pathogens *Cryptococcus neoformans* and *Cryptococcus gattii*. *FEMS Yeast Res.* 2006, *6*, 599–607, doi:10.1111/j.1567-1364.2006.00082.x.

37. You, M.; Xu, J. The Effects of Environmental and Genetic Factors on the Germination of Basidiospores in the *Cryptococcus gattii* Species Complex. *Sci Rep* 2018, *8*, 1–15, doi:10.1038/s41598-018-33679-2.

38. Cogliati, M. Global Molecular Epidemiology of *Cryptococcus neoformans* and *Cryptococcus gattii*: An Atlas of the Molecular Types. *Scientifica (Cairo)* 2013, *2013*, 675213, doi:10.1155/2013/675213.

39. Vogan, A.A.; Khankhet, J.; Samarasinghe, H.; Xu, J. Identification of QTLs Associated with Virulence Related Traits and Drug Resistance in *Cryptococcus neoformans*. *G3 (Bethesda)* 2016, *6*, 2745–2759, doi:10.1534/g3.116.029595.

40. Shahid, M.; Han, S.; Yoell, H.; Xu, J. Fitness Distribution and Transgressive Segregation across 40 Environments in a Hybrid Progeny Population of the Human-Pathogenic Yeast *Cryptococcus neoformans*. *Genome* 2008, *51*, 272–281, doi:10.1139/G08-004.

41. Meyer, W.; Aanensen, D.M.; Boekhout, T.; Cogliati, M.; Diaz, M.R.; Esposto, M.C.; Fisher, M.; Gilgado, F.; Hagen, F.; Kaocharoen, S.; *et al*. Consensus Multi-Locus Sequence Typing Scheme for *Cryptococcus neoformans* and *Cryptococcus gattii*. *Med. Mycol.* 2009, *47*, 561–570, doi:10.1080/13693780902953886.

42. Kumar, S.; Stecher, G.; Tamura, K. MEGA7: Molecular Evolutionary Genetics Analysis Version 7.0 for Bigger Datasets. *Mol Biol Evol* 2016, *33*, 1870–1874, doi:10.1093/molbev/msw054.

43. Skosireva, I.; James, T.Y.; Sun, S.; Xu, J. Mitochondrial Inheritance in Haploid x Non-Haploid Crosses in *Cryptococcus neoformans*. *Curr. Genet.* 2010, *56*, 163–176, doi:10.1007/s00294-010-0289-z.

44. Sia, R.A.; Lengeler, K.B.; Heitman, J. Diploid Strains of the Pathogenic Basidiomycete *Cryptococcus neoformans* Are Thermally Dimorphic. *Fungal Genetics and Biology* 2000, *29*, 153–163, doi:10.1006/fgbi.2000.1192.

45. Sun, S.; Xu, J. Genetic Analyses of a Hybrid Cross between Serotypes A and D Strains of the Human Pathogenic Fungus *Cryptococcus neoformans*. *Genetics* 2007, *177*, 1475–1486, doi:10.1534/genetics.107.078923.

46. Vogan, A.A.; Khankhet, J.; Xu, J. Evidence for Mitotic Recombination within the Basidia of a Hybrid Cross of *Cryptococcus neoformans*. *PLoS ONE* 2013, *8*, e62790, doi:10.1371/journal.pone.0062790.

47. Xu, J. Mitochondrial DNA Polymorphisms in the Human Pathogenic Fungus *Cryptococcus neoformans*. *Curr. Genet.* 2002, *41*, 43–47, doi:10.1007/s00294-002-0282-2.

48. Fredslund, J.; Schauser, L.; Madsen, L.H.; Sandal, N.; Stougaard, J. PriFi: Using a Multiple Alignment of Related Sequences to Find Primers for Amplification of Homologs. *Nucleic Acids Res* 2005, *33*, W516–W520, doi:10.1093/nar/gki425.

49. Hopfer, R.L.; Blank, F. Caffeic Acid-Containing Medium for Identification Of *Cryptococcus neoformans*. *J. CLIN. MICROBIOL.* 1976, *2*, 115-120.

50. Rueden, C.T.; Schindelin, J.; Hiner, M.C.; DeZonia, B.E.; Walter, A.E.; Arena, E.T.; Eliceiri, K.W. ImageJ2: ImageJ for the next Generation of Scientific Image Data. *BMC Bioinformatics* 2017, *18*, 529, doi:10.1186/s12859-017-1934-z.

51. Clinical Laboratory Standards Institue: Reference Method for Broth Dilution Antifungal Susceptibility Testing of Yeasts; Approved Standard, 3rd Ed, CLSI Document M27-A3, CLSI, Wayne, PA 2008.

52. R Core Team R: A Language and Environment for Statistical Computing. 2013.

53. Kamvar, Z.N.; Tabima, J.F.; Grünwald, N.J. Poppr: An R Package for Genetic Analysis of Populations with Clonal, Partially Clonal, and/or Sexual Reproduction. *PeerJ* 2014, *2*, e281, doi:10.7717/peerj.281.

54. Bates, D.; Mächler, M.; Bolker, B.; Walker, S. Fitting Linear Mixed-Effects Models Using Lme4. *Journal of Statistical Software* 2015, *67*, 1–48, doi:10.18637/jss.v067.i01.

55. Fox, J.; Weisberg, S. Visualizing Fit and Lack of Fit in Complex Regression Models with Predictor Effect Plots and Partial Residuals. *Journal of Statistical Software* 2018, *87*, 1–27, doi:10.18637/jss.v087.i09.

56. Wickham, H. Ggplot2: Elegant Graphics for Data Analysis. *Spring New York* 2009.

57. Lin, X.; Patel, S.; Litvintseva, A.P.; Floyd, A.; Mitchell, T.G.; Heitman, J. Diploids in the *Cryptococcus neoformans* Serotype A Population Homozygous for the Alpha Mating Type Originate via Unisexual Mating. *PLoS Pathog.* 2009, *5*, e1000283, doi:10.1371/journal.ppat.1000283.

58. Kavanaugh, L.A.; Fraser, J.A.; Dietrich, F.S. Recent Evolution of the Human Pathogen *Cryptococcus neoformans* by Intervarietal Transfer of a 14-Gene Fragment. *Mol. Biol. Evol.* 2006, *23*, 1879–1890, doi:10.1093/molbev/msl070.

59. Vogan, A.A.; Xu, J. Evidence for Genetic Incompatibilities Associated with Post-Zygotic Reproductive Isolation in the Human Fungal Pathogen *Cryptococcus neoformans*. *Genome* 2014, *57*, 335–344, doi:10.1139/gen-2014-0077.

60. Sun, S.; Xu, J. Chromosomal Rearrangements between Serotype A and D Strains in *Cryptococcus neoformans*. *PLoS ONE* 2009, *4*, e5524, doi:10.1371/journal.pone.0005524.

61. D'Souza, C.A.; Kronstad, J.W.; Taylor, G.; Warren, R.; Yuen, M.; Hu, G.; Jung, W.H.; Sham, A.; Kidd, S.E.; Tangen, K.; *et al*. Genome Variation in *Cryptococcus gattii*, an Emerging Pathogen of Immunocompetent Hosts. *mBio* 2011, *2*, doi:10.1128/mBio.00342-10.

62. Morrow, C.A.; Lee, I.R.; Chow, E.W.L.; Ormerod, K.L.; Goldinger, A.; Byrnes, E.J.; Nielsen, K.; Heitman, J.; Schirra, H.J.; Fraser, J.A. A Unique Chromosomal Rearrangement in the *Cryptococcus neoformans* var. *grubii* Type Strain Enhances Key Phenotypes Associated with Virulence. *mBio* 2012, *3*, doi:10.1128/mBio.00310-11.

63. Farrer, R.A.; Desjardins, C.A.; Sakthikumar, S.; Gujja, S.; Saif, S.; Zeng, Q.; Chen, Y.; Voelz, K.; Heitman, J.; May, R.C.; *et al*. Genome Evolution and Innovation across the Four Major Lineages of *Cryptococcus gattii*. *mBio* 2015, *6*, e00868-15, doi:10.1128/mBio.00868-15.

64. Birky, C.W. The Inheritance of Genes in Mitochondria and Chloroplasts: Laws, Mechanisms, and Models. *Annual Review of Genetics* 2001, *35*, 125–148, doi:10.1146/annurev.genet.35.102401.090231.

65. Xu, J. The Inheritance of Organelle Genes and Genomes: Patterns and Mechanisms. *Genome* 2005, *48*, 951–958, doi:10.1139/g05-082.

66. Yan, Z.; Xu, J. Mitochondria Are Inherited from the MATa Parent in Crosses of the Basidiomycete Fungus *Cryptococcus neoformans*. *Genetics* 2003, *163*, 1315–1325.

67. McClelland, C.M.; Chang, Y.C.; Varma, A.; Kwon-Chung, K.J. Uniqueness of the Mating System in *Cryptococcus neoformans*. *Trends in Microbiology* 2004, *12*, 208–212, doi:10.1016/j.tim.2004.03.003.

68. Voelz, K.; Ma, H.; Phadke, S.; Byrnes, E.J.; Zhu, P.; Mueller, O.; Farrer, R.A.; Henk, D.A.; Lewit, Y.; Hsueh, Y.-P.; *et al*. Transmission of Hypervirulence Traits via Sexual Reproduction within and between Lineages of the Human Fungal Pathogen

Cryptococcus gattii. *PLOS Genetics* 2013, *9*, e1003771, doi:10.1371/journal.pgen.1003771.

69. Wang, Z.; Wilson, A.; Xu, J. Mitochondrial DNA Inheritance in the Human Fungal Pathogen *Cryptococcus gattii*. *Fungal Genet. Biol.* 2015, *75*, 1–10, doi:10.1016/j.fgb.2015.01.001.

70. Hayles, J.; Nurse, P. Genetics of the Fission Yeast *Schizosaccharomyces pombe*. *Annu. Rev. Genet.* 1992, *26*, 373–402, doi:10.1146/annurev.ge.26.120192.002105.

71. Yan, Z.; Hull, C.M.; Heitman, J.; Sun, S.; Xu, J. SXI1alpha Controls Uniparental Mitochondrial Inheritance in *Cryptococcus neoformans*. *Curr. Biol.* 2004, *14*, R743-744, doi:10.1016/j.cub.2004.09.008.

72. Yan, Z.; Hull, C.M.; Sun, S.; Heitman, J.; Xu, J. The Mating Type-Specific Homeodomain Genes *SXI1* Alpha and *SXI2*a Coordinately Control Uniparental Mitochondrial Inheritance in *Cryptococcus neoformans*. *Curr. Genet.* 2007, *51*, 187–195, doi:10.1007/s00294-006-0115-9.

73. Yan, Z.; Sun, S.; Shahid, M.; Xu, J. Environment Factors Can Influence Mitochondrial Inheritance in the Fungus *Cryptococcus neoformans*. *Fungal genetics and biology: FG & B* 2007, *44*, 315–322, doi:10.1016/j.fgb.2006.10.002.

74. Govender, N.P.; Patel, J.; van Wyk, M.; Chiller, T.M.; Lockhart, S.R.; Group for Enteric, Respiratory and Meningeal Disease Surveillance in South Africa (GERMS-SA) Trends in Antifungal Drug Susceptibility of *Cryptococcus neoformans* Isolates Obtained through Population-Based Surveillance in South Africa in 2002-2003 and 2007-2008. *Antimicrob. Agents Chemother.* 2011, *55*, 2606–2611, doi:10.1128/AAC.00048-11.

75. Alizadeh, F.; Khodavandi, A.; Zalakian, S. Quantitation of Ergosterol Content and Gene Expression Profile of *ERG11* Gene in Fluconazole-Resistant *Candida albicans*. *Curr Med Mycol* 2017, *3*, 13–19, doi:10.29252/cmm.3.1.13.

76. Choi, Y.J.; Kim, Y.-J.; Yong, D.; Byun, J.-H.; Kim, T.S.; Chang, Y.S.; Choi, M.J.; Byeon, S.A.; Won, E.J.; Kim, S.H.; *et al*. Fluconazole-Resistant *Candida parapsilosis* Bloodstream Isolates with Y132F Mutation in *ERG11* Gene, South Korea. *Emerg Infect Dis* 2018, *24*, 1768–1770, doi:10.3201/eid2409.180625.

77. Gast, C.E.; Basso, L.R.; Bruzual, I.; Wong, B. Azole Resistance in *Cryptococcus gattii* from the Pacific Northwest: Investigation of the Role of *ERG11*. *Antimicrobial Agents and Chemotherapy* 2013, *57*, 5478–5485, doi:10.1128/AAC.02287-12.

78. Sionov, E.; Chang, Y.C.; Garraffo, H.M.; Dolan, M.A.; Ghannoum, M.A.; Kwon-Chung, K.J. Identification of a *Cryptococcus neoformans* Cytochrome P450 Lanosterol 14α-Demethylase (*Erg11*) Residue Critical for Differential Susceptibility between Fluconazole/Voriconazole and Itraconazole/Posaconazole. *Antimicrobial Agents and Chemotherapy* 2012, *56*, 1162–1169, doi:10.1128/AAC.05502-11.

79. Rodero, L.; Mellado, E.; Rodriguez, A.C.; Salve, A.; Guelfand, L.; Cahn, P.; Cuenca-Estrella, M.; Davel, G.; Rodriguez-Tudela, J.L. G484S Amino Acid Substitution in Lanosterol 14-α Demethylase (*ERG11*) Is Related to Fluconazole Resistance in a Recurrent *Cryptococcus neoformans* Clinical Isolate. *Antimicrobial Agents and Chemotherapy* 2003, *47*, 3653–3656, doi:10.1128/AAC.47.11.3653-3656.2003.

80. Xu, Y.; Chen, L.; Li, C. Susceptibility of Clinical Isolates of *Candida* Species to Fluconazole and Detection of *Candida albicans ERG11* Mutations. *J Antimicrob Chemother* 2008, *61*, 798–804, doi:10.1093/jac/dkn015.

81. Altamirano, S.; Fang, D.; Simmons, C.; Sridhar, S.; Wu, P.; Sanyal, K.; Kozubowski, L. Fluconazole-Induced Ploidy Change in *Cryptococcus neoformans* Results from the Uncoupling of Cell Growth and Nuclear Division. *mSphere* 2017, *2*, doi:10.1128/mSphere.00205-17.

82. Chang, Z.; Yadav, V.; Lee, S.C.; Heitman, J. Epigenetic Mechanisms of Drug Resistance in Fungi. *Fungal Genet Biol* 2019, *132*, 103253, doi:10.1016/j.fgb.2019.103253.

83. Li, X.; Cai, Q.; Mei, H.; Zhou, X.; Shen, Y.; Li, D.; Liu, W. The Rpd3/Hda1 Family of Histone Deacetylases Regulates Azole Resistance in *Candida albicans*. *J Antimicrob Chemother* 2015, *70*, 1993–2003, doi:10.1093/jac/dkv070.

84. Robbins, N.; Leach, M.D.; Cowen, L.E. Lysine Deacetylases Hda1 and Rpd3 Regulate Hsp90 Function Thereby Governing Fungal Drug Resistance. *Cell Reports* 2012, *2*, 878–888, doi:10.1016/j.celrep.2012.08.035.

85. Brandão, F.A.; Derengowski, L.S.; Albuquerque, P.; Nicola, A.M.; Silva-Pereira, I.; Poças-Fonseca, M.J. Histone Deacetylases Inhibitors Effects on *Cryptococcus neoformans* Major Virulence Phenotypes. *Virulence* 2015, *6*, 618–630, doi:10.1080/21505594.2015.1038014.

86. Lamoth, F.; Juvvadi, P.R.; Steinbach, W.J. Histone Deacetylase Inhibition as an Alternative Strategy against Invasive Aspergillosis. *Front Microbiol* 2015, *6*, 96, doi:10.3389/fmicb.2015.00096.

87. Iii, E.J.B.; Li, W.; Ren, P.; Lewit, Y.; Voelz, K.; Fraser, J.A.; Dietrich, F.S.; May, R.C.; Chatuverdi, S.; Chatuverdi, V.; *et al*. A Diverse Population of *Cryptococcus gattii* Molecular Type VGIII in Southern Californian HIV/AIDS Patients. *PLOS Pathogens* 2011, *7*, e1002205, doi:10.1371/journal.ppat.1002205.

88. Springer, D.J.; Billmyre, R.B.; Filler, E.E.; Voelz, K.; Pursall, R.; Mieczkowski, P.A.; Larsen, R.A.; Dietrich, F.S.; May, R.C.; Filler, S.G.; *et al*. *Cryptococcus gattii* VGIII Isolates Causing Infections in HIV/AIDS Patients in Southern California: Identification of the Local Environmental Source as Arboreal. *PLoS Pathog* 2014, *10*, doi:10.1371/journal.ppat.1004285.

89. Halliday, C.L.; Bui, T.; Krockenberger, M.; Malik, R.; Ellis, D.H.; Carter, D.A. Presence of Alpha and a Mating Types in Environmental and Clinical Collections of *Cryptococcus neoformans* var. *gattii* Strains from Australia. *J Clin Microbiol* 1999, *37*, 2920–2926, doi:10.1128/JCM.37.9.2920-2926.1999.

90. Firacative, C.; Roe, C.C.; Malik, R.; Ferreira-Paim, K.; Escandón, P.; Sykes, J.E.; Castañón-Olivares, L.R.; Contreras-Peres, C.; Samayoa, B.; Sorrell, T.C.; *et al*. MLST and Whole-Genome-Based Population Analysis of *Cryptococcus gattii* VGIII Links Clinical, Veterinary and Environmental Strains, and Reveals Divergent Serotype Specific Sub-Populations and Distant Ancestors. *PLoS Neglected Tropical Diseases* 2016, *10*, doi:10.1371/journal.pntd.0004861.

91. Lockhart, S.R.; Iqbal, N.; Harris, J.R.; Grossman, N.T.; DeBess, E.; Wohrle, R.; Marsden-Haug, N.; Vugia, D.J. *Cryptococcus gattii* in the United States: Genotypic Diversity of Human and Veterinary Isolates. *PLOS ONE* 2013, *8*, e74737, doi:10.1371/journal.pone.0074737.

92. Byrnes, E.J.; Bartlett, K.H.; Perfect, J.R.; Heitman, J. *Cryptococcus gattii*: An Emerging Fungal Pathogen Infecting Humans and Animals. *Microbes Infect* 2011, *13*, 895–907, doi:10.1016/j.micinf.2011.05.009.

93. Fraser, J.A.; Subaran, R.L.; Nichols, C.B.; Heitman, J. Recapitulation of the Sexual Cycle of the Primary Fungal Pathogen *Cryptococcus neoformans* var. *gattii*: Implications for an Outbreak on Vancouver Island, Canada. *Eukaryotic Cell* 2003, *2*, 1036–1045, doi:10.1128/ec.2.5.1036-1045.2003.

94. Fernandes, K.E.; Dwyer, C.; Campbell, L.T.; Carter, D.A. Species in the *Cryptococcus gattii* Complex Differ in Capsule and Cell Size Following Growth under Capsule-Inducing Conditions. *mSphere* 2016, *1*, doi:10.1128/mSphere.00350-16.

95. Upadhya, R.; Campbell, L.T.; Donlin, M.J.; Aurora, R.; Lodge, J.K. Global Transcriptome Profile of *Cryptococcus neoformans* during Exposure to Hydrogen Peroxide Induced Oxidative Stress. *PLOS ONE* 2013, *8*, e55110, doi:10.1371/journal.pone.0055110.

96. Ueno, K.; Yanagihara, N.; Otani, Y.; Shimizu, K.; Kinjo, Y.; Miyazaki, Y. Neutrophil-Mediated Antifungal Activity against Highly Virulent *Cryptococcus gattii* Strain R265. *Med Mycol* 2019, *57*, 1046–1054, doi:10.1093/mmy/myy153.

97. Missall, T.A.; Lodge, J.K.; McEwen, J.E. Mechanisms of Resistance to Oxidative and Nitrosative Stress: Implications for Fungal Survival in Mammalian Hosts. *Eukaryot Cell* 2004, *3*, 835–846, doi:10.1128/EC.3.4.835-846.2004.

98. Romero-Martinez, R.; Wheeler, M.; Guerrero-Plata, A.; Rico, G.; Torres-Guerrero, H. Biosynthesis and Functions of Melanin in *Sporothrix schenckii*. *Infect Immun* 2000, *68*, 3696–3703.

99. Gerik, K.J.; Bhimireddy, S.R.; Ryerse, J.S.; Specht, C.A.; Lodge, J.K. PKC1 Is Essential for Protection against Both Oxidative and Nitrosative Stresses, Cell Integrity, and Normal Manifestation of Virulence Factors in the Pathogenic Fungus *Cryptococcus neoformans*. *Eukaryot Cell* 2008, *7*, 1685–1698, doi:10.1128/EC.00146-08.

100. Brown, S.M.; Upadhya, R.; Shoemaker, J.D.; Lodge, J.K. Isocitrate Dehydrogenase Is Important for Nitrosative Stress Resistance in *Cryptococcus neoformans*, but Oxidative Stress Resistance Is Not Dependent on Glucose-6-Phosphate Dehydrogenase. *Eukaryotic Cell* 2010, *9*, 971–980, doi:10.1128/EC.00271-09.

101. Chiranand, W.; McLeod, I.; Zhou, H.; Lynn, J.J.; Vega, L.A.; Myers, H.; Yates, J.R.; Lorenz, M.C.; Gustin, M.C. CTA4 Transcription Factor Mediates Induction of Nitrosative Stress Response in *Candida albicans*. *Eukaryot Cell* 2008, *7*, 268–278, doi:10.1128/EC.00240-07.

102. Rieseberg, L.H.; Archer, M.A.; Wayne, R.K. Transgressive Segregation, Adaptation and Speciation. *Heredity* 1999, *83*, 363–372, doi:10.1038/sj.hdy.6886170.

103. Kagawa, K.; Takimoto, G. Hybridization Can Promote Adaptive Radiation by Means of Transgressive Segregation. *Ecology Letters* 2018, *21*, 264–274, doi:https://doi.org/10.1111/ele.12891.

104. Rieseberg, L.H.; Kim, S.-C.; Randell, R.A.; Whitney, K.D.; Gross, B.L.; Lexer, C.; Clay, K. Hybridization and the Colonization of Novel Habitats by Annual Sunflowers. *Genetica* 2007, *129*, 149–165, doi:10.1007/s10709-006-9011-y.

105. Xu, J. 2004. Genotype-environment interactions of spontaneous mutations affecting vegetative fitness in the human pathogenic fungus *Cryptococcus neoformans*. Genetics 168:1177-1188, doi: 10.1534/genetics.104.030031.

Chapter 5: Genetic and phenotypic diversities in experimental populations of diploid inter-lineage hybrids in the human pathogenic *Cryptococcus*

5.1 Preface

Genome instability can arise from events, such as genome doubling, chromosomal rearrangement, mitotic crossovers, gene deletion and gene conversion in diploid organisms. These events can also cause aneuploidy and loss of heterozygosity (LOH). The emergence of aneuploidy and LOH is considered as a major mechanism of generating genetic diversity. It has been revealed that exposure to the antifungal drug fluconazole can induce ploidy changes and LOH, allowing it to rapidly adapt to a new environment. However, the role of parental divergence in genome stability has not been well-documented in *Cryptococcus* hybrids. The results indicate that, compared to their respect ancestral clones, the evolved clones showed a range of changes in genomic DNA contents, genotypes and phenotypes. However, we found that neither the parental genetic divergence of each hybrid ancestral clone nor the mutation accumulation condition could be used to predict all the observed variations. Instead, both the parental genetic divergence and the MA conditions, as well as their interactions, contributed to the observed genotypic and phenotypic changes among the MA lines. This work is now published in Microorganisms 2021, 9(8), 1579. The referencing style in this chapter is as in the originally submitted manuscript. I am the primary contributor of this work.

5.2 Abstract

To better understand the potential factors contributing to genome instability and phenotypic diversity, we conducted mutation accumulation (MA) experiments for 120 days for seven diploid cryptococcal hybrids under fluconazole (10 MA lines each) and non-fluconazole conditions (10 MA lines each). The genomic DNA content, loss of heterozygosity (LOH) rate, growth ability, and fluconazole susceptibility were determined for all 140 evolved cultures. Compared to that of their ancestral clones, the evolved clones showed: (i) genomic DNA content changes ranging from ~22% less to ~27% more, and (ii) reduced, similar, and increased phenotypic values for each tested trait, with most evolved clones displaying increased growth at 40 °C and increased fluconazole resistance. Aside from the ancestral multi-locus genotypes (MLGs) and heterozygosity patterns (MHPs), 77 unique MLGs and 70 unique MPHs were identified among the 140 evolved cultures at day 120. The average LOH rates of the MA lines in the

absence and presence of fluconazole were similar at 1.27×10^{-4} and 1.38×10^{-4} LOH events per MA line per mitotic division, respectively. While LOH rates varied among MA lines from different ancestors, there was no apparent correlation between the genetic divergence of the parental haploid genomes within ancestral clones and LOH rates. Together, our results suggest that hybrids between diverse lineages of the human pathogenic *Cryptococcus* can generate significant genotypic and phenotypic diversities during asexual reproduction.

5.3 Introduction

A stable genome allows faithful transmission of genetic information from parent to progeny, ensuring genotypic and phenotypic stability within individual organisms or populations. However, genome instability is common and has been found in most organisms. Genome instability can be manifested in multiple forms and caused by various factors, such as genome doubling, chromosomal rearrangement, mitotic recombination, gene duplication, gene deletion, gene conversion, and transposition. Many of these changes involve double-strand DNA breaks, followed by repair through either the synthesis-dependent strand annealing using homologous sequences or non-homologous end joining [1,2]. Among these changes, gene deletion, gene conversion, and, to a lesser extent, mitotic recombination between homologous chromosomes, are commonly manifested as loss of heterozygosity (LOH) that can be detected using multiple molecular methods. Environmental stress, such as ultraviolet exposure and other high-energy radiation, can increase double-strand DNA breaks and elevate the LOH rates [3,4]. Spontaneous and induced LOH events were observed in diploid fungi, such as *Saccharomyces cerevisiae* and *Candida albicans* [5–9]. In addition, if there was a selection in favor of one of the alleles in the strain, the non-favored allele would likely be lost more frequently. For example, the antifungal drug fluconazole was shown to increase the frequencies of LOH events in *C. albicans*, resulting in aneuploidy and greater resistance to fluconazole [10]. Through LOH, diverse genotypes and phenotypes could be derived from a single diploid strain [11–13]. At present, most investigations of LOH focused on the impacts of environmental factors. Relatively little is known about the influences of genetic factors on LOH, such as that between genome sequence divergence of homologous chromosomes in diploid cells.

The human pathogenic *Cryptococcus* (HPC) is a group of basidiomycete yeasts and an excellent model for studying the genetic stability of hybrids and investigating how genome sequence divergence between homologous chromosomes can impact the LOH rates. HPC consists of two species complexes, the *Cryptococcus neoformans* species complex (CNSC) and the *Cryptococcus gattii* species complex (CGSC). Most strains of CNSC and CGSC are haploid, existing in one of two mating types, *MAT*α and *MAT***a**. These haploid yeast cells typically propagate asexually by budding until strains of the opposite mating-type (**a**-α) or the same mating-type (α-α) come into contact on substrates conducive for mating. The mating products are initially in a dikaryotic hyphal form that transitions into a transient diploid phase before meiosis to produce sexual spores (i.e., basidiospores). However, the diploid status can be induced and maintained through the hypha-to-yeast transition at 37 °C. In nature, most haploid strains are *MAT*α [14]. Although *MAT***a** strains are relatively rare, heterozygous diploid hybrids from **a**-α mating of HPC were frequently reported from environmental and clinical settings [6,9–12]. Both environmental and clinical hybrid isolates are either aneuploid or diploid, different from the haploid status of most non-hybrid strains [15,16-19]. Among the cryptococcal hybrids, serotype AD hybrids derived from the mating between *Cryptococcus neoformans* (serotype A) and *Cryptococcus deneoformans* (serotype D) are the most prevalent [20]. Serotype AD hybrid isolates are heterozygous at most loci but homozygous at some loci [11,15,21]. Yet, it remains unknown whether the observed homozygosity in natural hybrids was derived through meiosis, mitosis, or both.

Previous investigations of serotype AD hybrids showed that both meiosis and mitosis could generate diploid or aneuploid progeny, along with some loci being heterozygous while others being homozygous[13,15,19,21–23]. However, information on the genome stability of other cryptococcal hybrids, such as those of serotypes AB and BC, is very limited. In addition, two common indicators of genome instability are LOH and genomic DNA content change (i.e., ploidy change), such as the generation of aneuploidy. Aneuploidy was observed in a variety of organisms, including fungi, plants, and animals [15,24–27]. In the yeast *S. cerevisiae*, the induced chromosomal instability is often regulated by interactions between chromosomes leading to aneuploidy in cells [24]. Ploidy changes in cells are commonly observed in eukaryotes during sexual and

asexual reproduction, and aneuploidy can result from disruptions in many of the steps during cell cycles [28].

Experimental evolution is a valuable tool for studying the mechanisms of adaptation to specific environmental conditions. For example, experimental evolution revealed the genetic mechanisms for fluconazole resistance and adaptations to new environments in *C. albicans*, including LOH, aneuploidy, gene duplication, and novel mutations [10,29,30]. There are multiple types of experimental evolutionary approaches. One common type is mutation accumulation (MA), where a random individual (or pair of individuals in obligate sexual species) is chosen for the transfer to establish the next generation. This process maximizes genetic drift and enables diverse types of mutations to be accumulated. In HPC, a mutation accumulation experiment involving a laboratory serotype AD strain revealed evidence of LOH and ploidy changes [13]. Researchers also found that fluconazole stress increased the LOH frequency for markers on Chromosome 1 by over 50 folds compared to non-fluconazole stress, favoring the parental homolog associated with a higher fluconazole resistance. Two Chromosome 1 genes, *ERG11* (the fluconazole target gene) and *AFR1* (the transporter for triazoles), are associated with fluconazole resistance [31,32].

In this study, we aimed to investigate the genome instability of inter-lineage hybrids of HPC, including hybrids between lineages within CGSC and hybrids between CNSC and CGSC. Specifically, we were interested in whether genomes of hybrids from evolutionarily more divergent parental strains were more stable than those from evolutionarily more similar parents. On the one hand, the increased sequence divergence between more divergent homologous chromosomes could reduce the rate of homologous recombination, resulting in more stable genomes [33]. On the other hand, having more divergent genomes in the same nucleus may make it more difficult to coordinate cellular activities during cell cycles and render the hybrid genome less stable [34]. Aside from investigating the potential impact of parental sequence divergence on hybrid genome stability, we were also interested in whether sublethal fluconazole stress would influence hybrid genome stability. To address these questions, we conducted MA experiments on seven diploid cryptococcal hybrids over 800 mitotic generations under flu-

conazole stress and non-fluconazole stress conditions. For all 140 MA lines, we determined their genotypes and LOH by PCR-RFLP, genomic DNA contents by flow cytometry, growth under nine conditions, and susceptibility to fluconazole.

5.4 Materials and Methods

5.4.1 Ancestral clones

Seven diploid *Cryptococcus* hybrids from our previous work were used as the starting clones to initiate the MA experiments [23]. These original starting clones are referred to as ancestral clones, and their descendants derived from the MA lines are called evolved clones. These hybrid ancestral clones were from seven inter-lineage crosses within CGSC and between CGSC and CNSC. They were YMD72 (progeny of B4495 × JF101, VGI × VGIII cross), YMD36 (of WM779 × JF109, VGIV × VGIII cross), YMD135 (of R265 × B4546, VGII × VGIII cross), YMD165 (of CDC15 × JF109, VNI × VGIII cross), YMD10 (of KN99a × JF101, VNI × VGIII cross), YMD88 and YMD89 (of JEC21 × B4546, VNIV × VGIII cross). The percentage of nucleotide difference based on seven single-copy nuclear genes between parental strains for each of the seven hybrids is shown in Table 5.1.

5.4.2 Mutation accumulation (MA) experiments

It was estimated that the growth of one cell to ~10^6 cells takes three days under our experimental conditions, representing ~20 ± 1 mitotic divisions over three days of growth [35]. In the present study, each MA line underwent 40 successive transfers at every 72 h interval, equivalent to ~800 generations in total. At each transfer, cells from one random colony were used to establish the successive MA cultures. To obtain broad patterns about the new mutations and their mutational effects, twenty MA lines were established from each ancestral clone (all from the same colony), including ten MA lines cultured on the yeast extract-peptone-dextrose (YEPD) agar plates (the Y lines) and ten MA lines maintained on YEPD + 4 μg/mL fluconazole (YEPD-FLC) agar plates (the F lines) (as illustrated in Figure 5.1). All MA lines were incubated at 37 °C. In every 5 transfers representing ~100 mitotic generations, an aliquot of each MA line was

collected and stored at −80 °C. The MA phase lasted 120 days (i.e., ~800 mitotic generations), with the evolved cultures from days 15, 30, 45, 60, 75, 90, 105, and 120 stored and labeled as D15, D30, D45, D60, D75, D90, D105, and D120, respectively.

Table 5.1. Information on ancestral clones used in this study.

Crosses		Ancestral Clones	*MAT*a Parent (Lineage)	*MAT*α Parent (Lineage)	Parental Haploid Genome Divergence
Inter-lineage crosses within CGSC	VGI × VGIII	YMD72	B4495 (VGI)	JF101 (VGIII)	0.038
	VGIV × VGIII	YMD36	JF109 (VGIII)	WM779 (VGIV)	0.045
	VGII × VGIII	YMD135	B4546 (VGIII)	R265 (VGII)	0.135
Inter-lineage crosses between CNSC and CGSC	VNI × VGIII	YMD165	JF109 (VGIII)	CDC15 (VNI)	0.171
		YMD10	KN99a (VNI)	JF101 (VGIII)	0.171
	VNIV × VGIII	YMD88	B4546 (VGIII)	JEC21 (VNIV)	0.172
		YMD89	B4546 (VGIII)	JEC21 (VNIV)	0.172

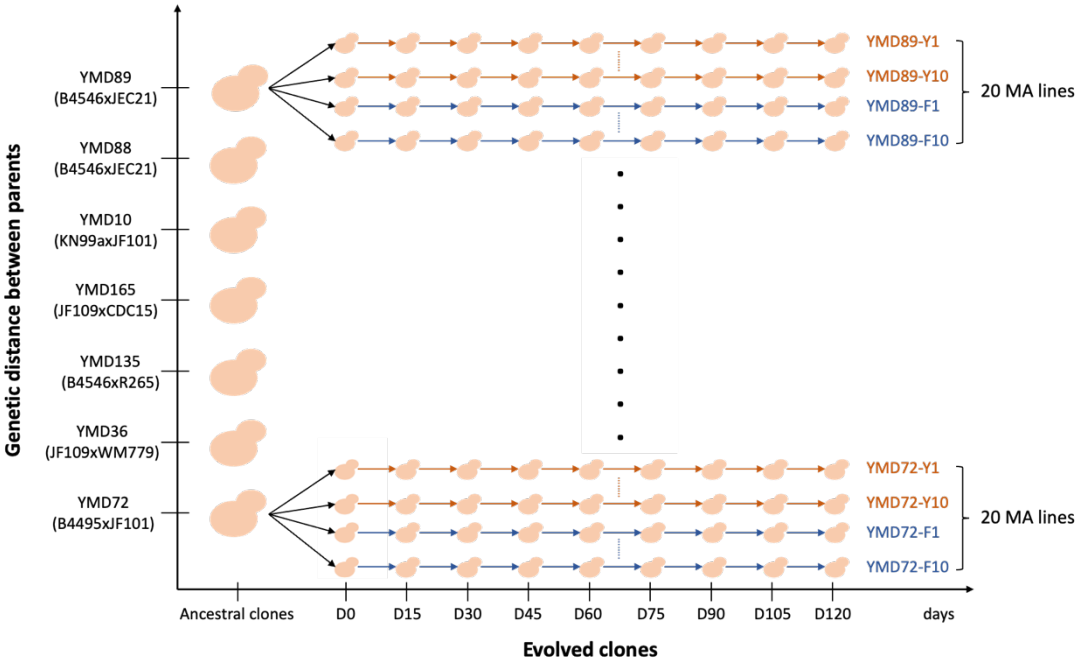

Figure 5.1. Schematic representation of mutation accumulation (MA) experiments. Seven diploid hybrids with diverse genetic backgrounds were used in this study. Each ancestral clone was used to establish 20 MA lines, including ten Y lines (cultured on YEPD agar plates) and ten F lines (cultured on YEPD + 4 µg/ml fluconazole agar plates). All MA lines were incubated at 37 °C. Each MA line underwent 40 transfers over 120 days, equivalent to about 800 mitotic generations.

5.4.3 Ploidy analysis of D120 cultures

The genomic DNA contents of the D120 cultures of all 140 MA lines and their respective ancestral clones were determined by fluorescence-activated cell sorting (FACS), using the protocol described previously [23]. In this analysis, the haploid parental strains were used as haploid controls, and the RAS D15 strain and seven ancestral clones were used as diploid references [23,36]. Data were analyzed and visualized by ModFit LT 5.0 (Verity Software House, Topsham, USA). The ploidy change of each MA line was computed as the percentage of change in peak FACS values between the D120 culture and its respective ancestral clone divided by the peak FACS value of the ancestral clone.

5.4.4 Detecting the loss of heterozygosity (LOH)

Thirteen nuclear genetic markers located on ten chromosomes and two mitochondrial markers were used to analyze the genotypes of the evolved clones in this study (as illustrated in Table S1). All seven ancestral clones were heterozygous at all or most of these nuclear loci [23]. Genotypic changes and occurrence of LOH among MA lines were determined using the PCR-RFLP approach. The specific markers, including their primers, PCR cycling conditions, restriction enzyme digests, gel electrophoresis, and allele scoring, were described in You and Xu [23]. The LOH rate per locus per generation was calculated as the total number of observed LOH events (total number of loci * total number of MA lines * total number of generations).

5.4.5 Growth studies in nine conditions

The growth abilities of haploid parental strains, diploid ancestral clones, and the D120 cultures of all 140 MA lines were quantified in nine conditions. Briefly, fresh cells of these cultures were collected and adjusted to a final concentration of ~10^6 cells/mL in three different liquid media, including RPMI (Roswell Park Memorial Institute; Buffalo, NY, USA) broth, YEPD broth, and YEPD-FLC broth (additional 4 μg/mL fluconazole was added to YEPD broth). These cells were inoculated in 96-well microtiter plates and incubated at three different temperatures (30 °C, 37 °C, and 40 °C)

for 3 days. OD600 values were measured on day 0 and day 3. Three biological replicates of each sample under each treatment were performed with three experimental repeats.

5.4.6 Susceptibility to fluconazole

For all D120 cultures of the 140 MA lines, the fluconazole minimal inhibitory concentration (MIC) was determined following the CLSI broth microdilution method (M27-A2) [37]. We examined fluconazole concentrations of 0 μg/mL, 0.5 μg/mL, 1 μg/mL, 2 μg/mL, 4 μg/mL, 8 μg/mL, 16 μg/mL, 32 μg/mL, 64 μg/mL, and 128 μg/mL. The MIC value was determined as the fluconazole concentration without visible growth. The MIC values of the original parental strains and the ancestral clones were also determined. One parental strain, CDC15, has a fluconazole MIC of 64 μg/mL and was used as a control [38]. The fluconazole susceptibility testing was repeated 3 times. To compare fluconazole susceptibility of the MA lines with their respective ancestral clones, we standardized the MIC values of D120 cultures of MA lines by calculating the fold changes of the evolved clones over their respective ancestral clones. The evolved clones with standardized values >2 meant that they were more than twice as resistant to fluconazole as their ancestral clones.

5.4.7 Statistical analyses

We evaluated the genotypic diversity of the evolved clones using the Shannon-Weiner Diversity index (H). Pearson correlation tests were used to determine the relationships between the parental genetic divergence of the hybrids and LOH rates, ploidy changes, multi-locus genotypic diversity, growth rates under nine conditions, and fluconazole susceptibility of evolved clones. We examined the effects of parental genetic divergence on the observed genetic and phenotypic changes. The effects of fluconazole stress on these genetic and phenotypic changes were estimated by comparing the observed changes between F lines and Y lines. In addition, we investigated the potential impacts of ancestral clones' fluconazole susceptibility on the changes of MICs of the evolved clones. The interaction effects of parental genetic divergence, fluconazole stress, and ancestral fluconazole susceptibility were evaluated. Generalized linear models were used to evaluate the relationships among the above factors using the R package 'lme4' [39]. The multi-locus genotypes (MLGs) and related statistics were determined

using the R package 'poppr' [40]. Data visualization was done performing the R package 'ggplot2' [41]. All statistical analyses and visualization of data were performed using R (version 4.0.3) [42].

5.5 Results

In this study, the ploidy changes, genotypic diversity, LOH, growth rates under nine conditions, and fluconazole MIC changes of all D120 cultures were determined. The multi-locus heterozygosity patterns and LOH rates were estimated based on multi-locus genotype data. We also estimated the effects of factors (i.e., parental genetic divergence and fluconazole stress) on the observed genetic and phenotypic changes, as well as the correlations between them. Below we describe the findings.

5.5.1 Ploidy changes among D120 cultures of 140 MA lines

Over 800 mitotic generations, more than 70% of D120 cultures showed different genomic DNA contents from their respective ancestral clones (as illustrated in Table 5.S1). They had a range of changed genomic DNA contents, from ~22% less to ~27% more than their ancestral clones (as illustrated in Figure 5.2). Interestingly, all 20 evolved clones from YMD72 had increased genomic DNA contents. For D120 cultures from each of the remaining six hybrids, both increases and decreases were found. D120 cultures from some hybrids showed predominantly increased genomic DNA contents (e.g., 19/20 D120 cultures of YMD36), while others showed more frequently decreased genomic DNA contents (e.g., 19/20 D120 cultures of YMD165). We found that 48 out of 70 D120 cultures maintained in the presence of fluconazole (F lines) and 42 out of 70 D120 cultures maintained in the absence of fluconazole (Y lines) showed increased genomic DNA contents. Overall, the D120 cultures in the F lines had significantly higher genomic DNA contents than those in the Y lines ($p < 0.001$).

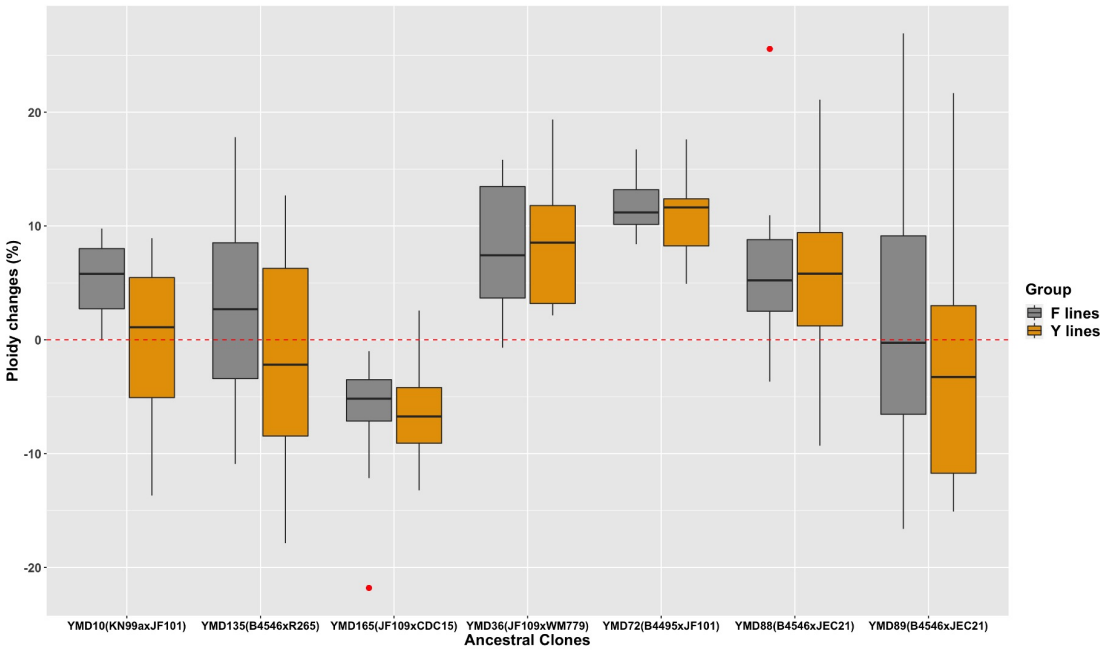

Figure 5.2. Ploidy changes of D120 cultures of MA lines from each ancestral clone. Y lines are in yellow, and F lines are in grey. Above 0 (the red dashed line) means an increased ploidy, and below 0 indicates a decreased ploidy.

5.5.2 Genotypic diversity among D120 cultures of 140 MA lines

As expected, all MA lines maintained the mtDNA genotypes as their respect ancestral clones (i.e., from the *MAT***a** parent, from the *MAT*α parent, or a recombinant genotype) at the two assayed mitochondrial loci (as illustrated in Table 5.S1). Based on PCR-RFLP results at the 13 nuclear loci, all seven ancestral clones were heterozygous at most or all the examined nuclear loci.

Among the D120 cultures of all 140 MA lines, we observed a total of 83 multilocus genotypes (MLGs), including six ancestral MLGs and 77 *de novo* MLGs. Surprisingly, none of the D120 cultures of YMD135 had the ancestral MLG (MLG.29). In addition, the D120 cultures from the seven ancestral clones showed different genotypic diversities (as illustrated in Table 5.2). Specifically, the D120 cultures of YMD89 had the highest genotypic richness with 17 MLGs, followed by that of YMD88 with 16 MLGs. In contrast, the D120 cultures of YMD165 had the lowest richness with only two MLGs. Consequently, the D120 cultures of YMD89 had the greatest genotypic diversity (H = 2.76), whereas the D120 cultures of YMD165 showed the lowest genotypic diversity (H = 0.42).

According to their multi-locus heterozygosity patterns (MHPs), these seven ancestral clones were assigned to two MHPs, MHP.16 and MHP.74 (as illustrated in Table 5.S1). Among the 140 D120 evolved cultures, 15 from the Y lines and 11 from the F lines shared MHP.74, and three each from the Y lines and F lines shared MHP.16. None of them reverted to the original *MAT***a** or *MAT*α haploid parental genotypes (i.e., MHP.1 and MHP.19). Among the remaining 108 MA lines, we found a total of 70 *de novo* MHPs, including eight MHPs shared between Y lines and F lines (MHP.35, MHP.39, MHP.50, MLP.69, MHP.70, MHP.71, MHP.72, and MHP.73), 34 MHPs were only found among Y lines, and 28 unique MHPs were found only in F lines.

Table 5.2. Genetic diversity among MA lines of each cross.

Ancestral clones	Number of MA lines	Number of multi-locus Genotypes (MLGs)	Shannon-Weiner Diversity Index (H)
YMD72	20	9	2.06
YMD36	20	14	2.39
YMD135	20	11	2.00
YMD165	20	2	0.42
YMD10	20	14	2.53
YMD88	20	16	2.69
YMD89	20	17	2.76

5.5.3 LOH among 140 MA lines

Among the 13 nuclear loci, LOH events were found at 11 loci. The only two loci without any detected LOH were the *MAT* locus and *CGNA* (as illustrated in Table 5.S1). Among the 11 loci with LOH, there were notable variations in the LOH frequencies. For example, locus *CNI01350* had the highest LOH frequency with 3.3×10^{-4} LOH events per MA line per mitotic division, while locus *ERG11* had the lowest LOH frequency with 5.36×10^{-5} LOH events per MA line per mitotic division. Aside from the overall differences in LOH frequencies among loci, there were also differences in the

timing of the LOH events (as illustrated in Table 5.S2). For example, some LOH events occurred very early during MA (e.g., within 100 mitotic generations), while others happened much later (e.g., after 700 mitotic generations).

In total, we detected 213 LOH events (97 in Y lines and 116 in F lines) accumulated over 800 mitotic generations among the 140 MA lines, corresponding to 1.27×10^{-4} LOH events per sample per locus per mitotic division. Of the two MA conditions, Y lines had a LOH frequency of 1.15×10^{-4} LOH events per MA line per mitotic division, whereas F lines had a frequency of 1.38×10^{-4} LOH events per MA line per mitotic division. The LOH rates varied among MA lines derived from different ancestors (as illustrated in Table 5.S2). The lowest was found from Y lines of YMD165 with a LOH rate of 8.33×10^{-6} LOH events per MA line per mitotic division. The highest was found from F lines of YMD88 with a LOH rate of 2.92×10^{-4} LOH events per MA line per mitotic division. In general, we found that Y lines and F lines derived from the same ancestral clones had similar LOH rates. However, in YMD88, the LOH rate of F lines was two times more than that of Y lines.

5.5.4 Growth rates of D120 cultures under nine environmental conditions

The D120 cultures showed diverse growth rates under the nine tested environmental conditions (as illustrated in Figure 5.3). Overall, the growth rates of D120 cultures were lower than their respective ancestral clones at 30 °C and 37 °C but higher at 40 °C. The results indicate that the cultures evolved at 37 °C had superior growth at 40 °C than their respective ancestral clones. We also observed growth differences among the three media. On average, the growth rates of D120 cultures were lower than their ancestral clones at all three temperatures in the RPMI and YEPD media. However, the D120 cultures grew faster than their respective ancestral clones in the YEPD-FLC medium at 37 °C and 40 °C. The average growth rates of D120 cultures from both Y lines and F lines were significantly greater at 40 °C than at 37 °C in the YEPD-FLC medium (p values < 0.001). The only exceptions were D120 cultures from the ancestral clone of YMD88 showing decreased growth in the YEPD-FLC medium at 40 °C. The findings suggest that the MA temperature at 37 °C can increase the growth ability of the evolved clones at a higher temperature (i.e., 40 °C).

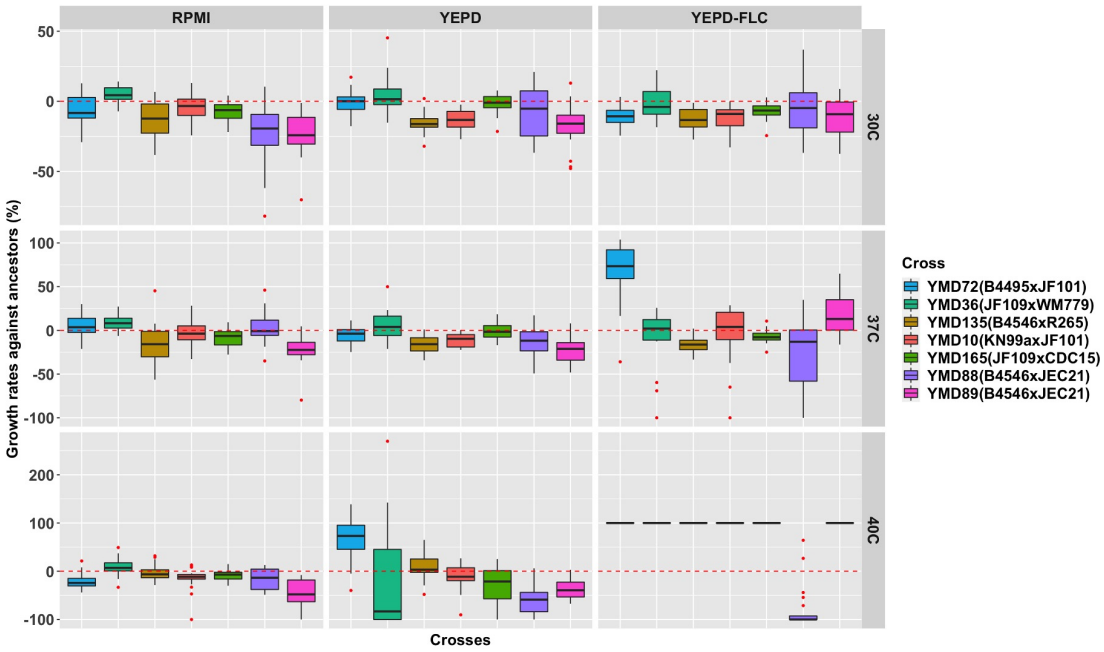

Figure 5.3. Growth rates of D120 cultures of 140 MA lines derived from each ancestral clone under nine environmental conditions.

5.5.5 Fluconazole MIC changes of D120 cultures

Among the D120 cultures, the fold changes of MIC values from their respective ancestral clones ranged from 0.5 to 8 (as illustrated in Table 5.S1 and Figure 5.4). Of the 140 D120 cultures, 82 (~59%) showed an increased fluconazole MIC, including four from F lines having an 8-fold increase, 16 from F lines, and 4 from Y lines having a 4-fold increase, and 30 from F lines and 28 from Y lines having a 2-fold increase. In total, 50 out of 70 (~71%) D120 cultures from F lines and 32 out of 70 (~46%) D120 cultures from Y lines had higher MIC values than their respective ancestor clones. In contrast, D120 cultures from one F line and nine Y lines had decreased fluconazole MIC compared to that of their ancestral clones. The remaining 48 (29 from Y lines and 19 from F lines) maintained the same MIC values as their respective ancestors. Overall, after 800 mitotic divisions, 130 out of the 140 MA lines (~93%) maintained or increased their fluconazole MIC.

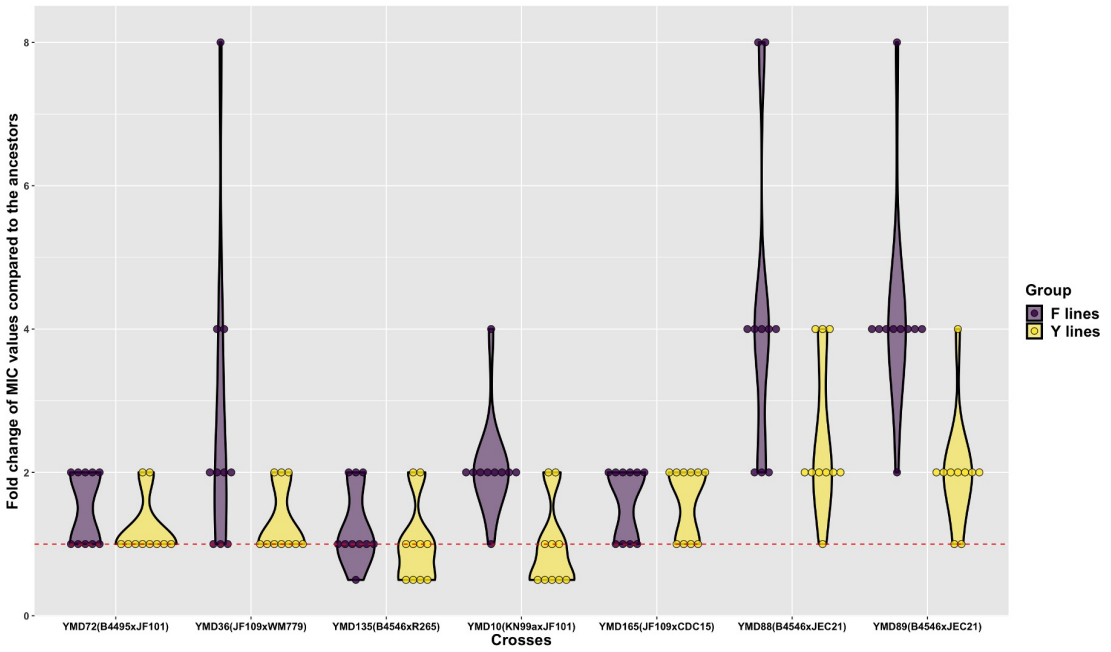

Figure 5.4. Fold changes of fluconazole MIC values among D120 cultures of 140 MA lines derived from each ancestral clone.

5.5.6 Relationship between parental genetic divergence and genetic and phenotypic changes among MA lines

The genetic distance between parental genomes within hybrids showed several significant correlations with genetic and phenotypic changes of evolved hybrid MA clones (as illustrated in Figure 5.5). Specifically, parental genetic distance within hybrids was significantly positively correlated with fluconazole MIC changes of both the Y lines ($r = 0.26$, $p < 0.001$) and the F lines ($r = 0.23$, $p < 0.001$). In contrast, it was significantly negatively correlated with ploidy changes of the Y lines ($r = -0.5$, $p < 0.001$) and the F lines ($r = -0.42$, $p < 0.001$). We also observed negative correlations between parental genetic distance and growth rates of the Y lines under all nine conditions and those of the F lines under six conditions (as illustrated in Figure 6). For example, there were negative correlations in YEPD-FLC medium at 40 °C ($r = -0.4$, $p = 0.015$ for Y lines; $r = -0.43$, $p = 0.008$ for F lines). Overall, our data indicate that parental genetic divergence significantly affected ploidy changes, fluconazole MIC changes, and growth rates under most tested conditions of both the Y lines and the F lines, as well as LOH rates of the F lines.

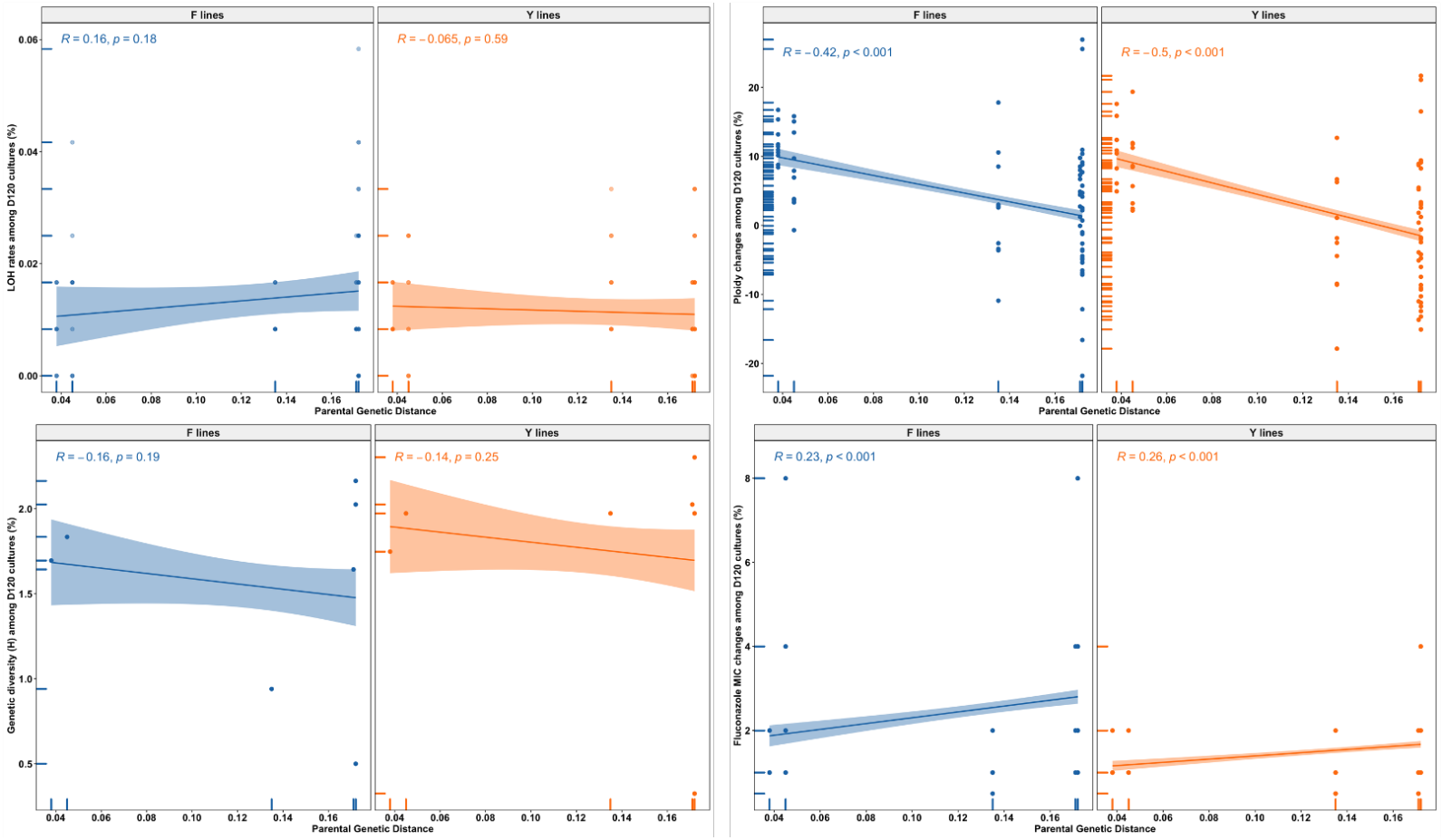

Figure 5.5. Relationships between parental genetic distance and genetic and fluconazole MIC changes of D120 cultures of 140 MA line. The genetic changes of the evolved clones include LOH rates, ploidy changes, and genotypic diversity.

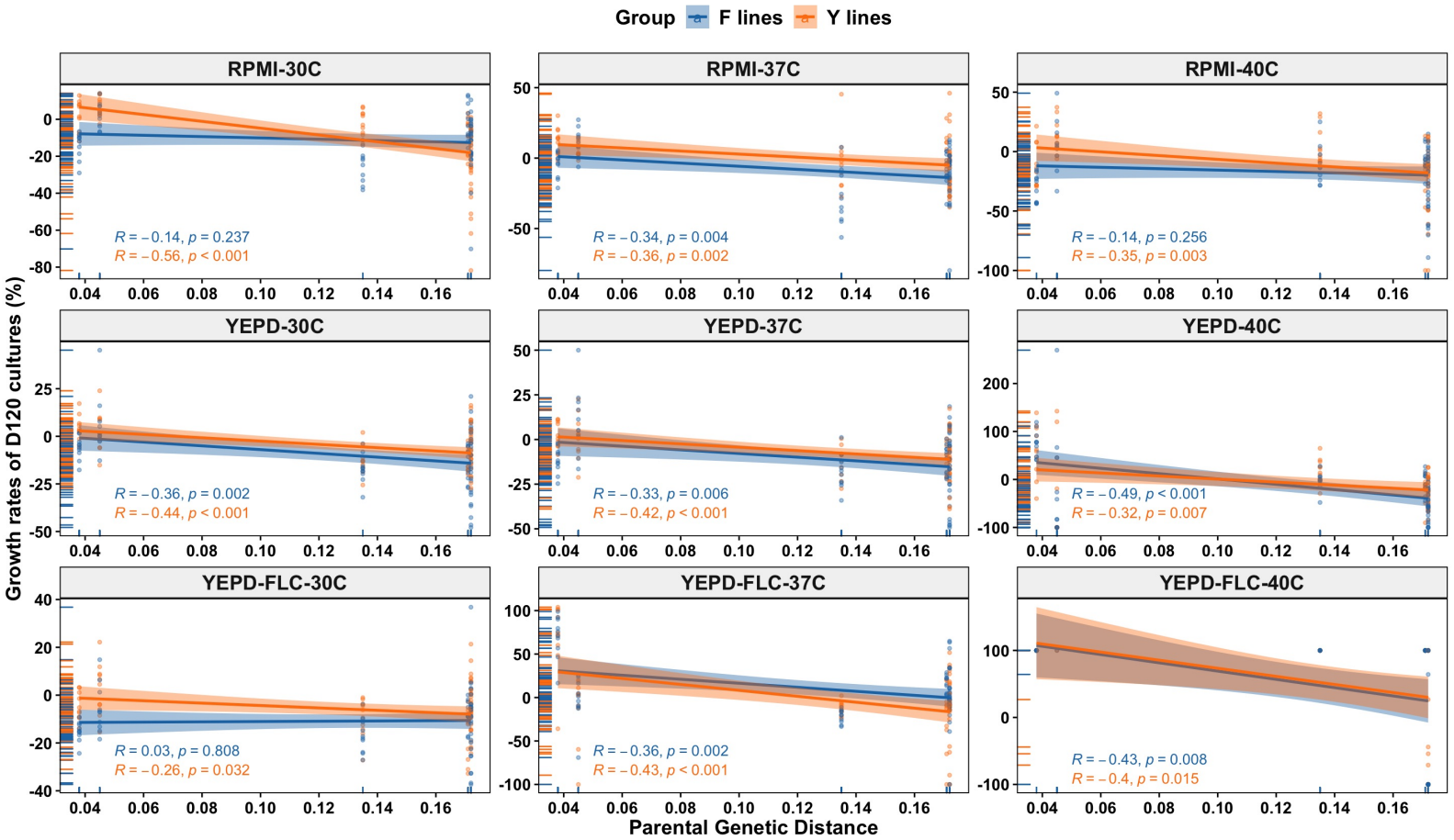

Figure 5.6. Relationships between parental genetic distance and growth rates of D120 cultures of 140 MA lines under nine environmental conditions.

5.5.7 Impacts of fluconazole stress on genetic and phenotypic changes among MA lines

Pairwise comparisons of D120 cultures between Y lines and F lines were used to evaluate the potential effects of fluconazole stress on the observed genetic and phenotypic changes. Overall, we found that D120 cultures from the Y lines and the F lines showed similar genetic diversity. There was no statistically significant difference in LOH rates between F lines and Y lines. Interestingly, D120 cultures from F lines showed greater increases in ploidy and fluconazole MIC than those from Y lines (p values < 0.001). In contrast, D120 cultures from the Y lines had on average higher growth rates than those from F lines under 7 of the 9 conditions, except for the YEPD-FLC medium at 37 °C and 40 °C. These results indicate that fluconazole stress could affect the ploidy levels and fluconazole MIC values of the evolved clones during mitotic divisions.

5.5.8 Relationships between the observed genetic changes and phenotypic changes among MA lines

We found several statistically significant correlations between the observed genetic changes (i.e., ploidy changes and LOH rates) and phenotypic changes (i.e., fluconazole MIC changes and growth rates) among the D120 cultures. For example, LOH rates of F lines were significantly positively correlated with fluconazole MIC changes ($r = 0.29$, $p = 0.013$), while negatively correlated with growth rates at 40 °C in the YEPD-FLC medium ($r = -0.61$, $p < 0.001$). However, for both F lines and Y lines, diverse correlations were observed when the analyses were conducted for the lines derived from individual strains (as illustrated in Figure 5.7). For example, LOH rates were significantly negatively correlated with fluconazole MIC changes of Y lines from YMD10 ($r = -0.62$, $p < 0.001$), while positively correlated with those of Y lines from YMD135 ($r = 0.37$, $p < 0.001$). Interestingly, for MA lines derived from YMD88, LOH rates were significantly positively correlated with fluconazole MIC changes of Y lines ($r = 0.47$, $p < 0.001$) but negatively correlated with those of F lines ($r = -0.36$, $p < 0.001$). We found similarly diverse correlations between LOH rates and growth rates, with ancestral clones, MA conditions (i.e., fluconazole stress and non-fluconazole condition), and

growth conditions contributing to the positive and negative correlations. For example, the D120 cultures of the Y lines from YMD165 showed a statistically significant positive correlation between their LOH rates and growth rates in the YEPD-FLC medium at 37 °C ($r = 0.71$, $p = 0.022$; as illustrated in Figure 5.S1).

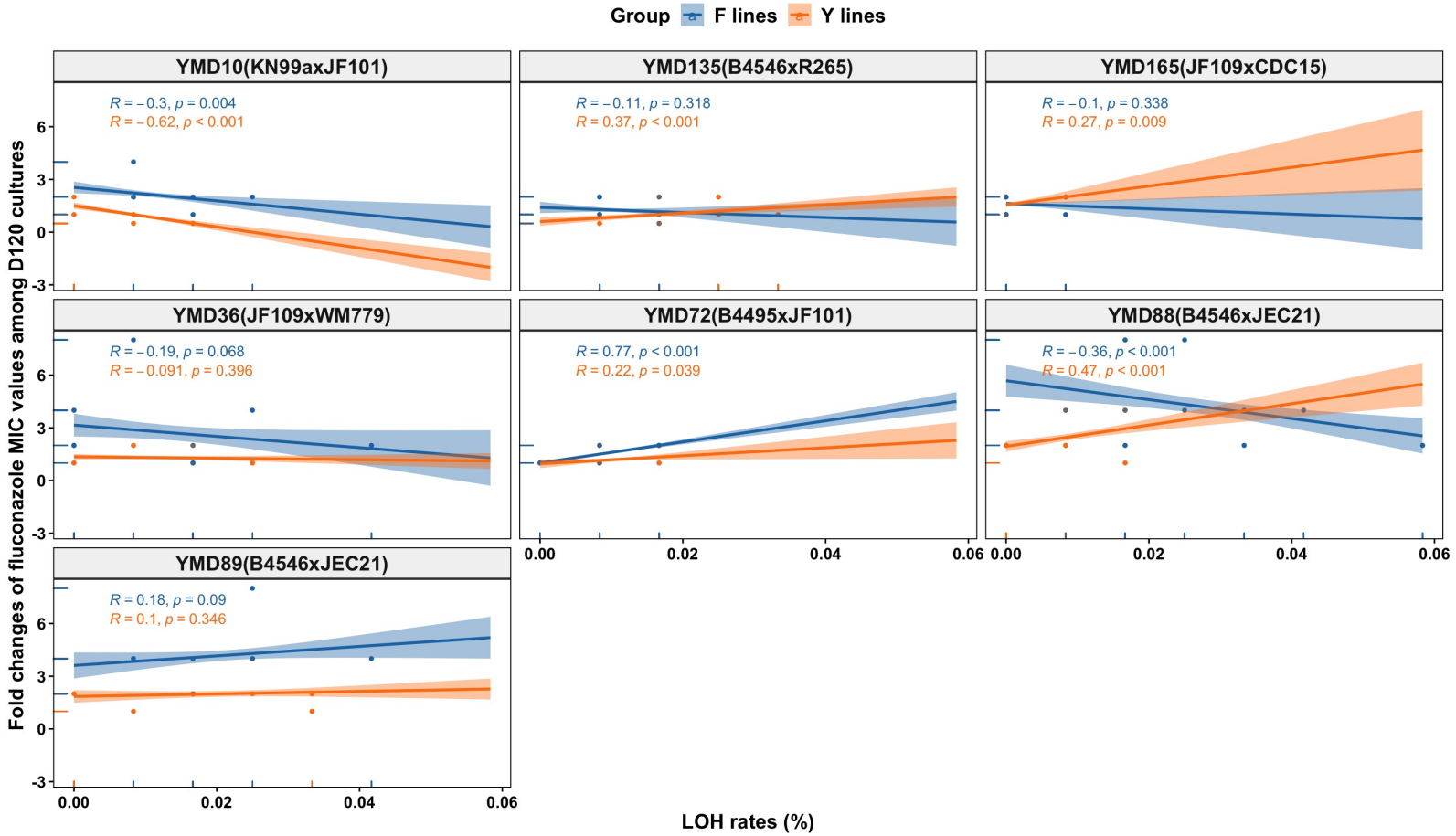

Figure 5.7. Relationship between LOH rates and fluconazole MIC value changes of D120 cultures of 140 MA lines from each ancestral clone.

Similar to the observed relationships between LOH rates and phenotypic changes among MA lines, a diversity of relationships between ploidy changes and phenotypic changes were also found. For example, we observed overall positive correlations between ploidy changes and growth rates for D120 cultures in Y lines in the RPMI medium (at 37 °C, r = 0.34, $p = 0.005$; and at 40 °C, r = 0.31, $p = 0.009$) but not in F lines. The D120 cultures from both F lines and Y lines from some ancestral clones showed positive correlations between ploidy changes and fluconazole MIC changes and growth rates, while those of others were negatively correlated or showed no association (as illustrated in Figures 5.8 and Figure 5.S2). For example, ploidy changes were positively correlated with fluconazole MIC changes of Y lines (r = 0.43, $p < 0.001$) but negatively associated with that of F lines (r = −0.21, $p = 0.048$). For growth rates in different media, ploidy changes were only negatively associated with the growth rates of D120 cultures in Y lines from YMD72 in the YEPD medium at 30 °C (r = −0.69, $p = 0.027$) and of Y lines from YMD89 in the YEPD-FLC medium at 30 °C (r = −0.7, $p = 0.025$). Overall, the relationships between the observed genetic changes and phenotypic changes varied among Y lines and F lines from different ancestral clones.

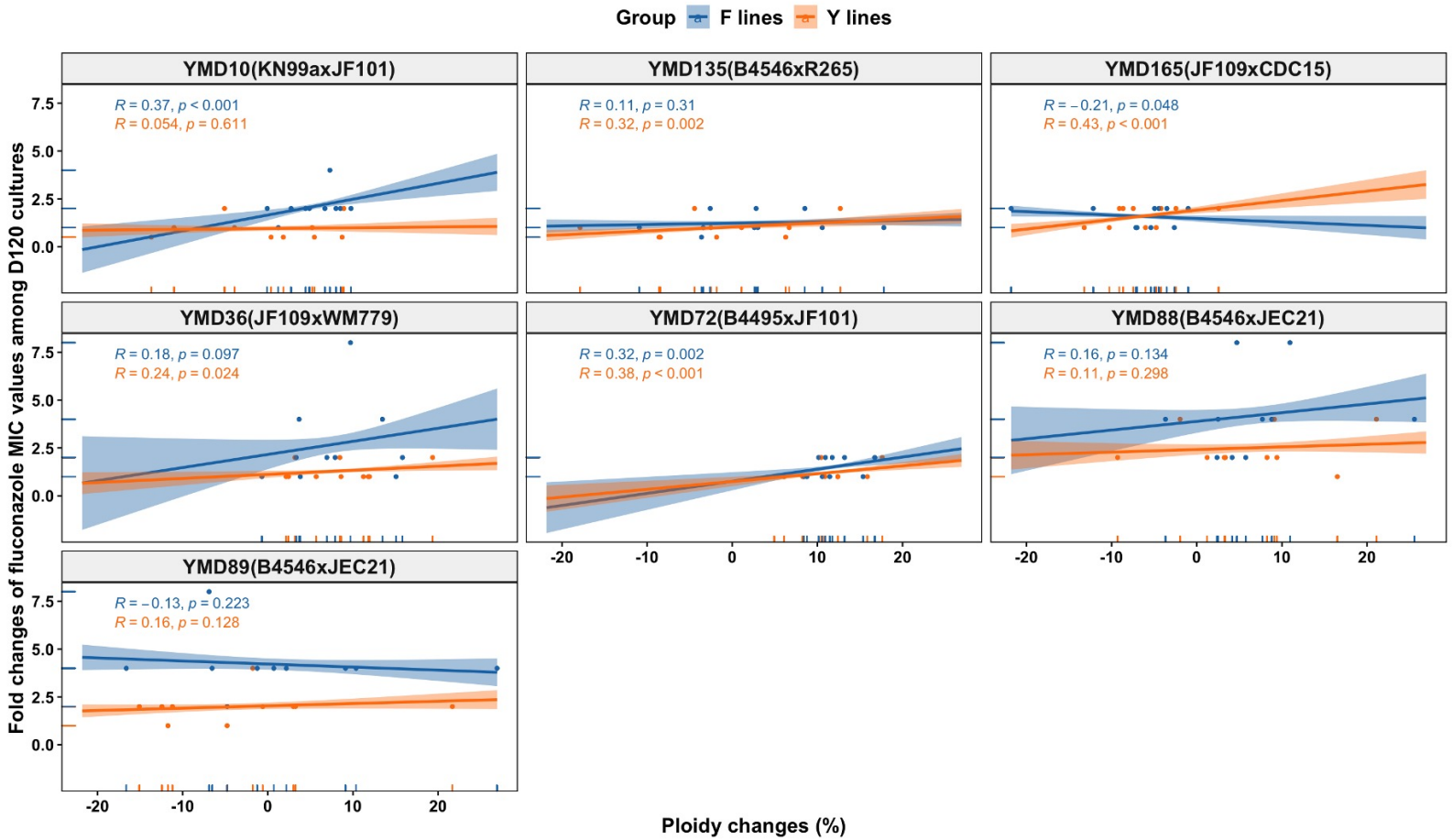

Figure 5.8. Relationship between ploidy changes and fluconazole MIC value changes of D120 cultures of 140 MA lines from each ancestral clone.

5.6 Discussion

Our study used mutation accumulation experiments to investigate the genome stability of seven diploid cryptococcal hybrids during mitotic divisions. We evaluated the effects of parental genetic divergence and fluconazole stress on genome stability, growth ability, and fluconazole susceptibility, as well as relationships between genetic and phenotypic changes. Below we discuss the potential mechanisms and implications for our findings.

5.6.1 Contributions of parental divergence to genetic changes

We investigated the effects of parental genetic divergence on LOH rates, ploidy changes, and genotypic diversity. For both Y lines and F lines, parental genetic divergence showed significant impacts on ploidy changes while not on LOH rates or genetic diversity. Our findings suggest that MA lines derived from more divergent parental pairs were like to have more stable ploidy levels over generations.

Cryptococcal lineages show from 2 – 17% of nucleotide sequence divergence at the whole genome level and are believed to have diverged from each other for 4.7 to 100 million years [43–49]. Previous studies revealed genetic incompatibilities between divergent parental strains and structural differences in chromosomes among divergent lineages in the human pathogenic *Cryptococcus* [50–53]. Ancestral clones (i.e., original hybrids), derived from genetically more closely related haploid parental strains, contained more similar chromosomal homologs with higher sequence similarities than that from more distantly related haploid parental strains. The more similar sequences and chromosomal structures between homologs of hybrids derived from more closely related haploid parents could contribute to a higher rate of homologous recombination and ploidy change during the extended asexual reproduction. Indeed, previous studies showed that as the genetic divergence between homologous sequences increases, the rate of homologous recombination decreases [54,55].

5.6.2 Contributions of fluconazole stress to genetic changes

By comparing the observed genetic changes between Y lines and F lines, we found that the tested fluconazole stress (4 μg/mL) contributed significantly to the ploidy status

of MA lines. The evolved clones under fluconazole stress (F lines) had higher ploidies on average than those under non-fluconazole stress lines (Y lines). Evidence that fluconazole stress can induce ploidy changes (e.g., aneuploidy) was reported in many species, such as *Candida albicans* and *Cryptococcus neoformans* [13,56,57]. Aneuploidy is generated due to the loss or gain of chromosomes or chromosomal segments within a genome. In humans, aneuploidy is often detrimental and linked to a variety of genetic disorders, such as Down syndrome (trisomy 21). However, when cells are exposed to stress, aneuploidy can provide a quick response through changes in gene dosage [26]. Fluconazole is an antifungal drug commonly administered to treat cryptococcosis, a severe disease caused by strains of HPC. Fluconazole can induce aneuploidy by disrupting the normal synchronization of chromosomal and cytoplasmic divisions in *C. albicans* [58]. In *C. neoformans*, pleiotropic effects of fluconazole on cell growth and mitotic division likely contribute to select for increased copies of chromosomes or chromosomal segments containing genes related to fluconazole stress response [56]. The continued fluconazole pressure during mutation accumulation for the F lines selects for cells with maintained or increased fluconazole resistance, contributing to their increased prevalence in subsequent MA cultures.

5.6.3 Interactions effects of factors on the observed changes among MA lines

In this study, we focused on the impacts of two factors separately on the genotypic and phenotypic changes of these hybrids during mutation accumulation. The results demonstrated that: (i) parental genetic distance can influence ploidy changes and growth rates among the D120 cultures of the MA lines under several conditions, and (ii) fluconazole stress can impact ploidy changes and fluconazole MIC changes. Interestingly, the analyses also indicated interaction effects of these two factors, with certain correlations found only in one of the two MA conditions. Indeed, our analyses showed interactions between parental genetic divergence and MA conditions on most observed phenotypic and genetic changes among the D120 cultures, including LOH rates, ploidy changes, genetic diversity, fluconazole MIC changes, and growth rates at 30 °C and 37 °C in the RPMI medium and at 40 °C in the YEPD-FLC medium. Because natural environments are heterogenous and cryptococcal hybrids can disperse across geographic regions and ecological niches, divergent genotypes with different phenotypic properties

could be evolved and selected from single hybrids through sexual reproduction, which could bring negative impacts to patients and our healthcare system.

5.6.4 Relationships between ploidy changes and phenotypic changes

Aneuploidy refers to gains and/or losses of individual chromosome (s) or chromosomal segment (s) from the normal chromosome set. The ploidy changes in aneuploid strains could directly alter the transcription level of many genes on the affected chromosome (s) and indirectly change the expressions of genes on other chromosomes. This is because most genetic and metabolic pathways contain genes from multiple chromosomes, and when some components of a pathway in one chromosome are activated or inhibited, other components in other chromosomes could also be affected. In the present study, we found that most MA lines deviated from the genomic DNA contents of their ancestral clones after ~800 mitotic generations, with both increased and decreased ploidy levels compared to their ancestral clones (as illustrated in Table 5.S1). Furthermore, ploidy changes were significantly correlated with fluconazole MIC changes and growth rates under several conditions. Previous research showed that specific aneuploidies can impact phenotypes in human pathogenic yeasts. For example, increased ploidies in several yeasts have shown enhanced antifungal drug resistance and greater growth rates under specific conditions [59–61]. However, decreased copy numbers of specific chromosomes could also lead to increased drug resistance. For example, in *C. albicans*, monosomy of chromosome 5 increases resistance to several antifungal drugs [62]. While specific ploidy changes can enhance the strains' survival under the selected stress conditions, in the absence of such stress, aneuploidy can have detrimental effects. Moreover, if there is no selective pressure to maintain the aneuploidy, aneuploidy often returns to euploidy [63]. At present, the conditions under which aneuploidy of the MA lines in our study will return to euploidy remain to be investigated.

5.6.4 Relationships between LOH and phenotypic changes

While no correlation was found between LOH rates and growth rates under most of the tested conditions for both Y lines and F lines, significant correlations were found

for MA lines derived from specific ancestral clones under certain conditions (as illustrated in Figure 5.S1). In addition, we found notable influences of LOH rates on fluconazole MIC changes of both Y lines and F lines (as illustrated in Figure 5.7).

Two genes on chromosome 1 were confirmed to be associated with fluconazole resistance in *C. neoformans*, *ERG11* and *CnAFR1*. *ERG11* encodes the fluconazole target enzyme lanosterol 14-α-demethylase, and *CnAFR1* is an ATP binding cassette (ABC) transporter-encoding gene [31,32,38]. A previous MA study on a serotype AD hybrid found that in the presence of high fluconazole concentration (32 μg/mL), most LOH events happened on chromosome 1, resulting in the loss of fluconazole-susceptible allele of *ERG11* [13]. Differently, in this study, we only observed six LOH events on the *ERG11* locus among D120 cultures of 140 MA lines, including three in Y lines and three in F lines. The reason for the different LOH rates of *ERG11* between these two studies was likely due to the different fluconazole concentrations used. In the current study, we used 4 μg/mL of fluconazole (vs. 32 μg/mL in the previous study), and the parental haploid strains could all grow on the agar medium containing 4 μg/mL of fluconazole. Another study found that chromosome 4 is the second most frequently formed disomy at high concentrations of fluconazole [64].

In this study, we did not find any relationship between LOH at any specific locus/loci and the increased fluconazole MIC values. However, by comparing heterozygous rates of the examined 13 nuclear loci together to fluconazole MIC changes, we found a significantly negative correlation between heterozygous rates and fluconazole MIC changes ($r = -0.28$, $p < 0.001$) among D120 cultures of F lines ($r = 0.28$, $p < 0.001$). In contrast, no correlation was found between them among the Y lines. In addition, the nuclear locus *CNI01350* had the highest LOH rate, and it is a QTL (quantitative trait locus) associated with cell size in *Cryptococcus neoformans* [38]. Altogether, our data suggest that the 4 μg/mL fluconazole stress in this study had an overall effect on heterozygosity but was not sufficient as a selective force for LOH at any specific locus.

5.7 Conclusions

In this study, we investigated the genetic and phenotypic changes of cryptococcal diploid hybrids after ~800 mitotic generations and examined the effects of potential factors on the observed changes. Our analyses revealed that asexual reproduction of

these hybrids under laboratory conditions could generate high genotypic and phenotypic diversities. Overall, we found that neither the parental genetic divergence of each hybrid ancestral clone nor the mutation accumulation condition (i.e., fluconazole stress and non-fluconazole condition) could be used to predict all the observed variations. Instead, both the parental genetic divergence and the MA conditions, as well as their interactions, contributed to the observed genotypic and phenotypic changes among the MA lines. Interestingly, significant correlations among MA lines from individual ancestors were frequently observed between certain genetic changes and phenotypic changes. In addition, most evolved lines showed increased fluconazole resistance, especially those maintained on medium containing fluconazole, suggesting that the treatment of infection by cryptococcal hybrids could present additional challenges over those by non-hybrids. For example, the presence of sublethal dose antifungals for the treatment of infections by hybrids might not kill these pathogens but instead facilitate the evolution of diverse genotypes and increased drug resistance. Together, our findings indicate the enormous potential of cryptococcal hybrids to generate genotypic and phenotypic diversities and that multiple factors can impact the production of such diversities. Future analyses of the genomes and transcriptomes of the evolved clones could help reveal their detailed genetic changes and the potential mechanisms contributing to the observed phenotypic differences among these clones.

5.8 Appendix

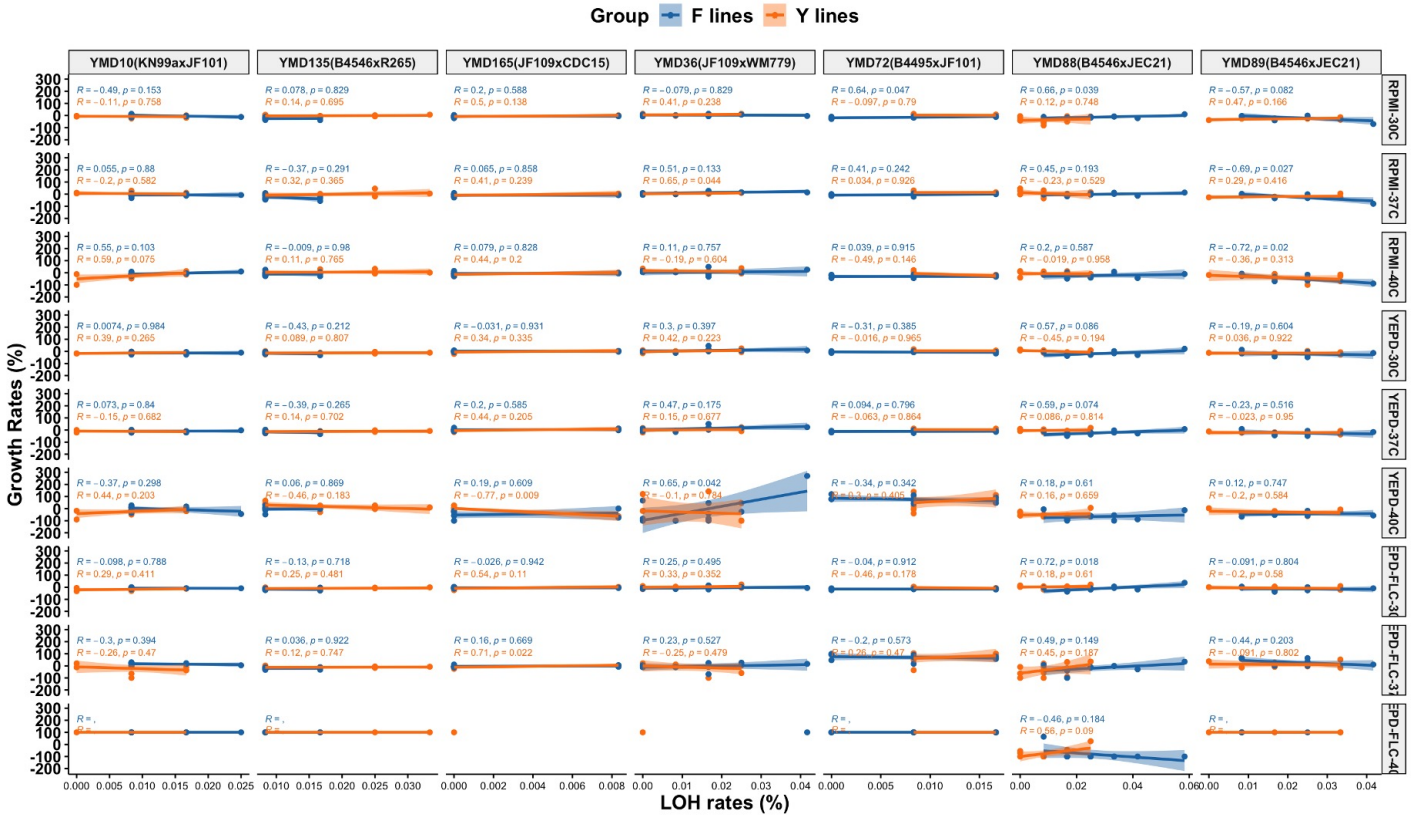

Figure 5.S1. Relationships between LOH rates and average growth rates of D120 cultures of 140 MA lines derived from each ancestor under each environmental condition.

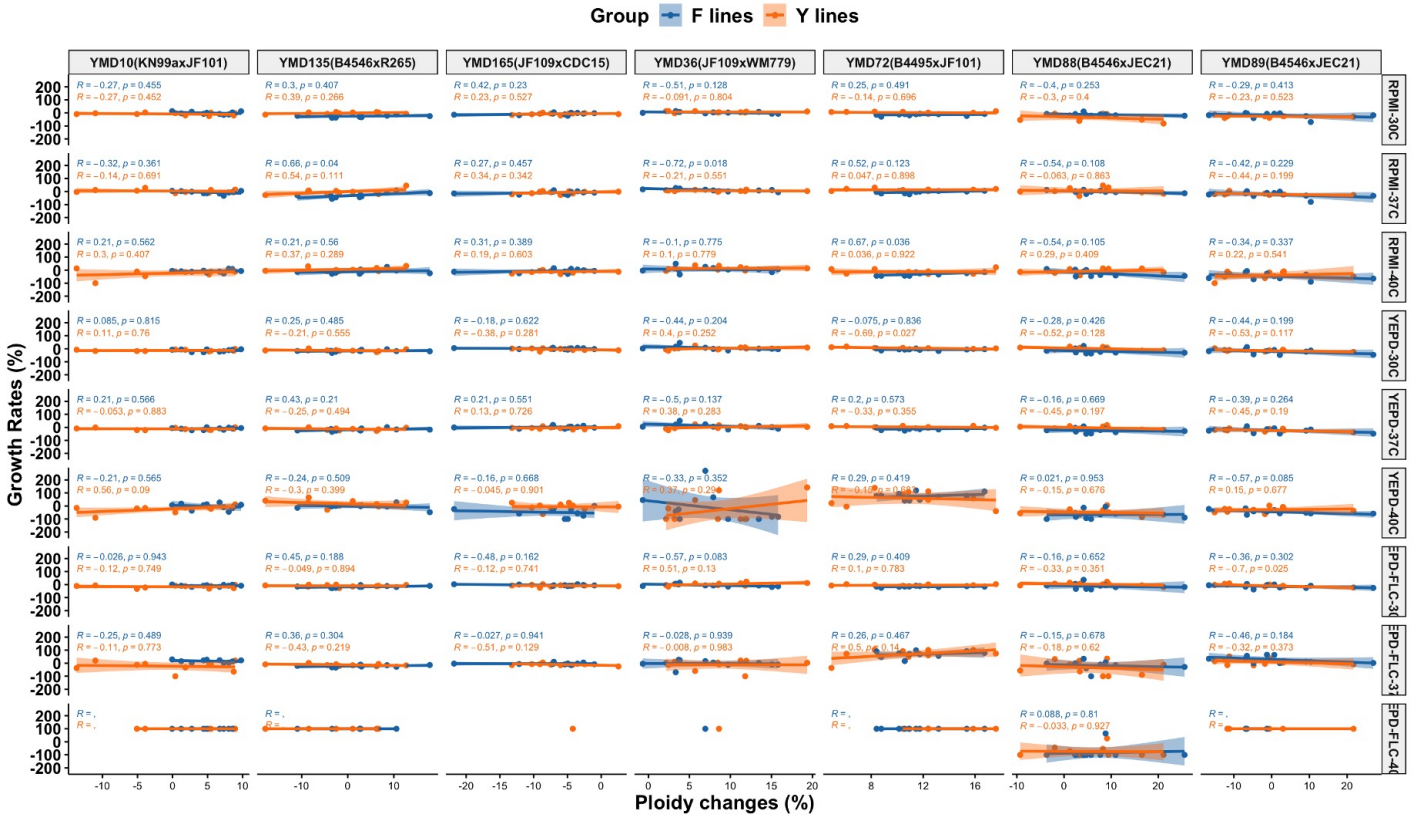

Figure 5.S2. Relationships between ploidy changes and average growth rates of D120 cultures of 140 MA lines derived from each ancestor under each environmental condition.

Table 5.S1. Details of MA lines, ploidy changes, fluconazole MIC changes, multi-locus genotypes, multi-locus heterozygosity patterns, nuclear genotyping and mitochondria genotying.

Group	Sample ID	Ploidy changes compared to ancestor (%)	Fluconazole MIC fold changes	Multi-locus genotypes (MLG)	Multi-locus heterozygosity patterns (MHP)	#LOH across 15 loci	Nuclear genotyping													Mitochondrial genotyping	
							URA5	MAT locus	ERG11	CNM00180	CGNA	CNB00360	CGNI	CNE00250	CNL06810	CGNM2	CNH02750	CNI01350	CNK01700	ND2	ND4
VGIxVGIII	B4495(*MAT* a parent)	NA	NA	MLG.1	MHP.1	NA	1	1	1	1	1	1	1	1	1	1	1	1	1	1	1
	JF101(*MAT* α parent)	NA	NA	MLG.2	MHP.19	NA	2	2	2	2	2	2	2	2	2	2	2	2	2	2	2
	YMD72(ancestor)	NA	NA	MLG.3	MHP.74	NA	3	3	3	3	3	3	3	3	3	3	3	3	3	2	2
	YMD72-Y1	4.93	1	MLG.8	MHP.73	1	3	3	3	3	3	3	3	3	3	3	3	3	2	2	2
	YMD72-Y2	12.39	1	MLG.7	MHP.72	1	3	3	3	3	3	3	3	3	3	3	3	3	1	2	2
	YMD72-Y3	8.26	1	MLG.8	MHP.73	1	3	3	3	3	3	3	3	3	3	3	3	3	2	2	2
	YMD72-Y4	6.09	1	MLG.8	MHP.73	1	3	3	3	3	3	3	3	3	3	3	3	3	2	2	2
	YMD72-Y5	17.61	2	MLG.4	MHP.51	1	3	3	3	3	3	1	3	3	3	3	3	3	3	2	2
	YMD72-Y6	10.87	1	MLG.6	MHP.71	1	3	3	3	3	3	3	3	3	3	3	3	1	3	2	2
	YMD72-Y7	12.39	1	MLG.9	MHP.34	2	2	3	3	3	3	3	3	3	3	3	3	1	3	2	2
	YMD72-Y8	12.39	1	MLG.5	MHP.59	2	3	3	3	3	3	3	3	2	3	3	3	3	2	2	2
	YMD72-Y9	10.43	2	MLG.10	MHP.50	2	3	3	3	3	3	1	3	3	3	3	3	1	3	2	2
	YMD72-Y10	15.87	1	MLG.8	MHP.73	1	3	3	3	3	3	3	3	3	3	3	3	3	2	2	2
	YMD72-F1	13.19	2	MLG.9	MHP.47	2	3	3	3	1	3	3	3	3	3	3	3	1	3	2	2
	YMD72-F2	16.74	2	MLG.7	MHP.72	1	3	3	3	3	3	3	3	3	3	3	3	3	1	2	2
	YMD72-F3	8.41	1	MLG.8	MHP.73	1	3	3	3	3	3	3	3	3	3	3	3	3	2	2	2
	YMD72-F4	8.77	1	MLG.3	MHP.74	0	3	3	3	3	3	3	3	3	3	3	3	3	3	2	2
	YMD72-F5	11.74	2	MLG.10	MHP.50	2	3	3	3	3	3	1	3	3	3	3	3	1	3	2	2
	YMD72-F6	15.36	1	MLG.3	MHP.74	0	3	3	3	3	3	3	3	3	3	3	3	3	3	2	2
	YMD72-F7	11.45	1	MLG.3	MHP.74	0	3	3	3	3	3	3	3	3	3	3	3	3	3	2	2
	YMD72-F8	10.58	1	MLG.6	MHP.71	1	3	3	3	3	3	3	3	3	3	3	3	1	3	2	2
	YMD72-F9	10.94	2	MLG.6	MHP.71	1	3	3	3	3	3	3	3	3	3	3	3	1	3	2	2
	YMD72-F10	10.14	2	MLG.9	MHP.47	2	3	3	3	1	3	3	3	3	3	3	3	1	3	2	2
VGIVxVGIII	JF109(*MAT* a parent)	NA	NA	MLG.11	MHP.1	NA	1	1	1	1	1	1	1	1	1	1	1	1	1	1	1
	WM779(*MAT* α parent)	NA	NA	MLG.12	MHP.19	NA	2	2	2	2	2	2	2	2	2	2	2	2	2	2	2
	YMD36(ancestor)	NA	NA	MLG.13	MHP.16	NA	1	3	3	3	1	3	3	3	3	3	3	1	3	1	1
	YMD36-Y1	2.43	1	MLG.13	MHP.16	0	1	3	3	3	1	3	3	3	3	3	3	1	3	1	1
	YMD36-Y2	11.24	1	MLG.13	MHP.16	0	1	3	3	3	1	3	3	3	3	3	3	1	3	1	1
	YMD36-Y3	5.69	1	MLG.22	MHP.11	3	1	3	3	3	1	2	3	3	3	3	2	1	1	1	1
	YMD36-Y4	19.36	2	MLG.21	MHP.10	2	1	3	3	3	1	2	3	3	3	2	3	1	3	1	1
	YMD36-Y5	11.94	1	MLG.19	MHP.8	3	1	3	3	1	1	3	3	3	3	1	2	1	3	1	1
	YMD36-Y6	11.80	1	MLG.20	MHP.9	2	1	3	3	1	1	3	3	3	3	1	3	1	3	1	1
	YMD36-Y7	8.61	1	MLG.13	MHP.16	0	1	3	3	3	1	3	3	3	3	3	3	1	3	1	1
	YMD36-Y8	8.47	2	MLG.25	MHP.14	1	1	3	3	3	1	3	3	3	3	2	3	1	3	1	1
	YMD36-Y9	2.15	1	MLG.14	MHP.2	3	1	3	1	3	1	1	3	3	2	3	3	1	3	1	1
	YMD36-Y10	3.19	2	MLG.23	MHP.12	1	1	3	3	3	1	2	3	3	3	3	3	1	3	1	1
	YMD36-F1	3.33	2	MLG.24	MHP.13	2	1	3	3	3	1	3	3	3	2	3	3	1	1	1	1
	YMD36-F2	6.94	2	MLG.18	MHP.7	5	1	3	3	1	1	1	3	3	3	2	2	1	1	1	1
	YMD36-F3	15.82	2	MLG.13	MHP.16	0	1	3	3	3	1	3	3	3	3	3	3	1	3	1	1
	YMD36-F4	9.72	8	MLG.26	MHP.15	1	1	3	3	3	1	3	3	3	3	3	2	1	3	1	1
	YMD36-F5	13.46	4	MLG.13	MHP.16	0	1	3	3	3	1	3	3	3	3	3	3	1	3	1	1
	YMD36-F6	3.68	4	MLG.16	MHP.5	3	1	3	3	2	1	3	3	3	2	2	3	1	3	1	1
	YMD36-F7	3.82	1	MLG.15	MHP.3	2	1	3	1	3	1	1	3	3	3	3	3	1	3	1	1
	YMD36-F8	7.91	2	MLG.13	MHP.16	0	1	3	3	3	1	3	3	3	3	3	3	1	3	1	1
	YMD36-F9	-0.69	1	MLG.17	MHP.6	2	1	3	3	2	1	3	3	3	3	2	3	1	3	1	1
	YMD36-F10	15.06	1	MLG.17	MHP.6	2	1	3	3	2	1	3	3	3	3	2	3	1	3	1	1

VGIIxVGIII	B4546(*MAT* **a** parent)	NA	NA	MLG.27	MHP.1	NA	1	1	1	1	1	1	1	1	1	1	1	1	1	1	1
	R265(*MAT* α parent)	NA	NA	MLG.28	MHP.19	NA	2	2	2	2	2	2	2	2	2	2	2	2	2	2	2
	YMD135(ancestor)	NA	NA	MLG.29	MHP.74	NA	3	3	3	3	3	3	3	3	3	3	3	3	3	1	1
	YMD135-Y1	6.28	0.5	MLG.40	MHP.70	1	3	3	3	3	3	3	3	3	3	3	3	2	3	1	1
	YMD135-Y2	1.09	1	MLG.39	MHP.72	1	3	3	3	3	3	3	3	3	3	3	3	3	1	1	1
	YMD135-Y3	-8.46	0.5	MLG.39	MHP.72	1	3	3	3	3	3	3	3	3	3	3	3	3	1	1	1
	YMD135-Y4	12.69	2	MLG.35	MHP.54	3	3	3	3	3	3	3	1	3	2	3	2	3	3	1	1
	YMD135-Y5	-2.52	1	MLG.31	MHP.37	4	3	3	2	3	3	3	1	1	1	3	3	3	3	1	1
	YMD135-Y6	-1.84	0.5	MLG.38	MHP.66	2	3	3	3	3	3	3	3	3	3	1	3	2	3	1	1
	YMD135-Y7	-17.87	1	MLG.39	MHP.72	1	3	3	3	3	3	3	3	3	3	3	3	3	1	1	1
	YMD135-Y8	-8.59	0.5	MLG.32	MHP.43	2	3	3	3	1	3	3	3	3	2	3	3	3	3	1	1
	YMD135-Y9	6.68	1	MLG.30	MHP.36	3	3	3	2	2	3	3	1	3	3	3	3	3	3	1	1
	YMD135-Y10	-4.43	2	MLG.34	MHP.53	2	3	3	3	3	3	3	1	3	1	3	3	3	3	1	1
	YMD135-F1	8.53	2	MLG.40	MHP.70	1	3	3	3	3	3	3	3	3	3	3	3	2	3	1	1
	YMD135-F2	10.57	1	MLG.40	MHP.70	1	3	3	3	3	3	3	3	3	3	3	3	2	3	1	1
	YMD135-F3	2.80	2	MLG.37	MHP.64	2	3	3	3	3	3	3	3	3	2	3	3	2	3	1	1
	YMD135-F4	-10.91	1	MLG.40	MHP.70	1	3	3	3	3	3	3	3	3	3	3	3	2	3	1	1
	YMD135-F5	3.00	1	MLG.40	MHP.70	1	3	3	3	3	3	3	3	3	3	3	3	2	3	1	1
	YMD135-F6	17.80	1	MLG.40	MHP.70	1	3	3	3	3	3	3	3	3	3	3	3	2	3	1	1
	YMD135-F7	2.59	1	MLG.40	MHP.70	1	3	3	3	3	3	3	3	3	3	3	3	2	3	1	1
	YMD135-F8	-2.59	2	MLG.40	MHP.70	1	3	3	3	3	3	3	3	3	3	3	3	2	3	1	1
	YMD135-F9	-3.41	1	MLG.33	MHP.46	2	3	3	3	1	3	3	3	3	3	3	3	2	3	1	1
	YMD135-F10	-3.62	0.5	MLG.36	MHP.62	2	3	3	3	3	3	3	3	3	1	3	3	2	3	1	1
VNIxVGIII	JF109(*MAT* **a** parent)	NA	NA	MLG.11	MHP.1	NA	1	1	1	1	1	1	1	1	1	1	1	1	1	1	1
	CDC15(MATα parent)	NA	NA	MLG.41	MHP.19	NA	2	2	2	2	2	2	2	2	2	2	2	2	2	2	2
	YMD165(ancestor)	NA	NA	MLG.42	MHP.74	NA	3	3	3	3	3	3	3	3	3	3	3	3	3	2	1
	YMD165-Y1	2.57	2	MLG.42	MHP.74	0	3	3	3	3	3	3	3	3	3	3	3	3	3	2	1
	YMD165-Y2	-13.22	1	MLG.42	MHP.74	0	3	3	3	3	3	3	3	3	3	3	3	3	3	2	1
	YMD165-Y3	-7.46	2	MLG.42	MHP.74	0	3	3	3	3	3	3	3	3	3	3	3	3	3	2	1
	YMD165-Y4	-2.44	2	MLG.42	MHP.74	0	3	3	3	3	3	3	3	3	3	3	3	3	3	2	1
	YMD165-Y5	-6.02	1	MLG.42	MHP.74	0	3	3	3	3	3	3	3	3	3	3	3	3	3	2	1
	YMD165-Y6	-4.20	2	MLG.42	MHP.74	0	3	3	3	3	3	3	3	3	3	3	3	3	3	2	1
	YMD165-Y7	-8.65	2	MLG.43	MHP.39	1	3	3	3	2	3	3	3	3	3	3	3	3	3	2	1
	YMD165-Y8	-9.09	2	MLG.42	MHP.74	0	3	3	3	3	3	3	3	3	3	3	3	3	3	2	1
	YMD165-Y9	-4.76	1	MLG.42	MHP.74	0	3	3	3	3	3	3	3	3	3	3	3	3	3	2	1
	YMD165-Y10	-10.28	1	MLG.42	MHP.74	0	3	3	3	3	3	3	3	3	3	3	3	3	3	2	1
	YMD165-F1	-7.14	1	MLG.42	MHP.74	0	3	3	3	3	3	3	3	3	3	3	3	3	3	2	1
	YMD165-F2	-4.45	2	MLG.42	MHP.74	0	3	3	3	3	3	3	3	3	3	3	3	3	3	2	1
	YMD165-F3	-12.16	2	MLG.42	MHP.74	0	3	3	3	3	3	3	3	3	3	3	3	3	3	2	1
	YMD165-F4	-21.80	2	MLG.42	MHP.74	0	3	3	3	3	3	3	3	3	3	3	3	3	3	2	1
	YMD165-F5	-2.63	1	MLG.43	MHP.39	1	3	3	3	2	3	3	3	3	3	3	3	3	3	2	1
	YMD165-F6	-1.00	2	MLG.43	MHP.39	1	3	3	3	2	3	3	3	3	3	3	3	3	3	2	1
	YMD165-F7	-3.51	2	MLG.42	MHP.74	0	3	3	3	3	3	3	3	3	3	3	3	3	3	2	1
	YMD165-F8	-5.39	1	MLG.42	MHP.74	0	3	3	3	3	3	3	3	3	3	3	3	3	3	2	1
	YMD165-F9	-4.95	2	MLG.42	MHP.74	0	3	3	3	3	3	3	3	3	3	3	3	3	3	2	1
	YMD165-F10	-7.02	1	MLG.42	MHP.74	0	3	3	3	3	3	3	3	3	3	3	3	3	3	2	1
	KN99a(*MAT* **a** parent)	NA	NA	MLG.44	MHP.1	NA	1	1	1	1	1	1	1	1	1	1	1	1	1	1	1
	JF101(*MAT* α parent)	NA	NA	MLG.2	MHP.19	NA	2	2	2	2	2	2	2	2	2	2	2	2	2	2	2
	YMD10(ancestor)	NA	NA	MLG.45	MHP.74	NA	3	3	3	3	3	3	3	3	3	3	3	3	3	1	1
	YMD10-Y1	8.93	2	MLG.50	MHP.55	1	3	3	3	3	3	3	1	3	3	3	3	3	3	1	1
	YMD10-Y2	5.21	1	MLG.53	MHP.57	1	3	3	3	3	3	3	3	1	3	3	3	3	3	1	1
	YMD10-Y3	-13.68	0.5	MLG.52	MHP.56	2	3	3	3	3	3	3	3	1	1	3	3	3	3	1	1
	YMD10-Y4	1.82	0.5	MLG.46	MHP.38	2	3	3	3	2	3	3	3	3	1	3	3	3	3	1	1
	YMD10-Y5	5.47	0.5	MLG.52	MHP.56	2	3	3	3	3	3	3	3	1	1	3	3	3	3	1	1
	YMD10-Y6	-5.08	2	MLG.45	MHP.74	0	3	3	3	3	3	3	3	3	3	3	3	3	3	1	1
	YMD10-Y7	8.73	0.5	MLG.51	MHP.60	1	3	3	3	3	3	3	3	2	3	3	3	3	3	1	1

VNIxVGIII	YMD10-Y8	-3.91	1	MLG.58	MHP.73	1	3	3	3	3	3	3	3	3	3	3	3	3	2	1	1
	YMD10-Y9	0.39	0.5	MLG.47	MHP.39	1	3	3	3	2	3	3	3	3	3	3	3	3	3	1	1
	YMD10-Y10	-11.01	1	MLG.45	MHP.74	0	3	3	3	3	3	3	3	3	3	3	3	3	3	1	1
	YMD10-F1	4.89	2	MLG.57	MHP.71	1	3	3	3	3	3	3	3	3	3	3	3	1	3	1	1
	YMD10-F2	9.77	2	MLG.55	MHP.63	1	3	3	3	3	3	3	3	3	1	3	3	3	3	1	1
	YMD10-F3	6.71	2	MLG.55	MHP.63	1	3	3	3	3	3	3	3	3	1	3	3	3	3	1	1
	YMD10-F4	8.53	2	MLG.57	MHP.71	1	3	3	3	3	3	3	3	3	3	3	3	1	3	1	1
	YMD10-F5	-0.07	2	MLG.57	MHP.71	1	3	3	3	3	3	3	3	3	3	3	3	1	3	1	1
	YMD10-F6	4.43	2	MLG.54	MHP.61	2	3	3	3	3	3	3	3	3	1	2	3	3	3	1	1
	YMD10-F7	8.01	2	MLG.49	MHP.52	3	3	3	3	3	3	3	1	3	1	2	3	3	3	1	1
	YMD10-F8	7.30	4	MLG.55	MHP.63	1	3	3	3	3	3	3	3	3	1	3	3	3	3	1	1
	YMD10-F9	2.74	2	MLG.56	MHP.69	1	3	3	3	3	3	3	3	3	3	3	2	3	3	1	1
	YMD10-F10	1.24	1	MLG.48	MHP.50	2	3	3	3	3	3	1	3	3	3	3	3	1	3	1	1
VNIVxVGIII	B4546(*MAT* a parent)	NA	NA	MLG.27	MHP.1	NA	1	1	1	1	1	1	1	1	1	1	1	1	1	1	1
	JEC21(*MAT* α parent)	NA	NA	MLG.59	MHP.19	NA	2	2	2	2	2	2	2	2	2	2	2	2	2	2	2
	YMD88(ancestor)	NA	NA	MLG.60	MHP.74	NA	3	3	3	3	3	3	3	3	3	3	3	3	3	1	1
	YMD88-Y1	16.51	1	MLG.72	MHP.58	2	3	3	3	3	3	3	3	2	3	3	1	3	3	1	1
	YMD88-Y2	3.24	2	MLG.75	MHP.68	1	3	3	3	3	3	3	3	3	3	3	1	3	3	1	1
	YMD88-Y3	21.10	4	MLG.64	MHP.18	1	1	3	3	3	3	3	3	3	3	3	3	3	3	1	1
	YMD88-Y4	3.36	2	MLG.60	MHP.74	0	3	3	3	3	3	3	3	3	3	3	3	3	3	1	1
	YMD88-Y5	1.22	2	MLG.60	MHP.74	0	3	3	3	3	3	3	3	3	3	3	3	3	3	1	1
	YMD88-Y6	9.42	2	MLG.74	MHP.69	1	3	3	3	3	3	3	3	3	3	3	2	3	3	1	1
	YMD88-Y7	-9.30	2	MLG.61	MHP.35	1	2	3	3	3	3	3	3	3	3	3	3	3	3	1	1
	YMD88-Y8	8.26	2	MLG.60	MHP.74	0	3	3	3	3	3	3	3	3	3	3	3	3	3	1	1
	YMD88-Y9	-1.96	4	MLG.69	MHP.45	2	3	3	3	1	3	3	3	3	3	3	1	3	3	1	1
	YMD88-Y10	9.11	4	MLG.68	MHP.44	3	3	3	3	1	3	3	3	3	3	1	2	3	3	1	1
	YMD88-F1	8.81	4	MLG.74	MHP.69	1	3	3	3	3	3	3	3	3	3	3	2	3	3	1	1
	YMD88-F2	5.75	2	MLG.73	MHP.67	2	3	3	3	3	3	3	3	3	3	3	2	2	3	1	1
	YMD88-F3	4.16	2	MLG.62	MHP.4	7	1	3	1	3	3	1	1	3	3	3	2	2	1	1	1
	YMD88-F4	25.57	4	MLG.65	MHP.40	5	3	3	3	1	3	1	1	3	3	3	3	2	1	1	1
	YMD88-F5	2.51	4	MLG.66	MHP.41	2	3	3	3	1	3	1	3	3	3	3	3	3	3	1	1
	YMD88-F6	10.95	8	MLG.70	MHP.48	3	3	3	3	3	3	2	3	1	3	3	2	3	3	1	1
	YMD88-F7	7.71	4	MLG.67	MHP.42	3	3	3	3	1	3	3	3	1	3	3	3	2	3	1	1
	YMD88-F8	-3.67	4	MLG.63	MHP.17	4	1	3	3	3	3	2	1	3	3	3	3	2	3	1	1
	YMD88-F9	2.39	2	MLG.63	MHP.17	4	1	3	3	3	3	2	1	3	3	3	3	2	3	1	1
	YMD88-F10	4.71	8	MLG.71	MHP.49	2	3	3	3	3	3	1	3	3	3	3	3	2	3	1	1
VNIVxVGIII	B4546(*MAT* a parent)	NA	NA	MLG.27	MHP.1	NA	1	1	1	1	1	1	1	1	1	1	1	1	1	1	1
	JEC21(*MAT* α parent)	NA	NA	MLG.59	MHP.19	NA	2	2	2	2	2	2	2	2	2	2	2	2	2	2	2
	YMD89(ancestor)	NA	NA	MLG.76	MHP.74	NA	3	3	3	3	3	3	3	3	3	3	3	3	3	2	1
	YMD89-Y1	-4.77	1	MLG.81	MHP.24	4	2	3	3	2	3	3	3	3	3	3	2	2	3	2	1
	YMD89-Y2	-11.73	1	MLG.91	MHP.35	1	2	3	3	3	3	3	3	3	3	3	3	3	3	2	1
	YMD89-Y3	21.69	2	MLG.89	MHP.32	2	2	3	3	3	3	3	3	3	3	3	2	3	3	2	1
	YMD89-Y4	-15.09	2	MLG.80	MHP.23	3	2	3	3	2	3	2	3	3	3	3	3	3	3	2	1
	YMD89-Y5	-0.59	2	MLG.76	MHP.74	0	3	3	3	3	3	3	3	3	3	3	3	3	3	2	1
	YMD89-Y6	-12.43	2	MLG.92	MHP.65	2	3	3	3	3	3	3	3	3	3	1	2	3	3	2	1
	YMD89-Y7	3.24	2	MLG.82	MHP.25	2	2	3	3	2	3	3	3	3	3	3	3	3	3	2	1
	YMD89-Y8	-11.20	2	MLG.85	MHP.27	4	2	3	3	3	3	2	1	3	3	3	3	2	3	2	1
	YMD89-Y9	3.01	2	MLG.79	MHP.22	4	2	3	3	2	3	2	3	3	3	3	3	2	3	2	1
	YMD89-Y10	-1.77	4	MLG.86	MHP.28	3	2	3	3	3	3	2	1	3	3	3	3	3	3	2	1
	YMD89-F1	-4.77	2	MLG.83	MHP.31	2	2	3	3	3	3	1	3	3	3	3	3	3	3	2	1
	YMD89-F2	9.13	4	MLG.90	MHP.33	2	2	3	3	3	3	3	3	3	3	3	3	2	3	2	1
	YMD89-F3	10.37	4	MLG.78	MHP.21	5	2	3	3	2	3	2	3	3	3	3	3	2	2	2	1
	YMD89-F4	2.18	4	MLG.84	MHP.26	3	2	3	3	3	3	2	2	3	3	3	3	3	3	2	1
	YMD89-F5	26.93	4	MLG.77	MHP.20	3	2	3	2	3	3	2	3	3	3	3	3	3	3	2	1
	YMD89-F6	-16.62	4	MLG.88	MHP.30	3	2	3	3	3	3	2	3	3	3	3	3	2	3	2	1
	YMD89-F7	-1.24	4	MLG.91	MHP.35	1	2	3	3	3	3	3	3	3	3	3	3	3	3	2	1

	YMD89-F8	-6.89	8	MLG.87	MHP.29	3	2	3	3	3	3	2	3	2	3	3	3	3	3	2	1
	YMD89-F9	-6.54	4	MLG.91	MHP.35	1	2	3	3	3	3	3	3	3	3	3	3	3	3	2	1
	YMD89-F10	0.71	4	MLG.87	MHP.29	3	2	3	3	3	3	2	3	2	3	3	3	3	3	2	1
Total LOH events							24	0	6	26	0	28	14	11	17	13	18	37	18	0	0
LOH frequency (per sample per mitotic division)							2.14E-04	0	5.36E-05	2.32E-04	0	2.50E-04	1.25E-04	9.82E-05	1.52E-04	1.16E-04	1.61E-04	3.30E-04	1.61E-04	0	0

Table 5.S2. The occurrence of LOH events among MA lines during mitotic divisions.

Ancestor	Loci	Sample ID	D0	D15	D30	D45	D60	D75	D90	D105	D120
YMD72	*URA5*	YMD72-Y7	3	2	2	2	2	2	2	2	2
	CNM00180	YMD72-F1	3	3	3	1	1	1	1	1	1
		YMD72-F10	3	3	3	1	1	1	1	1	1
	CNB00360	YMD72-Y5	3	3	3	3	3	3	3	1	1
		YMD72-Y9	3	1	1	1	1	1	1	1	1
		YMD72-F5	3	3	3	3	3	1	1	1	1
	CNE00250	YMD72-Y8	3	3	3	2	2	2	2	2	2
	CNI01350	YMD72-Y6	3	3	3	3	3	1	1	1	1
		YMD72-Y7	3	3	3	3	3	3	3	1	1
		YMD72-Y9	3	1	1	1	1	1	1	1	1
		YMD72-F1	3	1	1	1	1	1	1	1	1
		YMD72-F5	3	1	1	1	1	1	1	1	1
		YMD72-F8	3	1	1	1	1	1	1	1	1
		YMD72-F9	3	3	3	3	3	1	1	1	1
		YMD72-F10	3	1	1	1	1	1	1	1	1
	CNK01700	YMD72-Y1	3	2	2	2	2	2	2	2	2
		YMD72-Y2	3	1	1	1	1	1	1	1	1
		YMD72-Y3	3	2	2	2	2	2	2	2	2
		YMD72-Y4	3	2	2	2	2	2	2	2	2
		YMD72-Y8	3	2	2	2	2	2	2	2	2
		YMD72-Y10	3	2	2	2	2	2	2	2	2
		YMD72-F2	3	1	1	1	1	1	1	1	1
		YMD72-F3	3	3	3	2	2	2	2	2	2
	#LOH in Y lines		0	9	10	10	11	11	13	13	13
	#LOH in F lines		0	5	5	8	8	9	9	9	9
	Y lines-LOH frequency		8.67%, or 1.08 x 10-4 LOH events per sample per loucs per mitotic division								
	F lines-LOH frequency		6%, or 7.50 x 10-5 LOH events per sample per loucs per mitotic division								
YMD36	*ERG11*	YMD36-Y9	3	3	3	3	1	1	1	1	1
		YMD36-F7	3	1	1	1	1	1	1	1	1
	CNM00180	YMD36-Y5	3	3	3	3	3	3	3	1	1
		YMD36-Y6	3	3	3	3	1	1	1	1	1
		YMD36-F2	3	3	3	3	3	3	1	1	1
		YMD36-F6	3	2	2	2	2	2	2	2	2
		YMD36-F9	3	2	2	2	2	2	2	2	2
		YMD36-F10	3	2	2	2	2	2	2	2	2
	CNB00360	YMD36-Y3	3	3	3	3	2	2	2	2	2
		YMD36-Y4	3	3	3	3	3	3	2	2	2
		YMD36-Y9	3	3	3	1	1	1	1	1	1
		YMD36-Y10	3	3	3	3	2	2	2	2	2
		YMD36-F2	3	3	3	3	3	3	1	1	1
		YMD36-F7	3	1	1	1	1	1	1	1	1
	CNL06810	YMD36-Y9	3	3	3	3	3	3	3	2	2
		YMD36-F1	3	3	3	3	3	3	3	2	2
		YMD36-F6	3	3	2	2	2	2	2	2	2
	CGNM2	YMD36-Y4	3	2	2	2	2	2	2	2	2
		YMD36-Y5	3	3	3	3	3	3	3	3	1
		YMD36-Y6	3	3	3	3	1	1	1	1	1
		YMD36-Y8	3	3	3	2	2	2	2	2	2
		YMD36-F2	3	3	3	2	2	2	2	2	2
		YMD36-F6	3	2	2	2	2	2	2	2	2
		YMD36-F9	3	3	3	3	3	2	2	2	2
		YMD36-F10	3	3	3	2	2	2	2	2	2
	CNH02750	YMD36-Y3	3	3	3	3	2	2	2	2	2
		YMD36-Y5	3	3	2	2	2	2	2	2	2
		YMD36-F2	3	3	3	3	3	3	2	2	2
		YMD36-F4	3	3	3	3	3	3	2	2	2
	CNK01700	YMD36-Y3	3	3	3	1	1	1	1	1	1
		YMD36-F1	3	3	3	3	1	1	1	1	1
		YMD36-F2	3	3	3	3	3	3	1	1	1

	#LOH in Y lines		0	1	2	5	11	11	12	14	15
	#LOH in F lines		0	6	7	9	10	12	19	20	20
	Y lines-LOH frequency		10%, or 1.25 x 10-4 LOH events per sample per loucs per mitotic division								
	F lines-LOH frequency		11.33%, or 1.42 x 10-4 LOH events per sample per loucs per mitotic division								
YMD135	*ERG11*	YMD135-Y5	3	3	3	3	2	2	2	2	2
		YMD135-Y9	3	3	3	3	3	3	2	2	2
	CNM00180	YMD135-Y8	3	3	3	3	3	3	3	3	1
		YMD135-Y9	3	3	3	3	3	3	3	3	2
		YMD135-F9	3	3	3	3	1	1	1	1	1
	CGNI	YMD135-Y4	3	1	1	1	1	1	1	1	1
		YMD135-Y5	3	3	3	3	1	1	1	1	1
		YMD135-Y9	3	3	3	3	1	1	1	1	1
		YMD135-Y10	3	3	3	3	3	3	3	3	1
	CNE00250	YMD135-Y5	3	3	3	3	3	3	2	2	2
	CNL06810	YMD135-Y4	3	2	2	2	2	2	2	2	2
		YMD135-Y5	3	3	3	3	1	1	1	1	1
		YMD135-Y8	3	3	3	3	3	2	2	2	2
		YMD135-Y10	3	3	3	3	3	3	1	1	1
		YMD135-F3	3	3	3	3	3	3	2	2	2
		YMD135-F10	3	1	1	1	1	1	1	1	1
	CGNM2	YMD135-Y6	3	3	1	1	1	1	1	1	1
	CNH02750	YMD135-Y4	3	3	3	2	2	2	2	2	2
	CNI01350	YMD135-Y1	3	3	2	2	2	2	2	2	2
		YMD135-Y6	3	3	3	3	3	3	3	2	2
		YMD135-F1	3	2	2	2	2	2	2	2	2
		YMD135-F2	3	2	2	2	2	2	2	2	2
		YMD135-F3	3	2	2	2	2	2	2	2	2
		YMD135-F4	3	2	2	2	2	2	2	2	2
		YMD135-F5	3	3	3	3	3	3	3	2	2
		YMD135-F6	3	2	2	2	2	2	2	2	2
		YMD135-F7	3	2	2	2	2	2	2	2	2
		YMD135-F8	3	2	2	2	2	2	2	2	2
		YMD135-F9	3	2	2	2	2	2	2	2	2
		YMD135-F10	3	2	2	2	2	2	2	2	2
	CNK01700	YMD135-Y2	3	3	3	3	3	3	3	3	1
		YMD135-Y3	3	3	3	3	1	1	1	1	1
		YMD135-Y7	3	3	3	3	3	3	3	1	1
	#LOH in Y lines		0	2	4	5	10	11	14	16	20
	#LOH in F lines		0	10	10	10	11	11	12	13	13
	Y lines-LOH frequency		13.33%, or 1.67 x 10-4 LOH events per sample per loucs per mitotic division								
	F lines-LOH frequency		8.67%, or 1.08 x 10-4 LOH events per sample per loucs per mitotic division								
YMD165	CNM00180	YMD165-Y7	3	3	2	2	2	2	2	2	2
		YMD165-F5	3	3	2	2	2	2	2	2	2
		YMD165-F6	3	3	3	3	2	2	2	2	2
	#LOH in Y lines		0	0	1	1	1	1	1	1	1
	#LOH in F lines		0	0	1	1	2	2	2	2	2
	Y lines-LOH frequency		0.67%, or 8.33 x 10-6 LOH events per sample per loucs per mitotic division								
	F lines-LOH frequency		1.33%, or 1.67 x 10-5 LOH events per sample per loucs per mitotic division								
YMD10	*CNM00180*	YMD10-Y4	3	3	3	3	2	2	2	2	2
		YMD10-Y9	3	2	2	2	2	2	2	2	2
	CNB00360	YMD10-F10	3	3	1	1	1	1	1	1	1
	CGNI	YMD10-Y1	3	1	1	1	1	1	1	1	1
		YMD10-F7	3	3	3	3	3	3	3	3	1
	CNE00250	YMD10-Y2	3	3	1	1	1	1	1	1	1
		YMD10-Y3	3	3	3	3	3	3	3	1	1
		YMD10-Y5	3	1	1	1	1	1	1	1	1
		YMD10-Y7	3	3	2	2	2	2	2	2	2
	CNL06810	YMD10-Y3	3	3	3	3	3	3	3	3	1
		YMD10-Y4	3	3	3	3	3	3	3	3	1
		YMD10-Y5	3	3	3	3	3	3	3	3	1
		YMD10-F2	3	3	3	3	3	3	3	3	1
		YMD10-F3	3	3	3	3	1	1	1	1	1
		YMD10-F6	3	3	3	3	1	1	1	1	1
		YMD10-F7	3	3	3	3	3	3	1	1	1
		YMD10-F8	3	3	3	3	3	1	1	1	1
	CNH02750	YMD10-F9	3	3	3	3	3	3	3	2	2

	CGNM2	YMD10-F6	3	3	3	3	2	2	2	2	2
		YMD10-F7	3	3	3	3	3	3	2	2	2
	CNI01350	YMD10-F1	3	1	1	1	1	1	1	1	1
		YMD10-F4	3	1	1	1	1	1	1	1	1
		YMD10-F5	3	1	1	1	1	1	1	1	1
		YMD10-F10	3	1	1	1	1	1	1	1	1
	CNK01700	YMD10-Y8	3	3	3	2	2	2	2	2	2
	#LOH in Y lines		0	3	5	6	7	7	7	8	12
	#LOH in F lines		0	4	5	5	8	9	11	11	13
	Y lines-LOH frequency		8%, or 1 x 10-4 LOH events per sample per loucs per mitotic division								
	F lines-LOH frequency		8.66%, or 1.08 x 10-4 LOH events per sample per loucs per mitotic division								
YMD88	*URA5*	YMD88-Y3	3	3	3	3	1	1	1	1	1
		YMD88-Y7	3	3	3	2	2	2	2	2	2
		YMD88-F3	3	3	3	3	3	3	1	1	1
		YMD88-F8	3	3	3	3	3	3	1	1	1
		YMD88-F9	3	3	1	1	1	1	1	1	1
	ERG11	YMD88-F3	3	3	3	3	3	3	1	1	1
	CNM00180	YMD88-Y9	3	3	1	1	1	1	1	1	1
		YMD88-Y10	3	1	1	1	1	1	1	1	1
		YMD88-F4	3	3	3	3	3	1	1	1	1
		YMD88-F5	3	3	3	1	1	1	1	1	1
		YMD88-F7	3	3	3	3	3	3	3	1	1
	CNB00360	YMD88-F3	3	3	3	3	3	3	1	1	1
		YMD88-F4	3	3	1	1	1	1	1	1	1
		YMD88-F5	3	3	3	3	3	1	1	1	1
		YMD88-F6	3	3	3	3	3	3	2	2	2
		YMD88-F8	3	3	3	3	3	3	2	2	2
		YMD88-F9	3	2	2	2	2	2	2	2	2
		YMD88-F10	3	3	3	1	1	1	1	1	1
	CGNI	YMD88-F3	3	3	3	3	3	3	1	1	1
		YMD88-F4	3	3	3	3	3	3	3	1	1
		YMD88-F8	3	3	3	3	3	3	1	1	1
		YMD88-F9	3	1	1	1	1	1	1	1	1
	CNE00250	YMD88-Y1	3	3	3	3	3	3	3	3	2
		YMD88-F6	3	3	3	1	1	1	1	1	1
		YMD88-F7	3	3	3	3	3	3	1	1	1
	CGNM2	YMD88-F3	3	3	3	1	1	1	1	1	1
	CNH02750	YMD88-Y1	3	3	3	3	3	3	3	3	1
		YMD88-Y2	3	3	3	3	3	3	3	3	1
		YMD88-Y6	3	3	3	2	2	2	2	2	2
		YMD88-Y9	3	3	3	3	3	3	3	3	1
		YMD88-Y10	3	3	3	3	3	3	3	3	2
		YMD88-F1	3	3	3	3	3	3	3	3	2
		YMD88-F2	3	3	3	3	3	3	3	3	2
		YMD88-F3	3	3	3	3	3	3	2	2	2
		YMD88-F6	3	3	3	3	3	3	3	3	2
	CNI01350	YMD88-F2	3	3	3	3	3	3	3	3	2
		YMD88-F3	3	3	3	3	3	3	2	2	2
		YMD88-F4	3	3	3	3	3	3	3	3	2
		YMD88-F7	3	2	2	2	2	2	2	2	2
		YMD88-F8	3	3	3	3	3	2	2	2	2
		YMD88-F9	3	3	2	2	2	2	2	2	2
		YMD88-F10	3	2	2	2	2	2	2	2	2
	CNK01700	YMD88-F3	3	3	3	1	1	1	1	1	1
		YMD88-F4	3	3	3	3	3	3	3	1	1
	#LOH in Y lines		0	1	2	4	5	5	5	5	11
	#LOH in F lines		0	4	7	12	12	15	26	29	33
	Y lines-LOH frequency		6.67%, or 8.33 x 10-5 LOH events per sample per loucs per mitotic division								
	F lines-LOH frequency		23.34%, or 2.92 x 10-4 LOH events per sample per loucs per mitotic division								
		YMD89-Y1	3	2	2	2	2	2	2	2	2
		YMD89-Y2	3	2	2	2	2	2	2	2	2
		YMD89-Y3	3	2	2	2	2	2	2	2	2
		YMD89-Y4	3	2	2	2	2	2	2	2	2
		YMD89-Y7	3	2	2	2	2	2	2	2	2
		YMD89-Y8	3	2	2	2	2	2	2	2	2
		YMD89-Y9	3	2	2	2	2	2	2	2	2

YMD89	*URA5*	YMD89-Y10	3	2	2	2	2	2	2	2	2
		YMD89-F1	3	2	2	2	2	2	2	2	2
		YMD89-F2	3	2	2	2	2	2	2	2	2
		YMD89-F3	3	2	2	2	2	2	2	2	2
		YMD89-F4	3	2	2	2	2	2	2	2	2
		YMD89-F5	3	2	2	2	2	2	2	2	2
		YMD89-F6	3	2	2	2	2	2	2	2	2
		YMD89-F7	3	2	2	2	2	2	2	2	2
		YMD89-F8	3	2	2	2	2	2	2	2	2
		YMD89-F9	3	2	2	2	2	2	2	2	2
		YMD89-F10	3	2	2	2	2	2	2	2	2
	ERG11	YMD89-F5	3	3	3	3	3	3	3	3	2
	CNM00180	YMD89-Y1	3	2	2	2	2	2	2	2	2
		YMD89-Y4	3	2	2	2	2	2	2	2	2
		YMD89-Y7	3	3	3	3	3	2	2	2	2
		YMD89-Y9	3	2	2	2	2	2	2	2	2
		YMD89-F3	3	3	3	3	3	3	3	3	2
	CNB00360	YMD89-Y4	3	3	3	2	2	2	2	2	2
		YMD89-Y8	3	3	3	3	3	3	3	3	2
		YMD89-Y9	3	3	3	2	2	2	2	2	2
		YMD89-Y10	3	3	3	3	3	3	3	2	2
		YMD89-F1	3	3	1	1	1	1	1	1	1
		YMD89-F3	3	3	2	2	2	2	2	2	2
		YMD89-F4	3	3	2	2	2	2	2	2	2
		YMD89-F5	3	3	3	2	2	2	2	2	2
		YMD89-F6	3	2	2	2	2	2	2	2	2
		YMD89-F8	3	3	2	2	2	2	2	2	2
		YMD89-F10	3	2	2	2	2	2	2	2	2
	CGNI	YMD89-Y8	3	1	1	1	1	1	1	1	1
		YMD89-Y10	3	1	1	1	1	1	1	1	1
		YMD89-F4	3	2	2	2	2	2	2	2	2
	CNE00250	YMD89-F8	3	3	2	2	2	2	2	2	2
		YMD89-F10	3	3	3	2	2	2	2	2	2
	CGNM2	YMD89-Y6	3	3	3	3	3	3	3	3	1
	CNH02750	YMD89-Y1	3	3	3	3	3	3	3	3	2
		YMD89-Y3	3	3	3	3	3	3	3	3	2
		YMD89-Y6	3	3	3	3	3	3	3	3	2
	CNI01350	YMD89-Y1	3	3	3	3	3	3	3	3	2
		YMD89-Y8	3	3	3	3	2	2	2	2	2
		YMD89-Y9	3	3	2	2	2	2	2	2	2
		YMD89-F2	3	2	2	2	2	2	2	2	2
		YMD89-F3	3	2	2	2	2	2	2	2	2
		YMD89-F6	3	2	2	2	2	2	2	2	2
	CNK01700	YMD89-F3	3	3	2	2	2	2	2	2	2
	#LOH in Y lines		0	13	14	16	17	18	18	19	25
	#LOH in F lines		0	16	22	24	24	24	24	24	26
	Y lines-LOH frequency		16.67%, or 2.08 x 10-4 LOH events per sample per loucs per mitotic division								
	F lines-LOH frequency		17.33%, or 2.17 x 10-4 LOH LOH events per sample per loucs per mitotic division								

5.9 References

1. Pâques, F.; Haber, J.E. Multiple Pathways of Recombination Induced by Double-Strand Breaks in *Saccharomyces Cerevisiae*. *Microbiol Mol Biol Rev* **1999**, *63*, 349–404.

2. Chang, H.H.Y.; Pannunzio, N.R.; Adachi, N.; Lieber, M.R. Non-Homologous DNA End Joining and Alternative Pathways to Double-Strand Break Repair. *Nat Rev Mol Cell Biol* **2017**, *18*, 495–506.

3. Rastogi, R.P.; Richa; Kumar, A.; Tyagi, M.B.; Sinha, R.P. Molecular Mechanisms of Ultraviolet Radiation-Induced DNA Damage and Repair. *J Nucleic Acids* **2010**, *2010*.

4. Garm, C.; Moreno-Villanueva, M.; Bürkle, A.; Larsen, L.A.; Bohr, V.A.; Christensen, K.; Stevnsner, T. Genetic and Environmental Influence on DNA Strand Break Repair: A Twin Study. *Environ Mol Mutagen* **2013**, *54*, 414–420.

5. Gerstein, A.C.; Kuzmin, A.; Otto, S.P. Loss-of-Heterozygosity Facilitates Passage through Haldane's Sieve for *Saccharomyces Cerevisiae* Undergoing Adaptation. *Nature Communications* **2014**, *5*, 3819.

6. Dunkel, N.; Julia-Blaß; Rogers, P.D.; Morschhäuser, J. Mutations in the Multi-drug Resistance Regulator MRR1, Followed by Loss of Heterozygosity, Are the Main Cause of MDR1 Overexpression in Fluconazole-Resistant *Candida Albicans* Strains. *Mol Microbiol* **2008**, *69*, 827–840.

7. Hiraoka, M.; Watanabe, K.; Umezu, K.; Maki, H. Spontaneous Loss of Heterozygosity in Diploid *Saccharomyces Cerevisiae* Cells. *Genetics* **2000**, *156*, 1531–1548.

8. Nguyen, D.T.; Wu, B.; Long, H.; Zhang, N.; Patterson, C.; Simpson, S.; Morris, K.; Thomas, W.K.; Lynch, M.; Hao, W. Variable Spontaneous Mutation and Loss of Heterozygosity among Heterozygous Genomes in Yeast. *Molecular Biology and Evolution* **2020**, *37*, 3118–3130.

9. Ciudad, T.; Hickman, M.; Bellido, A.; Berman, J.; Larriba, G. Phenotypic Consequences of a Spontaneous Loss of Heterozygosity in a Common Laboratory Strain of *Candida Albicans*. *Genetics* **2016**, *203*, 1161–1176.

10. Forche, A.; Abbey, D.; Pisithkul, T.; Weinzierl, M.A.; Ringstrom, T.; Bruck, D.; Petersen, K.; Berman, J. Stress Alters Rates and Types of Loss of Heterozygosity in Candida Albicans. *mBio* **2011**, *2*.

11. Li, W.; Averette, A.F.; Desnos-Ollivier, M.; Ni, M.; Dromer, F.; Heitman, J. Genetic Diversity and Genomic Plasticity of *Cryptococcus Neoformans* AD Hybrid Strains. *G3 (Bethesda)* **2012**, *2*, 83–97.

12. Lin, X.; Nielsen, K.; Patel, S.; Heitman, J. Impact of Mating Type, Serotype, and Ploidy on the Virulence of *Cryptococcus Neoformans*. *Infect Immun* **2008**, *76*, 2923–2938.

13. Dong, K.; You, M.; Xu, J. Genetic Changes in Experimental Populations of a Hybrid in the *Cryptococcus Neoformans* Species Complex. *Pathogens* **2019**, *9*.

14. Kwon-Chung, K.J.; Bennett, J.E. Distribution of Alpha and Alpha Mating Types of *Cryptococcus Neoformans* among Natural and Clinical Isolates. *Am J Epidemiol* **1978**, *108*, 337–340.

15. Lengeler, K.B.; Cox, G.M.; Heitman, J. Serotype AD Strains of *Cryptococcus Neoformans* Are Diploid or Aneuploid and Are Heterozygous at the Mating-Type Locus. *Infect Immun* **2001**, *69*, 115–122.

16. Bovers, M.; Hagen, F.; Kuramae, E.E.; Hoogveld, H.L.; Dromer, F.; St-Germain, G.; Boekhout, T. AIDS Patient Death Caused by Novel *Cryptococcus Neoformans* × *C. Gattii* Hybrid. *Emerg Infect Dis* **2008**, *14*, 1105–1108.

17. Bovers, M.; Hagen, F.; Kuramae, E.E.; Diaz, M.R.; Spanjaard, L.; Dromer, F.; Hoogveld, H.L.; Boekhout, T. Unique Hybrids between the Fungal Pathogens *Cryptococcus Neoformans* and *Cryptococcus Gattii*. *FEMS Yeast Research* **2006**, *6*, 599–607.

18. Lin, X.; Litvintseva, A.P.; Nielsen, K.; Patel, S.; Floyd, A.; Mitchell, T.G.; Heitman, J. AADα Hybrids of *Cryptococcus Neoformans*: Evidence of Same-Sex Mating in Nature and Hybrid Fitness. *PLOS Genetics* **2007**, *3*, e186.

19. Ni, M.; Feretzaki, M.; Li, W.; Floyd-Averette, A.; Mieczkowski, P.; Dietrich, F.S.; Heitman, J. Unisexual and Heterosexual Meiotic Reproduction Generate Aneuploidy and Phenotypic Diversity *De Novo* in the Yeast *Cryptococcus Neoformans*. *PLoS Biol* **2013**, *11*.

20. Samarasinghe, H.; Xu, J. Hybrids and Hybridization in the *Cryptococcus Neoformans* and *Cryptococcus Gattii* Species Complexes. *Infection, Genetics and Evolution* **2018**, *66*, 245–255.

21. Cogliati, M.; Esposto, M.C.; Tortorano, A.M.; Viviani, M.A. *Cryptococcus Neoformans* Population Includes Hybrid Strains Homozygous at Mating-Type Locus. *FEMS Yeast Res* **2006**, *6*, 608–613.

22. Vogan, A.A.; Khankhet, J.; Xu, J. Evidence for Mitotic Recombination within the Basidia of a Hybrid Cross of *Cryptococcus Neoformans*. *PLoS One* **2013**, *8*.

23. You, M.; Xu, J. What Are the Best Parents for Hybrid Progeny? An Investigation into the Human Pathogenic Fungus *Cryptococcus*. *Journal of Fungi* **2021**, *7*, 299.

24. Ravichandran, M.C.; Fink, S.; Clarke, M.N.; Hofer, F.C.; Campbell, C.S. Genetic Interactions between Specific Chromosome Copy Number Alterations Dictate Complex Aneuploidy Patterns. *Genes Dev* **2018**, *32*, 1485–1498.

25. Birchler, J.A. Aneuploidy in Plants and Flies: The Origin of Studies of Genomic Imbalance. *Seminars in Cell & Developmental Biology* **2013**, *24*, 315–319.

26. Gilchrist, C.; Stelkens, R. Aneuploidy in Yeast: Segregation Error or Adaptation Mechanism? *Yeast* **2019**, *36*, 525–539.

27. Todd, R.T.; Forche, A.; Selmecki, A. Ploidy Variation in Fungi – Polyploidy, Aneuploidy, and Genome Evolution. *Microbiol Spectr* **2017**, *5*.

28. Bennett, R.J.; Forche, A.; Berman, J. Rapid Mechanisms for Generating Genome Diversity: Whole Ploidy Shifts, Aneuploidy, and Loss of Heterozygosity. *Cold Spring Harb Perspect Med* **2014**, *4*.

29. Weil, T.; Santamaría, R.; Lee, W.; Rung, J.; Tocci, N.; Abbey, D.; Bezerra, A.R.; Carreto, L.; Moura, G.R.; Bayés, M.; et al. Adaptive Mistranslation Accelerates the Evolution of Fluconazole Resistance and Induces Major Genomic and Gene Expression Alterations in *Candida Albicans*. *mSphere* **2017**, *2*.

30. Huang, M.; McClellan, M.; Berman, J.; Kao, K.C. Evolutionary Dynamics of *Candida Albicans* during In Vitro Evolution. *Eukaryotic Cell* **2011**, *10*, 1413–1421.

31. Rodero, L.; Mellado, E.; Rodriguez, A.C.; Salve, A.; Guelfand, L.; Cahn, P.; Cuenca-Estrella, M.; Davel, G.; Rodriguez-Tudela, J.L. G484S Amino Acid Substitution in Lanosterol 14-Alpha Demethylase (ERG11) Is Related to Fluconazole Resistance in a Recurrent *Cryptococcus Neoformans* Clinical Isolate. *Antimicrob Agents Chemother* **2003**, *47*, 3653–3656.

32. Posteraro, B.; Sanguinetti, M.; Sanglard, D.; La Sorda, M.; Boccia, S.; Romano, L.; Morace, G.; Fadda, G. Identification and Characterization of a *Cryptococcus*

Neoformans ATP Binding Cassette (ABC) Transporter-Encoding Gene, CnAFR1, Involved in the Resistance to Fluconazole. *Mol Microbiol* **2003**, *47*, 357–371.

33. Modrich, P.; Lahue, R. Mismatch Repair in Replication Fidelity, Genetic Recombination, and Cancer Biology. *Annu Rev Biochem* **1996**, *65*, 101–133.

34. De Storme, N.; Mason, A. Plant Speciation through Chromosome Instability and Ploidy Change: Cellular Mechanisms, Molecular Factors and Evolutionary Relevance. *Current Plant Biology* **2014**, *1*, 10–33.

35. Xu, J. Estimating the Spontaneous Mutation Rate of Loss of Sex in the Human Pathogenic Fungus *Cryptococcus Neoformans*. *Genetics* **2002**, *162*, 1157–1167.

36. Sia, R.A.; Lengeler, K.B.; Heitman, J. Diploid Strains of the Pathogenic Basidiomycete *Cryptococcus Neoformans* Are Thermally Dimorphic. *Fungal Genet Biol* **2000**, *29*, 153–163.

37. Clinical Laboratory Standards Institue: Reference Method for Broth Dilution Antifungal Susceptibility Testing of Yeasts; Approved Standard, 3rd Ed, CLSI Document M27-A3, CLSI, Wayne, PA 2008.

38. Vogan, A.A.; Khankhet, J.; Samarasinghe, H.; Xu, J. Identification of QTLs Associated with Virulence Related Traits and Drug Resistance in *Cryptococcus Neoformans*. *G3 Genes|Genomes|Genetics* **2016**, *6*, 2745–2759.

39. Bates, D.; Mächler, M.; Bolker, B.; Walker, S. Fitting Linear Mixed-Effects Models Using Lme4. *Journal of Statistical Software* **2015**, *67*, 1–48.

40. Kamvar, Z.N.; Tabima, J.F.; Grünwald, N.J. Poppr: An R Package for Genetic Analysis of Populations with Clonal, Partially Clonal, and/or Sexual Reproduction. *PeerJ* **2014**, *2*, e281.

41. Wickham, H. Ggplot2. *WIREs Computational Statistics* **2011**, *3*, 180–185.

42. R Core Team R: A Language and Environment for Statistical Computing. 2013.

43. Farrer, R.A.; Chang, M.; Davis, M.J.; Dorp, L. van; Yang, D.-H.; Shea, T.; Sewell, T.R.; Meyer, W.; Balloux, F.; Edwards, H.M.; et al. A New Lineage of *Cryptococcus Gattii* (VGV) Discovered in the Central Zambezian Miombo Woodlands. *mBio* **2019**, *10*.

44. Hagen, F.; Khayhan, K.; Theelen, B.; Kolecka, A.; Polacheck, I.; Sionov, E.; Falk, R.; Parnmen, S.; Lumbsch, H.T.; Boekhout, T. Recognition of Seven Species in the

Cryptococcus Gattii/*Cryptococcus Neoformans* Species Complex. *Fungal Genet Biol* **2015**, *78*, 16–48.

45. Kidd, S.E.; Guo, H.; Bartlett, K.H.; Xu, J.; Kronstad, J.W. Comparative Gene Genealogies Indicate That Two Clonal Lineages of *Cryptococcus Gattii* in British Columbia Resemble Strains from Other Geographical Areas. *Eukaryot Cell* **2005**, *4*, 1629–1638.

46. Xu, J.; Vilgalys, R.; Mitchell, T.G. Multiple Gene Genealogies Reveal Recent Dispersion and Hybridization in the Human Pathogenic Fungus *Cryptococcus Neoformans*. *Mol Ecol* **2000**, *9*, 1471–1481.

47. Ngamskulrungroj, P.; Gilgado, F.; Faganello, J.; Litvintseva, A.P.; Leal, A.L.; Tsui, K.M.; Mitchell, T.G.; Vainstein, M.H.; Meyer, W. Genetic Diversity of the *Cryptococcus* Species Complex Suggests That *Cryptococcus Gattii* Deserves to Have Varieties. *PLOS ONE* **2009**, *4*, e5862.

48. Casadevall, A.; Freij, J.B.; Hann-Soden, C.; Taylor, J. Continental Drift and Speciation of the *Cryptococcus Neoformans* and *Cryptococcus Gattii* Species Complexes. *mSphere* **2017**, *2*.

49. Sharpton, T.J.; Neafsey, D.E.; Galagan, J.E.; Taylor, J.W. Mechanisms of Intron Gain and Loss in *Cryptococcus*. *Genome Biol* **2008**, *9*, R24.

50. Hu, G.; Liu, I.; Sham, A.; Stajich, J.E.; Dietrich, F.S.; Kronstad, J.W. Comparative Hybridization Reveals Extensive Genome Variation in the AIDS-Associated Pathogen *Cryptococcus Neoformans*. *Genome Biol* **2008**, *9*, R41.

51. Vogan, A.A.; Xu, J. Evidence for Genetic Incompatibilities Associated with Post-Zygotic Reproductive Isolation in the Human Fungal Pathogen *Cryptococcus Neoformans*. *Genome* **2014**, *57*, 335–344.

52. Sun, S.; Xu, J. Chromosomal Rearrangements between Serotype A and D Strains in *Cryptococcus Neoformans*. *PLOS ONE* **2009**, *4*, e5524.

53. D'Souza, C.A.; Kronstad, J.W.; Taylor, G.; Warren, R.; Yuen, M.; Hu, G.; Jung, W.H.; Sham, A.; Kidd, S.E.; Tangen, K.; et al. Genome Variation in *Cryptococcus Gattii*, an Emerging Pathogen of Immunocompetent Hosts. *mBio* **2011**, *2*.

54. Fujitani, Y.; Kobayashi, I. Effect of DNA Sequence Divergence on Homologous Recombination as Analyzed by a Random-Walk Model. *Genetics* **1999**, *153*, 1973–1988.

55. Opperman, R.; Emmanuel, E.; Levy, A.A. The Effect of Sequence Divergence on Recombination Between Direct Repeats in Arabidopsis. *Genetics* **2004**, *168*, 2207–2215.

56. Altamirano, S.; Fang, D.; Simmons, C.; Sridhar, S.; Wu, P.; Sanyal, K.; Kozubowski, L. Fluconazole-Induced Ploidy Change in *Cryptococcus Neoformans* Results from the Uncoupling of Cell Growth and Nuclear Division. *mSphere* **2017**, *2*.

57. Stone, N.R.H.; Rhodes, J.; Fisher, M.C.; Mfinanga, S.; Kivuyo, S.; Rugemalila, J.; Segal, E.S.; Needleman, L.; Molloy, S.F.; Kwon-Chung, J.; et al. Dynamic Ploidy Changes Drive Fluconazole Resistance in Human Cryptococcal Meningitis. *J Clin Invest* **2019**, *129*, 999–1014.

58. Harrison, B.D.; Hashemi, J.; Bibi, M.; Pulver, R.; Bavli, D.; Nahmias, Y.; Wellington, M.; Sapiro, G.; Berman, J. A Tetraploid Intermediate Precedes Aneuploid Formation in Yeasts Exposed to Fluconazole. *PLoS Biol* **2014**, *12*, e1001815.

59. Pavelka, N.; Rancati, G.; Zhu, J.; Bradford, W.D.; Saraf, A.; Florens, L.; Sanderson, B.W.; Hattem, G.L.; Li, R. Aneuploidy Confers Quantitative Proteome Changes and Phenotypic Variation in Budding Yeast. *Nature* **2010**, *468*, 321–325.

60. Sionov, E.; Lee, H.; Chang, Y.C.; Kwon-Chung, K.J. *Cryptococcus Neoformans* Overcomes Stress of Azole Drugs by Formation of Disomy in Specific Multiple Chromosomes. *PLoS Pathog* **2010**, *6*, e1000848.

61. Semighini, C.P.; Averette, A.F.; Perfect, J.R.; Heitman, J. Deletion of *Cryptococcus Neoformans* AIF Ortholog Promotes Chromosome Aneuploidy and Fluconazole-Resistance in a Metacaspase-Independent Manner. *PLoS Pathog* **2011**, *7*, e1002364.

62. Yang, F.; Kravets, A.; Bethlendy, G.; Welle, S.; Rustchenko, E. Chromosome 5 Monosomy of *Candida Albicans* Controls Susceptibility to Various Toxic Agents, Including Major Antifungals. *Antimicrobial Agents and Chemotherapy* **2013**, *57*, 5026–5036.

63. Selmecki, A.; Forche, A.; Berman, J. Aneuploidy and Isochromosome Formation in Drug-Resistant *Candida Albicans*. *Science* **2006**, *313*, 367–370.

64. Ngamskulrungroj, P.; Chang, Y.; Hansen, B.; Bugge, C.; Fischer, E.; Kwon-Chung, K.J. Characterization of the Chromosome 4 Genes That Affect Fluconazole-Induced Disomy Formation in *Cryptococcus Neoformans*. *PLOS ONE* **2012**, *7*, e33022.

Chapter 6: Conclusions

Overall, my PhD thesis examined the effects of parental divergence on three distinct areas: (i) the mating success and hybrid spore germination under different conditions; (ii) the genotypic diversity and phenotypic variations under diverse environmental conditions among progeny; (iii) genome stability of diploid hybrids through laboratory experimental evolution. Below, I summarize my major findings and make suggestions for further research.

6.1 Main findings and future prospects

In Chapter 2, we reviewed the prevalence of hybridization in fungi and its role in fungal evolution and adaptation. We showed evidence for the advantages of using HPC as model organisms to study the evolutionary dynamics and mechanisms of genomic plasticity, and to investigate the genotypic and phenotypic consequences of hybridization. This review set the stage for the three subsequent chapters of using HPC to understand the relationship between parental divergence and hybrid performance.

In Chapter 3, I investigated the effects of multiple genetic and environmental factors on the germination of basidiospores from diverse intra-lineage and inter-lineage crosses. We found that VGIII strains are more fertile than strains of other molecular types in the human pathogenic *Cryptococcus*. Previously, genetic incompatibility between *C. neoformans* and *C. neoformans* was identified (Vogan & Xu, 2014). Here, we provided evidence of genetic incompatibility between CNSC and CGSC and between divergent lineages/molecular types in CGSC. Basidiospores are considered to be the infectious propagules that cause cryptococcosis. Consistent with observations in serotype AD hybrids from previous studies, basidiospore germination from crosses conducted from this work was also highly variable (Forsythe *et al*., 2016; Lengeler *et al*., 2001; Vogan *et al*., 2013). Basidiospores of intra-lineage crosses had an overall higher germination rate. However, different from serotype AD hybrids, the genetic distance between parents did not significantly influence the spore germination in other kinds of cryptococcal hybrids examined in this study. Instead, the germination of basidiospores can be affected by multiple factors, such as high temperatures. At present, the genetic bases for the highly variable basidiospore germination rates among HPC hybrids are largely unknown. As these spores are considered the dominant infectious propagules, further investigations on the genetic mechanisms could help revealing mechanisms of

pathogenesis, especially at the initial stages of infection. One area of potential future research is to investigate the genotypes and genome sequences of a large number of germinated spores and to infer the potential lethal allelic combinations associated with non-viable hybrids.

In Chapter 4, I determined the relationships between parental divergence (genetic and phenotypic) and progeny phenotypes using diverse genetic crosses in the human pathogenic *Cryptococcus*. We observed multiple patterns of relationships between parents and their progeny under different phenotypic traits. Previous studies on serotype AD hybrid fitness also found similar diversities (Li *et al*., 2012; Lin *et al*., 2007; Shahid *et al*., 2008). Although parental genetic divergence is significantly associated with progeny phenotypes under some traits, it is not likely to predict progeny phenotypes only based on parental divergence. Our results suggest the enormous capacity and potential of cryptococcal hybrids in adapting to diverse ecological niches. This work also expands the knowledge of genotypic and phenotypic consequences of hybridization in the human pathogenic *Cryptococcus*. Potential follow-up research includes investigating more phenotypes related to survival in conditions simulating both natural and clinical environments, as well as the genetic bases for the observed genotypic and phenotypic variations among hybrids. Such investigations can involve multi-omics approaches to identify the differences in transcriptomes, proteomes, and metabolomes among hybrids that show diverse phenotypes.

In Chapter 5, I investigated the genetic and phenotypic changes of inter-lineage diploid hybrids in the human pathogenic *Cryptococcus* by means of mutation accumulation (MA) experiments. This work revealed high genotypic and phenotypic diversities generated during asexual reproduction. Also, we found that parental genetic divergence, mutation accumulation conditions, and their interaction can contribute to the observed genotypic and phenotypic diversities. However, our analyses showed no apparent correlation between parental genome divergence and genome stability of hybrids. Additionally, previous MA experiments under drug stress in *Canadia albicans* and *Cryptococcus neoformans* species complex found the formation of disomy in specific chromosomes (i.e., drug-resistance related) (Dong *et al*., 2019; Forche *et al*., 2011). However, this did not occur among hybrids examined in this study, suggesting that a

relatively low dose of drug stress might not be likely to induce more loss of heterozygosity events. One potential area of future research to understand the genetic bases for the observed phenotypic variations among the evolved clones and between the evolved clones and their respective ancestral clones is to identify both the large-scale and the fine-scale genomic changes (e.g., genome structural rearrangements, SNPs, INDELs, and copy number variants) among them.

6.2 References

Dong, K., You, M., & Xu, J. (2019). Genetic Changes in Experimental Populations of a Hybrid in the *Cryptococcus neoformans* Species Complex. Pathogens, 9(1).

Forche, A., Abbey, D., Pisithkul, T., Weinzierl, M. A., Ringstrom, T., Bruck, D., Petersen, K., & Berman, J. (2011). Stress Alters Rates and Types of Loss of Heterozygosity in Candida albicans. MBio, 2(4).

Forsythe, A., Vogan, A., & Xu, J. (2016). Genetic and environmental influences on the germination of basidiospores in the *Cryptococcus neoformans* species complex. Scientific Reports, 6(1), 33828.

Lengeler, K. B., Cox, G. M., & Heitman, J. (2001). Serotype AD Strains of *Cryptococcus neoformans* Are Diploid or Aneuploid and Are Heterozygous at the Mating-Type Locus. Infection and Immunity, 69(1), 115–122.

Li, W., Averette, A. F., Desnos-Ollivier, M., Ni, M., Dromer, F., & Heitman, J. (2012). Genetic Diversity and Genomic Plasticity of *Cryptococcus neoformans* AD Hybrid Strains. G3: Genes|Genomes|Genetics, 2(1), 83–97.

Lin, X., Litvintseva, A. P., Nielsen, K., Patel, S., Floyd, A., Mitchell, T. G., & Heitman, J. (2007). αADα Hybrids of *Cryptococcus neoformans*: Evidence of Same-Sex Mating in Nature and Hybrid Fitness. PLOS Genetics, 3(10), e186.

Shahid, M., Han, S., Yoell, H., & Xu, J. (2008). Fitness distribution and transgressive segregation across 40 environments in a hybrid progeny population of the human-pathogenic yeast *Cryptococcus neoformans*. Genome, 51(4), 272–281.

Vogan, A. A., Khankhet, J., & Xu, J. (2013). Evidence for Mitotic Recombination within the Basidia of a Hybrid Cross of *Cryptococcus neoformans*. PLoS ONE, 8(5).

Vogan, A. A., & Xu, J. (2014). Evidence for genetic incompatibilities associated with post-zygotic reproductive isolation in the human fungal pathogen *Cryptococcus neoformans*. Genome, 57(6), 335–344.